NUTRIENT-DEPENDENT EFFECTS OF THE AUTOPHAGY-LYSOSOMAL INHIBITOR, CHLOROQUINE, ON CELL DEATH AND LYSOSOMAL FUNCTIONALITY

A thesis presented by

Laura Gallagher

In fulfilment of the requirement for the degree of

Doctor of Philosophy

2017

Strathclyde Institute of Pharmacy and Biomedical Sciences

University of Strathclyde

This thesis is the result of the author's original research. It has been composed by the author and has not been previously submitted for examination which has led to the award of a degree.

Signed:

Date:

ACKNOWLEDGEMENTS

Firstly I would like that thank my supervisors Dr Edmond Chan and Dr Marie Boyd. Ed's support and advice throughout the whole project has been greatly appreciated, especially when things may not have gone to plan, results were unexpected, and the project began to deviate from that which we had originally planned. The support and training he has provided me with will stay with me for the rest of my career. I would also like to thank the past and present members of my lab group, for their continued support and the positive atmosphere they created in the lab during my time here at Strathclyde. An additional mention goes to my funding body, Cancer Research UK, without them this work would not have been possible.

Since taking the leap to move to Scotland just over 4 years ago, I have made some amazing friends here at Strathclyde. I would particularly like to thank Chelsey and Rachel for making my time in Glasgow so special. You know you have made friends for life when they can put up with seeing you during the day at university and then again when you get home, I could not have asked for better housemates and best friends. My boyfriend, David, also deserves a special mention for supporting me through the final year of my PhD. There may have been a few tears and tantrums this past year but his advice, calmness, and love has got me through with my sanity still intact.

Finally I would like to mention my friends and family back in Manchester. They were so supportive of my move to Scotland to complete my PhD, even though it meant I wouldn't get to see them so often. I also give a special mention to my mum and dad, who have shaped me into the person I am today and who I strive to make proud every day. Also to my grandparents, who I know will be very happy and proud to say they have a Doctor in the family.

This is a big thank you to everyone who has helped and supported me over the past 4 years…..maybe you'll get to see more of me now.

PUBLICATIONS

Gallagher, L.E., Chan, E.Y., 2013. Early signalling events of autophagy. *Essays Biochem,* 55: p1-15.

Gallagher, L.E., Williamson, L.E., Chan, E.Y.*, 2016. Advances in autophagy regulatory mechanisms. *Cells,* 5: 24.

POSTER COMMUNICATIONS

2nd UK Autophagy conference, Edinburgh, 14-15th April 2016. Gallagher, L.E., Chan, E.Y., Interference with glucose metabolism confers resistance toward Chloroquine-induced cytotoxicity in metastatic breast cancer cells.

EACR conference series “A matter of life or death: Mechanisms and Relevance of Cell Death for Cancer Biology and Treatment”, Amsterdam, 28th-30th Jan 2016. Gallagher, L.E., Chan, E.Y., Interference with glucose metabolism confers resistance toward Chloroquine-induced cytotoxicity in metastatic breast cancer cells.

1st UK Autophagy conference, Warwick, 6-7th May 2015. Gallagher, L.E., Chan, E.Y., Lower glucose metabolism leads to resistance toward the chemotherapeutic drug, Chloroquine, in metastatic breast cancer cells.

Visualising Cancer: Microscopy and Beyond, Beatson Institute, Glasgow, 12th Sept 2014. Gallagher, L.E., Chan, E.Y., Reduced cell metabolism enhances resistance to the chemotherapeutic drug, Chloroquine, in breast cancer cells.

ORAL COMMUNICATIONS

CRUK Glasgow Centre Annual Symposium, 11th September 2015. Gallagher, L.E., Chan, E.Y., Chloroquine as an anti-cancer treatment: Resistance mechanism linked to glucose metabolism.

TABLE OF CONTENTS

Chapter 1

Chapter 2

Chapter 3

Chapter 4

Chapter 7

LIST OF FIGURES

Chapter 1.

Chapter 3.

Chapter 5.

Chapter 6.

LIST OF TABLES

Chapter 1.

Chapter 2.

Chapter 5.

ABBREVIATIONS

2DG	2-Deoxyglucose
4E-BP1	Eukaryotic translation initiation factor 4E-binding protein 1
ACC	Acetyl-CoA carboxylase
AICAR	5-Aminoimidazole-4-carboxamide ribonucleotide
Ambra1	Autophagy And Beclin 1 Regulator 1
AMPK	5'AMP-activated protein kinase
AQ	Amodiaquine
ATG	Autophagy-related gene
ATM	*Ataxia telangiectasia mutated*
Bax	BCL2-Associated X protein
Bcl-2	B-Cell CLL/Lymphoma 2
CASTOR	Cellular Arginine Sensor for mTORC1
CK2	Casein kinase 2
CMA	Chaperone mediated autophagy
CML	Chronic myeloid leukaemia
COP-II	Coat protein complex-II
CPX	Ciprofloxacin
CQ	Chloroquine
CXCL12	C-X-C Motif Chemokine Ligand 12
CXCR4	C-X-C chemokine receptor type 4
DCA	Dichloroacetate
DFCP1	Double FYVE domain-containing protein1
DMEM	Dulbecco's modified eagle's medium
DNA	Deoxyribonucleic acid
EBSS	Earle's balanced salt solution
EMT	Epithelial to Mesenchymal transition
ER	Endoplasmic reticulum
ERES	ER exit sites
ERGIC	ER-Golgi intermediate compartment
FBS	Fetal bovine serum
FIP200	Focal adhesion kinase family interacting protein of 200kDa
GAP	GTPase-Activating Protein
GATOR	GTPase-activating protein (GAP) activity toward Rags
GDP	Guanosine-diphosphate
GEF	Guanine Nucleotide Exchange Factor
GLS	Glutaminase
GPCR	G-protein coupled receptors

GTP	Guanosine-triphosphate
HCQ	Hydroxychloroquine
HDAC	Histone deacetylases
HER-2	Human epidermal growth factor receptor-2
HK	hexokinase
Hsc70	Heat shock protein 70
hTERT	Telomerase reverse transcriptase
IM	Isolation membrane
IM	Imatinib Mesylate
IMAT	IM-associated tubules
LAMP	Lysosome-associated membrane proteins
LC3	Microtubule-associated protein 1A/1B-light chain 3
LC3-II	LC3-phosphatidylethanolamine conjugate
LIR	LC3-interacting region
LLOME	Leucyl-Leucyl-O-Methyl ester
LMP	Lysosomal membrane permeabilisation
LTR	Lysotracker Red
MAM	Mitochondria-associated membranes
MDM2	Mouse double minute 2 homolog
MEF	Mouse embryonic fibroblasts
mLST8	Mammalian lethal with SEC13 protein 8
MMP2	Matrix Metalloproteinases
MP	Methyl pyruvate
MTD	Maximum tolerated dose
mTOR	Mechanistic target of rapamycin
mTORC1	Mechanistic target of rapamycin complex 1
NAC	N-Acetyl-L-Cysteine
PARP	Poly ADP ribose polymerase
PBS	Phosphate buffered saline
PDH	Pyruvate dehydrogenase
PDK	Pyruvate dehydrogenase kinase
PDK1	*Phosphoinositide dependent kinase* 1
PFA	Paraformaldehyde
PI3K	Phosphoinositide 3-kinase
PI3P	Phosphatidylinositol 3-phosphate
PIP_2	Phosphatidylinositol 4,5-bisphosphate
PIP_3	Phosphatidylinositol (3,4,5)-trisphosphate
PP2A	Protein phosphatase 2A
PQ	Primaquine

PRAS40	Proline-rich Akt substrate, 40kDa
PTEN	Phosphatase and tensin homolog
PUMA	p53 upregulated modulator of *apoptosis*
Rag	Ras-related GTPase
Ragulator	Rag regulator complex
Raptor	Regulator-associated protein of mTOR
Ras	Derived from 'Rat Sarcoma'
Rheb	Ras homolog enriched in brain
ROS	Reactive oxygen species
RTK	Receptor tyrosine kinases
Rubicon	RUN domain protein as Beclin 1-interacting and cysteine-rich containing
S6K1	Ribosomal protein S6 kinase beta-1
SLC38A9	Human member 9 of the solute carrier family 38
TBC1D7	TBC1 Domain Family Member 7
TBK1	TANK-binding kinase 1
TCA	Tricarboxylic acid cycle
TKI	Tyrosine kinase inhibitors
TMZ	Temozolomide
TNBC	Triple negative breast cancer
Tom20	Translocase of outer membrane 20
TSC	Tuberous sclerosis complex
Ub	Ubiquitin
UBA	Ubiquitin binding domain
ULK1	Unc-51-like kinase 1
UVRAG	UV radiation resistance-associated gene protein
v-ATPase	Vacuolar-type H+ ATPase
VCAM1	Vascular cell adhesion molecule-1
VEGF	Vascular endothelial growth factor
VPS34	Vacuolar protein sorting-associated protein 34
WIPI	WD-repeat protein interacting with phosphoinositides

ABSTRACT

There is huge potential for targeting pro-survival autophagy as a cancer therapeutic strategy, but this approach has not yet been fully realised due to the complex involvement of autophagy for cancer biology. In early stages of transformation, autophagy acts as a tumour suppressor, whilst in a developed tumour, autophagy aids cancer cell survival contributing to resistance. This thesis aimed to interrogate the role of autophagy for survival in metastatic breast cancer using the 4T1 mouse mammary carcinoma model. Investigations utilised the autophagy-lysosomal inhibitor Chloroquine (CQ) since this compound is currently in clinical trials for a variety of blood and solid cancers, including breast cancer. Here, the mechanisms of CQ and furthermore, the potential of combining this drug with metabolic targeting strategies were investigated.

In doing this, an unexpected resistance mechanism linking glucose metabolism and CQ was uncovered. In clonogenic assays, CQ induced cell death that cooperated with other therapeutic stressors such as ionising irradiation and PI3K-Akt inhibition. CQ and the metabolic stress of serum starvation produced cell death within 24hrs; however, unexpectedly, further glucose starvation or hexokinase inhibition fully rescued cell viability. The cytotoxic effects of CQ were found to be autophagy-independent as knockdown of ATG proteins did not mimic CQ. As the form of cell death in our model did not resemble classical caspase-dependent apoptosis or necrosis, it was hypothesised the cytotoxic effects of CQ were potentially triggering lysosome membrane permeabilisation. Indeed, CQ treatment did lead to marked lysosomal stress and enlargement, suggestive of LMP. In contrast, while CQ was still able to enter and deacidify the lysosome in glucose starved cells, it failed to induce enlargement.

Our data indicate that glucose metabolic rate has a profound influence on the efficacy of CQ to target lysosomes and to induce LMP-mediated death. These effects may be reducing clinical outcomes of CQ in cancer cells with reduced glucose metabolism.

Chapter 1

Introduction

1.1 CANCER

Cancer is considered a group of diseases characterised by unregulated cell growth and the spread of rogue cells from the site of origin to invade distant sites in the body (Pecorino, 2008). Cancer and associated diseases are estimated to affect up to 2.5 million people in the UK, with this figure expected to rise to 4 million by 2030 (Maddams et al., 2012). Strikingly, predictions are that by 2020, almost half of the population (47%) will be diagnosed with cancer during their lifetime (MacmillanCancerSupport, 2013).

Despite the collective term of cancer encompassing over 200 different subtypes, more than half of cases are attributed to just 4 specific forms of cancer. The latest available statistics provided by Cancer Research UK show these to be breast (15%), prostate (13%), lung (13%), and bowel (12%) cancers. The high incidence rate of cancers, in particular the most common forms, is mirrored by the mortality rates. Indeed, cancer accounts for more than a quarter of deaths (2011, UK), and statistics show the majority of these deaths (46%) are attributed to breast, prostate, lung and bowel carcinomas. While treatment options for cancer and in turn the mortality rate have improved dramatically over the past few decades, there is still a clear clinical gap for more effective therapies. The basis for the development of these therapies is knowledge of the dis-regulated biology driving tumorigenesis and maintenance of oncogenic cells.

1.1.i The biological hallmarks of cancer cells

Cancer tumorigenesis is often regarded as a multi-step process, arising from genetic alterations (mutations), leading to a normal human cell transforming into a malignant cancer cell with uncontrolled replication (Pecorino, 2008). However, while the genetic changes between cancer phenotypes may differ, six common key biological features underpinning cancer development and progression were seminally outlined by Hanahan and Weinberg (Hanahan and Weinberg, 2000), and further explored in a more recent revision of this review (Hanahan and Weinberg, 2011) These have been defined as: (1) unregulated proliferation independent of growth signals; (2) insensitivity to anti-growth signals; (3) evasion of apoptosis; (4) unlimited replicative potential; (5) sustained angiogenesis; and (6) tissue invasion and metastasis. These

key hallmarks are outlined in **Figure 1.1**; highlighted are some of the key events, drivers, and signalling pathways discussed in each section. Since these fundamental biological pathways are modelled to drive disease in patients, many current cancer therapeutics strategies target one or more of these key pillars, as summarised below. As this thesis is ultimately interested in identifying strategies to target cancer cells, the rationale for experiments presented were built on a foundation of cancer cell biology.

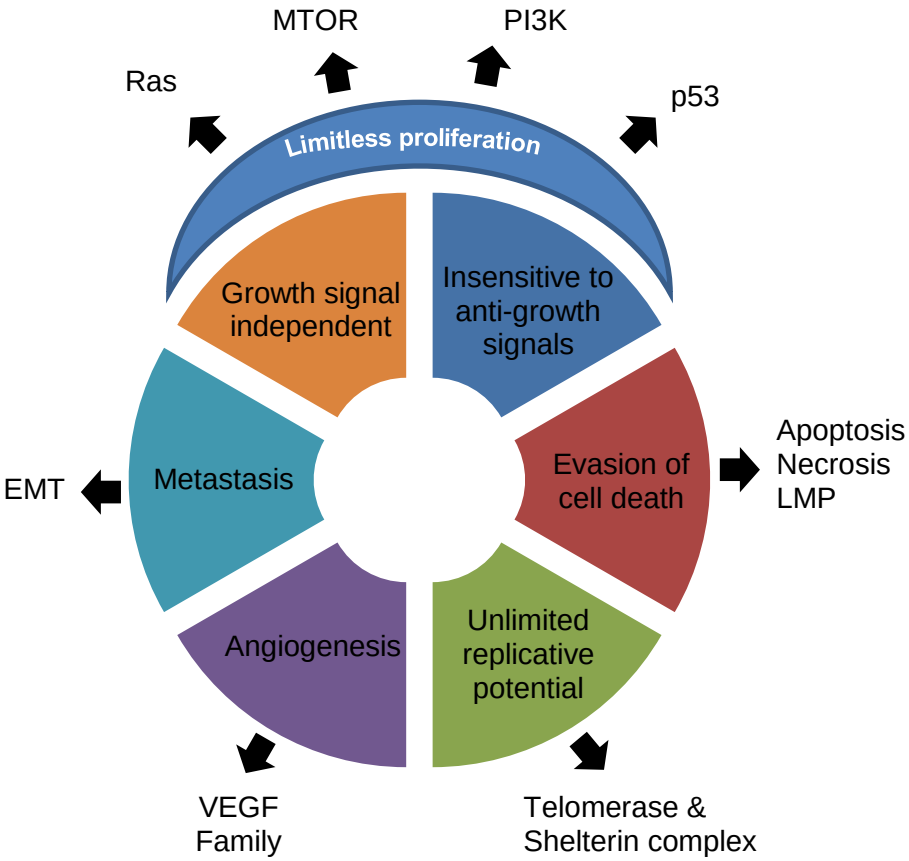

Fig 1.1. Critical 6 hallmarks of cancer proposed by Hanahan and Weinberg. The 6 essential hallmarks of cancer are outlined here. These include growth signal independence and insensitivity to anti-growth signals, which together lead to limitless proliferation capabilities. Further biological hallmarks proposed were evasion of cell death, unlimited replicative potential, angiogenesis, and metastasis. We have highlighted with arrows the key related events in each biological hallmark that contribute to the pathogenesis of cancers and which will be discussed in this section.

Limitless proliferation capabilities of cancer

Normal cells require external growth factor signals to divide, whereas cancer cells can grow independently of these signals. It has been shown that cancer cells acquire the ability to short-circuit growth factor pathways via mutations. For instance, there may be a change in sensitivity to growth signals via receptor up-regulation, allowing cells to proliferate in response to just basal levels of growth factor. Other mechanisms of growth signal autonomy include mutations within growth factor signal transducers or receptors leading to constitutive activation of proliferative pathways. In the alternate vein, cancer cells may also render themselves insensitive to anti-growth signals, thereby maintaining themselves in a proliferative state. Normal cells are not actively dividing and are maintained in this state via exit of the cell cycle. Thus, when mutations occur within essential checkpoint proteins of the cell cycle, cancer cells are able to evade the safety check and sustain their proliferate state.

The diversity of mutations in different cancer phenotypes is vast. However, there are certain frequently mutated proteins which play a role in driving oncogenic proliferation across multiple cancer types. In a mutational analysis of 12 major cancers, the most frequently mutated gene across the pan-cancer cohort was *TP53* (42% of cancers). The respective protein encoded by this gene, p53, has a dual role in cell cycle regulation and apoptosis. Therefore, inactivating mutations of *TP53* can drive unregulated proliferation. Similarly, many of the genes most frequently mutated across all cancers analysed were those with a role in activating proliferative signalling, for example *PI3KCA* (17.8%), *PTEN* (9.7%), *KRAS* (6.7%), and *MTOR* (3%) (Kandoth et al., 2013). The high incidence of mutations in these proteins makes them highly attractive drug targets in the development of new cancer therapeutics.

Interestingly both PI3KCA and Phosphatase and tensin homolog (PTEN) are involved in the phosphoinositide 3-kinase (PI3K) signalling axis (Maehama and Dixon, 1998, Stambolic et al., 1998), suggesting dis-regulation of this pathway has a particularly strong role during oncogenesis. Positioned downstream of both receptor tyrosine kinases (RTK) and G-protein coupled receptors (GPCR), the PI3K lipid kinases act as major downstream effector pathway in regulating multiple cellular processes, including proliferation. While there are three classes of PI3K, it is Class I

enzymes that are the best characterised. The Class IA heterodimer consists of two components, the p110 catalytic subunit and a p85 regulatory subunit (Carpenter et al., 1990). Upon receptor activation, PI3K is recruited to the plasma membrane, where activated p110 is able to generate phosphatidylinositol (3,4,5)-trisphosphate (PIP_3). This membrane lipid acts to recruit and bind AKT at the plasma membrane, shifting AKT conformation and allowing subsequent activation (T308) by phosphoinositide dependent kinase 1 (PDK1) (Alessi et al., 1997, Andjelkovic et al., 1997).

Activating mutations in the p110α catalytic subunit (protein encoded for by PI3KCA gene) have been identified in a range of cancers from colorectal to lung (Samuels et al., 2004). These mutant proteins were shown to express increased kinase activity, and enhanced downstream activation of the PI3K target proteins such as AKT. Furthermore, colorectal cancer cells expressing these mutants could proliferate independently of growth factor signals (Samuels et al., 2005). PI3KCA mutant driven proliferation has been further confirmed in a variety of cancers including cervical (Ma et al., 2000), breast (Isakoff et al., 2005), and tongue (Chen et al., 2011b). While p110α is a catalytic driver of the PI3K pathway, PTEN acts as tumour suppressor, negatively regulating the PI3K proliferative pathway. PTEN is a lipid phosphatase, supressing the PI3K pathway by converting PIP_3 to PIP_2, and thus reducing the cellular levels of PIP_3 present to continually activate downstream components of the pathway. Because of the nature of this growth-supressing role it is unsurprising that the majority of oncogenic mutations within this protein are loss-of-function (Li et al., 1997, Steck et al., 1997). Again, this protein has been shown to be frequently mutated in a broad range of cancers. Despite the numerous mutations affecting the PI3K signalling axis, to date only one therapeutic compound (Idelalisib) targeting this pathway has been approved by the FDA, although many other drugs are being examined in Phase I/II clinical trials (Furman et al., 2014). However, many alternate strategies targeting cancer growth are aiming to target other oncogenes frequently mutated such as Ras (derived from Rat Sarcoma virus) and mTOR.

The Ras pro-oncogenic GTPases are encoded by three distinct genes: *HRAS*, *NRAS*, and *KRAS*; and similar to PI3K, these sit downstream of RTKs. Upon receptor activation, initial downstream signalling events at the plasma membrane are activated including the assembly of guanine nucleotide exchange complexes to transform inactive GDP-bound Ras to active GTP-bound Ras. Activated Ras in turn

triggers as one main effector pathway the Raf-MEK-ERK (MAPK) cascade (Santarpia et al., 2012). One of the key responses of this pathway is the nuclear translocation of ERK to drive phosphorylation and mediate the degradation of transcription factors involved in tumour suppression and cell cycle regulation, such as those in the Forkhead Box O (FOXO) family. For example, ERK-mediated phosphorylation of the tumour suppressive FOXO3a transcription factor at several serine residues has been shown to enhance its degradation through interaction with MDM2, an E3 ubiquitin-protein ligase (Yang et al., 2008). Therefore, degradation of such transcription factors via aberrantly activated Ras-MAPK signalling can lead to unregulated cell proliferation in cancer cells. Indeed, transforming mutations in the Ras family (H-Ras, K-Ras, and N-Ras) were originally identified in human cancer more than 30 years ago (Chang et al., 1982, Parada et al., 1982, Santos et al., 1982, Taparowsky et al., 1983). Although isoform specific mutations amongst certain cancers have been noted, a recent catalogue of somatic mutations in cancer (COSMIC) study showed that of the 3 Ras genes it was K-Ras that was mutated most frequently (Forbes et al., 2011). This could highlight K-Ras as an important therapeutic target for a variety of cancer phenotypes, especially with respect to inhibition of oncogenic proliferation.

Similar to Ras proteins, there is also a high frequency of *MTOR* mutations across multiple cancer types (Sato et al., 2010, Murugan et al., 2013, Grabiner et al., 2014). Mechanistic target of rapamycin (mTOR) is the catalytic kinase subunit of two individual protein complexes, mTORC1 and mTORC2, although the first of these complexes is more well-defined in its biological roles. While multiple functions and interactions of mTORC1 have been identified, mTORC1 initially was best understood and appreciated for its role in protein synthesis, thus explaining why gain-of-function mutations in mTOR can drive unregulated proliferation. In this primary mechanism, active mTORC1 directly phosphorylates key translational regulatory factors, such as eukaryotic translation initiation factor 4E binding protein (4E-BP1) and S6 kinase 1 (S6K1) to drive mRNA transcription and translation (Ma and Blenis, 2009). It is important to note that MTORC1 closely interacts and cross-talks with other essential proliferative signalling pathways. The mTORC1 pathway can receive signals downstream of the PI3K-Akt and Ras-MAPK cascades, which indicates the potential for oncogenic mutations within these axes to also drive aberrant activation of the mTOR pathway (Manning et al., 2002, Inoki et al., 2002, Carriere et al., 2008). As such, mTOR inhibition has had been long-standing

strategy for cancer therapy; two compounds, everolimus and temsirolimus (which are derivatives of rapamycin), have already received FDA- and EMA-approval for a variety of cancers (Pazdur, 2013a, Pazdur, 2013b).

Importantly, while the PI3K signalling axis, Ras GTPases, and mTOR complexes are strongly implicated in oncogenic proliferation, they are also tightly linked to autophagy regulation. This catabolic process is itself described to play a role in both cancer cell survival and tumorigenesis. Autophagy and its regulation by nutrient sensing and mTORC1 will be explored further in later sections of this chapter.

Evasion of cell death

Perhaps one of the most important hallmarks of cancers is their ability to evade cell death and apoptosis. Apoptosis programmed cell death is typically characterised by DNA fragmentation, chromatin condensation, and blebbing of the plasma membrane. Through activation of apoptosis, a dying cell causes minimal damage to its surrounding environment. For example, when a normal human cell suffers DNA damage, it is typically programmed to die via apoptosis. However, many cancer cells have the ability to elude this process. This can be attributed to the apparent imbalance between pro-apoptotic and anti-apoptotic proteins and the corresponding signals in cancer cells. Many cancer cells have a clear down-regulation or mutation in the pro-apoptotic protein p53 (as in (Kandoth et al., 2013).

As mentioned earlier, p53 plays a role in proliferation by controlling the transcription of cell cycle proteins. However, p53 is also known to have a key role during the initiation of apoptosis. Activation of p53 can be triggered by numerous events, but a key driver in cancer cells is DNA damage, such as that which occurs in response to radiation or anti-cancer therapies. DNA damage typically triggers activation of cell cycle checkpoint proteins, such as ataxia telangiectasia mutated (ATM), which phosphorylate p53. This phosphorylation event has a dual role in preventing p53-MDM2 (Mouse double minute 2 homolog) interaction, an interaction which normally leads to p53 ubiquitination and degradation (Cheng and Chen, 2010). As such ATM leads to stabilisation of p53 and activation of downstream signalling. If the DNA damage is extensive and non-repairable, activated p53 goes on to trigger apoptosis.

Indeed, a role for p53 in apoptosis induction was first noted in 1991 (Yonishrouach et al., 1991), where expression of wild-type p53 in myeloid leukaemia cells led to a

reduction in cell viability and clear biological hallmarks of apoptosis (e.g. fragmented nuclei and chromatin condensation). Further work has shown p53 primarily initiates apoptosis through transcriptional up-regulation of pro-apoptotic proteins such as BCL2-Associated X protein (Bax) (Miyashita and Reed, 1995) and p53 upregulated modulator of apoptosis (PUMA) (Nakano and Vousden, 2001), or down-regulation of anti-apoptotic proteins such as B-Cell CLL/Lymphoma 2 (Bcl-2) (Wu et al., 2001). In addition to this primary role, a small fraction of p53 can localise to mitochondria and directly interact with and antagonise anti-apoptotic protein Bcl-2 (Tomita et al., 2006). Alternatively, it has also been reported that cytosolic p53 can activate Bax, via a transcription-independent mechanism, to trigger the apoptosis cascade (Chipuk et al., 2003, Chipuk et al., 2004).

Activation of p53-driven apoptosis is important for the efficacy of many DNA damaging cancer therapies. When this pathway is compromised, through mutations and/or an imbalance in pro-apoptotic or anti-apoptotic signalling proteins, cancer cells are able to evade cell death. Multiple studies have shown a correlation between p53 mutation and chemotherapeutic resistance. For example, a study in ovarian cancer patients showed that p53 mutations were common (56% tumours), and more importantly that cisplatin or carboplatin resistance was frequent in patients with p53 alterations (Reles et al., 2001). Similarly, mutated or null p53 has been linked with chemotherapeutic resistance in non-small cell lung cancer (Rusch et al., 1995), leukaemias (Wattel et al., 1994), and breast cancer (Aas et al., 1996).

While evasion of apoptotic cell death is one of the key cancer hallmarks and is highly implicated in chemotherapy resistance, cancer cells are also susceptible to other forms of programmed cell death. Indeed, alternative p53-independent apoptosis has been identified, though the mechanisms defining these vary from caspase-2 mediated events (Sidi et al., 2008) to p73-mediated pathways (Gong et al., 1999, Irwin et al., 2000).

As explored in my experiments of chapter 5, necroptosis and lysosomal membrane permeabilisation (LMP) cell death pathways are also increasingly being investigated for their role in cancer biology. Indeed, crosstalk between the apoptotic and LMP signalling pathways has been frequently observed **(Fig. 1.2).** LMP is defined as the leakage of the lysosomal contents, in particular degradative proteases, into the cytosol to trigger controlled cell death (Boya and Kroemer, 2008). The key mediators of LMP cell death are the lysosomal cathepsin proteases, in particular Cathepsins B,

D, and L (Boya and Kroemer, 2008, Oberle et al., 2010). The leakage of the cathepsin proteases has been shown to induce secondary apoptotic signalling, such as activation of the apoptotic machinery not limited to but including mitochondria and the caspases (Boya et al., 2003, Droga-Mazovec et al., 2008, Conus et al., 2008). In turn, many of the same stimuli can activate both apoptosis and LMP, including reactive oxygen species (ROS) and p53, as highlighted in Fig 1.1 (Erdal et al., 2005, Li et al., 2007, Huai et al., 2013). Alternatively, lysosomotropic detergents and compounds have been identified to be potent inducers of LMP, such as the autophagy-lysosomal inhibitor Chloroquine (one focus of this thesis) (Seitz et al., 2013, Liang et al., 2015) and the lysosomal detergent, Leucyl-Leucyl-O-methyl ester (LLOME) (Aits et al., 2015b).

Nevertheless, targeting cancer cells ability to evade cell death, whether that is via apoptosis, LMP or necrosis is one of the key challenges of current cancer therapeutics.

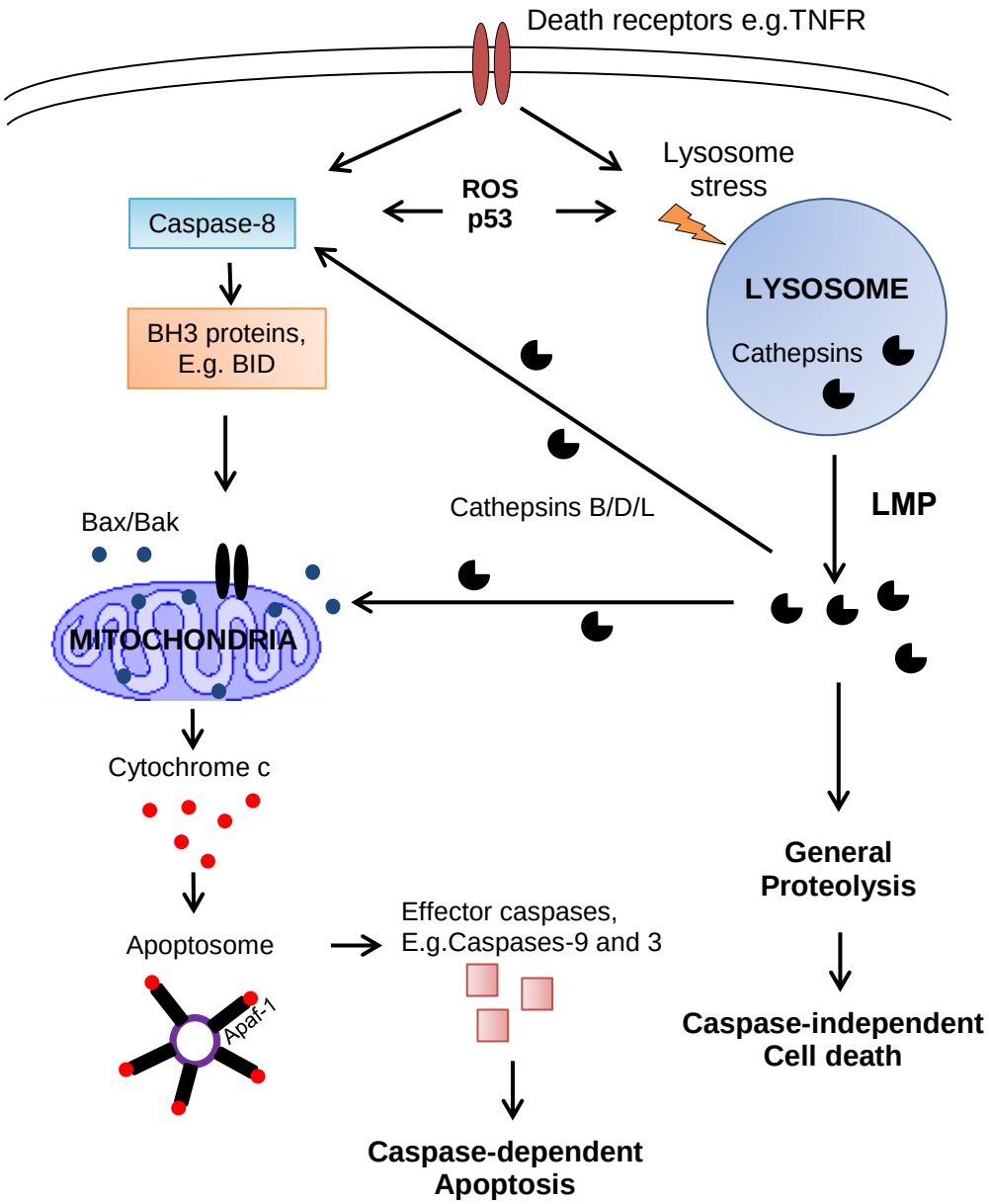

Fig. 1.2 The interplay between apoptosis and LMP. Various treatments have been identified to induce LMP including, ROS, p53, and more specific lysosomal stressors, such as lysosomotropic drugs. While LMP offers an alternative mode of cell death in cancer cells, numerous points of crosstalk between LMP and apoptosis have been defined. Cathepsins are key mediators of cleavage-dependent activation of pro-apoptotic proteins, such as caspase-8, Bax and Bak. Through apoptotic events downstream of mitochondrial cytochrome c release LMP can in turn induce secondary apoptotic events, as well as inducing cell death via LMP alone.

Unlimited replicative potential

One of the remarkable features of cancer cells is their seemingly limitless replicative potential in comparison to normal human cells. This continuous replicative potential has long been linked to cancer cells ability to maintain telomere DNA, repeated TTAGGG sequences that are located at the ends of chromosomes. Non-transformed cells display shortening of these chromosomal ends after each round of replication. This offers an inbuilt counting device which allows for a certain number of cell divisions (Hayflick limit) before a cell enters a state of senescence, where cells are still alive but stop growing. However, cancer cells are able to bypass senescence via upregulation of the enzyme telomerase, which stabilises or expands the length of the telomeres. Telomerase is a reverse transcriptase that is sufficient on its own to add new sections of DNA to the telomere ends. Importantly, early studies on telomerase expression in cancer biopsy samples identified 90% of tumours showed evidence of telomerase activity, whereas all normal non-cancerous tissue samples contain undetectable levels (Kim et al., 1994). Furthermore, introduction of the catalytic subunit of telomerase (hTERT) in combination with oncogenes was able to induce the conversion of normal human epithelial cells into cells with clear tumorigenic properties, such as anchorage-independent growth and the ability to form tumours in nude mice (Hahn et al., 1999).

In addition to telomerase, alternative mechanisms of telomere protection have been identified in cancer cells. The shelterin complex formed of 6 individual telomere-associated proteins, including telomere repeat factor-1 (TRF-2) and -2 (TRF-2) has been shown to protect the telomeres from degradation (Broccoli et al., 1997, Houghtaling et al., 2004, Ye et al., 2004). The basic mechanism of this shelterin complex involves the formation of t-loop structures in the DNA which prevents the DNA being targeted by DNA repair executioner proteins (Fouche et al., 2006, Amiard et al., 2007). Taken together, these mechanisms of telomere protection allow cancer cells to have unlimited replicative potential, promoting tumour growth.

Angiogenesis

As stated previously, the fifth hallmark of cancer is sustained angiogenesis. Whilst the other hallmarks of cancer described allow the formation of a malignant mass of tumour cells, angiogenesis occurs once a tumour has formed and is more a tumour-physiology feature of cancer rather than a cellular feature. Tumours notably contain

areas of severe hypoxia and in order for the residing cancer cells to receive nutrients and oxygen they must initiate angiogenesis - the formation of new blood vessels triggered by the angiogenic switch (i.e. a balance between angiogenic inducers and inhibitors) (Pecorino, 2008).

Angiogenesis is typically a multi-step process whereby pro-angiogenic factors secreted in the vicinity of the tumour site initiate a cascade of basement membrane degradation and extracellular matrix (ECM) remodelling. Endothelial cells (EC) become activated, displaying proliferation and migration, and finally, tube formation and stabilisation of EC in the context of newly formed aberrant tumour blood vessels. While multiple pro-angiogenic factors have been identified (TNFα, bFGF, EGF), vascular endothelial growth factor (VEGF) has been investigated most extensively. VEGF(-A) is a member of a family of structurally related proteins, including VEGF-B, VEGF-C, VEGF-D, and placental growth factor (PlGF). These factors mediate angiogenic events via binding to the receptor tyrosine kinases, VEGFR1 and VEGFR2 (Carmeliet, 2005). Upon binding to its receptor, VEGF triggers signalling pathways including PI3K and Ras-MAPK cascades, to drive proliferation and migration of vascular endothelial cells.

In addition to its roles in directly stimulating the proliferation of endothelial cells, VEGF has also been suggested to have a multi-faceted role in all stages of angiogenesis. VEGF has been shown to protect newly formed tumour vascular cells from apoptosis (Gerber et al., 1998, Nor et al., 1999) and mediate secretion of ECM degrading enzymes, for example matrix metalloproteinases (MMPs) (Unemori et al., 1992, Wang and Keiser, 1998), to promote continued angiogenic development. The upregulation of VEGF is common in hypoxic areas of a tumour. Indeed, hypoxia has been shown to regulate VEGF expression via HIF1α in multiple cancer settings (Forsythe et al., 1996, Horiuchi et al., 2002, Buchler et al., 2003). Furthermore, there is evidence suggesting that activation of oncogenes, for example K-Ras, can lead to increased expression of VEGF (Rak et al., 1995). Taking together the multiple drivers for VEGF transcription and activation in cancer, it is not surprising that serum and plasma levels of this angiogenic signal are elevated across a range of cancer phenotypes, including gastric cancer (Karayiannakis et al., 2002), and are often associated with a poor prognosis and metastatic disease (Gasparini, 2000, Ishigami et al., 1998).

Due to its potent role in initiating and sustaining angiogenesis, VEGF and its receptors have been implicated in neovascularisation of many solid tumours and as such the formation of metastases. The VEGF family has been an attractive target for anti-angiogenic therapies (Vasudev and Reynolds, 2014). The earliest of these to receive FDA approval was Bevacizumab (Avastin), a monoclonal antibody for VEGF-A that is licensed for use in a range of cancers from metastatic colorectal to non-small cell lung cancer. Since the approval of this anti-VEGF therapy in 2004, many more anti-angiogenic therapies have been developed and approved for use in patients. Sunitinib, used to treat patients with renal cell or gastrointestinal stromal tumours, is a small molecule RTK inhibitor that inhibits VEGFR1, 2 and 3, as well as a range of other RTKs such as PDGFR and c-kit. Alternatively, sorafenib, used for renal cell and hepatocellular carcinomas, is also a small molecule RTK inhibitor, affecting an overlapping profile of targets with sunitinib (Meadows and Hurwitz, 2012). It is notable however, that with the exception of Bevacizumab in severe cases of glioblastoma, these anti-angiogenic therapies are rarely given as single therapy, and rather are administered as part of a combinatory treatment strategy. This may be in part due to angiogenesis being a secondary later event in cancer progression and tumour sustenance rather than the cause of tumorigenesis and malignant transformation.

Metastasis

All of the above hallmarks of cancer are important for initiation and maintenance of a malignant tumour. However it is the final hallmark, the process of invasion and metastasis that is the major series of events leading to death from cancer. Although, the incidence of metastases may differ between cancer types, the most common sites for metastases are the lung, liver, brain, and bone. For example, secondary tumours in the liver account for around 25% of all solid organ metastases (Ahuja, 2007). Furthermore, the increased mortality rate upon metastases is reflected in the reduced median survival rates in patients with untreated brain metastases (Sawaya, 2001). In addition to reducing the survival time of a patient, metastases are also implicated in severe morbidities, such as bone metastases resulting in bone pain and hypercalcemia.

The biological event of metastasis is a multistep process (depicted in **Figure 1.3**) by which tumour cells disseminate from their primary site and migrate to form tumours

at secondary sites (Pecorino, 2008). In the first instance, this process involves the escape of neoplastic cells from the primary tumour followed by subsequent loss of cellular adhesion and increased motility. These metastatic tumour cells undergo intravasation into the vasculature, and must acquire the ability to survive whilst in transit in the circulation. When these cells reach an organ microenvironment, they begin the process of extravasation from the bloodstream to the secondary site, and finally, colonisation of the secondary site to form micro-metastases (Gupta and Massague, 2006).

Exactly how tumour cells choose secondary sites has been explored by the seed and soil theory. Originally posed by Paget in 1889, this theory postulated that tumour cell seeds grow only in the specific microenvironment of particular organs, the soil (Paget, 1989). For example, late stage breast cancer patients are frequently found to develop bone metastases. It is suggested that multiple subpopulations of tumour cells with alternate genetic profiles reside within the primary tumour, and certain tumour cells overexpressing a subset of specialised genes will have a higher propensity to metastasise to specific organ sites. Breast cancer cells over-expressing C-X-C chemokine receptor type 4 (CXCR4) are commonly found to metastasise to the bone (Kang et al., 2003); the ligand of this receptor, C-X-C Motif Chemokine Ligand 12 (CXCL12), is highly expressed by resident stromal cells in the bone niche (Muller et al., 2001). Alternatively, cell populations over-expressing genes such as the cell adhesion receptor, *VCAM1*, and the matrix metalloproteinase, *MMP2*, preferentially metastasised to the lungs (Minn et al., 2005).

Whilst the process of metastasis and sites of secondary tumours is now better understood, the mechanism of how they take the initial steps towards metastasis is comparatively unclear. It has been proposed that epithelial-mesenchymal transition (EMT) is intimately involved in driving metastasis. EMT is a programme by which epithelial cells lose cell-cell adhesion, and undergo a conversion from epithelial-like cells to cells with a mesenchymal morphology that possess enhanced migratory and invasive abilities (Heerboth et al., 2015). It is therefore suggested that EMT contributes to the dissociation of cancer cells from tumours originating from epithelial tissues (Hanahan and Weinberg, 2011). Initiation of the EMT process stems from the loss of expression of adhesion molecules regulating cell-cell attachment. E-cadherin is one such molecule that is frequently down-regulated prior

to EMT and reduction in E-cadherin is associated with increased invasiveness of tumour cells (Onder et al., 2008).

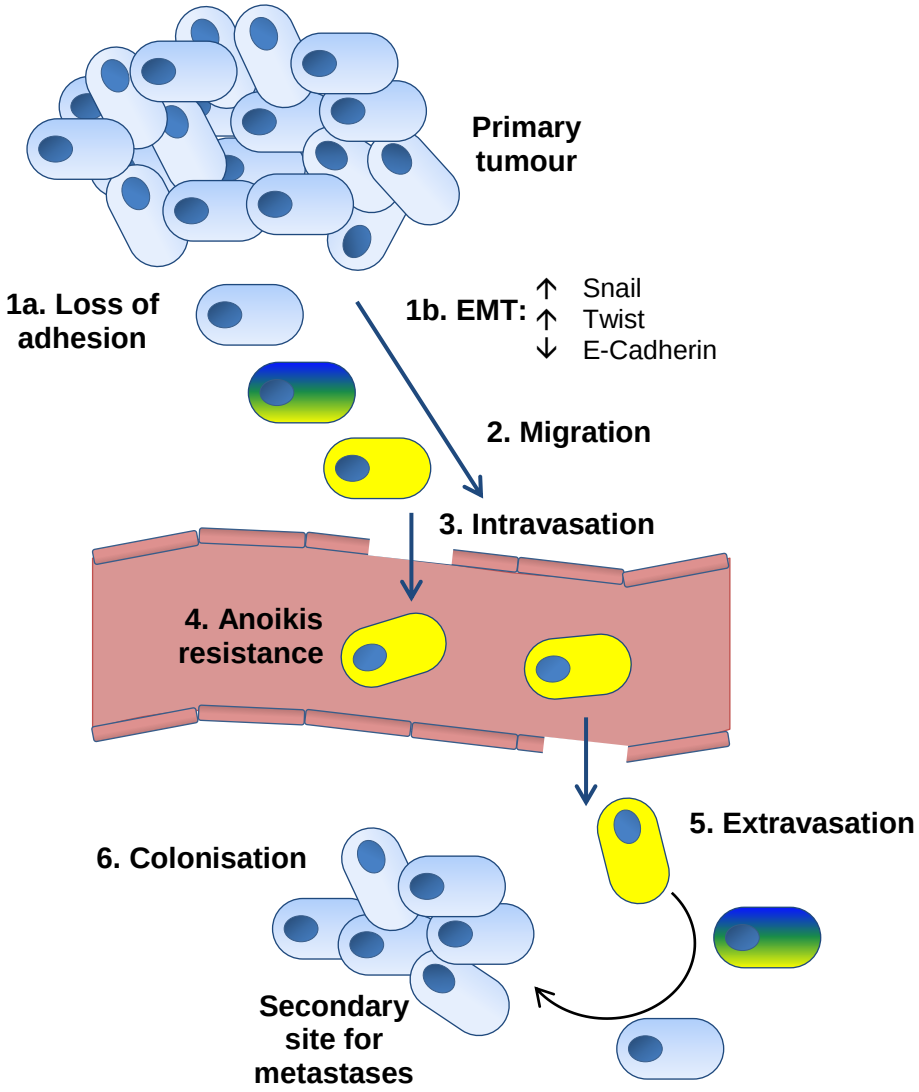

Fig 1.3. Epithelial mesenchymal transition (EMT) and the metastatic process. The metastatic process is key in the pathogenesis of aggressive cancer phenotype. It is typically described as a multistep process characterised by (1) Loss of adhesion within the primary tumour, as such a key driver for this event is EMT, (2) Increased motility and migration, (3) Intravasation into the local circulating blood supply, (4) Cell survival while in transit, (5) Extravasation to the secondary site (often termed a niche or 'soil'), (6) Colonisation and formation of distant metastases.

Similarly, transcription factors such as Snail and Twist have also been implicated in the progression of EMT. Snail has been shown to directly down-regulate E-cadherin expression (Batlle et al., 2000), as wells as repressing other key genes involved in cell adhesion such as claudins (Ikenouchi et al., 2003). Furthermore, it has been shown in multiple studies that snail increases the invasive capacity of cancer cells; prostate cancer cell lines with over-expression of Snail exhibited increased cell invasion. Conversely, shRNA against Snail decreased the invasiveness of these cell lines (Osorio et al., 2016). Furthermore, Snail inhibition in breast cancer cells (MCF-7) reduced invasive capabilities in both 2D and 3D assays (Vistain et al., 2015). Thus, snail can be inextricably linked to an invasive metastatic cancer phenotype. The transcription factor, Twist, has also been shown to contribute to EMT and this has been linked with breast cancer metastasis. Suppression of Twist in highly metastatic breast cancer cells inhibited metastasis from the breast to the lung. Similarly, in human breast tissue samples, high expression of Twist correlated with a more invasive metastatic cancer phenotype (Yang et al., 2004a). Therefore a large body of work has shown there is a direct link between EMT and metastasis, and furthermore, this has been observed in multiple cancer phenotypes including breast cancer, the cancer type which is the focus of this thesis.

1.1.ii Breast cancer

Breast cancer is one of the four most common cancers in the UK; in fact it is the most common cancer accounting for 15% of new cancer diagnoses. Furthermore, it is estimated that 1 in 8 women will be diagnosed with breast cancer during their lifetime, although diagnosis is more common in women over 65 (46% of cases). Although breast cancer has the highest incidence in the UK, breast cancer therapy has vastly improved with 78% of patients now surviving for 10 or more years; improvements in treatment and the development of awareness campaigns have seen death rates due to breast cancer fall by 40% since the mid-80s (Statistics from (CancerResearchUK, 2013). However, while survival rates for women diagnosed at the early stages of breast cancer are favourable, late diagnosis is still a major clinical problem with only 15% of women expected to survive beyond 5 years when diagnosed with stage IV cancer. The lack of effective treatment at this stage is

largely due to the formation of metastases. In addition, there are also still major clinical barriers to overcome in relation to recurrent and resistant breast cancers.

In this thesis, we are investigating the effects of a catabolic process, autophagy, in metastatic breast cancer. Indeed, autophagy has been shown to facilitate the development of chemotherapeutic-resistant breast cancer phenotypes. It has been implicated in resistance to the Human epidermal growth factor receptor-2 (HER-2) monoclonal antibody trastuzumab (Herceptin) (Vazquez-Martin et al., 2009), anti-estrogen drugs such as Tamoxifen (Schoenlein et al., 2009), and anthracyclines such as epirubicin (Sun et al., 2011). Based on these outcomes, targeting autophagy is increasingly being investigated as a therapeutic option for many solid tumours, including those originating in breast tissue. The biology underlying this catabolic process and its implications in cancer are described further in section 1.2 and 1.3.

1.2 AUTOPHAGY

Autophagy is the conserved cellular process whereby damaged organelles and cellular proteins are sequestered in double membrane vesicles, known as autophagosomes, and targeted to the lysosomes for degradation. The term autophagy was coined in 1963 by de Duve when he used it to describe the presence of vesicles containing degraded cellular proteins and organelles (Yang and Klionsky, 2010). Since this discovery, three main types of autophagy have been noted: micro-autophagy, macro-autophagy and chaperone-mediated autophagy (CMA). In micro-autophagy cellular components are sequestered in a specific or non-specific manner directly by the lysosomes. CMA only degrades soluble proteins and requires the unfolded proteins to be directly translocated across the lysosome membrane via chaperone proteins (heat shock protein 70 (hsc70)) and membrane receptors (Lysosome-associated membrane proteins (LAMP)). During macro-autophagy (referred to as autophagy for the remainder of the thesis), cellular components are sequestered in a double-membrane cytosolic vesicle, termed the autophagosome. The autophagosomes fuse with lysosomes or endosomes, after which the inner membrane and contents are broken down and released back into the cytosol through membrane permeases (Mizushima et al., 2008, Xie and Klionsky, 2007).

1.2.i The regulation of autophagy by autophagy-related proteins

The activation and formation of the autophagosome is reliant on key **A**u**t**opha**g**y-related signalling proteins (Atg proteins), which are differentially expressed over the 3 stages of autophagosome formation -- initiation, nucleation, and elongation and closure -- as outlined in **Fig 1.4**.

Autophagosomes originate from phagophores (or isolation membranes (IM)), which are currently understood to be membrane structure assembly sites derived from the endoplasmic reticulum (ER) or other membrane sources such as the mitochondria, the Golgi, the plasma membrane and recycling endosomes (Ravikumar et al., 2010, Longatti et al., 2012, Puri et al., 2013, Axe et al., 2008, Hailey et al., 2010). Despite the identification of multiple membrane sources, the general model of isolation membrane formation centres on the ER. Early studies noted an association between ER membranes and autophagosomes in starved hepatocytes (Dunn, 1990). Further

evolution of studies using fluorescent tagged autophagy constructs has led to mechanistic insights of isolation membrane formation being elucidated. A notable event is the recruitment of the omegasome marker double FYVE domain-containing protein1 (DFCP1) to phosphatidylinositol 3-phosphate (PI3P)-enriched phagophore (cradle) assemblies localised to the ER (Axe et al., 2008). The omegasome is a compartment within the cell specific to autophagosome biogenesis. However the function of DFCP1 is still unknown as inhibiting its expression does not inhibit autophagy (Axe et al., 2008). Further work has supported the hypothesis of specific IM formation sites; termed the 'cradle model', it has been observed that cup-shaped regions of the ER membrane provide structural support to forming IMs (Hayashi-Nishino et al., 2009). In addition, ER linked $DFCP1^{+}$ tubular membrane structures, IM-associated tubules (IMATs), have recently been identified to join the edges of the IM, providing further support to the forming autophagosome (Uemura et al., 2014). Indeed, IMAT formation was abrogated in MEFs with a ULK1 complex deficiency, but was still present in MEFs with defects in the autophagy conjugation pathways (described later). This data supports a model in which IM formation occurs proximal to cradle-shaped omegasome sites, and the ULK1 complex is necessary for membrane assembly.

As adhered to above, in mammalian cells autophagosome initiation and autophagy induction relies on activation of the unc-51-like kinase 1 (ULK1) complex (Ganley et al., 2009, Hosokawa et al., 2009a, Chan et al., 2009). This consists of the serine/threonine protein kinase ULK1 (or related family member ULK2), ATG13, focal adhesion kinase family interacting protein of 200kDa (FIP200) (Hara et al., 2008) and ATG101 (Hosokawa et al., 2009b, Mercer et al., 2009).

The ULK1/2 complex integrates signals from the master nutrient sensors, mechanistic target of rapamycin complex (mTORC1) and 5'AMP-activated protein kinase (AMPK), and transmits information to the downstream autophagic machinery. In nutrient rich conditions, mTORC1 directly associates with the ULK1 complex via the raptor subunit (Hosokawa et al., 2009a). In the current predominant model, associated mTORC1 mediates phosphorylation of ATG13 and ULK1 at the Ser^{757} site leading to a potent inhibition of ULK1 kinase activity (Kim et al., 2011). In contrast, during amino acid starvation, mTORC1 dissociates from the ULK1/2 leading to the auto-phosphorylation of ULK1/2 possibly at Thr180 in the ULK kinase activation loop (Bach et al., 2011). Following this activation ULK1 phosphorylates

ATG13 (Ser318) and FIP200 at sites not completely understood (Joo et al., 2011, Jung et al., 2009) To this date over 30 phosphorylation sites have been identified on ULK1 indicative of an important role for the function of the protein.

The ULK1 complex is poised as the primary initiating protein kinase of the autophagy cascade. An essential interaction is that of ULK1 and Beclin1; under amino acid starvation ULK1 has been shown to phosphorylate Beclin-1 on Ser14, and in turn enhances activity of the autophagic Beclin1 complex (Russell et al., 2013). This is a key step in the initiation and nucleation of autophagosomes. Importantly, DFCP1 localisation to omegasome sites is driven by PI3P, the formation of which is dependent on activation of VPS34. This requires the functional interaction of Beclin 1 with ATG14L and p150 in an autophagosome formation-specific PI3K complex to activate VPS34 at the membrane formation sites (Itakura et al., 2008, Russell et al., 2013). It is interesting to note, that multiple Beclin-1 complexes have been identified with differential roles in autophagy activation. While ATG14L complexes were shown to drive autophagosome formation, complexes containing UV radiation resistance-associated gene protein (UVRAG), RUN domain protein as Beclin 1-interacting and cysteine-rich containing (Rubicon) and Autophagy And Beclin 1 Regulator 1 (Ambra1) were shown to regulate autophagosome trafficking (Zhong et al., 2009). This differential interaction places ATG14L as a key effector in IM initiation and nucleation. Indeed, under starvation conditions preventing ATG14L translocation to ER membranes abrogated omegasome formation (Matsunaga et al., 2010). Furthermore, ATG14L has been shown to contain a conserved region which binds to PI3P (Fan et al., 2011), thereby ATG14L also has an essential role in anchoring the Beclin-1 complex at the forming autophagosome.

Anchoring of this complex at the autophagosome initiation site generates an abundance of PI3P, which not only aids in membrane initiation through recruitment of DFCP1 but also recruits other effector proteins that aid in expansion of the IM. These include members of the WD-repeat protein interacting with phosphoinositides (WIPI) family to the phagophore (Itakura and Mizushima, 2010). Indeed, WIPI2 has been identified to connect membrane initiation events with the autophagic conjugate, ATG5-ATG12-ATG16L, and consequently elongation and closure of the autophagosome. Here, a direct binding interaction was observed between WIPI2b

and ATG16L, which aided in recruiting the ATG16L conjugate to initiation membranes (Dooley et al., 2014).

The importance of this step is recognised in the cross over between the two conjugation systems required for autophagosome elongation and closure. In making the ATG12-ATG5-ATG16L conjugate, first ATG12 is made in a C-terminal glycine exposed form, which is activated by the E1 enzyme (ATG7) and transferred to the E2 enzyme (ATG10) (Mizushima et al., 1998). This enables ATG12 to form a conjugate with ATG5, which further interacts with ATG16L1 to broaden the complex. The ATG12-ATG5 portion of this complex is necessary for the second conjugation system, which ultimately leads to the formation of light chain 3-II (LC3-II). ATG12-ATG5 has been shown to directly bind LC3 (ATG8) and stimulate the E2 enzyme, ATG3, thus promoting its lipidation to LC3-II (or LC3-PE) (Fujita et al., 2008, Sakoh-Nakatogawa et al., 2013).

While formation of the autophagosome involves this step-wise series of initiation, nucleation and elongation events at ER membranes, further defined ER exit sites (ERES) have also been shown to play a role in elongation of the autophagosome (Zoppino et al., 2010). These ER specific sites are the centre for protein sorting into coat protein complex-II (COP-II) vesicles and Golgi trafficking (Brandizzi and Barlowe, 2013). However, recent studies of autophagy have now revealed a separate membrane structure receiving ERES vesicles, the ER-Golgi intermediate compartment (ERGIC), to be important in elongation and maturation of autophagosomes (Ge et al., 2013). Using cell-free studies, membranes isolated from ERGIC fractions displayed an abundance of LC3 lipidation activity, whilst those from mitochondria-associated membranes (MAMs) did not. In addition, the production of COP-II vesicles containing the LC3 lipidating machinery has been demonstrated to be intimately dependent to PI3P (Ge et al., 2014). Taken together, the current model proposes that Beclin1-ATG14L-VPS34 complexes associate with IM formation sites (forming PI3P), which consequently mature into membranes associated with ERES and ERGIC. However, it has alternatively been proposed that Beclin1-ATG14L-VPS34 localises with COP-II vesicles whilst being trafficked to ERGIC, and current data has failed to discriminate between either of these models. An important development in this field has now demonstrated ATG13 (part of the ULK1 complex) to directly associate with isolated components of ERGIC, suggesting further interplay between autophagy, ULK1 and ERGIC (Karanasios et al., 2016).

In addition to the autophagy specific proteins localising to forming autophagosomes, less specific cargo and adaptor proteins are also recruited, including p62. Through recognition of damaged or aggregated proteins marked with ubiquitin (Ub), a 76 amino acid residue globular protein, p62 was the first protein shown to have an ubiquitin-mediated adaptor function in autophagy (Pankiv et al., 2007). P62 contains both a C-terminal ubiquitin-binding domain (UBA) (Ciani et al., 2003) and a LC3-interacting region (LIR) (Pankiv et al., 2007, Ichimura et al., 2008). It has been reported that under proteasome inhibition ULK1 kinase can phosphorylate Ser407 in the p62 UBA. This was subsequently shown to destabilise the UBA dimer interface, allowing further phosphorylation of the UBA domain by kinases such as casein kinase 2 (CK2) or TANK-binding kinase 1 (TBK1) (Lim et al., 2015, Matsumoto et al., 2011, Pilli et al., 2012, Ro et al., 2014). This series of events acted to increase the affinity of p62 for ubiquitin, making it an efficient Ub-receptor and adaptor protein. Indeed, p62 knockout in both mice and *Drosophila* has shown p62 to play an essential role in ubiquitinylated protein aggregation and the autophagic clearance of these aggregates (Nezis et al., 2008, Bartlett et al., 2011). Separately, the interaction between p62 and LC3 via the LIR domain has been shown to be necessary for p62 autophagic degradation, but it was not required for p62 translocation to autophagosome formation sites (Itakura and Mizushima, 2011). This could suggest that upstream factors such as ULK1, which has been identified to directly interact with p62, recruit p62 to the autophagosome formation site prior to membrane formation. Whether this is the case or not, p62 remains an important autophagic marker, as increased levels of p62 are routinely observed during autophagy inhibition.

The mechanisms behind the formation of the autophagosome and thus activation of autophagy are important as they allow us to pinpoint key molecular targets for silencing or inhibiting autophagy, as well as detecting the activation of autophagy experimentally.

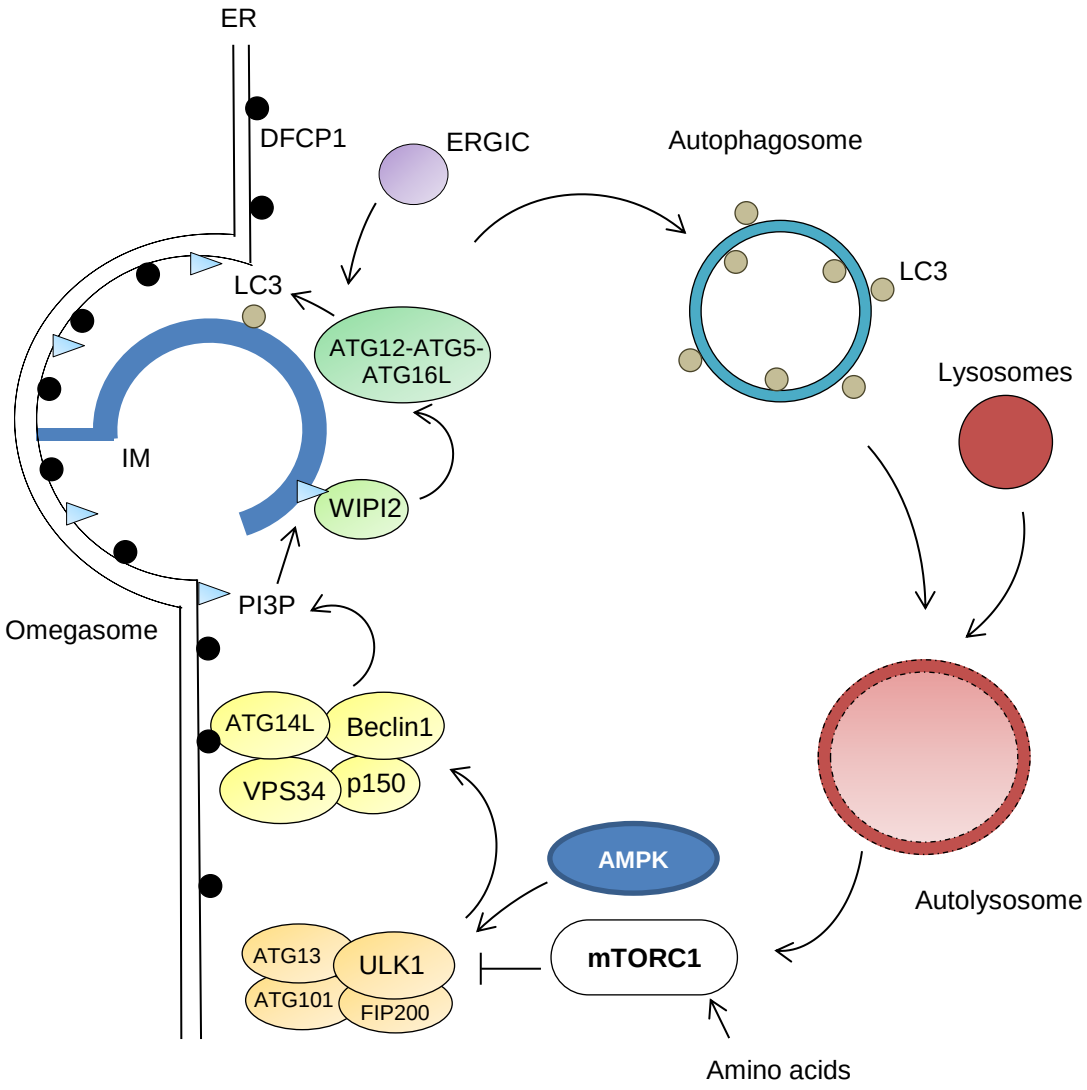

Fig 1.4. Key autophagy signalling events and formation of the autophagosome. Autophagosome membrane initiation is driven by the key initiator ULK1 complex, whose activity ultimately lies under the control of the master nutrient regulators, mTORC1 and AMPK. Upon activation ULK1 drives a series of signalling events, recruiting Beclin1 complex to the isolation membrane formation site (omegasome lined with DFCP1). Beclin1 produces PI3P, which recruits further proteins required for nucleation and elongation of the membrane, namely WIPI2, ATG12-ATG5-ATG16L conjugate, and LC3. The LC3 lipidation activity has recently been shown to be linked to other ER-membrane compartments, such as ERGIC. Digestion of autophagosome contents occurs upon fusion with lysosomes and formation of the acidic autolysosome containing essential degradative proteases.

1.2.ii Nutrient regulation of autophagy

While autophagy can be activated in response to various stimuli, the canonical activation pathway linked to nutrient starvation is the best characterised (Codogno et al., 2012) and is one such focus of the research outlined in this thesis. This nutrient dependent canonical pathway is primarily driven by two kinases, mTORC1 and AMPK, both of which have phosphorylating activity upon ULK1, the essential initiator protein in autophagy activation. Autophagy regulation by both of these nutrient-dependent kinases will be discussed further here.

AMPK regulation of ULK1

The positive regulation of autophagy by AMPK has been substantiated by the mechanism directly linking interactions between AMPK and ULK1. Seminal work identified two serine sites (S317, S777) within the ULK1 protein that were directly phosphorylated by AMPK under glucose starvation (Kim et al., 2011). Further evidence in this model was that phosphorylation of S317 and S777 was abrogated in AMPK DKO cells and by the AMPK inhibitor, compound C. Furthermore, the phosphorylation of these specific serine sites was shown to be essential for the induction of autophagy in response to glucose starvation -- the induction of autophagy under glucose withdrawal was significantly reduced in ULK1S317/S777A mutant cells compared to wild-type. This showed that inhibition of AMPK-mediated phosphorylation of ULK1 was sufficient to block nutrient starvation induced autophagy. In addition, these modified-ULK1 cells which were less able to utilise autophagy, were also less able to resist glucose starvation-induced apoptosis. This work supported a clear role for AMPK in the activation of ULK1 kinase and in turn autophagy.

Interestingly, S317 and S777 are not the only AMPK-phosphorylation sites on ULK1 that have been identified. Additional sites (S467, S555, T574, and S637) were identified with functional roles for survival following nutrient stress and mitophagy (Egan et al., 2011). Originally identified using bioinformatics, these sites were confirmed as targets for AMPK using mass spectrometry and phospho-specific antibodies. For example, purified AMPK could induce S467 and S555 phosphorylation using *in vitro* assays. Treatment of cells with the AMP-mimetic, AICAR, led to p-S555 on endogenous ULK1. In assessing the biological outcome of these phosphorylation events, cells expressing an AMPK non-phosphorylatable

ULK1 mutant had severely accumulated p62 levels, defective mitophagy, and were unable to survive nutrient stress in culture.

Indeed, the role for S555 phosphorylation has been further examined with respect to mitophagy in more recent studies. Following hypoxia stress, p-S555 was required for directing ULK1 translocation to the mitochondria (Tian et al., 2015). In this study, it was shown that p-S317 and p-S555 increased upon hypoxia. Furthermore, a ULK1-S555A mutation significantly reduced the translocation of ULK1 to the mitochondria under hypoxic conditions. Importantly, ULK1 KO cells were unable to undergo mitophagy. Reconstitution with a phosphomimetic S555D mutant rescued the formation of autophagosomes directed toward mitochondria, whereas expression of the S555A mutant could not restore efficient mitophagy. These data implicated p-S555 is a key event in hypoxia-driven mitophagy, as well as that driven by nutrient stress.

Another suggested role for ULK1-S555 phosphorylation is to mediate the binding between 14-3-3 proteins and ULK1 kinase (Bach et al., 2011). A direct nutrient-dependent interaction between GST-14-3-3 and ULK1 was observed, with the strength of this interaction increasing with glucose or amino acid starvation. A positive role for AMPK was implicated in this interaction based on data showing that an AMPK simulating drug, A769662, or AMPK-activating drug, phenformin, further increased interaction. Using immuno-precipitation, this regulation was shown to be through direct AMPK-ULK1 binding. Thus, taking these studies into consideration, the current consensus behind AMPK regulation of autophagy is that it positively regulates ULK1 activation via phosphorylation of multiple serine/threonine sites to drive autophagy in response to nutrient stress, as indicated in **Fig 1.5**.

Intriguingly, while these studies depict a multi-faceted role for AMPK regulation of ULK1, AMPK has been shown to regulate other essential proteins involved in autophagy signalling. As described earlier, the class III PI3K (VPS34) promotes autophagosome formation and in turn autophagy induction. An intricate mechanism was also identified in which AMPK differentially regulated both non-autophagy VPS34 complexes (lacking autophagy adaptors ATG14L or UVRAG) and pro-autophagy VPS34 complexes (containing ATG14L or UVRAG) (Kim et al., 2013a). Upon glucose starvation, non-autophagy VPS34 complexes displayed decreased activity as measured by a lipid kinase assay, whereas pro-autophagy complexes

displayed increased activity. These events were attributed to AMPK mediated phosphorylation of Beclin 1 (S91/S94) and VPS34 (T163/S165) specifically in response to glucose starvation. Phosphorylation of Beclin1 was essential for the activation of the pro-autophagic complex containing ATG14L and in turn induction of autophagy. In contrast, VPS34 phosphorylation was required to inhibit non-autophagy complexes. The switch between whether AMPK phosphorylation mediated inhibition or activation of the complex was determined by the presence of ATG14L. The binding of ATG14L was proposed to make Beclin1 a better substrate for AMPK, thus leading to activation of the pro-autophagic VPS34 complexes.

The evidence together highlights how multiple mechanisms likely arise downstream of AMPK to mediate autophagy regulation. There is thus a level of cross-talk that is still not fully understood for the cell to integrate signals to Beclin 1, VPS34 and ULK1, which signal together in their own dedicated mechanisms. It is important to note the studies primarily used glucose starvation to drive AMPK-mediated ULK1 and VPS34 phosphorylation. However, alternative nutrient starvation conditions, i.e. amino acid withdrawal, have been shown to regulate autophagy through a second major kinase complex, mTORC1. The regulation of autophagy by mTORC1 is comparatively better understood than the AMPK mechanisms. The mTORC1 regulatory complex and potential crosstalk with AMPK will be discussed next. Nevertheless, the multiple regulatory pathways so far described demonstrate wider potential for different nutrient stressors to stimulate autophagy induction via distinct but overlapping mechanisms.

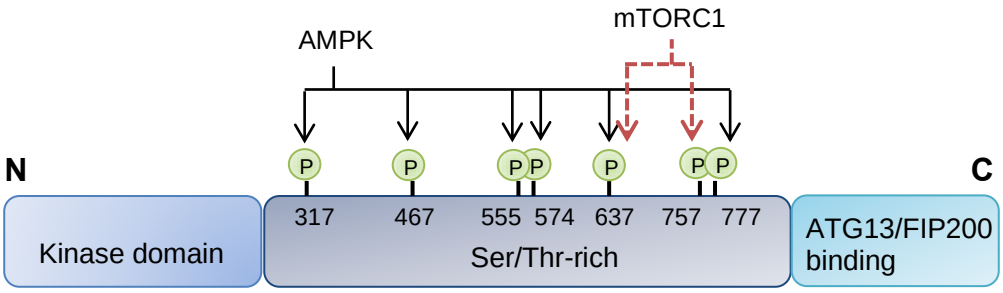

Fig 1.5. AMPK and mTORC1 phosphorylation sites with ULK1. Multiple phosphorylation sites for AMPK and mTORC1 have been identified to date within the Ser/Thr-rich domain of ULK1. Direct activating interactions between AMPK and ULK1 at S317, S777, S467, S555, T754, and S637 have been identified. While some overlap between the AMPK and mTORC1 sites exists (S637), phosphorylation of S757 by mTORC1 is the best characterised inhibitory modification on ULK1.

MTORC1 regulation of ULK1

MTORC1 has been inextricably linked to ULK1 regulation and thus control of autophagy activation. The core components of this complex have been identified as mTOR, Raptor (regulator-associated protein of mTOR), and mLST8 (mammalian lethal with SEC13 protein 8) (Yip et al., 2010, Aylett et al., 2016). In addition, these core components can be further regulated via sub-units such as PRAS40 (proline-rich Akt substrate, 40kDa). In this respect PRAS40 typically binds to mTORC1 to inhibit its activity. However phosphorylation of PRAS40 protein by AKT, downstream of growth factor signalling, can lead to detachment and increase mTORC1 activity (Vander Haar et al., 2007). This provides one mechanism linking growth factors as well as amino acids in the regulation of mTORC1 function.

In contrast to the AMPK-mediated phosphorylation of activating sites within ULK1, mTORC1 phosphorylates ULK1 at proposed inhibitory sites. The most widely reported of these mTORC1-mediated modifications is at serine 757, which was shown to inhibit ULK1 function (Kim et al., 2011). Autophagy activation generally correlated with a reduction in p-S757 levels, confirming loss of mTORC1 phosphorylating activity coincides with autophagy induction. This was confirmed by Kang *et al.,* 2013; here mutation of the mTORC1 phosphorylation site strongly reduced mTORC1-mediated phosphorylation of ULK1, and led to an increased sensitivity to rapamycin or amino acid starvation induced autophagy (Kang et al., 2013). Interestingly, it was noted that phosphorylation or functional mutations in ULK1-S757 could decrease the binding between ULK1 and AMPK, suggesting crosstalk between these two nutrient sensing modules to drive autophagy activation (Kim et al., 2011). In this interplay model, mTORC1 was proposed to negatively regulate the ability of AMPK to bind and activate ULK1.

As with AMPK, mTORC1 can phosphorylate multiple sites within ULK1. In addition to ULK1-S757, an alternative mTORC1-regulated site has been noted at ULK1-S637 (Shang et al., 2011, Wong et al., 2015). Interestingly, experiments comparing mTORC1 inhibition via amino acid starvation or rapamycin has shown differential dynamics in autophagy activation despite similarly blocking mTORC1 activity. In this way, amino acid starvation produced a much more rapid induction of autophagy. This difference was attributed to a secondary mechanism occurring in nutrient starved cells involving the protein phosphatase 2A (PP2A) (Wong et al., 2015). Only

starvation triggered dissociation of PP2A from its negative regulator Alpha4, allowing this phosphatase to de-phosphorylate ULK1 specifically on the S637 site leading to subsequent autophagy induction. Functional coordination between the S637 and S757 sites, the full set of cellular phosphatases, and interaction with AMPK signalling remain finer details that require further study. Nonetheless, the studies summarised here illustrate the importance of mTORC1 phosphorylation at specific sites in negatively regulating autophagy both with respect to ULK1 activation and its interactions with other proteins.

MTORC1 sensing of amino acids at the lysosome

Autophagy is commonly viewed to be activated following starvation of nutrients, the most potent of which are amino acids. Alternatively, we can also consider how evolution has linked positive amino acid sensing signals via mTORC1 to suppress catabolic autophagy. Understanding how amino acids activate mTORC1 ultimately improves our understanding of autophagy regulation. A long series of studies in recent years have shed substantial light on the detailed upstream signalling events of mTORC1. Interestingly, these studies outline how nutrient sensitivity is intimately linked with lysosomal cell biology, highlighting how downstream structures and organelles are interconnected with early cell signalling. These emerging models thus provide a link between early and late stage autophagy flux.

It is now well established that the lysosome plays a role as a signalling scaffold sensing acute amino acid levels leading to mTORC1 activation, as well as being the primary organelle involved in the later degradative stages of autophagy. A key observation was that mTORC1 translocates to the lysosome and that this is necessary for its activation by amino acids (Sancak et al., 2008, Kim et al., 2008, Sancak et al., 2010) (summarised in **Fig 1.6)**. Based on the current model, mTORC1 activation is typically associated with direct interactions between mTORC1 subunits and the Ras-related GTPases (Rags) at the surface of the lysosomes. Rag GTPases (A-D) are key components of the Ragulator-mTORC1 complex at the lysosome. In the active state GTP-bound Rag A (or Rag B) is associated with GDP-bound Rag C (or Rag D), and this in turn binds the Raptor subunit of mTORC1 to facilitate the association with lysosomal membranes and mediate amino acid signalling (Sancak et al., 2008, Sancak et al., 2010). Indeed, mTORC1 inhibition

was impaired in MEFs expressing constitutively active RagA, and thus these cells displayed an autophagy-deficient phenotype (Efeyan et al., 2013).

Amino acids sensing by the mTORC1-Rag complex has been a fundamentally important question. How are RagA/B activated by amino acid availability? One critical feature of the Rag GTPases is their positioning at the lysosomal membrane. This localisation is mediated through their interaction with the lysosomal resident scaffold, the Ragulator complex (composed of p18 (LAMTOR1/C11orf59); p14 (LAMTOR2/ROBLD3); MP1 (LAMTOR3/MAPKSP1); LAMTOR4 (C7orf59); and LAMTOR5 (HBXIP)). In addition to the Rag-Ragulator complexes, the vacuolar-ATPase (v-ATPase) also co-operates in the amino acid sensing and translocation of mTORC1 to the lysosome. The combination of the Rag-Ragulator complex and v-ATPase at the lysosome creates an efficient docking site which acts to anchor mTORC1 to the lysosome (Zoncu et al., 2011). Indeed, binding between the Ragulator and the v-ATPase V1 domain was weakened by amino acid stimulation. Although speculative, it has been proposed that this amino acid sensitive interaction may free the Ragulator from the v-ATPase to regulate the Rag GTPases. Supporting this proposed model, it has been shown that Ragulator acts as a guanine nucleotide exchange factor (GEF) for the Rag GTPases, and this activity is dependent on amino acid availability and v-ATPase interactions (Bar-Peled et al., 2012). The v-ATPase was shown to strongly bind to Ragulator upon both glucose and amino acid starvation suggesting a crossover of nutrient dependent signalling at the lysosome (Efeyan et al., 2013). Importantly, v-ATPase is also an essential proton pump driving the acidification of the lysosome, a process intricately linked with autophagy activation, in particular the later degradative stages. This is one such example of how the early signalling mechanisms of autophagy are linked with the final execution stages of the process.

Other work from two independent groups has highlighted the complexity of amino acid sensing by specific cellular receptors. These studies identified the solute carrier family 38 (SLC38A9) to function upstream of the v-ATPase-Ragulator-Rag complex. Using tandem affinity purification coupled with LC-MS/MS, SLC38A9 was found to interact with all 5 members of the Ragulator/ mTORC1 complex, as well as the four Rag GTPases (Rebsamen et al., 2015). The SLC38A9.1 was found to be the preferential isoform that bound Ragulator, Rag A, Rag C, and endogenous components of the v-ATPase proton pump (Wang S., 2015). Importantly,

knockdown of SLC38A9 supressed the activation of mTORC1 by amino acids, and conversely overexpression of SLC38A9 led to mTORC1 insensitivity towards to amino acid starvation and resulted in an autophagy-deficient cell phenotype. Interestingly, SLC938A9.1 was shown to be a preferential Arginine (Arg) sensor in stimulating mTORC1 activity; genetic deletion of SLC38A9.1 was only shown to block Arg-induced mTORC1 activation, while that induced by Leucine remained intact (Wang S., 2015). Further work showed that amino acid stimulation was able to weaken the interaction between SLC38A9 and the ragulator. This further supports the proposed model of amino acid stimulation leading to free Ragulator to impart its GEF activity upon RagA/B. Although in this case, while v-ATPase inhibition abrogated mTORC1 signalling in control cells, it did not induce full blockade of mTORC1 signalling in cells overexpressing SLC38A9.1, suggesting that v-ATPase and SLC38A9 may represent independent mechanisms of Ragulator-Rag control.

While mTORC1 activity is intricately linked to GTP-loading of the Rag GTPases, mTORC1 is conversely inactivated when RagA/B return to their GDP-bound state. Another key mechanism that has emerged in recent years links the stress inducible proteins termed Sestrins (sesn1-3) to mTORC1 signalling and amino acid sensing. Sestrin function for mTORC1 intimately involves the GTPase-activating protein (GAP) activity toward Rags (GATOR) complexes. The GATOR1 complex (consisting of subunits DEPDC5, Nprl2 and Nprl3) acts as a GAP for Rags A and B, therefore inhibiting activation of the mTORC1 complex at the lysosome (Bar-Peled et al., 2013). The GATOR2 complex (consisting of Mios, WDR24, WDR59, Seh1L and Sec13) is the endogenous negative regulator of GATOR1 (Bar-Peled et al., 2013). GATOR2 allows mTORC1 to be activated by blocking the inhibitory activity of GATOR1.

Previous data has suggested that Sestrins regulate mTORC1 via AMPK (Budanov and Karin, 2008). However, expression of Sestrins led to a strong inhibition of p70S6K phosphorylation, an indication of inhibition of MTORC1 signalling, even in AMPKα-/- MEFs suggesting that Sestrins can also work through a mechanism independently of AMPK (Parmigiani et al., 2014). More recent studies have suggested an alternate model whereby Sestrins inhibit the activity of GATOR2 through direct binding, leading to mTORC1 inhibition via GATOR1 activation. For example, Sestrins were shown to bind GATOR2, but not GATOR1 complexes (Parmigiani et al., 2014, Chantranupong et al., 2014), and this interaction was

promoted by amino acid starvation. Further studies have pinpointed this amino acid sensing GATOR2 mediated control of mTORC1 activity to be altered by Leucine. Here leucine was shown to bind to Sestrin 2 and subsequently disrupt Sestrin2-GATOR2 interactions, leading to activation of the mTORC1 pathway (Wolfson et al., 2016, Saxton et al., 2016b). Based on this observation we could speculate that Sestrins play a role in amino acid-dependent inactivation of mTORC1, and in turn initiation of autophagy.

In alternative mechanism of GATOR 2 modulation, an arginine sensing CASTOR1-CASTOR2 complex has recently been identified. CASTOR1 (Cellular Arginine Sensor for mTORC1) was shown to directly interact with GATOR2 upon arginine deprivation, and in turn inhibit mTORC1 activity. Conversely, in the presence of arginine the interaction between CASTOR1 and GATOR2 was disrupted and mTORC1 was active (Chantranupong et al., 2016, Saxton et al., 2016a). It interesting to note, that SLC38A9 was also identified as a preferential arginine sensing component of the mTORC1 regulatory machinery (Wang S., 2015), therefore this work highlighted an alternative mechanism of how arginine controls mTORC1 activity.

The summary above highlights mechanisms that drive mTORC1 translocation to the lysosome for activation of downstream signalling or alternatively mechanisms that negatively regulated MTORC1 activity. It is now well accepted that mTORC1, once at the lysosome, becomes fully activated via further stimulatory signals driven by the Rheb (Ras homolog enriched in brain) GTPase (Long et al., 2005). Rheb GTP levels (and hence activation) is under the control of the tuberous sclerosis heterodimer (TSC) complex, made up of TSC1, TSC2, & TBC1D7 (tre2-bub2-cdc16-1 domain family member 7). TSC2 acts a GAP for Rheb (Tee et al., 2003, Inoki et al., 2003), and TSC1 is a scaffold for TSC2 and TBC1D7, stabilising the protein complex (Dibble et al., 2012).

The TSC complex essentially acts as an inhibitor of MTORC1 signalling. The generally accepted view recognises the TSC2 pathway as the main driver for growth factor activation of mTORC1. Insulin has been shown to initiate PI3K/AKT mediated phosphorylation of TSC2 (Inoki et al., 2002, Cai et al., 2006), and subsequentl TSC1/2 dissociation from the lysosome (Menon et al., 2014). This presents a model whereby growth factors promote MTORC1 activity via protection of Rheb inactivation.

However, recent studies have indicated further levels of crosstalk and signal integration. Demetriades et al., 2014, recently outlined a model whereby the Rag complex and amino acids also contribute to Rheb regulation. Amino acid removal promoted Rag GTPases in their inactive confirmations (RagA-GDP and RagC-GTP) to recruit TSC2 to the lysosome where it can inactivate Rheb and co-operate to induce mTORC1 release from the lysosome. In their experimental systems, MTORC1 could only be fully released from the lysosome when both Rag GTPases & Rheb were inactivated. This requires TSC2 to be present at the lysosome, and it is therefore an essential component needed in the amino acid sensing pathways. In support of this, mTORC1 remained localised at the lysosome, even under amino acid starvation condition in TSC2 null MEFs. In addition, while control MEFS activated autophagy on aa-starvation, shown by LC3A accumulation of the lipidated form and p62 degradation, TSC2 null MEFs were autophagy impaired (Demetriades et al., 2014). In addition to amino acid starvation mediation of MTORC1 activity, using a lysosomal tethered-TSC2, another group were able to show TSC dissociation from the lysosome was needed to activate MTORC1 via growth factor/insulin stimulation (Menon et al., 2014). However, in contrast to the data above, they also showed TSC2 lysosomal localisation was not altered by amino acid starvation, therefore there still remains conflicting evidence in this area of autophagy and MTORC1 control.

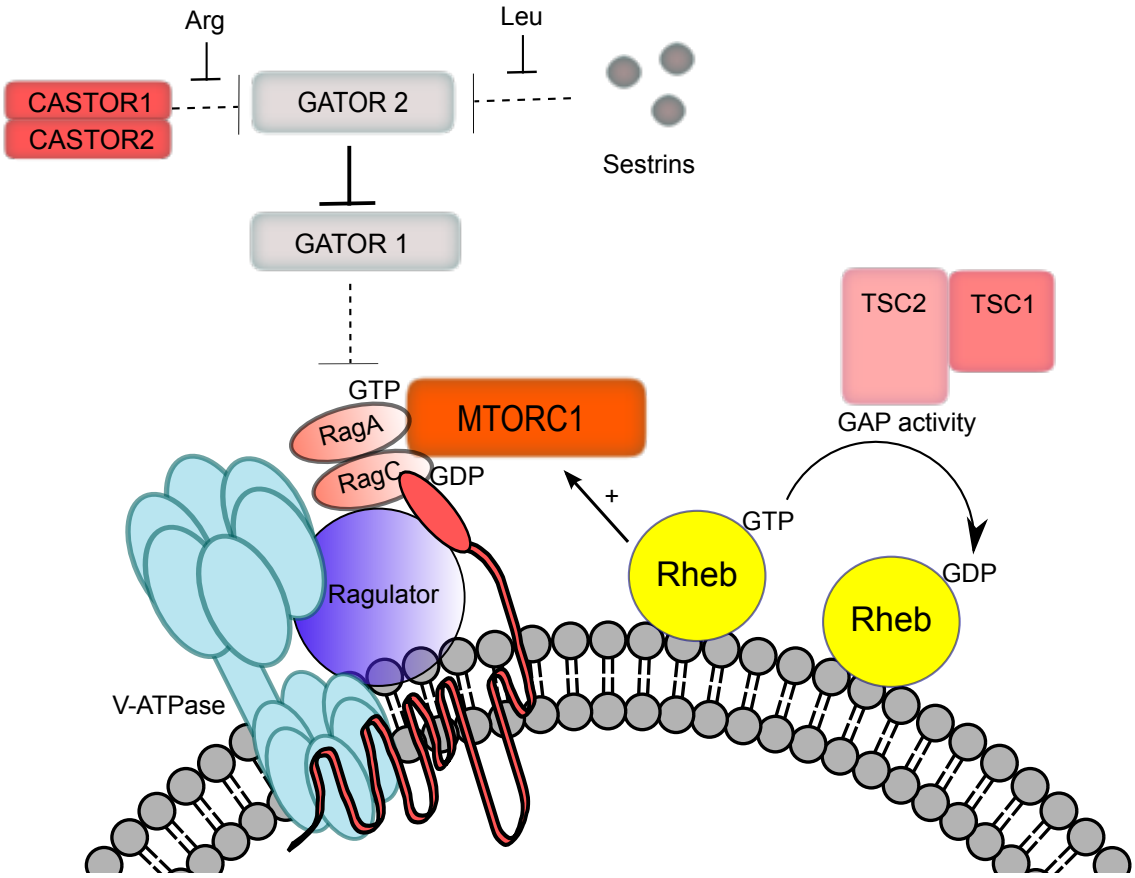

Amino acids present, MTORC1 is active.

Fig 1.6. Nutrient sensing of mTORC1 at the lysosome. The mTORC1 complex is localised and activated at the lysosome by an intricate network of protein complexes. The interaction between the v-ATPase, Ragulator complex and the Rag GTPases is essential in anchoring mTORC1 at the lysosome. When localised to the lysosome, mTORC1 can be activated by the additional GTPase Rheb, whose activation lies under the control of the TSC2/TSC1 complex. Negative regulators of mTORC1 include the Sestrins, GATOR and CASTOR complexes, which can be further regulated by specific amino acids, such as Leucine and Arginine. One amino acid sensing component of mTORC1 activation has recently been identified as SLC38A9, however further amino acid sensors remain to be identified.

1.3. The role of autophagy in cancer

1.3.i Autophagy as a tumour suppressor

The role of autophagy in cancer is complex due to dual roles for both tumour cell survival and tumour suppression as summarised in **Figure 1.7**. Early evidence for the role of autophagy in cancer did point towards a tumour suppressive role. A key effector protein involved in autophagy regulation, Beclin1, was identified as a tumour suppressor by Liang *et al*, 1999. *Beclin1* was found to be mono-allelically absent in 45-75% of human breast and ovarian cancer cases. Furthermore, over-expression of Beclin1 in MCF-7 cells led to upregulation of autophagy and this correlated with reductions in cell proliferation, clonigenicity in soft agar studies, and *in vivo* tumorigenesis (Liang et al., 1999).

The tumour suppressive function of Beclin1 and autophagy was confirmed by multiple studies showing loss of autophagy regulatory genes promoted spontaneous tumour development in mouse models. Beclin1 heterozygous mice more frequently developed lymphomas, lung or liver tumours compared to wild type mice, and concurrent with previous studies these mice had decreased capacity to initiate autophagy, as measured in starved muscle tissue (Yue et al., 2003). In addition to Beclin1, alternative autophagy genes when knocked out, could also give rise to spontaneous tumour development. Mice with mosaic deletion of *ATG5* were noted to develop liver tumours specifically; moreover, liver-specific deletion of *ATG7* resulted in formation of benign liver adenomas (Takamura et al., 2011). *ATG4C* deletion, one of the essential mediators involved in priming LC3 for lipidation, increased susceptibility to formation of MCA carcinogen-induced fibrosarcomas (Marino et al., 2007). In support of data generated from knockout mouse models, autophagy regulators ATG4, ATG5, and ATG12 have all been shown to be deleted and/or mutated in human cancers, including gastric and colorectal carcinomas (Kang et al., 2009).

As a model for the tumour suppressive function of autophagy, $Beclin^{+/-}$ or $ATG5^{-/-}$ iBMK autophagy-deficient cells display accumulation of p62, ubiquitin-containing protein aggregates, reactive oxygen species, and damaged organelles (mitochondria) (Mathew, 2009). Furthermore, failure to regulate these pathways, in particular p62 levels, arising from autophagy deficiency led to activation of the DNA damage response, and in turn promoted tumorigenesis. p62-EGFP expression in

autophagy-deficient cells led to increased γ-H2AX positive nuclear staining (marker of DNA damage) and importantly increased tumour volumes as compared to their autophagy competent counterparts. This p62 driven mechanism of tumorigenesis was also identified by Takamura *et al*., 2011 (Takamura et al., 2011); here tumours originating from ATG7-deleted mice showed evidence of p62 accumulation and genome damage. Furthermore, concurrent deletion of p62 significantly reduced the volume of $ATG7^{-/-}$ driven tumours. Taken together, this evidence would suggest that autophagy inhibits accumulation of critical key signalling proteins such as p62, thereby suppressing cell and genomic damage, thus reducing initiation of cancer.

1.3.ii Autophagy promotes survival of established tumour cells

Conversely, autophagy is also well recognised to promote survival and resistance in cancer cells, and indeed this is the fundamental rationale for autophagy inhibition as anti-cancer therapy. The premise is that cellular stress will activate autophagy and lead to the cancer cells gaining reliance on autophagy for survival (Mathew, 2007). For example, it is estimated that a large proportion of tumours contain regions which are subject to hypoxic conditions. Hypoxia has been shown to be a major stressor leading to autophagy activation, especially in the context of cancer cells, and this stress-response pathway aids survival under hypoxic conditions. Hypoxia was shown to upregulate autophagy in BE human colorectal carcinoma cells as measured by GFP-LC3 puncta expression. siRNA-mediated ATG5 knockdown abrogated this biochemical response and moreover reduced cell viability of colorectal cancer cells subjected to hypoxic conditions (Wilkinson et al., 2009). These data clearly support a beneficial role for autophagy in hypoxia. In agreement with these findings, hypoxia correlated with an induction of autophagy in both human glioblastoma cell lines and primary cells, as shown by altered p62 and LC3-II expression (Hu et al., 2012). Inhibition of autophagy via 3-methylamine (3-MA) or Bafilomycin was able to reduce the levels of hypoxia-induced autophagy and in conjunction, increased cell death in response to hypoxic stress, primarily through promoting apoptosis.

In addition to hypoxia, another frequent cellular stress tumour cells encounter is nutrient starvation. Of course, this is a key driver of autophagy activation through the canonical autophagy pathway, downstream of mTORC1 and AMPK (as described in

section 1.2). Thus, it is unsurprising cancer cells exposed to a nutrient-deficient environment utilise autophagy for survival. Following extreme nutrient starvation, defined as combined glucose, amino acid and serum withdrawal, pancreatic carcinoma cells (PANC-1) displayed rapid upregulation of autophagy as shown by multiple methods of LC3 readouts (Kim et al., 2015). Autophagy inhibition, with CQ or ATG5 knockdown, promoted nutrient starvation induced cell death. In agreement, autophagy provided protection against less extensive nutrient starvation in multiple other studies. Amino acid-starvation induced autophagy contributed to the survival of colorectal cancer cells both *in vitro* and *in vivo* (Sato et al., 2007). Intriguingly, a more recent study showed that deprivation of just one of the essential amino acids, Arginine, led to activation of pro-survival autophagy in ovarian cancer cells (Shuvayeva et al., 2014). Here, the cell viability and proliferative capacity of Arg-depleted SKOV3 cells was significantly decreased when autophagy was inhibited (CQ or siRNA Beclin1) compared to control cells. These studies discussed here depict a clear role for pro-survival autophagy in multiple cancer phenotypes subjected to cellular or metabolic stress.

In an alternative cancer-promoting effect, autophagy has been shown to be required to support metabolism and mitochondria functionality within cancer cells. Expression of Ras isoforms with activating mutations, H-ras^{V12} and K-ras^{V12}, increased levels of basal autophagy in iBMK cells (Guo et al., 2011). However, interestingly Ras-driven cell lines, while having increased basal autophagy, were not then susceptible to induction of starvation induced autophagy, while control cells were. In further exploration of these effects, human cancer cell lines carrying Ras mutations also had high basal autophagy, and this was subsequently shown to facilitate the growth and survival of these cell lines (H1299, PC-3, PANC-1). Interestingly, the mechanism identified to be supporting autophagy-driven cell survival and growth in Ras expressing cancers was maintenance of mitochondrial function. Here genetic knockout of ATG5, ATG7, Beclin1, and p62, all led to abnormal mitochondrial morphology, loss of mitochondria membrane potential and signs of defective mitophagy. This data together suggested that autophagy was required to maintain a pool of healthy mitochondria to support cancer cell survival and growth. Similarly, autophagy has also been shown to support mitochondrial metabolism in BRAF^{V600E} lung tumours, here ATG7 deletion resulted in accumulation of mitochondria, in which a smaller fraction of these were determined functional compared to wild-type counterparts (Strohecker et al., 2013). Interestingly, the addition of glutamine was

sufficient to rescue loss of cell survival in ATG7 deficient cell lines in response to starvation. Subsequent studies showed autophagy deficient cells to be reliant on glutamine for survival, utilising glutamine in the tricarboxylic acid (TCA) cycle. Separately, this work was repeated in K-Ras^{G12D} non-small cell lung cancer, with comparable findings. Again ATG7 deficient tumours had defective mitochondria, which correlated with reduced tumour burden, and arrested proliferation (Guo et al., 2013). Taken together these studies support a role for autophagy in maintaining functional mitochondria for cancer cell metabolism, and ultimately cell survival.

Autophagy has also been shown to be cytoprotective, allowing cancer cells to survive chemo- or radio-therapy, and ultimately aid their recovery to form treatment-resistant tumours (O'Donovan, 2011). The tyrosine kinase inhibitors (TKI), Gefitinib and Erlotinib, have been shown to upregulate autophagy *in vitro*, and abolishing this response enhanced their cytotoxic actions (Han et al., 2011). Furthermore, the PI3K/mTOR inhibitor, NVP-BEZ235, has been shown to induce autophagy (Liu et al., 2009), and combination with autophagy inhibitors improves NVP-BEZ235 efficacy in multiple cancer cell lines including breast (Ji et al., 2015), and neuroblastoma (Seitz et al., 2013).

As well as chemotherapy, autophagy can also promote radio-resistant cancer phenotypes. The induction of autophagy by γ-irradiation has been shown to contribute to resistance to radiation in glioma cells *in vitro* (Lomonaco et al., 2009). A dose-dependent relationship between radiation and autophagy induction could be shown in malignant glioma cells (Jo et al., 2015). Indeed many breast cancer cells have been shown to be more sensitive to radiation-induced cell death in the presence of an autophagy inhibitor. Cytoprotective autophagy was induced upon irradiation in ER+ ZR-75-1 breast cancer, and both pharmacological inhibition of autophagy (chloroquine) or shRNA genetic suppression (ATG5 or 7) increased the radio-sensitivity of these cells (Wilson et al., 2011). This effect was confirmed by the same research group in MCF-7 breast carcinoma (Bristol et al., 2012). Interestingly, differences have been observed between radio-resistant and radio-sensitive breast cancer cell lines with respect to autophagy upregulation. MDA-MB-231 cells, noted to be radio-resistant, exhibited significant increases in autophagy markers such as LC3-II upon irradiation, whereas HBL-100 cells, considered to be radio-sensitive, did not activate autophagy (Chaachouay et al., 2011). The autophagy response was shown to be cytoprotective as pre-treatment with an autophagy inhibitor reduced the

clonogenic capacity of irradiated radio-resistant cells. These studies are just a snapshot of a vast array supporting a pro-survival role for autophagy with respect to cellular stress, radio-, and chemo-therapy. Furthermore, they promote a clear rationale for the inhibition of autophagy as a potential anti-cancer therapy.

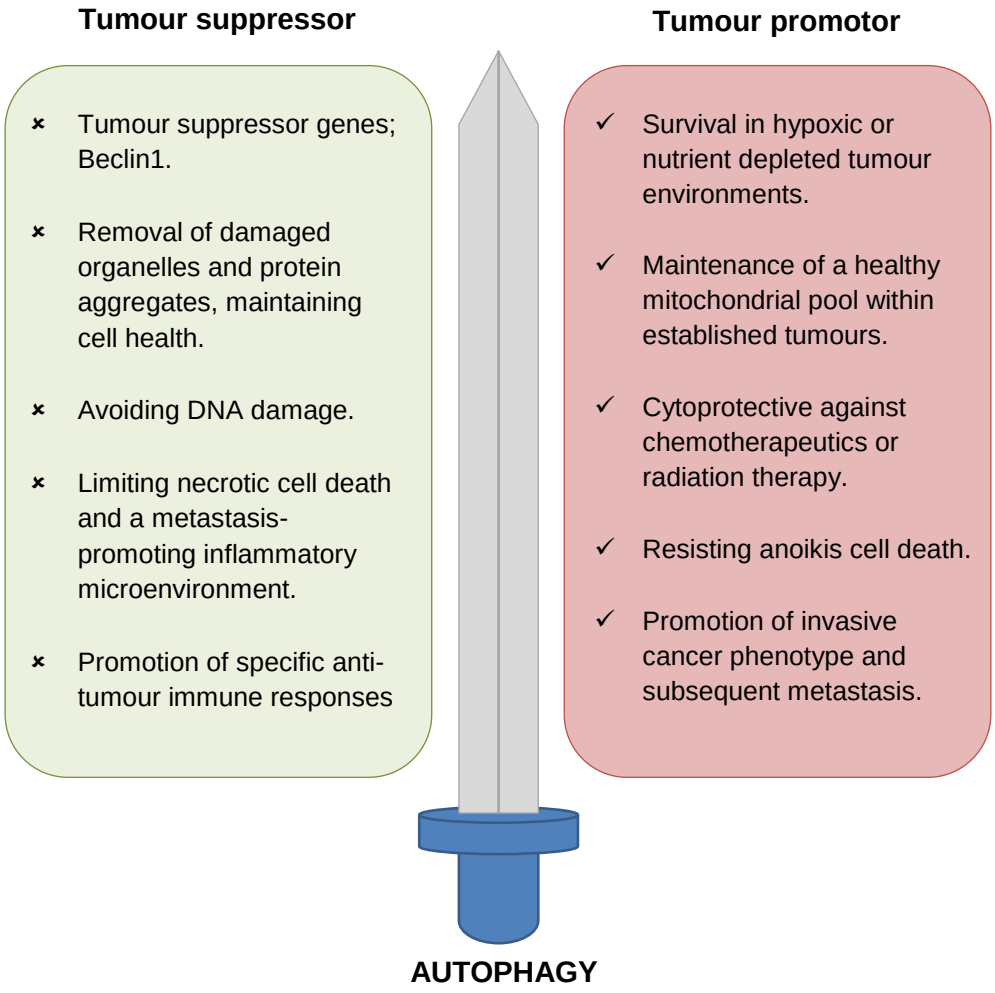

Fig 1.7. The double edged sword of autophagy. Autophagy has been shown to have opposing role in cancer pathology, acting both as a tumour suppressor during early cancer initiation, and later as a cancer promotor within established tumours. Here we summarise a selection of evidence supporting each of these roles.

1.3.iii Autophagy as an anti-metastatic factor

The rationale for targeting autophagy to reduce cancer cell survival has been extended for treatment of metastatic cancer. Similar to the dual roles of autophagy in autonomous cancer cell survival, the findings on autophagy for metastasis similarly highlight conflicting data (or duality) describing both pro-metastatic and anti-metastatic roles. However, as with autophagy in basic cancer cell biology, the majority of papers do point towards a pro-metastatic role of autophagy. Both sides of evidence are outlined below.

During metastasis, cells undergo stress as they adapt to new microenvironments. Thus, it is likely that autophagy is activated during metastasis. A model proposed nearly 10 years ago suggested that autophagy could serve as tumour suppressor by limiting metastasis (Degenhardt, 2006, Mathew, 2007). Autophagy would be up-regulated during the initial primary events of metastasis, including hypoxia, metabolic stress, and the loss of extracellular matrix (ECM) contacts. During these hypoxia and metabolic stresses, many tumour cells would undergo necrotic cell death, inducing an inflammatory niche at the primary tumour sites, and creating a favourable microenvironment for metastasis to progress. However, autophagy could promote cell health and survival under such conditions. Thus, induction of autophagy within the primary tumour may limit the level of cell death and necrosis, thereby inhibiting inflammation and suppressing metastasis (Degenhardt, 2006, Bingle, 2002).

An alternate example of this anti-inflammatory role for autophagy in preventing metastasis is the autophagy-regulated release of an essential immune modulator by cells programmed to die. High-mobility group B1 (HMGB1) activates an anti-tumour response and restricts metastasis through TLR-4 signalling mechanisms (Yang et al., 2010). Using the epithelial growth factor diphtheria toxin (DT-EGF) which selectively kills cells expressing EGFR, it was found that only dying cells (gliomas) which had high levels of autophagy released HMGB1, and this correlated with a non-apoptotic mode of cell death. Alternatively, in cells with low autophagy (epithelial type tumour cells), HMBG1 was not released and these cells died via apoptosis (Thorburn et al., 2009a, Thorburn et al., 2009b). Therefore these data suggested that autophagy was required for HMGB1 release and subsequent anti-tumour immune responses.

With respect to alternative mechanisms, the autophagy inducer, rapamycin, has frequently been shown to prevent metastasis in *in vivo* models. Rapamycin reduced tumour growth and formation of distant metastases in a mouse model of non-small cell lung cancer (NSCLC) (Boffa et al., 2004). In agreement, rapamycin also reduced the incidence of pulmonary metastases in a renal cell carcinoma SCID mouse model (Luan et al., 2003). However, as evident below, the beneficial effects of rapamycin in reducing metastasis may be dependent on the cancer type and mouse model used.

1.3.iv Autophagy as a pro-metastatic factor

More recent studies have shown opposing effects for rapamycin, in which autophagy promoted metastasis. In a 4T1 mammary carcinoma model, using immune-competent mice, after tumour resection surgery administration of rapamycin (thereby activation of autophagy) greatly increased the metastatic potential of the remaining population of aggressive breast cancer cells (Lin et al., 2015). Furthermore, in the 4T1 mouse model, rapamycin in combination with sunitinib (TKI anti-angiogenic therapy) was identified to promote lung metastasis despite reducing primary tumour growth (Yin et al., 2014).

How could autophagy promote the metastasis cascade? For one mechanism, we can recall that for metastasis, the tumour cell must have the ability to resist anoikis, a form of programmed cell death (as reviewed in (Paoli et al., 2013). Anoikis is induced by anchorage-dependent cells losing their cell-ECM attachments. A metastasising cell must lose ECM contact in order to move away from the primary tumour and towards the circulation and so anoikis would be expected to be activated during some stage of metastasis. It has been shown autophagy protects detached cells from anoikis-linked death. In a 3D mammary epithelial culture, inhibition of autophagy via knockdown of ATG12 protein enhanced anoikis death (Fung, 2008). Therefore, autophagy may compensate for the loss of extrinsic signals which usually promote metabolism, allowing the cells to survive detachment from the ECM.

In a later study using shRNA targeting of ATG12 (key component of the ATG8/LC3 conjugation system), it was shown that inhibition of autophagy inhibited the invasion of glioma cells in a 3D organotypic model (Macintosh, 2012). Based on this, the

authors concluded that autophagy plays a key role in the initiation of metastasis, i.e. the primary stage of metastasis, invasion. This correlation between autophagy and metastasis has further been supported by observations in clinical human tumour samples. An analysis of almost 1400 tumours, including breast carcinomas and melanomas, indicated an association between LC3B puncta, a marker of activated autophagosomes, and tumour cell invasion. Patients who showed signs of activated autophagy within the tumours typically had a poorer prognosis (Lazova, 2012).

In addition, a recent paper by Li *et al*., 2016, highlighted essential metastatic properties within MDA-MB-231 cells that may contribute to their high levels of invasive behaviour (Li et al., 2016). It was shown that this metastatic cell line could continue to proliferate even under nutrient starvation conditions, and this correlated with induction of autophagy. Furthermore, subpopulations of these cells, selected through being exposed to 5 rounds of culture in amino acid free media, had heightened sensitivity to rapamycin-induced autophagy activation compared to the parental population and upon rapamycin treatment displayed an increasingly invasive phenotype. Thus, these data confirmed that autophagy can confer the ability to survive under nutrient stress (an essential feature of metastatic cells) and can increase their invasiveness.

Using an alternate approach, it has been identified that inhibition of autophagy can decrease migratory and invasive capabilities of a metastatic breast cancer cell line (Sharifi et al., 2016). Interestingly, knockdown of autophagy (via ATG5 or ATG7 shRNA) in 4T1 murine mammary carcinoma cells did not alter cell growth or viability characteristics even under metabolic stress. However, it had a profound influence on the *in vitro* motility of these tumour cells in collagen transwell assays as well as the *in vivo* metastatic potential – i.e. autophagy ablation resulted in reduced numbers of macro-metastases present in the lungs and livers compared to parental cells. Importantly, the authors proposed a potential mechanism as to how autophagy can promote metastasis. Focal adhesion complexes, essential molecules involved in maintaining cell-ECM attachment, undergo disassembly when metastasis is occurring; however, this disassembly process is reduced in autophagy-deficient cells. This was attributed to autophagy-deficient 4T1 cells having elevated levels of the focal adhesion kinase substrate, paxillin. The authors suggest paxillin is typically degraded by autophagy. Thus, abrogation of the pathway leads to stabilisation of the paxillin and inhibition of metastasis. Thus, there is a growing body of diverse

evidence for autophagy as a pro-metastatic factor. Therefore, developing therapies which inhibit autophagy may decrease the likelihood of metastases forming.

As autophagy has dynamic and opposing roles in cancer, it is critical to understand the relationship between cancer development stages and autophagy function in order to be in a better position to rationally utilise autophagy modulation as a therapeutic target. Inhibiting autophagy may prove effective in increasing sensitivity to chemotherapy and decrease the potential for patients to relapse. However, increasing autophagy prior to tumorigenesis may help prevent tumour initiation. Taking this into consideration, the experiments of this thesis explored the potential of utilising an autophagy inhibitor to modulate cell survival in a metastatic breast cancer cell line.

1.3.iv Can autophagy inhibition be a successful anti-cancer therapy?

Chloroquine (CQ) is a lysosomotropic agent that prevents acidification of the lysosome/endosome. CQ accumulates and upon protonation becomes trapped in the lysosome; due to its weak basic activity this leads to an increase in lysosomal pH and subsequently inhibition of lysosome-resident degradative enzymes (such as cysteine proteases) which require an acidic pH for optimal activity. This disruption prevents further fusion of lysosomes with autophagosomes or endosomes, thus preventing overall protein degradation within the lysosome (Pasquier, 2016). CQ has been used as an anti-malarial drug since its development in the 1940s (Slater, 1993) and was very effective. It acts against the plasmodium parasite by accumulating, via a weak-base mechanism in the acidic food vacuole of intraerythrocytic trophozoites. Once in the food vacuole, the equivalent of the lysosome in the malaria parasite, there are two main theories of how CQ leads to death of the malarial parasite. CQ has been demonstrated to reduce the activity of heme polymerase enzyme, the enzyme responsible for converting toxic free heme to hemozoin pigment, through a potential pH-dependent mechanism although this has not been directly shown (Slater, 1993). In an alternative mechanism, CQ has been proposed and indeed demonstrated to form a complex with free heme, thereby preventing its conversion into hemozoin (Sullivan et al., 1998). However, clinical resistance to CQ is now quite prevalent, and newer drugs are replacing this once well-used prophylactic and therapeutic treatment (Reddy, 2012).

Due to the development of resistance in malaria, CQ has more recently been investigated for its use in cancer (Solomon and Lee, 2009). Multiple studies in mouse models of cancer have shown autophagy-lysosomal inhibition with CQ and its derivatives can enhance the effectiveness of a variety of anti-cancer treatments. Further to this, a range of clinical trials have been launched investigating the effectiveness of combination treatments of cancer therapies and CQ.

Chloroquine: pre-clinical evaluation

As summarised above, it is still a matter of debate as to the specific contexts that determine whether autophagy contributes towards tumour suppression or tumour cell survival. However, there is substantial rationale to inhibit autophagy in

combination with anti-cancer treatments. Initial primary studies have shown autophagy inhibition to be an effective anti-cancer therapeutic strategy.

In an *in vivo* model of *myc*-induced lymphoma, CQ treatment in cells with inactive p53 impaired tumour growth but did not led to regression of the cancer (Amaravadi et al., 2007). However, combination of CQ with tamoxifen-inducible p53 activation led to a delay in tumour recurrence. In this study, complete clinical regression of the tumours was detected in 81% of mice treated with tamoxifen/CQ as compared to only 8% in mice receiving tamoxifen/PBS. Non-apoptotic tumour cells derived from tamoxifen/PBS mice showed evidence of autophagy after 24 and 48hrs. In contrast, by 48hrs of Tamoxifen/CQ treatment tumours consisted largely of remains of apoptotic cells, suggesting tumour cells with activated p53 were using autophagy to resist apoptosis. To confirm that *in vivo* effects of CQ were due to an autophagy blockade, ATG5 shRNA was used as a genetic comparison; ATG5 knockdown reduced viability of tumour cells also. However, combination with CQ did not further decrease this (i.e. the effect of CQ was lost in autophagy-deficient cells). Overall, this suggests that autophagy does indeed aid in tumour cell survival, and that blocking autophagy with CQ enhances p53-dependent apoptosis. Similarly, Maclean *et al*. (Maclean et al., 2008), presented evidence that blockade of the end-stage of autophagy by CQ, induced p53-dependent cell death; here they noted p53-null cells were resistant to the effects of CQ. These two key papers provided insight into the potential role for autophagy in cancer cell survival, as highlighted here one important mechanism of autophagy in cancer cells was in resisting apoptosis, in particular p53-driven apoptotic signals. Therefore, using CQ to block autophagy was identified to be an effective strategy to boost apoptotic events in tumours.

Complementing these studies, blockade of autophagy via CQ has been shown to potentiate a number of anti-cancer therapies including TKI. Imatinib mesylate (IM) is the standard first-line therapy for treatment of chronic myeloid leukaemia (CML). Development of resistance has led to progression of second generation TKI including dasatinib and nilotinib. Bellodi *et al.* showed that CQ can sensitise CML blast crisis cells to co-treatment with TKI (Bellodi et al., 2009). The authors demonstrated IM treatment caused cell stress and autophagy activation in blast crisis cell lines and primary patient CML cells, suggesting that autophagy could be aiding the resistance of cells upon IM treatment. Supporting this idea, combination of IM with CQ potentiated cell death in the CML blast crisis cells, and this was

mimicked by ATG5 or ATG7 knockdown. Additionally, other data showed CQ-mediated blockade of autophagy in combination with second generation TKIs, dasatinib and nilotinib, led to near complete eradication of CML stem cells. Thus, in CML, CQ seemed to be an effective sensitiser for combination therapies supporting progression in clinical trials (as discussed in later section).

More widely, other studies have shown similar sensitising effects of CQ in different contexts, including CQ sensitising colon cancer to anti-angiogenic (Bevacizumab) and cytotoxic (oxaliplatin) therapies (Selvakumaran, 2013). Studies examining the effects of CQ in breast cancer have also demonstrated a strong beneficial potential. Comparison of trastuzumab-refractory vs. -sensitive breast cancer cells showed increased autophagic flux was present in refractory cells, thus linking autophagy to resistance towards therapy. Indeed, CQ treatment of refractory cells pushed them towards a trastuzumab-sensitive phenotype, with both evidence from reductions in cell viability *in vitro* and decreased xenograft growth in mice (Cufi et al., 2013).

This beneficial effect has been confirmed in multiple breast cancer categories including triple negative breast cancers (TNBC). One such study examined the potential combination of autophagy inhibition with recombinant human arginase, a therapy which depletes L-arginine levels, and has been shown to be an effective cancer therapeutic strategy in leukaemia cells (Hernandez et al., 2010, Morrow et al., 2013). Here, the cytotoxicity of recombinant human arginase was increased following blockade of autophagy either through siRNA-Beclin1, or importantly, through CQ treatment (Wang et al., 2014). Indeed, a more recent study has further supported this model, showing that CQ specifically targets stem cell populations within the TNBC subtype (Liang et al., 2016). These experiments showed that CQ and autophagy inhibition effectively eliminated the cancer stem cell population in TNBC via impairment of DNA repair. In agreement with the emerging trend, combination treatment of carboplatin with CQ resulted in a reduction in growth of platinum-resistant TNBC xenografts. Thus, this set of pre-clinical *in vitro* and *in vivo* data supports the rationale for use of CQ as an effective adjuvant therapy for a number of different cancer types.

The majority of studies on CQ in cancer focussed on its sensitising effects to chemo- or radio-therapy, as CQ has limited efficacy as a single agent. However, one strategy has been the development of modified more active CQ derivatives with increased potency in blocking autophagy as well as decreasing tumour growth as a

single agent (McAfee et al., 2012). The lead compound in this study was Lys-01, which was a compound with 2 aminoquinoline rings, a triamine linker, and C-7 chlorine added onto the original structure of CQ. The authors found that Lys01 was 10-fold more potent than CQ or hydroxychloroquine (HCQ) at inhibiting autophagy. In addition, Lys01 induced near complete cell death in melanoma (1205Lu) and CQ-resistant (HCC827) cell lines. Lys05, a more soluble analogue of Lys01, enabled further *in vivo* studies. In this way, Lys05 was shown to potently reduce tumour volume and weight, with an induction of greater numbers of autophagic vesicles in tumour cells than HCQ. Furthermore, lower doses of Lys05 could produce anti-tumour activity without dose-limiting toxicity. These data suggest that new CQ derivatives would be more effective drugs to enter into clinical trials than the original compounds. In any case, a sufficient body of evidence had already accumulated from *in vitro* and pre-clinical studies demonstrating CQ to potentiate cytotoxic effects for a range of chemotherapeutics, including TKI and hormonal-based therapies, such as tamoxifen. Based on these positive outcomes in pre-clinical studies, CQ and HCQ (structures shown in **Fig 1.8**) were already taken forward into a number of clinical trials for a broad range of cancers in combination with a number of cancer therapies.

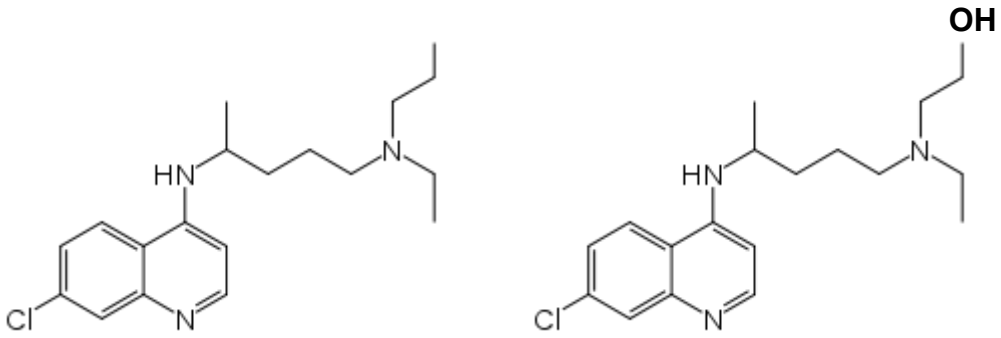

Chloroquine (CQ) Hydroxychloroquine (HCQ)

Fig 1.8. The chemical structures of CQ and HCQ. The CQ derivative HCQ differs only by the addition of a hydroxyl group (highlighted in bold) on the side chain.

Chloroquine clinical trials

CQ is being tested in multiple clinical trials against a variety of cancers, both as a single therapy or, more commonly, an adjuvant to other established therapies. The majority of CQ or HCQ clinical trials are in or have just completed Phase I/II studies, investigating maximum tolerated dose (MTD) safety, and are now moving forward into Phase II. Currently a search for HCQ clinical trials in cancer yields over 50 clinical trials worldwide. Five key published clinical trials assessing CQ in Phase I (MTD) and Phase II (efficacy) are described below, and are summarised alongside other ongoing clinical trials in **Table 1.1**. Notably, these studies use CQ or HCQ; HCQ differs only from CQ by the addition of a hydroxyl group on the side chain (highlighted in **Figure 1.8**), and it is proposed this alteration makes the molecule more lipophilic thus less efficient in crossing plasma membranes, although it is preferred in clinical trials due to greater solubility (Browning, 2014).

The first of these example studies examined the combination of HCQ with temozolomide (TMZ) in advanced solid tumours (patient examples included breast, colon, and head and neck) and melanoma (Rangwala, 2014b). This study noted that MTD was never reached for HCQ in this cohort of patients (from 200 – 1200mg/day), although the conclusion was finally 600mg twice a day to use for phase II trials. Autophagy inhibition was confirmed using electron micrographs of peripheral blood mononuclear cells, which showed significant accumulation of autophagic vehicles in comparison to pre-treatment samples. In a beneficial outcome, 10% of the 29 patients remaining at the end of the trial showed a partial response (defined as minimum 30% reduction in the sum of diameters of target lesions) to HCQ and TMZ treatment and a further 27% had stable disease (no shrinkage, but no progression either). It is of note, that as this was a dose-escalation study no control patients receiving TMZ alone were available to compare the effectiveness of combination therapy with. Despite this, the temozolomide combination study showed HCQ to be safe and tolerable, and to have potential anti-tumour activity in melanoma and advanced solid cancers (Rangwala, 2014b).

In a further example of the potential clinical benefits of HCQ, it has been tested in combination with the histone deacetylase (HDAC) inhibitor, Vorinostat (Zolinza, Merck), in patients with advanced solid tumours (Mahalingam, 2014). HDAC enzymes contribute to epigenetic regulation of gene expression, and thus can

contribute to the reprogramming of cancer biology to further drive progression of disease (Falkenberg and Johnstone, 2014). These authors had previously shown that Vorinostat induces protective autophagy, leading to resistance against the drug and that combination with CQ overcame this in a colon cancer cell model and *in vivo* colon cancer xenograft model (Carew et al., 2010). In the Phase I arm, the MTD concluded was 600mg/day HCQ in combination with 400mg Vorinostat. In the phase II arm of the trial, 11 out of the final 24 patients available for evaluation had a partial response or stabilised disease as a result of HCQ and HDAC inhibitor combination. Promisingly, one patient with renal cell carcinoma who had previously failed 7 lines of prior cancer therapies had a partial response to therapy, showing inhibition of autophagy in this case benefited resistant cancer phenotypes.

As a further example of where HCQ may benefit resistant or relapsed cancer phenotypes, the effects of HCQ were examined in patients with relapsed/refractory myeloma in combination with bortezomib (Velcade, Millennium Pharmaceuticals), a proteasome inhibitor. This was reported as an effective anti-cancer combination in a Phase I/II trial (Vogl, 2014). Here no dose-limiting toxicities were noted, although as with other studies described a similar dosing regimen of 600mg (twice a day here) was recommended. In all patients autophagic vacuole accumulation was observed in bone marrow plasma cells, indicative of effective autophagy blockade with HCQ. Out of the 22 patients available for assessment at the end of the study, 45% of these patients had a period of stable disease, 14% had minor responses, and 14% had partial responses to combination therapy. However, again as this was primarily a dosing study there was no group for comparison between bortezomib alone and combination with HCQ. Of interest, patients shown to be previously refractory to bortezomib treatment achieved stable disease when this was combined with HCQ in this trial. This again supported the potential for HCQ in maximising the response to therapeutics which patients may have previously shown resistance to.

In a similar clinical trial to that investigating HCQ in advanced solid tumours and melanoma, and alternative study examined the use of HCQ in combination with radiation and TMZ (Temodal, Merck) co-treatment in 92 patients with newly diagnosed Glioblastoma multiforme (Rosenfeld, 2014). They confirmed HCQ could achieve autophagy inhibition, as seen by autophagic vacuole accumulation and increases in the LC3II/I ratio, in patients receiving over 800mg/day but also in those treated with lower non-toxic dose levels. However, during the Phase I arm of the

study to establish the MTD, the dosage was limited to 600mg/day due to toxicity; with side effects including maculopapular rashes, anaemia and low counts for: white blood cells, lymphocytes, neutrophils, and platelets (at doses above 600mg/day). While autophagy could be achieved in some patients at safe doses of HCQ, this could not be consistently achieved for all patients. Furthermore, in continued phase II analysis no significant improvements in the median overall survival rates were made by the addition of HCQ in comparison to radiation and temozolomide co-treatment without HCQ. Thus, this phase I/II Glioblastoma HCQ trial suggests details need to be further optimised in the clinic to produce the desired effects observed in basic studies; for example a major limiting factor of this study was the inability to consistently achieve autophagy inhibition in patients. It is also important to note, this was the only trial comparing combination with and without HCQ. While the others studies described here showed some clinical benefits of HCQ, they do not make the same comparisons as this study, thus it cannot be determined with HCQ combination strategies have an advantage over single therapies at this stage.

In a further example of autophagy inhibition being difficult to achieve with HCQ in a clinical trial setting, HCQ has also been tested in combination with temsirolimus (Torisel, Pfizer), an MTOR inhibitor, in advanced solid tumours and melanoma (Rangwala, 2014a) in Phase I/II trials. While unlike the study with TMZ in glioblastoma, no MTD was reached in combination strategies with Torisel, although a recommended dose of 600mg twice a day was set. However, proper autophagy inhibition was only observed (via tumour biopsy) in patients treated with this maximum set dose of 1200mg/day HCQ. It is also interesting to note that in patients who experienced clinical benefits, positron emission tomography showed that addition of HCQ to temsirolimus induced a metabolic stress on the cancer cells. Thus, HCQ was producing autophagy/lysosomal related metabolic stress in some responding patients as expected. Unfortunately, stable disease was the best outcome of these clinical trials, meaning no clinical regression of disease was seen with HCQ treatment. Despite this, stable disease was observed in 74% of melanoma patients taken into the phase II stage of the trial. However, as other studies have demonstrated a regression of disease with HCQ combination therapies, this clinical trial was not as successful in comparison.

The conflicting results between clinical trials suggest the efficacy and safety of HCQ is dependent on the drug combination, disease phenotype, and treatment schedule.

Nevertheless, these studies demonstrate HCQ may be useful as a future adjuvant to existing cancer chemotherapies, and even be effective at treating resistant cancer phenotypes.

Cancer Phenotype	Drug Combination	NCT identifier/status	Phase
Glioblastoma multiforme	HCQ,Temozolomide, Radiation	NCT00486603 (results available)	I/II
Advanced solid tumours and melanoma	HCQ,Temozolomide	NCT n/a (results available)	I/II
Advanced solid tumours and melanoma	HCQ, Temsirolimus	NCT n/a (results available)	I/II
Advanced solid tumours	HCQ, Vorinostat	NCT n/a (results available)	I/II
Relapsed/refractory myeloma	HCQ, Bortezomib	NCT00568880 (results available)	I/II
Chronic Myeloid Leukemia	HCQ, Imatinib	NCT01227135 (active, no results yet)	II
Non-small cell lung cancer	HCQ, Erlotinib	NCT01026844 (results available)	II
Metastatic pancreatic cancer	HCQ	NCT01273805 (results available)	II
Metastatic ER+ Breast cancer	HCQ	NCT02414776 (currently recruiting)	I

Table 1.1. CQ/HCQ clinical trials. Small sub-selection of 59 clinical trials using HCQ in cancer as listed on clinicaltrials.gov.

1.4 Hypothesis and Aims

There is extensive direct evidence that autophagy can play a pro-survival role in established tumours, including both breast cancer phenotypes and aggressive metastatic cancer. Moreover, there is a rationale provided by literature evidence for targeting autophagy to improve current cancer therapeutic regimes, i.e. irradiation and chemotherapy. As such the main hypothesis being investigated in this thesis is that autophagy is a beneficial metabolic process that contributes to the survival of a metastatic breast cancer cell line under multiple cellular stressors. The initial strategy for *in vitro* investigations utilised CQ as a pharmacological method of inhibiting autophagy. Here we hypothesise that CQ sensitises 4T1 breast cancer cells to a range of cellular stressor (outlined below) via interfering with the autophagy cascade, and will promote cell death.

The aims of this PhD study are to:

(1) Use the 4T1 murine mammary carcinoma cell line to determine whether multiple cellular stressors; irradiation, growth factor deprivation, and candidate chemotherapeutic compounds, can be potentiated by CQ treatment in metastatic breast cancer phenotypes.

(2) Use genetic ablation of autophagy signalling proteins to determine if any sensitising effects of CQ are due to inhibition of autophagy, or due to lysosomal targeting.

(3) Compare alternate metabolic stressors, i.e. serum, glucose, and/or amino acid starvations, to assess if these differentially affect autophagy activation and/or cell survival responses.

(4) Investigate the mechanism for any potential differences observed between alternate nutrient starvations and whether any cell survival or biochemical responses we see in 4T1 cells are conserved in other cell types.

(5) Identify the potential mechanism of cell death with respect to CQ.

Chapter 2

Materials and Methods

2.0. Materials and methods

2.1 Cell culture

4T1 cells (Miller et al., 1983, Aslakson and Miller, 1992) were purchased from the American Type Culture Collection (ATCC) (ATCC CRL-2539) and cultured in Dulbecco's modified eagle medium (DMEM) with 4.5g/L glucose (Lonza #BE12-614F) supplemented with 10% fetal bovine serum (Labtech #FCS-SA), 4mM L-Glutamine (Lonza #BE17-605E), and 100U/mL Penicillin/Streptomycin (Lonza #DE17-602E) in a humidified incubator with 5% CO_2 at 37^{o}C. Both mouse embryonic fibroblasts (MEF) and UVW glioma cells (obtained from Marie Boyd, (Boyd et al., 2001)) were cultured using the same method. Wildtype and KO MEF were derived from ATG5-/- or ULK1/2 DKO embryos (Kuma et al., 2004, McAlpine et al., 2013). Cell stocks were normally maintained in 10cm cell culture dishes (Greiner Cellstar). Sub-culturing was performed using standard operating procedure with phosphate buffered saline (PBS #BE17-605E) (Lonza) washing and dissociation using trypsin/-EDTA (Lonza #BE17-161E). Cells were counted using a Neubauer haemocytometer, and cell density calculated dependent on the experiment to be performed.

2.2 Stable knockdown of autophagy-related proteins in 4T1 cells

Beclin1 mouse pLKO shRNA (TRCN0000087290) constructs were obtained from Open Biosystems (now Dharmacon); ATG7 mouse pLKO shRNA (*number 1,* TRCN0000092163) was a kind gift from Kevin Ryan (University of Glasgow), and pLKO scrambled shRNA was obtained from Addgene (#1864).

Table 2.1: Antisense sequences for Scrambled, Beclin1, and ATG7 shRNA.

Target protein	Antisense Sequence
Scrambled	GAGCGAGGGCGACTTAACCTTAGG
Beclin1	TTAAACTCACTATACTCCCGC
ATG7	TATTATTGAGTTCAGAGCTGG

Lentiviruses containing the various shRNA were made in HEK293FT cells transfected with specific shRNA-containing pLKO, pCMV HIV, pCMV VSVG

lentiviral packaging plasmids (kind gift of T. Holyoake, University of Glasgow) (in respective ratio of 3:2:1) and standard calcium phosphate as a transfection method. After 2 days, virus was collected from HEK293FT cell media, supplemented with polybrene (Sigma #TR-1003) and clarified using Millex-GP 0.22µm syringe filters (Millipore #SLGP033RS). 4T1 cells were transduced with lentivirus containing pLKO beclin1 shRNA, pLKO ATG7 shRNA, or scrambled pLKO using polybrene (2µg/ml). After puromycin selection (10µg/ml) for 1-2 weeks, to establish a stably knocked down cell line, cells were allowed to grow in normal growth media (DMEM/FBS).

2.3 CRISPR-Cas9 mediated knockout of Hexokinase 2 in 4T1 cells

2.3.i Digestion of the lentiCRISPRv2 plasmid

Use of CRISPR-Cas9 constructs to target a specific gene of interest, here HK2, results in site-specific double-strand cleavage of target DNA, in turn activating double-strand break repair machinery. Repair of these double-strand breaks by non-homologous end joining leads to deletions/mutations of the target gene and thus disruption of correct gene transcription and translation, effectively creating a gene knock-out cell line.

We re-derived a CRISPR-Cas9 lentivirus targeting Hexokinase 2 (HK2). Briefly, the lentiCRISPRv2 (one vector system) plasmid (Addgene #52961) (Sanjana et al., 2014), was digested with BsmB1 (Biolabs #R0580S) and gel purified (QIAquick gel extraction kit, Qiagen) according to the manufacturer's instructions. A sample of this product was checked by agarose gel for size and purity.

2.3.ii Annealing and ligating HK2 oligo sequences

Forward and reverse primer oligonucleotide sequences (1µl of each, final [10µM]) corresponding to mouse HK2 (CRISPR2-Gecko library, found at genome-engineering.org/gecko) (**Table 2.2**) were mixed with 1µl 10X T4 ligation buffer (New England Biolabs, B0202S), 7µl water and annealed using an optimised Thermo-cycler program (95^{o}C 5mins, followed by reduction in temperature to 25^{o}C at a rate of 6^{o}C/min). The final annealed oligonucleotide product was diluted 1/200 to give 50nM final concentrations.

For ligation of the annealed oligos with digested lentiCRISPRv2, 50ng digested plasmid was mixed with 1µl above diluted oligonucleotides, 1µl 10X ligation buffer,

and 0.5µl T4 DNA ligase (Biolabs #M0202S) in a final volume of 10µl. Ligations were carried out overnight at 16^0C.

Table 2.2: HK2 oligo forward and reverse sequences. Oligo overhang regions underlined.

Sequence name	Oligo Sequence (5' to 3')
Hk2MGLibA_24424_F	CACCGACTTCCGTGTGCTCCGAGTA
Hk2MGLibA_24424_R	AAACTACTCGGAGCACACGGAAGTC
Hk2MGLibA_24425_F	CACCGACTAAGGGGTTCAAGTCCAG
Hk2MGLibA_24425_R	AAACCTGGACTTGAACCCCTTAGTC
Hk2MGLibA_24426_F	CACCGATACCTCATCCAGTTTCGTC
Hk2MGLibA_24426_R	AAACGACGAAACTGGATGAGGTATC

2.3.iii Molecular cloning

The ligated product (5µl) was transformed into chemically competent DH5α *E.coli* (100µl) (Invitrogen #12297016) using standard heat shock conditions (20mins on ice, 42^oC 40secs, 1min on ice). Using a standard molecular biology protocol, transformed *E.coli* was transferred on LB-Ampicillin plates and bacterial colonies grown overnight. Colonies were picked and grown overnight in 2ml LB-Amp and the DNA plasmid extracted and purified using QIAprep Spin miniprep kit (Qiagen #27104) as per manufacturer's instructions. The final DNA plasmid product was confirmed by sequencing with the sequencing primer LKO1.5' (GACTATCATATGCTTACCGT) (GATC Biotech, SupremeRun^{TM}).

To amplify the final lentiCRISPRv2 plasmids, confirmed vectors were re-transformed into competent DH5α *E.coli* and grown in LB-Amp broth (200ml) and purified using Qiagen Plasmid Maxi kit (Qiagen #12163). The final DNA yield (A260 / A280 purity) was measured on the Ultrospec 2100 Pro-spectrophotometer (Amersham Biosciences). The final DNA plasmid product was further confirmed for intact guide with sequencing using primer LKO1.5'.

2.3.iv Production of HK2-CRISPR-Cas9 lentivirus

Lentiviruses containing the various HK2 targeting lentiCRISPRv2 were made in HEK293FT cells by transfection with HK2-lentiCRISPRv2 plasmids, pCMV HIV and pCMV VSVG packaging plasmids and standard calcium phosphate method as described above. Virus was collected after 2 days and purified using syringe filers as described above.

2.3.v Viral transfection of 4T1 cells and derivation of CRISPR clonal cell lines

4T1 cells were transduced with high (neat viral supernatant) or low (diluted 5x in DMEM media) titre lentivirus stocks containing HK2-lentiCRISPRv2 plasmids using polybrene (2µg/ml) and left to grow for 48hrs. Cells were selected for lentivirus transduction using puromycin selection (10µg/ml) for 1-2 weeks. To establish stable HK2-CRISPR clonal cell lines, we isolated and expanded colonies (a maximum of 8 per virus). Targeting of HK2 protein in clones was confirmed via western blot as described further below.

2.4 Clonogenic survival assays

2.4.i Assessment of CQ on cell viability in combination with cellular stressors

Cells ($5x10^3$/ml) were plated in Greiner Nunclon surface 6-well cell culture plates (or in some cases (Quinine and LMP studies) 12 well cultures plates were used). 24hrs after seeding, fresh full nutrient growth media was replenished. Following a further 24hrs, cells were stimulated for 24hrs with the following nutrient starvation conditions +/- CQ (25µM) (Sigma #C6628). For serum starvation, full nutrient DMEM was replaced with DMEM (containing 4.5g/L glucose, 4mM L-glutamine and 100U/ml Penicillin/streptomycin as above) with no FBS supplement. For glucose starvation, we used glucose-free DMEM media containing 4mM L-Glutamine (Gibco #11966-025), but no FBS and no Penicillin/streptomycin. For amino starvation, DMEM was replaced with Earle's balanced salt solution (EBSS) (Sigma #E2888), with no supplementation of L-Glutamine or Penicillin/streptomycin. Of note, EBSS contains 1.0g/L glucose. In each case, cells were washed in nutrient starvation media once, before final 24hr incubation.

To examine whether CQ sensitises 4T1 cells to ionising irradiation, following 2hrs pre-treatment with CQ (25µM) (in normal full nutrient DMEM) cells were exposed to

ionising irradiation at 1Gy, 4Gy, or 10Gy doses in X-Rad 225, RPS services. Plates were then returned to normal incubator 5% CO_2 37^{o}C conditions for a 24hr post stress period, before media was replenished and cells were left to grow for a further three days.

We also conducted clonogenic assays using the standard protocol described here with administration of the PI3K/AKT inhibitor, NVP-BEZ-235 (stock 1mM, kind gift from T.Holyoake, University of Glasgow), at a final concentration range of 50-200nM, +/- CQ, diluted in normal full nutrient DMEM.

In all clonogenic experiments performed, after 24hrs stimulation cells were changed back into full nutrient DMEM and left to grow for 3-5 days. At the experimental endpoint, cells were stained with Giemsa stain (Sigma #48900). Briefly, cells were fixed in 1:1 mix of PBS: methanol (1min) followed by a post-fix incubation in 100% methanol (1min) before staining with Giemsa (5mins). To quantify clonogenic survival assays, Giemsa stain was solubilised in 30% acetic acid, and absorbance at 560nm measured on the Ultrospec 2100 Pro spectrophotometer (Amersham Biosciences), adapted from method used in (Bristol et al., 2013). Giemsa blue uptake represented the % of viable cells after differential nutrient starvations or drug treatments, and thus when used in conjunction with clonogenic assays could determine the potential survival and re-population of cells post treatment.

2.4.ii Examination of the nutrient-dependency of CQ-induced cell death

We examined the dependency of CQ on specific nutrient availability to induce cell death using clonogenic assays as described above. As both glucose and amino acid starved conditions listed above were also in the absence of serum, we performed experiments using re-supplementation of dialysed FBS (Sigma #F0392) to dissect effects from the different nutrients. Here, cells were starved of: 1) serum; 2) serum and glucose; or 3) serum and amino acids; as described above for 24hrs. Alternatively, cells were treated with glucose or amino acid starvation alone (via addition of 1% dialysed FBS to the respective conditions).

To examine whether the effects of CQ-induced cell death were dependent on serum or glucose concentration, we performed titration experiments. Cells were treated for 24hrs using standard DMEM (Lonza #BE12-614F) containing differing

concentrations of FBS ranging from 10% to 0% (v/v) as in indicated in the respective figure legends. In a separate experiment, we examined the effect of glucose starvation on CQ-induced cell death. Here, cells were treated for 24hrs with serum-free media containing differing final concentrations of glucose: 4.5g/L (Lonza #BE12-614F), 2.25g/L (50:50 mixture of 4.5g/l and 0.0g/L media), 1.0g/L (ThermoFisher Scientific #12320032), or 0.0g/L (Gibco / Life Technologies #11966-025).

We assessed the potential for glutamine to be a factor in supporting cell survival under glucose-deplete conditions again using clonogenic assays as described above. Here the cells were treated for 24hrs using previously described nutrient starvations or alternatively using serum, glucose and glutamine-free media (ThermoFisher Scientific #A1443001). In addition, cells were also treated for 24hrs with serum, glucose and glutamine-free media (ThermoFisher Scientific #A1443001) containing 4mM glutamine supplementation (Lonza #BE17-605E).

2.5. Western blot analysis

Cell lysates were prepared by lysis on ice in TNTE-FB buffer (150mM Sodium Chloride (NaCl), 20mM Tris pH7.5, 5mM Ethylenediaminetetraacetic acid (EDTA), 10mM Sodium fluoride (NaF), 40mM Beta-glycerol phosphate, 0.3% TX100) supplemented with 1x complete protease inhibitor (Roche #11 873 580 001) for 15mins. Supernatants were harvested using cell scraping technique and samples centrifuged at 4^{o}C (12,000rpm, 5mins). Protein lysate from each sample was mixed with 1.5x Laemmli Sample Buffer containing β-mercaptoethanol (1:2 ratio), heated to 95^{o}C for 5 minutes and loaded onto NuPage 4-12% Bis-Tris pre-cast Gels (Life Technologies, U.K) and run for 40mins at 180V in NuPage MES-SDS running buffer (Life Technologies, U.K). A pre-stained molecular weight marker (Sigma #SDS7B2), indicating proteins from 26kDa to 180kDa **(Table 2.3)** was used as standard. Proteins were transferred onto Immobilon-FL transfer membranes (Millipore, U.K), in Towbin transfer buffer (250mM Tris, 2mM Glycine, 20% (v/v) methanol) using a submerged wet-transfer apparatus (Idea Scientific Company, Minneapolis U.S.A) at 20V for 35mins.

Transferred proteins were visualised using Ponceau-S stain (Sigma #P7170-1L), before cutting and separating appropriate regions for incubation with primary antibodies. Membranes were blocked with 5% non-fat dry milk-TBS for 1hr at room

temperature (RT). After washing with TBS (150mM NaCl, 25mM Tris-base pH 7.4), membranes were incubated with diluted primary antibody (**Table 2.4**) at 4^{o}C overnight, with the exception of actin (RT, 2hrs). Primary antibodies were typically made up in TBS unless stated otherwise below. For all antibodies, membranes were washed 3 times (3 x 5mins) with 0.05% Tween-20 TBS. Appropriate secondary antibodies were chosen (**Table 2.4**, all at 1:5000 dilution) and made up in a 1:1 mixture of TBS: 5% milk-TBS. Membranes were incubated with secondary antibody for 1hr (RT, dark). Following 3 washes (3 x 5mins) with 0.05% Tween-20 TBS, membranes were analysed and quantified using the LICOR odyssey infrared imager and Image Studio v2.0 software. Blots were quantified typically as ratios of protein over the loading control actin, with the exception of LC3-II, which was quantified as a ratio of LC3-II/LC3-I protein. Real protein expression was calculated as sample signal minus background signal.

Table 2.3: Sigma molecular weight marker proteins

Pre-stained protein	**Weight (Da)**
α_2–macroglobulin from human blood plasma	180,000
β-galactosidase from E.Coli	116,000
Lactoferrin from human milk	90,000
Pyruvate kinase from rabbit muscle	58,000
Fumarase from porcine heart	48,500
Lactic dehydrogenase from rabbit muscle	36,500
Triosephosphate isomerase from rabbit muscle	26,600

Table 2.4. Primary and Secondary Antibodies for western blot analyses. Dilution factors, incubation conditions and final concentrations (where available) indicated.

Target protein	Primary Antibody	Secondary Antibody
LC3	Mouse monoclonal (clone 5F10) [Nanotools #0231-100] 1:200, final [0.5µg/ml]	Alexa Fluor® 680 goat anti-mouse IgG (H+L) [ThermoScientific, A-21057]; final [0.4µg/ml]
p62/ SQSTM1 (mouse)	Guinea pig polyclonal [Progen #GP62-C]; 1:500	DyLight™ 680 goat anti-guinea pig IgG (H+L) [KPL, 072-06-17-06]; final [0.2µg/ml]
Beclin	Mouse monoclonal [BD Bioscience #612113]; 1:500, final [0.5µg/ml]	Alexa Fluor® 680 goat anti-mouse IgG (H+L) ThermoScientific, A-21057]; final [0.4µg/ml]
ATG7	Rabbit monoclonal [Cell signalling #8558]; 1:1000 (5%w/v BSA, TBS, 0.1%Tween20)	DyLight™ 800 conjugated goat anti-rabbit IgG {H+L) [ThermoScientific]; final [0.2µg/ml]
P-ACC (S79)	Rabbit polyclonal [Cell signalling #3661]; 1:1000 (5%w/v BSA,TBS, 0.1%Tween20)	DyLight™ 800 conjugated goat anti-rabbit IgG {H+L) [ThermoScientific]; final [0.2µg/ml]
P-AMPKα (T172)	Rabbit monoclonal [Cell signalling #2535S]; 1:1000 (5%w/v BSA,TBS, 0.1%Tween20)	DyLight™ 800 conjugated goat anti-rabbit IgG {H+L) [ThermoScientific]; final [0.2µg/ml]
Caspase-3 (8G10)	Rabbit monoclonal [Cell signalling #9665S]; 1:1000 (5%milk, TBS, 0.1%Tween20)	DyLight™ 800 conjugated goat anti-rabbit IgG {H+L) [ThermoScientific]; final [0.2µg/ml]
PARP	Mouse monoclonal [BD Pharmingen #556362]; 1:1000	AlexaFluor® 680 goat anti-mouse IgG (H+L) [ThermoScientific, A-21057]; final [0.4µg/ml]
Hexokinase II (C64G5)	Rabbit monoclonal [Cell signalling #2867S]; 1:1000 (5%milk, TBS, 0.1%Tween20)	DyLight™ 800 conjugated goat anti-rabbit IgG {H+L) [ThermoScientific]; final [0.2µg/ml]
Actin	Mouse monoclonal (Ab-5) [BD Bioscience #612657]; 1:1000, final [0.25 µg/ml]	Alexa Fluor® 680 goat anti-mouse IgG (H+L) [ThermoScientific, A-21057]; final [0.4µg/ml]

2.6. Fluorescence microscopy

2.6.i Intracellular staining of autophagy, mitochondrial and lysosomal markers

Cells were plated at $1x10^4$/ml on fibronectin (Sigma #F1141) coated coverslips in 24-well plates. Coverslips were coated by exposure to 10µg/ml fibronectin for 5mins. Media was typically replenished and cells treated the next day as indicated in figures. After treatments cells were fixed with 3.2% Paraformaldehyde (PFA) (Agar Scientific #R1026) for 20 minutes and then washed in PBS.

Cells were permeablised with 0.2% Triton X-100 (Sigma #T-9284) for autophagy marker staining (LC3, p62/SQSTM1) or lysosomal staining (LAMP). Cells were blocked with 0.2% (v/v) gelatin (Sigma #G6144) for 20 minutes. Cells were then incubated with the relevant primary antibodies as listed in **Table 2.5;** all antibodies were made up in 0.2% gelatin. Following incubation with the primary antibody (20mins, 4^oC), coverslips were washed 3 times in PBS before incubation with complimentary secondary antibodies (20mins, RT, dark). Cells were washed 3 times in PBS and mounted on glass slides using 4mM Mowiol 4-88 (Sigma #81381), and viewed by Epi-fluorescent (Nikon, Eclipse E600) and confocal microscopes (Leica, SP5).

Intensity of autophagy markers, LC3 and p62, were quantified using Image J; the cytoplasmic region of interest was quantified for fluorescence intensity. 30 cells per condition were analysed, and the average of three independent experiments taken.

LAMP staining was used to detect morphology of the lysosome. We used LAMP as an indicator of lysosomal diameter; this was quantified using Image J (where images were taken on Epi-fluorescent microscope) or LAS AF Lite (where images were taken on confocal). Length of the diameter was measured using a line-drawing tool within software for 10 lysosomes per cell, 30 cells per condition. Final data was derived from the average of 3 independent experiments.

Mitochondrial elongation was quantified using a line-drawing tool within Image J, from images taken on the Epi-fluorescent microscope. 10 mitochondria per cell, 30 cells per condition were analysed, for a pilot experiment as a basis for other PhD students work. Confocal images were taken to give a clearer image of mitochondrial elongation.

2.6.ii Lysotracker Red staining as an indicator of lysosomal acidification

To detect lysosomal acidification, 4T1 cells were plated at $2.5x10^4$/ml on fibronectin coated coverslips and after 24hrs in culture the media was replenished. Following a further 24hrs, cells were treated as indicated in the respective figure legends, with 50nM Lysotracker Red DND-99 (LTR) (Life technologies #L7528) added in the final 30mins of incubation. Cells were washed with PBS and fixed with 3.2% PFA for 20mins. Coverslips were mounted on glass slides using Permafluor (ThermoScientific #TA-030-FM). Cells were immediately imaged using confocal microscopy (Leica, SP5) to avoid light-deactivation of fluorescence.

LTR intensity was quantified as staining intensity within a cytoplasmic region of interest within the cells using LAS AF Lite software. 30 cells per condition were analysed, and raw data normalised as fold changes from control cells (basal acidity). Data was averaged from 3 independent experiments.

Table 2.5. Primary and Secondary Antibodies used for immunofluorescent imaging. Antibody dilution factors and final concentrations (where available) are indicated.

Protein	Primary antibody	Secondary antibody
LC3B	Rabbit monoclonal [Cell signalling #2775S]; 1:200	Anti-rabbit Alexa Fluor® 555 (Molecular probes, Invitrogen #A21428); 1:500, final [4µg/ml]
p62	Guinea pig polyclonal [Progen #GP62-C]; 1:200	Anti-guinea pig Alexa Fluor® 555 (Molecular probes, Invitrogen #A21435): 1:500, final [4µg/ml]
LAMP	Rat monoclonal [BD Biosciences #553792]; 1:200, final [2.5µg/ml]	Anti-rat Alexa Fluor® 555 (Molecular probes, Invitrogen #21434); 1:500, final [4µg/ml]
Tom20	Rabbit polyclonal [Santa Cruz #sc-11415]; 1:200, final [1µg/ml]	Anti-rabbit Alexa Fluor® 555 (Molecular probes, Invitrogen #A21428); 1:500, final [4µg/ml]

2.7. Live cell imaging

Cells were plated at $5x10^4$/ml in 24-well dishes, and treated with nutrient starvations +/- CQ as described for clonogenic assays. Cells were analysed using the Incucyte™ Zoom live-cell imaging system (Essen Bioscience) contained within an incubator at standard growth conditions (5%CO_2. 37^{o}C). Using the Incucyte™ Cell Confluence proliferation assay programme within the Incucyte™ software, we measured cell growth (as an increase in confluency) over the 24hr starvation period, followed by 24hrs in fresh full nutrient media. This programme was set to capture 1 image/well every 1hr using a 4X objective, phase contrast channel. Data points are averages of 2 wells, experiment performed once during a trial of instrument within research institute.

2.8. Examination of signalling and metabolic pathways using pharmacological compounds

2.8.i Analysis of glycolysis.

We performed clonogenic assays and imaging experiments on 4T1 cells exposed to 2-deoxyglucose (2-DG) 2.5mM or 5mM (Sigma #D8375), an inhibitor of hexokinase (Bertoni, 1981). Alternatively, we assessed the effects of alternative glycolysis inhibitors dichloroacetate (DCA, 5mM) (Sigma #347795) (Clark et al., 1987) and gossypol (GP, 20μM) (Sigma #G8761) (Yu et al., 2001).

2.8.ii Analysis of AMPK activation and energy dependency

We performed clonogenic assays with the AMPK activator, 5-Aminoimidazole-4-carboxamide ribonucleotide (AICAR, 1mM final concentration, Sigma #A9978), and used this activator as a positive control in western blot analysis to ascertain AMPK activation under alternate nutrient starvations. To assess changes in energy levels of 4T1 cells, we conducted clonogenic cell survival assays, using methyl pyruvate (10mM final concentration, Sigma #371173) and galactose (0.1%w/v (5mM) final, Sigma #G0750) as alternative cellular carbon energy sources.

2.8.iii Analysis of AKT influence on 4T1 cell survival.

Clonogenic cell survival assays comparing alternative nutrient starvation conditions in combination with CQ (25μM) as described previously were carried out in the absence and presence of the AKT inhibitor API-2 (5μM) (Tocris #2151).

2.9 Comparison of CQ versus alternative quinoline compounds

We compared the nutrient dependency, cell killing and lysosomal effects of alternative quinoline compounds: Primaquine (PQ) (Sigma #160393) and Amodiaquine (AQ) (Sigma #A2799) with CQ. Each of these was made up in the same vehicle, water.

Immunofluorescent LAMP1 and LTR imaging experiments were carried out as described previously and treatment times are indicated in the appropriate figure legends. Additionally, we performed parallel clonogenic survival assays (as

described) comparing CQ, PQ and AQ-mediated cell death responses in relation to nutrient availability.

2.10 Analysis of CQ-induced cell death mechanisms.

2.10.i Analysis of classical apoptotic and necroptotic pathways

Induction of apoptosis in cells subjected to serum starvation +/- CQ (25μM) (where indicated in presence of caspase-3 inhibitor, 10μM z-DEVD-FMK (Tocris #2166)) was analysed by measuring PARP and caspase-3 cleavage via western blot. Staurosporine (1μM, Tocris #1285) was used as a positive control in the lysate experiment as this is a known activator of apoptosis (Belmokhtar et al., 2001). To assess whether cell death induced by CQ was dependent upon apoptosis, clonogenic survival assays were performed in the presence and absence of z-DEVD-FMK, as indicated.

Alternatively, to determine the potential involvement of necroptosis, we performed clonogenic assays in the presence of a RIP1 inhibitor, 20μM Necrostatin-1 (Sigma #N9037). This was within the recommended range for use, 1-100μM, EC50 490nM in Jurkat cells (Degterev et al., 2005, Degterev et al., 2008).

Clonogenic assays were also performed with the addition of N-acetyl cysteine (NAC, stock made fresh on day of use), to determine if ROS production contributed to cell death. Clonogenic assays were set-up following our standard protocol in the presence or absence of 10mM NAC (Sigma #A7250).

2.10.ii Analysis of the lysosomal membrane permeabilisation cell death pathway

We compared the effects of CQ against two characterised LMP inducers, Leucyl-Leucyl-O-Methyl ester (LLOME, Sigma #L7393) (Aits et al., 2015b) and ciprofloxacin (CPX, Sigma #17850) (Boya et al., 2003) to examine whether the cell death induced by CQ was comparable to other LMP-inducing drugs. We performed clonogenic cell survival assays as described above with alternate nutrient starvation conditions in the presence or absence of 25μM CQ, 5mM LLOME, or 150μg/ml CPX.

To ascertain whether these LMP-inducing compounds exerted similar effects on the lysosome as CQ, we performed immunofluorescent image analysis as described

above using LAMP as a marker. Here, we measured lysosomal diameter in response to nutrient starvations in the absence or presence of 25μM CQ, 5mM LLOME, or 150μg/ml CPX. To further understand the interrelationship between lysosomal enlargement and lysosomal deacidification, we performed parallel LAMP and LTR imaging studies in the same experiments.

As a direct method of measuring the induction of LMP, we utilised a digitonin based extraction assay (Groth-Pedersen et al., 2007, Aits et al., 2015a). Cells were plated at $1x10^4$/ml in 12 well tissue culture plates and the following day treated using the nutrient starvation and drug combination conditions and times indicated in figure legends. After treatment, the media was removed from the cells, cells were washed with PBS and were then incubated on ice for 15mins in a minimal volume (200μl/well) extraction buffer (*250mM sucrose, 20mM Hepes pH 7.5, 10mM KCl, 1.5mM $MgCl_2$, 1mM EDTA, 1mM pefablock,)* containing the desired concentration of Digitonin (Sigma #D141) (as indicated in figure). We used concentrations ranging from 25μg/ml – 50μg/ml to extraction cytosolic fractions and 200μg/ml - 300μg/ml to extract whole cell fractions.

Enzymatic reactions were set up in 96-well plates as follows: 50μl of reaction buffer (*50mM sodium acetate pH 6.0, 4mM EDTA, 8mM DTT, 1mM pefablock)* containing the cathepsin B substrate (20μM z-Arg-Arg-7-amido-4-methylcoumarin hydrochloride (zRR-AMC, Sigma #C5429)) was added to one volume (50μl) of the supernatant from the extraction step and mixed by pipetting. The plate was scanned after 20mins incubation at 30^{o}C using the POLARstar Omega plate reader (BMG Labtech) *(wavelength excitation 355nm, emission 460nm)* to detect liberation of AMC fluorophore. Cathepsin activity was calculated in relative fluorescence units (RFU), as signal from sample minus a blank control (water).

Chapter 3

Investigation of the sensitising effects of CQ in a 4T1 metastatic breast cancer cell model and the influence of nutrient conditions on CQ efficacy

3.1 Introduction

While autophagy has been implicated in both tumour suppression and tumour cell survival, the inhibition of this highly conserved degradative process has been identified as a potential strategy for targeting and committing cancer cells to die. The anti-malarial compound Chloroquine (CQ), with its lysosomotropic properties and ability to block end-stage autophagy degradation, has been heavily utilised to study this potential anti-cancer approach (Bellodi et al., 2009, Liang et al., 2014). Indeed, along with its derivative hydroxychloroquine (HCQ), CQ remains the only 'autophagy inhibitor' being advanced through anti-cancer clinical trials to date (Duffy et al., 2015). Despite this, data being released from ongoing clinical trials is mixed with respect to supporting CQ as an anti-cancer therapy. Some studies have reported that CQ failed to achieve efficient autophagy inhibition in patients unless administered at extremely high doses (Rosenfeld, 2014, Rangwala, 2014a). However, other studies reported that CQ could indeed inhibit autophagy at reasonable doses and in turn improve concurrent therapy outcomes (Rangwala, 2014b). Thus, the application of CQ in the clinic is still unclear. The opposing findings of current clinical trials could suggest that the potential therapeutic benefits from CQ treatment are dependent upon the combination strategy used and other such factors as disease phenotype.

The potential for CQ *in vitro* has been investigated across multiple cancer phenotypes and in combination with varied approved cancer therapeutics. For instance, CQ improved the efficacy of the TKI Imatinib mesylate in CML blast crisis cells (as a model of advanced CML) (Bellodi et al., 2009), and has been shown to sensitise colon cancer cells to anti-angiogenic (Bevacizumab) and platinum (oxaliplatin) drugs (Selvakumaran, 2013). Importantly for the research outlined by this thesis, CQ has also been identified to have sensitising properties with respect to breast cancer therapeutics such as Herceptin and carboplatin in multiple cell models, including TNBCs (Cufi et al., 2013, Liang et al., 2016). However, there is still a question as to whether the beneficial effects of CQ in these cancer cell lines are dependent on the inhibition of autophagy. While some studies have shown genetic ablation of autophagy mimicked the effects of CQ, others have shown opposing results. For example, investigations using CQ in the CML blast crisis cells showed genetic knockdown of ATG5 or ATG7 replicated the benefits of CQ treatment (Bellodi et al., 2009). Conversely, Maycotte et al., 2012, showed

knockdown of ATG12 or Beclin1 did not mimic the sensitising effects of CQ in model of metastatic breast cancer (Maycotte et al., 2012). Taking into consideration the conflicting data describing the autophagy inhibitory properties of CQ in cell models and the recent outcomes from clinical trials suggesting that in some contexts autophagy inhibition with CQ in patients is difficult to achieve, there still remains doubt over whether CQ could be an effective treatment for cancer.

Here, the sensitising properties of CQ were examined in a highly metastatic murine mammary carcinoma cell line. 4T1 breast cancer cells were originally derived from a spontaneously arising mammary tumour in wild-type BALB/c mice by Fred Miller and colleagues at the Karmonos Cancer Institute (Miller et al., 1983). They have been shown to be highly metastatic, completing all stages of metastasis and forming visible nodules in the lung, as well as metastasising to the bone, liver, and brain (Aslakson and Miller, 1992, Eckhardt et al., 2005, Tao et al., 2008). Indeed, the metastatic profile of these cells resembles the metastasis which occurs in stage IV human breast cancer. Furthermore, 4T1 mammary carcinoma cells are poorly immunogenic, therefore can be injected into immunocompetent mice. This is important as many *in vivo* cancer studies are performed in immunodeficient mice which does not reflect human disease in which the immune system interacts and plays a role in the development and progression of cancer (Yang et al., 2004a, Tao et al., 2008, Chen, 2011). Indeed, this cell line has been used in various studies into breast cancer biology, but in particular with reference to metastasis. Using this cell model, the transcription factor, Twist, was identified to be up-regulated in highly metastatic cells compared to non-metastatic phenotypes and was found to contribute to EMT (Yang et al., 2004a). Furthermore, the hypoxia-inducible protein, carbonic anhydrase 9 (CAIX), was shown to promote metastasis in the 4T1 metastatic breast cancer model (Lou et al., 2011). These studies show the 4T1 is a highly effective model for metastatic research.

The 4T1 model of metastatic breast cancer has been previously used for investigating the effects of autophagy inhibition with respect to cell survival and metastasis. Using this model, work by Maycotte *et al*., 2012 shown that CQ sensitised 4T1 cells to the PI3K inhibitor LY294002, mTOR inhibitor rapamycin, and chemotherapeutic compound cisplatin (Maycotte et al., 2012). In addition, *in vivo* work performed by Jiang *et al.,* 2010, showed that CQ could significantly inhibit the growth of 4T1 tumours and induce apoptosis as a single agent (Jiang et al., 2010).

Taken together these two papers indicate the beneficial effects of CQ in 4T1 cancer cells have previously been observed. Depending on the study, CQ has been shown to have the potential to have an effect on its own, as well as sensitising to chemotherapeutic or drug treatments (though this effect might be independent of autophagy). In using this highly aggressive metastatic model of breast cancer, we aimed to characterise the sensitising effects of CQ on *in vitro* cell survival with a focus on nutrient stressors. Based on our experimental outcomes, we aimed in the long run for our insights to directly translate into further studies of 4T1 *in vivo* tumour growth and metastatic responses.

In a revised version of the key hallmarks of cancer (Hanahan and Weinberg, 2011), the dysregulation of cancer metabolism is highlighted as a key event in maintenance of tumour growth and survival. Otto Warburg first noted cancer cells to have an altered metabolic profile in comparison to 'normal' cells (Warburg et al., 1927, Warburg, 1956); it is now generally accepted that cancer cells favour glycolysis as a primary source of energy-generating metabolism even under aerobic conditions where mitochondrial oxidation would usually be utilised. This high dependency on glucose has thus been termed the 'Warburg effect'. In this chapter, the potential of CQ to enhance cell death in response to specific withdrawal of nutrients and inhibition of glycolysis is investigated using glucose withdrawal and glycolysis inhibitors; the glycolysis pathway and inhibitor targets are highlighted in Figure 3.1. Here glycolysis begins with conversion of glucose to glucose-6-phosphate by the rate limiting enzyme hexokinase, inhibited by 2-DG (Parniak and Kalant, 1985). Through a series of glucose conversion steps the final product of glycolysis is pyruvate which can be further metabolised into substrates for the TCA cycle (Acetyl CoA). Inhibition of the final stages of glycolysis and pyruvate metabolism is being investigated as a potential anti-cancer therapeutic strategy using DCA and Gossypol (Delaney et al., 2015, Le et al., 2010) therefore providing rationale for use of these compounds in CQ combination studies.

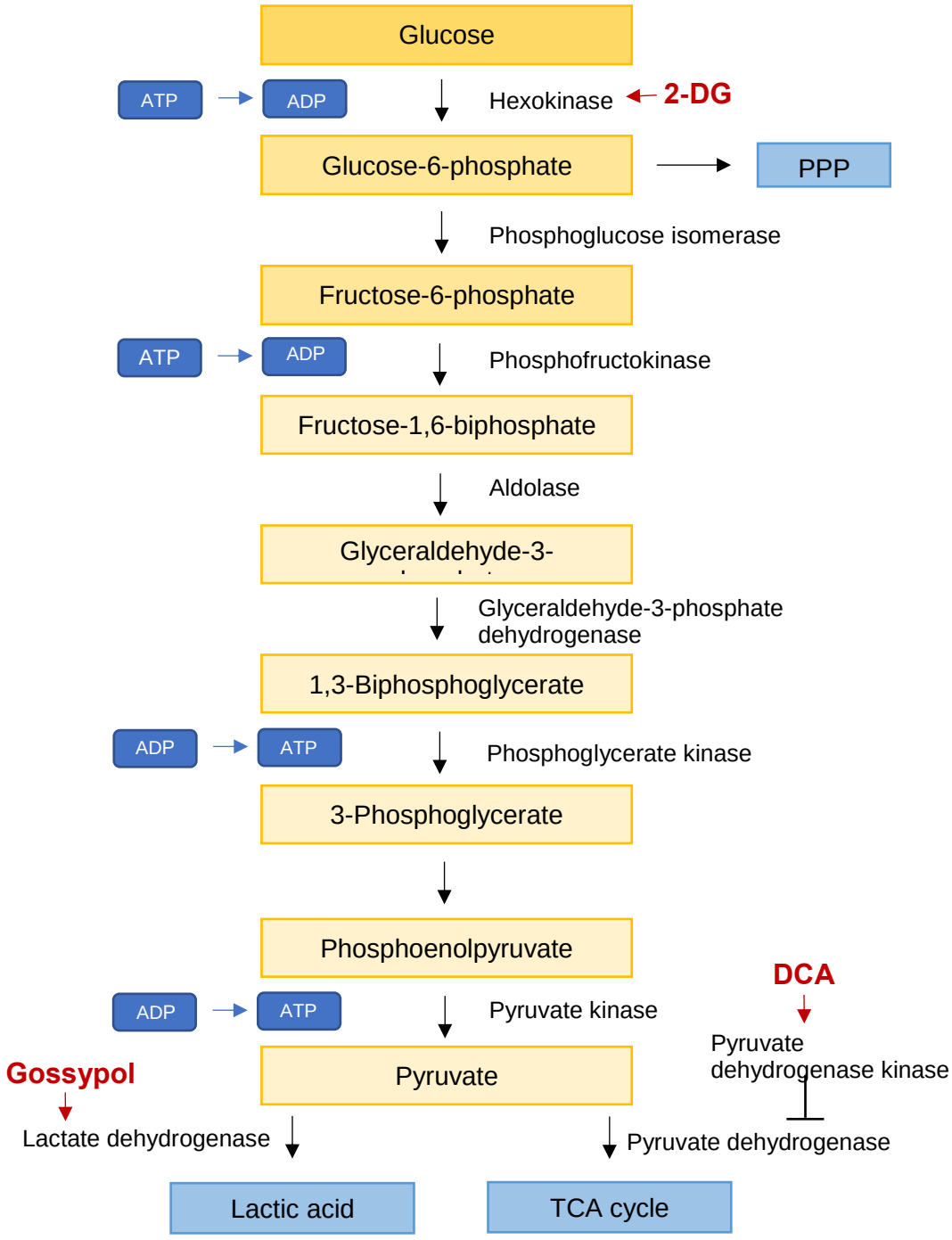

Figure 3.1. The Glycolysis pathway and glycolysis inhibitor target proteins. The glycolysis pathway is frequently mutated in cancer and/or tumour cells. Here the key stages of glycolysis are outlined including glucose conversion to glucose-6-phosphate by hexokinase, the formation of pyruvate by pyruvate kinase, and the downstream conversion of pyruvate into substrates available for alternative pathways e.g. TCA cycle. The targets within this pathway of 3 glycolysis inhibitors used in studies described by this thesis are outlined above.

In this chapter, the ability of CQ to sensitise 4T1 mammary carcinoma cells to varied cellular stressors was assessed and characterised. In addition, the responses of 4T1 cells to activate autophagy with respect to differential nutrient starvations were examined. Using 4T1 cells, the objectives of this chapter were to:

(1) Examine the potential for CQ to sensitise breast cancer cells to γ-irradiation, PI3K/mTOR inhibitor NVP-BEZ-235, and/or nutrient stress with respect to *in vitro* cell survival.

(2) Investigate whether autophagy is induced under alternate nutrient starvation conditions.

(3) Determine whether the effects of CQ are dependent on autophagy inhibition using genetic ablation of autophagy.

(4) Compare CQ efficacy (on *in vitro* cell survival) under alternate nutrient stressors and investigate any differences observed.

3.2 Results

Autophagy is a conserved cellular process whereby damaged organelles and cellular proteins are sequestered into autophagosome membranes, and targeted to the lysosomes. Autophagy can be induced by a variety of stresses including hypoxia, nutrient starvation, and anti-cancer therapies (Wilkinson et al., 2009, Kim et al., 2015, Jo et al., 2015). Thus, it is hypothesised that activation of autophagy allows the cell to survive environmental insults. Conversely, inhibition of autophagy would promote cell death under stress, such as the withdrawal of nutrients, exposure to radiation, or chemotherapeutics. Initial plans were to inhibit autophagy via genetic silencing of ULK1 in 4T1 cells; however the retrovirus used did not produce efficient knockdown as measured by PCR (data not included). To test the hypothesis that autophagy inhibition would induce cell death in the context of cellular stress, the effects of the well-established autophagy-lysosomal inhibitor, Chloroquine (CQ) were examined.

3.2.i Chloroquine, an autophagy-lysosomal inhibitor, sensitises 4T1 cells to metabolic stress, irradiation, and chemotherapeutics

For initial experiments, the survival of 4T1 cells when subjected to growth factor deprivation via serum withdrawal, using clonogenic survival assays was examined. Using 24hr treatments, CQ alone (25μM) displayed minimal cytotoxic activity, as did serum starvation alone. However, we found that a blockade of autophagy using CQ, simultaneously with serum withdrawal led to a strong reduction in cell survival **(Fig 3.2a)**. Furthermore, this effect was concentration-dependent; a reduction in CQ-dependent cell survival was noted as the concentration of foetal calf serum was gradually reduced **(Fig 3.2b)**. A 50% decrease in the serum concentration (from 10% to 5% final FBS v/v) was sufficient to induce cell death ($p<0.05$) when coupled with CQ. A serum concentration of 0.5% further reduced cell survival, similar to full withdrawal of serum.

In addition to sensitising 4T1 cells to serum starvation-induced cell death, the potential of CQ to sensitise 4T1 cells to other forms of cancer therapy-related cell stress such as DNA-damaging irradiation was explored. An up-regulation in autophagy has been noted in breast cancer cell lines, MDA-MB-231 and HBL-100,

in response to ionising irradiation (Chaachouay et al., 2011), and more recently CQ has been shown to promote γ-irradiation induced cell death in cancer stem cells resistant to radiation (Firat et al., 2012). Data presented here demonstrated that CQ also potentiated the effects of irradiation-induced cell death **(Fig 3.3a).** Irradiation alone was able to induce cell death in 4T1 cells in a dose-dependent manner (clearly observed only with 10Gy). However, 2hrs pre-treatment of the cells with CQ sensitised the cells to irradiation. Lower doses of irradiation were needed to illicit the same level of cell death; in the presence of CQ 4Gy irradiation was sufficient to induce the same decrease in clonogenic survival potential as 10Gy irradiation alone.

As CQ sensitised 4T1 cells to growth factor/serum deprivation, CQ potentiation of cell death mediated by inhibition of specific growth factor-induced signalling pathways, namely PI3K/AKT, was examined. The PI3K/mTOR inhibitor, NVP-BEZ-235 was utilised for the purposes of these studies. This compound has been identified to potently inhibit these proteins through direct binding to the ATP-binding cleft and has previously demonstrated efficacy when used in combination with other anti-cancer agents, such as temozolomide (Maira et al., 2008). Furthermore pre-clinical investigations combining NVP-BEZ-235 and CQ in both neuroblastoma and neuroendocrine cancer cell lines have demonstrated synergy between these two compounds (Seitz et al., 2013, Avniel-Polak et al., 2015). Importantly, NVP-BEZ-235 has then been investigated in clinical trials for potential treatment of neuroendocrine tumours (Clinical trial identifier NCT01658436) and advanced renal cell carcinoma (Clinical trial identifier NCT01453595 (N. Fazio, 2014, M Carlo. and JJ Hsieh., 2016). Here, cell death in our 4T1 mammary carcinoma cell model was induced by PI3K/mTOR kinase inhibitor NVP-BEZ-235 in a dose-dependent manner. Furthermore, cell death for each dose of NVP-BEZ-235 was potentiated by co-addition of CQ **(Fig 3.3b).** Together these findings show CQ has potentiating activity to the effects of growth factor starvation (metabolic stress), PI3K cell signalling inhibitors, and radiation.

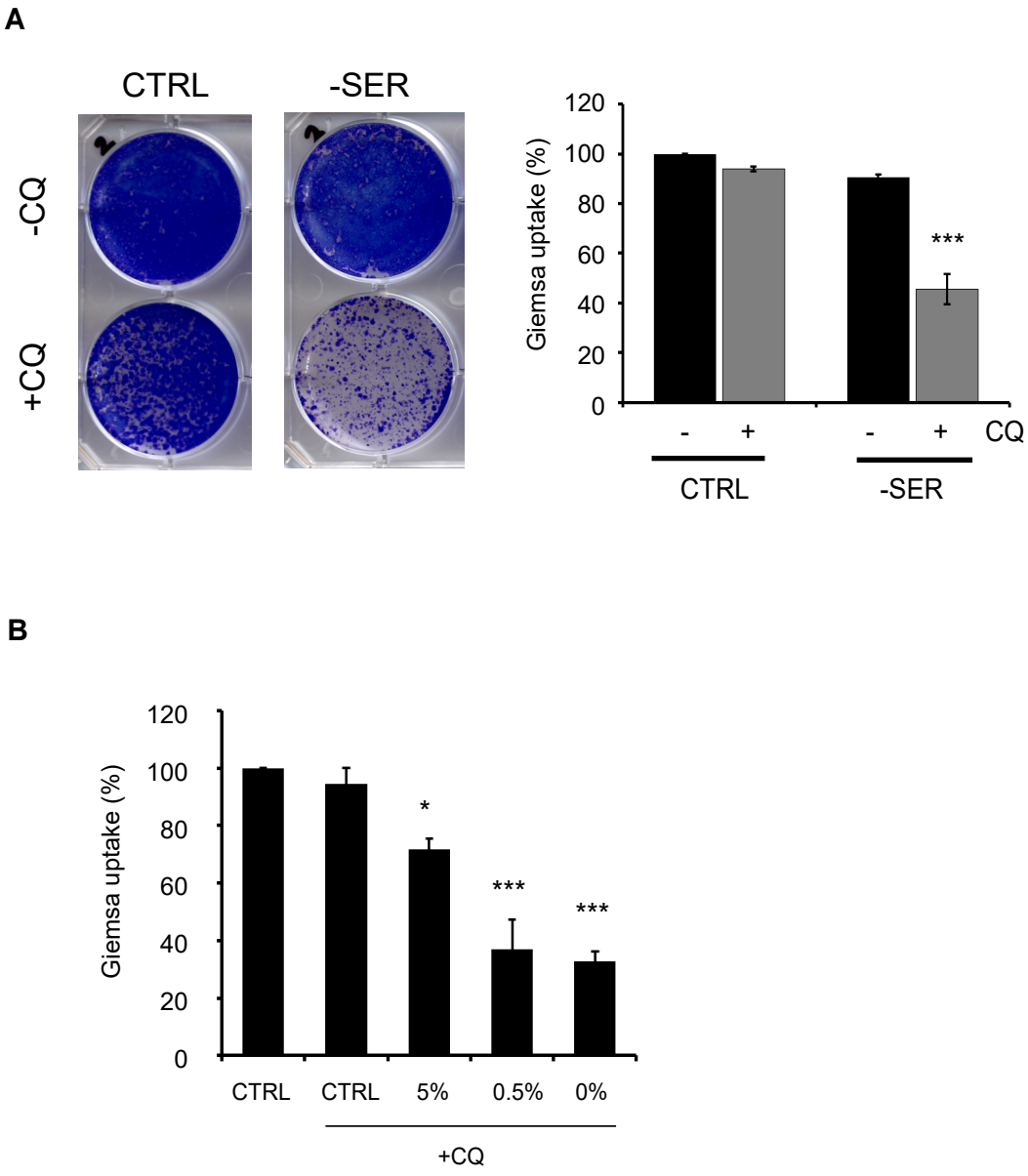

Fig 3.2: Chloroquine sensitises 4T1 cells to growth factor deprivation.

(A) 4T1 cells were treated with full nutrient (CTRL) or serum-free DMEM (-SER) +/- CQ (25μM) as indicated for 24hrs. The media was changed to normal full nutrient drug-free growth media and after 3 days cells were stained with Giemsa blue, and cell viability quantified as described in Methods. Giemsa uptake shown as % of ctrl one-way ANOVA with Tukey post-test, comparison to untreated control (***P < 0.001), n=3 technical replicates, errors bars +/- SEM.

(B) 4T1 cells were treated with DMEM containing differing FBS concentrations +CQ (25μM) as indicated. Cell viability was measured as in (A). Giemsa uptake as % of control, one-way ANOVA with Tukey post-test, comparison to untreated control (***P < 0.001, *p<0.05), n=3 technical replicates, errors bars +/- SEM.

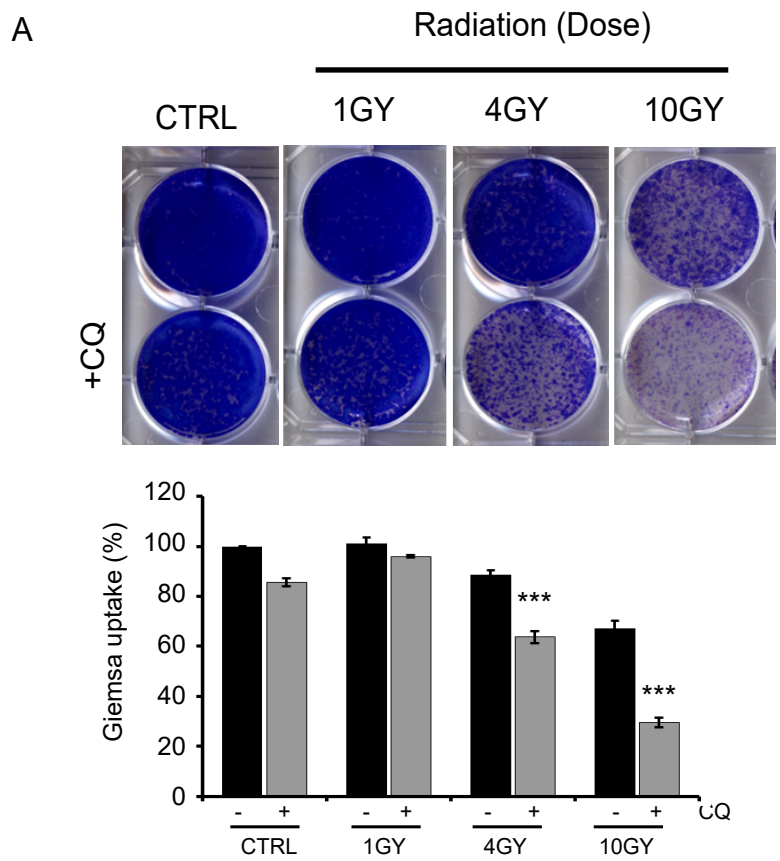
A
Radiation (Dose)
CTRL
1GY
4GY
10GY
+CQ
Giemsa uptake (%)
120
100
80
60
40
20
0
***
***
- + - + - + - + CQ
CTRL
1GY
4GY
10GY

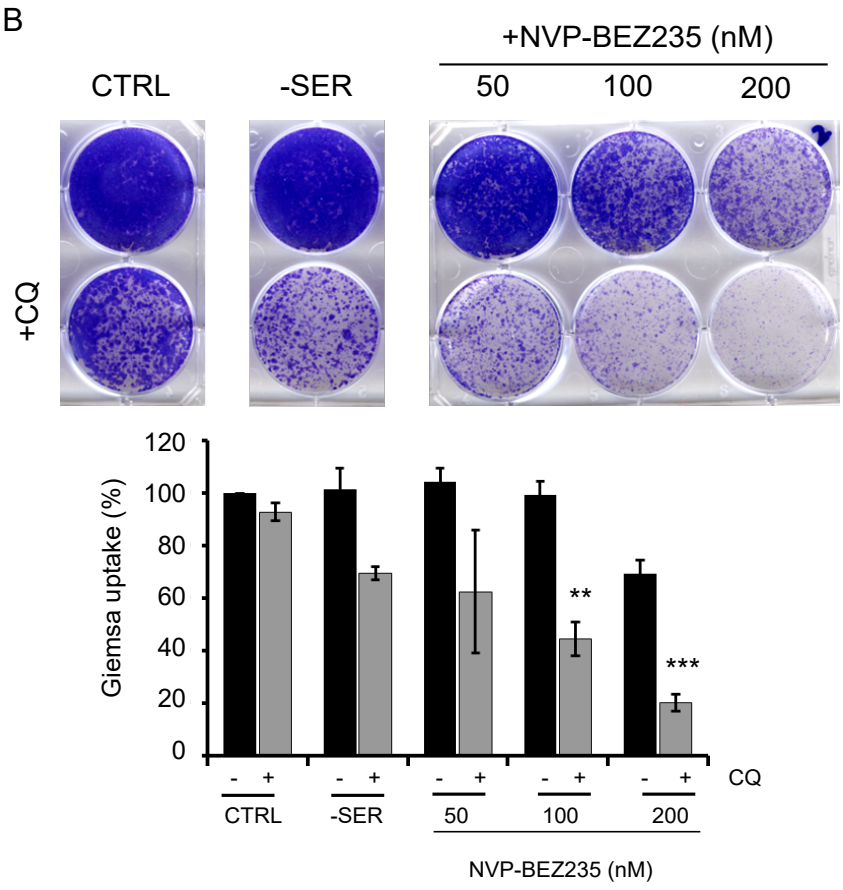
B
+NVP-BEZ235 (nM)
CTRL
-SER
50
100
200
+CQ
Giemsa uptake (%)
120
100
80
60
40
20
0
**
***
- + - + - + - + - + CQ
CTRL
-SER
50
100
200
NVP-BEZ235 (nM)

Fig 3.3 (previous page): Chloroquine sensitises 4T1 cells to therapeutic stressors; ionising irradiation and dual mTOR-AKT inhibition.

(A) 4T1 cells were exposed to increasing doses of irradiation and incubated +/- CQ (25μM) as indicated for 24hrs. Media was replenished and cell viability assessed as in Fig 3.1. Giemsa uptake shown as % of control, one-way ANOVA with Tukey post-test, comparison to respective treatment (-)CQ (***P < 0.001), n=3 technical replicates, errors bars +/-SEM.

(B) 4T1 cells were treated with the dual mTOR/PI3K inhibitor, NVP-BEZ-235, at increasing doses +/-CQ (25μM) as indicated for 24hrs. Media was replenished and cell viability assessed as in Fig 3.1. Giemsa uptake shown as % of control, one-way ANOVA with Tukey post-test, comparison to respective treatment (-) CQ (**P < 0.01, ***P < 0.001), n=3 technical replicates, errors bars +/-SEM.

3.2.ii Autophagic flux activation is nutrient selective

It is well documented that alternate nutrient starvations, namely glucose starvation vs. amino acid starvation, initiate formation of autophagosomes and the activation of autophagy through different signalling cascades. As stated previously, glucose starvation has been shown to activate AMPK signalling, whilst amino acid starvation initiates autophagy through the inactivation of mTORC1 signalling. In the current prominent model, both of these pathways converge on ULK1, leading to a crosstalk of distinct phosphorylation events, which together signal activation of autophagy (Kim et al., 2011). However, recent evidence has highlighted potential discrepancies with this accepted model of autophagy activation in response to nutrient stress. In some instances, glucose starvation has led to inhibition of autophagy rather than induction of the process (Ramirez-Peinado et al., 2013, Moruno-Manchon et al., 2013). In light of these results, the effects of different nutrient starvation conditions on their ability to induce autophagy in 4T1 cells was compared.

In **Fig 3.4a** autophagy activation in 4T1 cells was first confirmed in response to starvation of either glucose or amino acids. The conversion of LC3-I to LC3-II is a standard readout for the activation of autophagy. However, western blots can often be difficult to interpret as an increase in LC3-II is also seen when autophagy is blocked at the lysosome. CQ was used as a further tool to block autophagy degradative flux. As expected, large accumulation of LC3-II with just 3hrs CQ treatment was observed. Interestingly, there were clear differences in the LC3-II levels in glucose- vs. amino acid- starved cells. Glucose-starved cells showed a high level of LC3-II, when quantified as either a ratio over LC3-I protein or LC3-II over actin, which could be interpreted as activation of autophagy. However, the amount of LC3-II present in the cell lysates was very similar to the accumulation seen with CQ-mediated blockade of autophagy. In contrast, the LC3-II levels in amino acid-starved cells were low in comparison. These data could suggest that glucose starvation actually mediates a block of autophagy rather than activation. Amino acid activation is interpreted to stimulate both LC3-II generation during the formation of the autophagosome and subsequent protein turnover.

To investigate these different effects further, flux through the autophagy pathway was blocked in the presence of nutrient starvations **(Fig 3.4b)**. As seen in the previous experiment, a marked differences were observed in the LC3-II content of the cell lysates of glucose- vs. amino acid-starved cells (both condition also lacking

serum). To clarify, effects from just serum starvation were also measured. Cells starved of serum alone induced a relatively smaller amount of LC3-I to LC3-II conversion as compared to amino acid (and serum) starvation. When autophagy flux was blocked with CQ, there were marked increases in the ratio of LC3-II/LC3-I in control, serum-starved, and amino acid-starved conditions. However, this was not the case in glucose-starved cells. This could indicate as proposed that glucose starvation does not initiate flux through the autophagy pathway, but instead inhibits it. As a second autophagy measure, p62/SQSTM1 protein levels, an adaptor protein broken down during the autophagy process, were analysed. Overall, effects were not as dramatic, but quantification suggested that glucose starvation induced increases in p62, whereas amino acid starvation did not. CQ treatment did not further increase p62 levels following glucose starvation, but did following the other nutrient starvation conditions to varying extents. This correlation between LC3II and p62 data again suggests glucose starvation may block autophagy flux rather than stimulate it.

Since differences between glucose- vs. amino acid-starvation were unexpected, and also to clarify effects suggested from p62 immunoblotting, autophagy induction driven by alternate nutrient stressors was further investigated by fluorescent cell imaging. These analyses showed that p62 **(Fig 3.5a)** or LC3 **(Fig 3.5b)** puncta intensity increased to a greater extent in glucose starved cells in comparison to amino acid starved. CQ treatment also strongly increased p62 and LC3 puncta as expected from a lysosomal block. Furthermore, the puncta intensity in glucose starved cells was similar to that of CQ treatment.

Our results indicated that 4T1 cells differently sensed glucose- vs. amino acid-starvation. To further investigate the differential effects of alternate nutrient starvations, the mitochondria morphology upon glucose or amino acid starvation was examined. It has been suggested to avoid undergoing mitophagy mitochondria have the potential to shift from a small, fragmented phenotype to a more elongated (or tubulated) morphology (Rambold et al., 2011). Here, mitochondria were stained with an antibody targeting the outer mitochondrial membrane protein, translocase of outer membrane protein 20 (Tom20), and mitochondrial length and shape measured using confocal microscopy **(Fig 3.6)**. Again, there were stark differences in the response of the cells to specific nutrient starvations. In glucose starved cells, mitochondria remained small and rounded in shape, similar to untreated cells. In

contrast, amino acid starvation induced significant mitochondrial tubulation and elongation. Taken into context with previous findings, the mitochondrial tubulation we observed under amino acid starvation could be interpreted as a response to avoid mitophagy. As this response was not observed under glucose starvation, this may suggest mitophagy was not induced by the specific withdrawal of glucose. These data again highlight and corroborates the robust differences in 4T1 cell nutrient-sensing responses.

In summary, our studies into the nutrient sensitivity of 4T1 cells have identified clear differences following glucose vs. amino acid starvation. While amino acid starvation induces a marked induction of autophagy, glucose starvation elicits characteristics of autophagy inhibition similar to that of autophagy-lysosomal inhibitors.

Fig 3.4 (next page): Amino acid starvation and glucose starvation have opposing effects on autophagic flux in 4T1 cells

(A) 4T1 cells were treated with full nutrient DMEM (CTRL), serum- and glucose-free DMEM (-GLC), or serum- and amino acid-free media (-AA) for 3hrs. Alternatively, cells were incubated with CQ (25μM) under full nutrient conditions for 3hrs. Cells were lysed and LC3 protein assessed via western blot analysis. Actin was used as a loading control. Immunoblotting was quantified as described in Methods and expressed as either LC3-II normalised to Actin (arbitrary units) or as the LC3-II/LC3-I ratio. Data are representative of 4 western blots.

(B) 4T1 cells treated with the indicated nutrient conditions +/- CQ (25μM) for 4hrs. Cells were lysed and LC3 and p62 proteins assessed via western blot analysis. Actin was used as a loading control. Data are representative of 3 western blots.

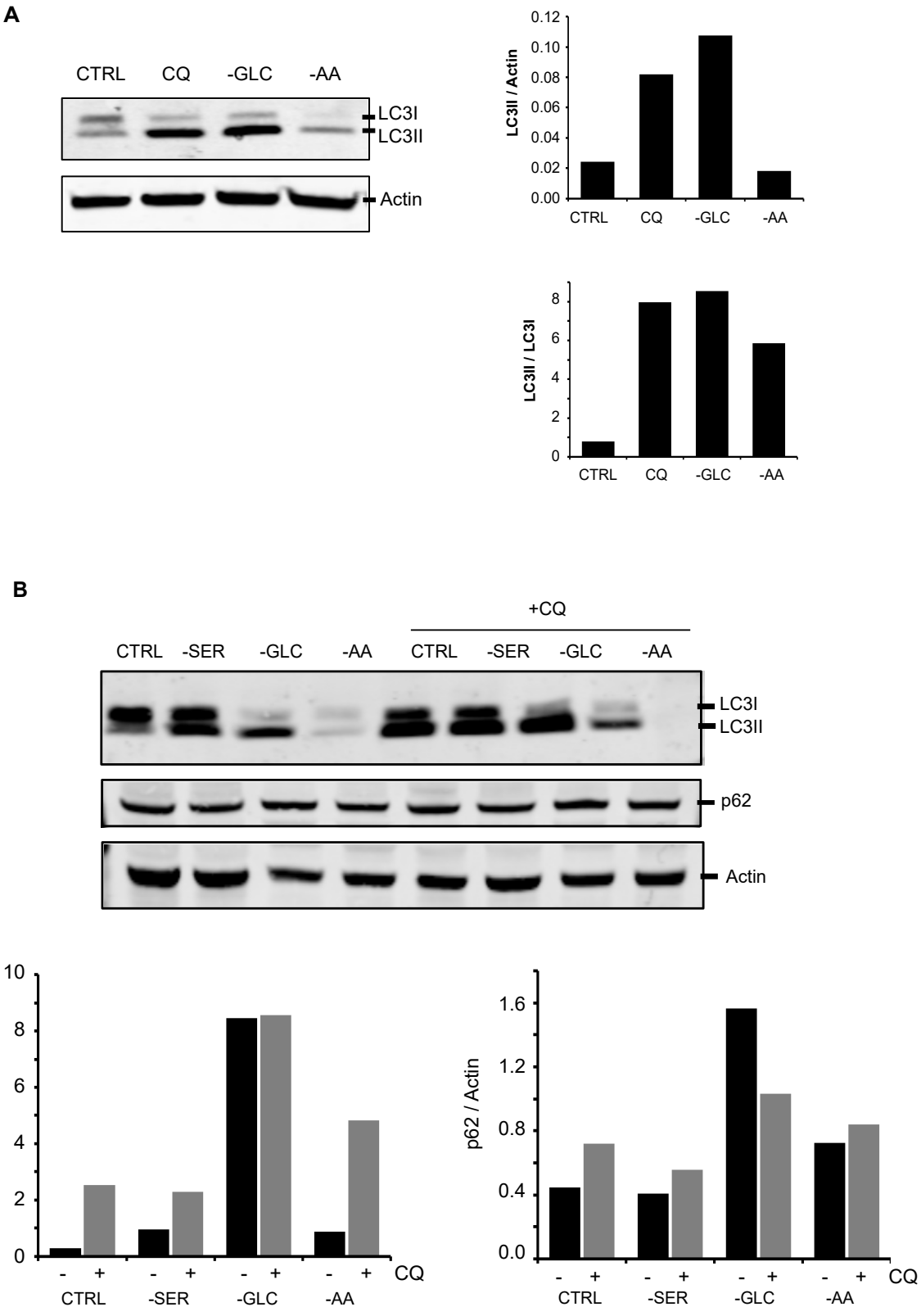
A
CTRL
CQ
-GLC
-AA
LC3I
LC3II
Actin
LC3II / Actin
0.12
0.10
0.08
0.06
0.04
0.02
0.00
CTRL
CQ
-GLC
-AA
LC3II / LC3I
8
6
4
2
0
CTRL
CQ
-GLC
-AA
B
+CQ
CTRL
-SER
-GLC
-AA
CTRL
-SER
-GLC
-AA
LC3I
LC3II
p62
Actin
LC3II / LC3I
10
8
6
4
2
0
- + - + - + - +
CQ
CTRL
-SER
-GLC
-AA
p62 / Actin
1.6
1.2
0.8
0.4
0.0
- + - + - + - +
CQ
CTRL
-SER
-GLC
-AA

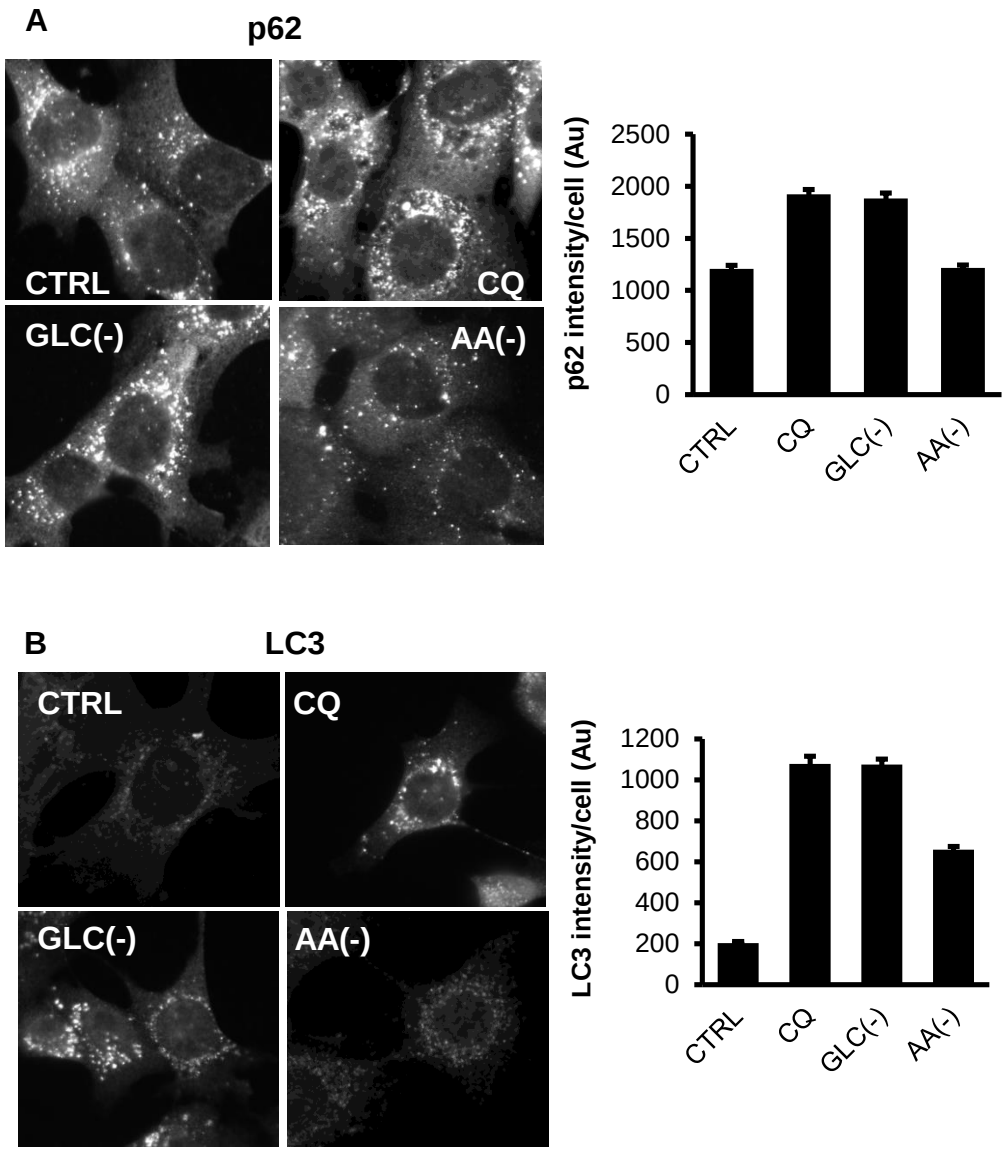

Fig 3.5: Glucose starvation leads to a block in autophagic flux in 4T1 cells. 4T1 cells were treated with CQ (25μM), glucose-free and serum-free (GLC(-)) media or amino acid-free and serum-free media (AA(-)) for 8hrs. Cells were fixed and stained for (A) p62 or (B) LC3. Images were captured by epifluorescent microscopy. p62 and LC3 puncta intensity were measured in 30 cells per condition as described in Methods. Data shown are mean p62 or LC3 puncta intensity / cell, n=3 independent experiments, errors bars +/- SEM.

Fig 3.6 (next page): Mitochondrial morphology differs in response to amino acid or glucose starvation

4T1 cells were treated with glucose-free and serum-free media (-GLC) or amino acid-free and serum-free media (-AA) for 4hrs. Cells were fixed and stained for Tom20. Images were captured by confocal microscopy. Mitochondrial length was quantified; measuring 10 mitochondria per cell, 30 cells per condition. Each data point represents the average mitochondrial length per cell. Data are representative of pilot experiment (a basis for other PhD students work).

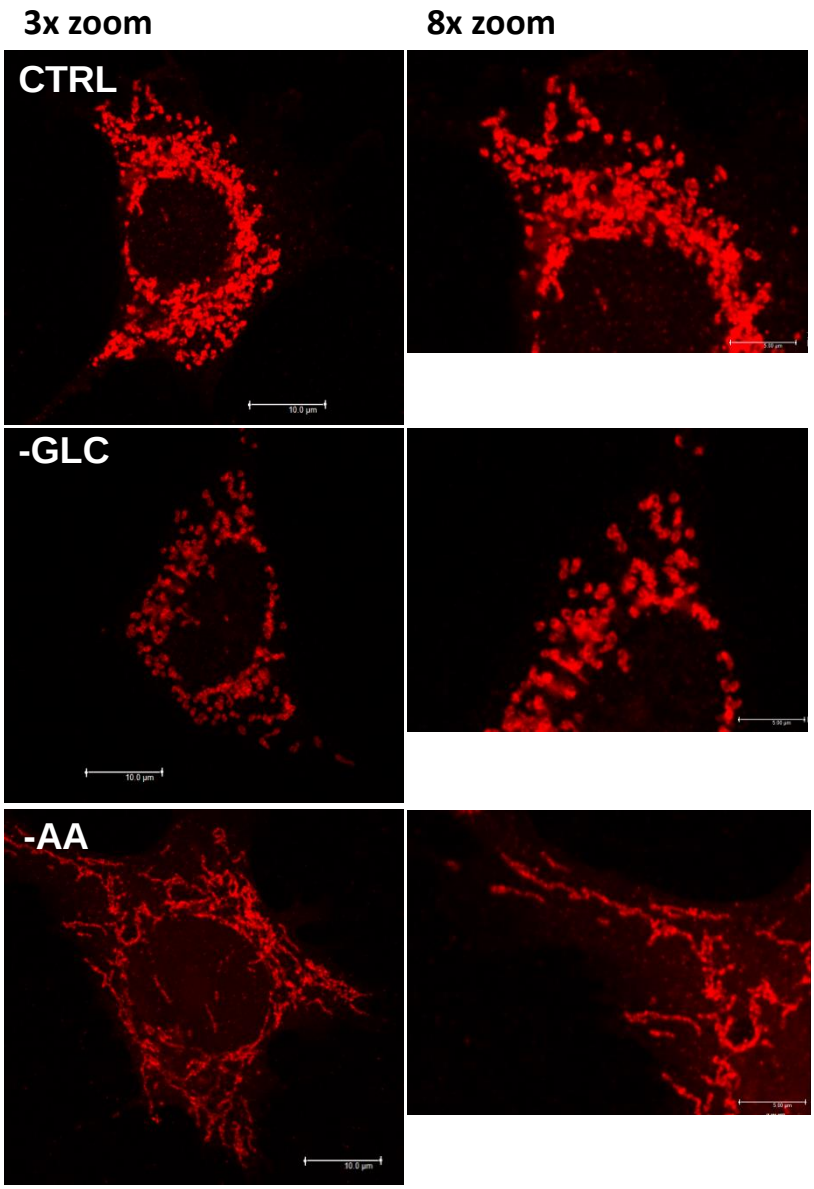
3x zoom
8x zoom
CTRL
-GLC
-AA

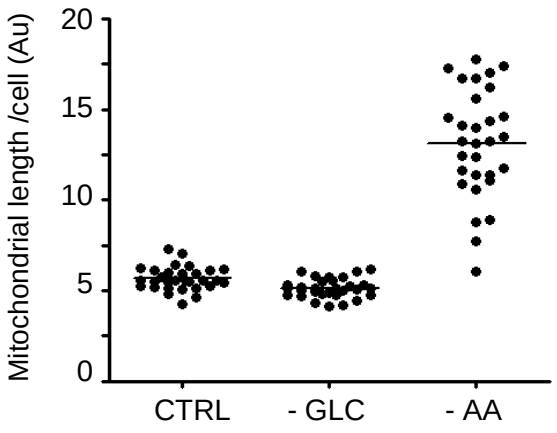
Mitochondrial length /cell (Au)
20
15
10
5
0
CTRL
- GLC
- AA

3.2.iii Chloroquine potentiates 4T1 cell death in an autophagy-independent manner.

CQ potentiated cell death in response to metabolic stress, radiation, and chemotherapeutics, but how this was related to inhibition of the autophagy pathway was not clear. CQ would be expected to block the autophagy pathway when used in the context of long term (24hr) survival assays and in longer term *in vivo* or within clinical settings.

As expected, treatment of 4T1 cells with CQ (25μM) over a 3 day time-course induced accumulation of LC3-II by western blot analysis **(Fig 3.7a)**. Furthermore, these longer term treatments now led to clear p62 accumulation. Autophagy block and accumulation of LC3 and p62 puncta was also observed following 24hr treatment **(Fig 3.7b)**. These data indicate that CQ is effective at blocking lysosomal autophagic flux when used at 24hrs and longer. However, a decrease in p62 levels and the ratio of LC3-II/-I was noted after 3 days of CQ exposure, which could be due to a gradual reduction in the activity of the drug over time.

Since CQ can affect several essential processes in the cell, the extent that CQ-mediated cell death was through autophagy inhibition was determined. Our approach was to determine if genetic knockdown of autophagy was similar to CQ treatment in generating cell death. Parallel experiments in 4T1 cell lines with stable knockdown of key autophagy genes, Beclin1, part of the essential class III PI3K complex, and ATG7, a key player in the LC3 conjugation system were performed. Efficiency of knockdowns in 4T1 cells was first confirmed by blotting. ATG7 and Beclin1 expression levels were sufficiently reduced by their respective shRNA. However, only knockdown of ATG7 produced a clear functional knockdown of autophagy. Amino acid starvation failed to initiate an autophagy response in ATG7 knockdown cells, indicated by no change in the LC3-II to LC3-I ratio. Interestingly, Beclin1 knockdown only produced a relatively mild impairment of starvation-induced LC3 conversion **(Fig 3.8)**.

For modulation of viability, as in previous experiments, CQ strongly sensitised wildtype 4T1 cells to serum-starvation induced cell death. However, stable knockdown of ATG7 did not mimic CQ activity in combination with serum withdrawal. Similarly, stable knockdown of Beclin1 did not mimic the sensitising effects of CQ to serum withdrawal **(Fig 3.8)**. These results indicate that genetic

inhibition of autophagy does not have the same effects as CQ at sensitising cells to serum deprivation mediated death.

To further test this idea, clonogenic assays were repeated in ATG5 knock-out MEFs. ATG5 is a vital component of the ATG12-ATG5-ATG16L1 conjugate, which 'coats' the outer surface of the phagophore and is absolutely required for the predominant canonical forms of autophagy (Mizushima et al., 1998). Strikingly, ATG5 knock-out MEFs, which are completely ablated in autophagy did not show any increased sensitivity to serum starvation **(Fig 3.9a)**. For control, in wild-type MEFs (derived in parallel to ATG5 knockout MEFs) CQ potentiated serum starvation-induced cell death as expected, although CQ alone at this dose had particularly strong cytotoxic effects and this line of wild-type MEFs also forms more heterogeneous sets of clones in clonogenic growth assays.

To further clarify the role of autophagy, clonogenic assays in ULK DKO MEFs, deficient in both ULK1 and ULK2 isoforms (McAlpine et al., 2013) were performed. As with ATG5 KO MEFs, autophagy deficient cells lacking ULK1/2 were not hypersensitive to serum starvation **(Fig 3.9b)**. However, combination of serum starvation and CQ did lead to marked cell death compared to untreated control cells, indicating CQ still potentiated cell death in autophagy-deficient contexts. For comparison, in wild-type MEFs (prepared in parallel to the ULK1/2 DKO line) CQ again sensitised to serum deprivation. Considering these data, the inhibition of autophagy through knockdown or knockout of essential regulatory factors could not replicate the potentiating ability of CQ and CQ may still have inhibitory activity in autophagy-deficient cells.

To further explore the relationship between CQ-mediated cell killing and autophagy, to potential for CQ to sensitise to cell death in autophagy-deficient contexts was examined. In ATG5 KO MEFs, serum starvation did not result in a shift in cell viability. However, addition of CQ, both alone and in combination with serum starvation, led to overt cell death **(Fig 3.10a)**. The potential of CQ to exert cell killing in autophagy-deficient cells was further examined using Atg7 knockdown 4T1 cells, which displayed a clear functional impairment of autophagy **(Fig 3.8)**. Treatment of autophagy-deficient 4T1 cell lines with CQ resulted in significant cell death when applied as a single agent and also potentiated nutrient starvation-induced cell death **(Fig 3.10b)**. As CQ potentiation of nutrient stress to induce cell death was maintained in a number of autophagy-deficient contexts, we concluded that CQ-

mediated sensitisation to cell death predominantly occurs via an autophagy-independent mechanism, contrary to expectations.

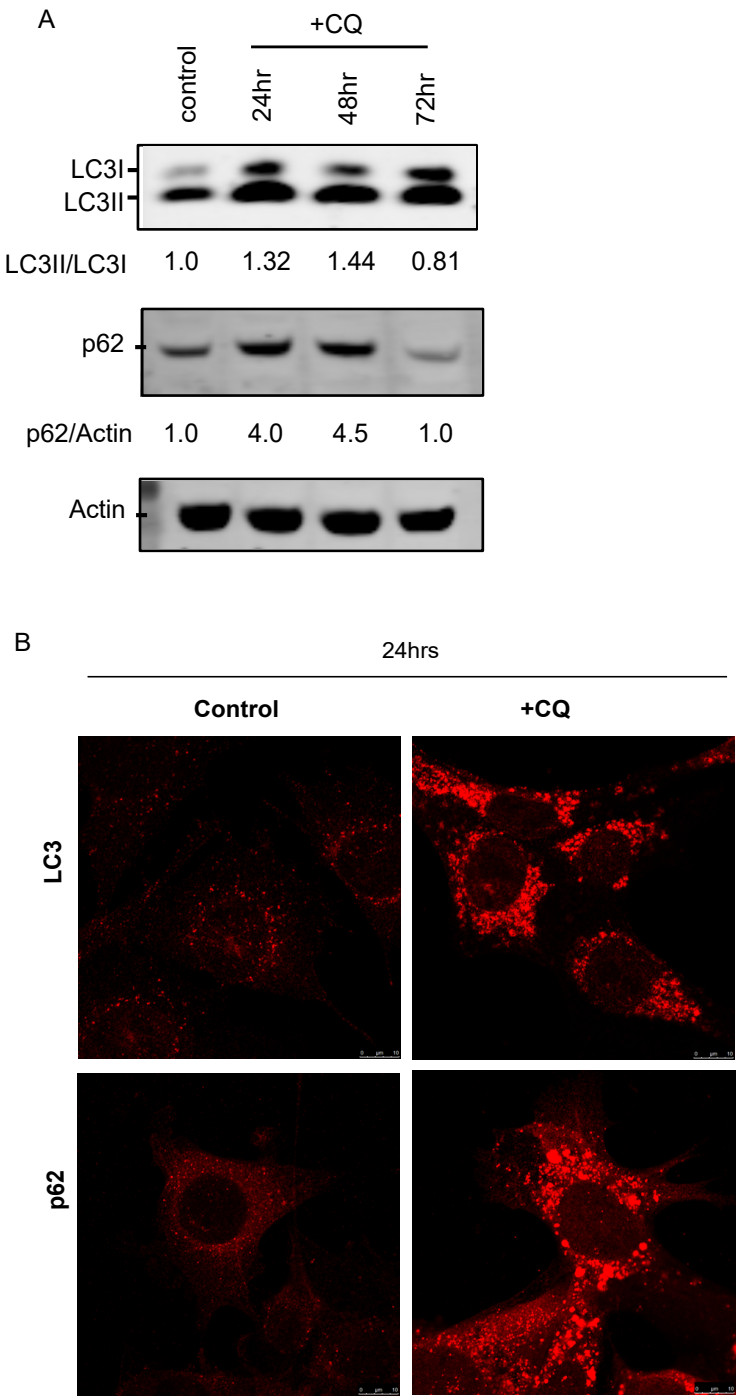

Fig 3.7: CQ induces accumulation of autophagy proteins LC3 and p62.

(A) 4T1 cells were treated under full nutrient conditions with CQ (25μM) for up to 72 hrs. Cells were lysed and analysed for LC3 and p62 protein expression as described in Fig 3.3. Quantification expressed as fold change in LC3 -II/-I ratio and p62/actin, n=1.

(B) 4T1 cells were treated with CQ (25μM) for 24hrs . Cells were fixed and stained for p62 or LC3 and imaged by confocal microscopy, n=1.

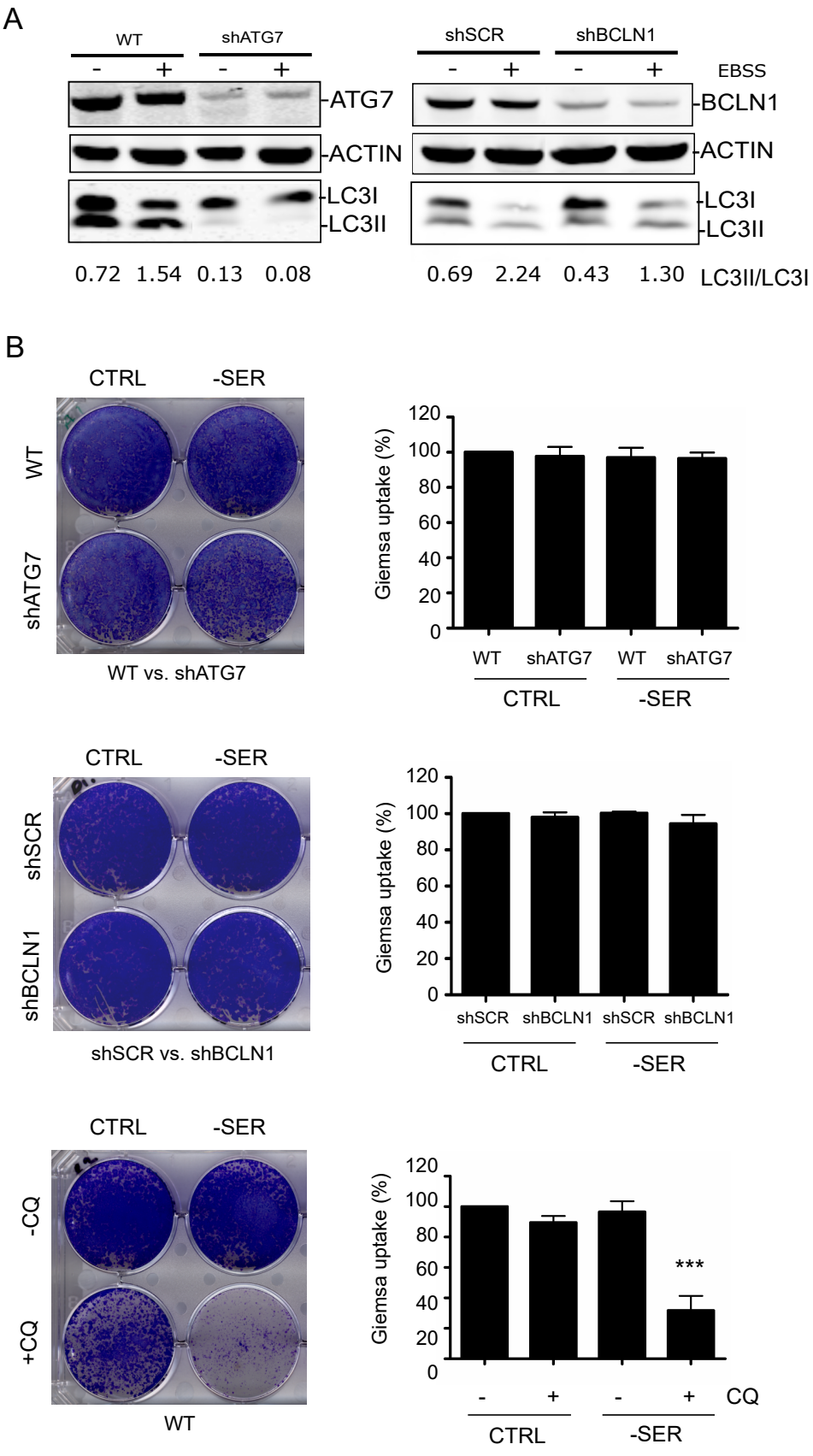
A
WT
shATG7
shSCR
shBCLN1
- + - +
- + - +
EBSS
ATG7
ACTIN
LC3I
LC3II
BCLN1
ACTIN
LC3I
LC3II
0.72 1.54 0.13 0.08
0.69 2.24 0.43 1.30
LC3II/LC3I
B
CTRL -SER
WT
shATG7
WT vs. shATG7
Giemsa uptake (%)
120
100
80
60
40
20
0
WT shATG7 WT shATG7
CTRL -SER
CTRL -SER
shSCR
shBCLN1
shSCR vs. shBCLN1
Giemsa uptake (%)
shSCR shBCLN1 shSCR shBCLN1
CTRL -SER
CTRL -SER
-CQ
+CQ
WT
Giemsa uptake (%)
***
- + - + CQ
CTRL -SER

Fig 3.8 (previous page): CQ sensitises to growth factor stress independent of autophagy inhibition

(A) 4T1 cells lines were generated stably carrying pLKO ATG7 shRNA, pLKO scrambled (SCR) shRNA, or pLKO Beclin1 (BCLN1) shRNA. Knockdown of target proteins was assessed using western blot analysis for Beclin1 and ATG7, as well as functional inhibition of autophagy being examined through conversion of LC3I to LC3II +/- amino acid starvation (EBSS) 2hrs. The LC3-II/LC3-I ratios are shown below the LC3 immunoblot.

(B) shATG7 or shBCLN1 cells were treated with full nutrient (CTRL) or serum-free DMEM (-SERUM) for 24hrs. Bottom panel: As a control, wild-type 4T1 cells were treated +/- CQ (25μM) in either full nutrient (CTRL) or serum-free DMEM (-SERUM) conditions (24hrs) for comparison. The media was replenished and 3 days later cell viability was assessed as in Fig 3.1. Giemsa uptake shown as % of control, one-way ANOVA with Tukey post-test, comparison to untreated control (***P<0.001), n=3 technical replicates, errors bars +/-SEM.

Fig 3.9 (next page): CQ sensitises to growth factor stress independent of autophagy inhibition in MEFs

(A) Wild-type or autophagy deficient (ATG5 -/-) MEFs were treated with full nutrient (CTRL) or serum-free DMEM (-SER) for 24hrs. Wild-type MEFs were treated +/- CQ (25μM) for comparison. The media was replenished and 3 days later cell viability was assessed as in Fig 3.1. Giemsa uptake shown as % of control, one-way ANOVA with Tukey post-test, comparison to untreated control (**P<0.01), n=3 technical replicates, errors bars +/-SEM.

(B) Wild-type (1SVN) or autophagy deficient ULK DKO (4SVN) MEFs were treated with full nutrient (CTRL) or serum-free DMEM (-SER) for 24hrs +/- CQ (25μM). The media was replenished and 3 days later cell viability was assessed as in Fig 3.1. Giemsa uptake shown as % of control, one-way ANOVA with Tukey post-test, comparison to untreated control (**P<0.01, ***P<0.001), n=3 technical replicates, errors bars +/-SEM.

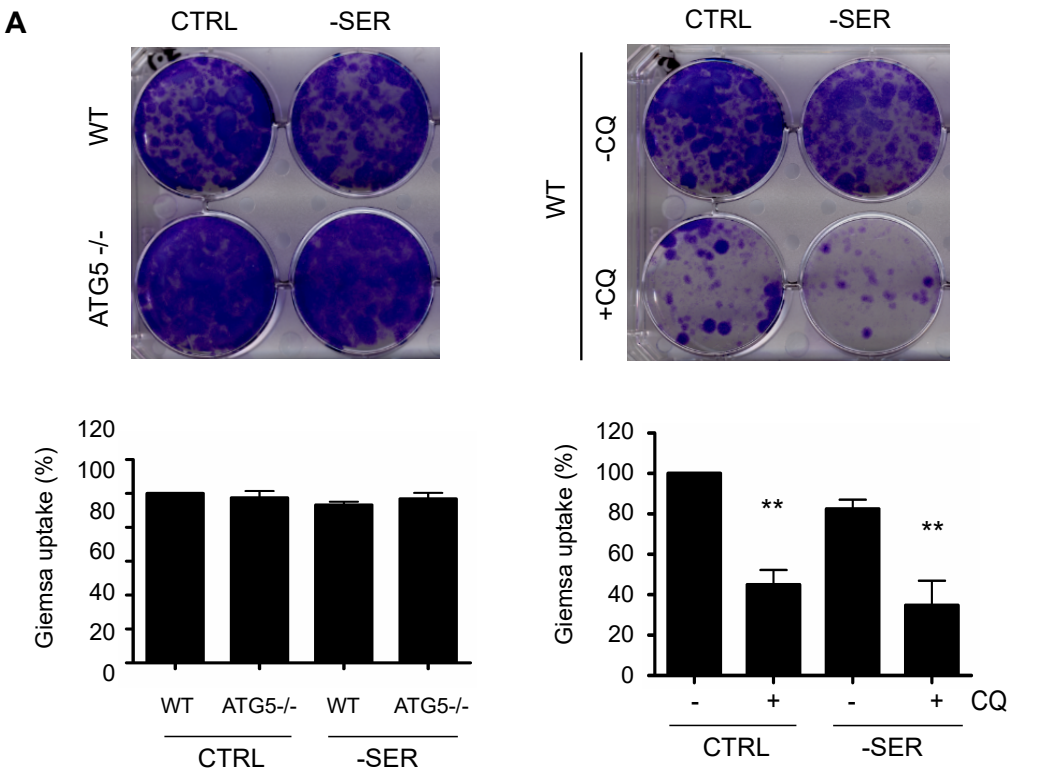
A
CTRL
-SER
WT
ATG5 -/-
Giemsa uptake (%)
120
100
80
60
40
20
0
WT
ATG5-/-
WT
ATG5-/-
CTRL
-SER
CTRL
-SER
WT
-CQ
+CQ
Giemsa uptake (%)
**
**
-
+
-
+
CQ
CTRL
-SER

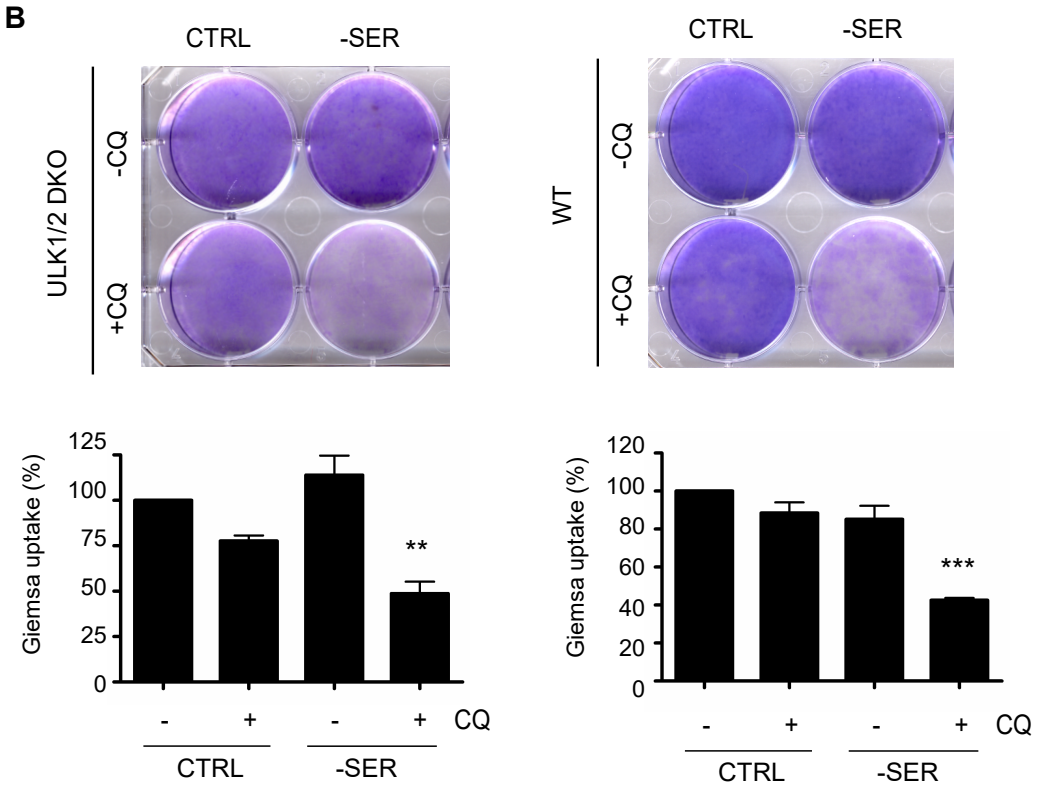
B
CTRL
-SER
ULK1/2 DKO
-CQ
+CQ
Giemsa uptake (%)
125
100
75
50
25
0
**
-
+
-
+
CQ
CTRL
-SER
CTRL
-SER
WT
-CQ
+CQ
Giemsa uptake (%)
120
100
80
60
40
20
0
***
-
+
-
+
CQ
CTRL
-SER

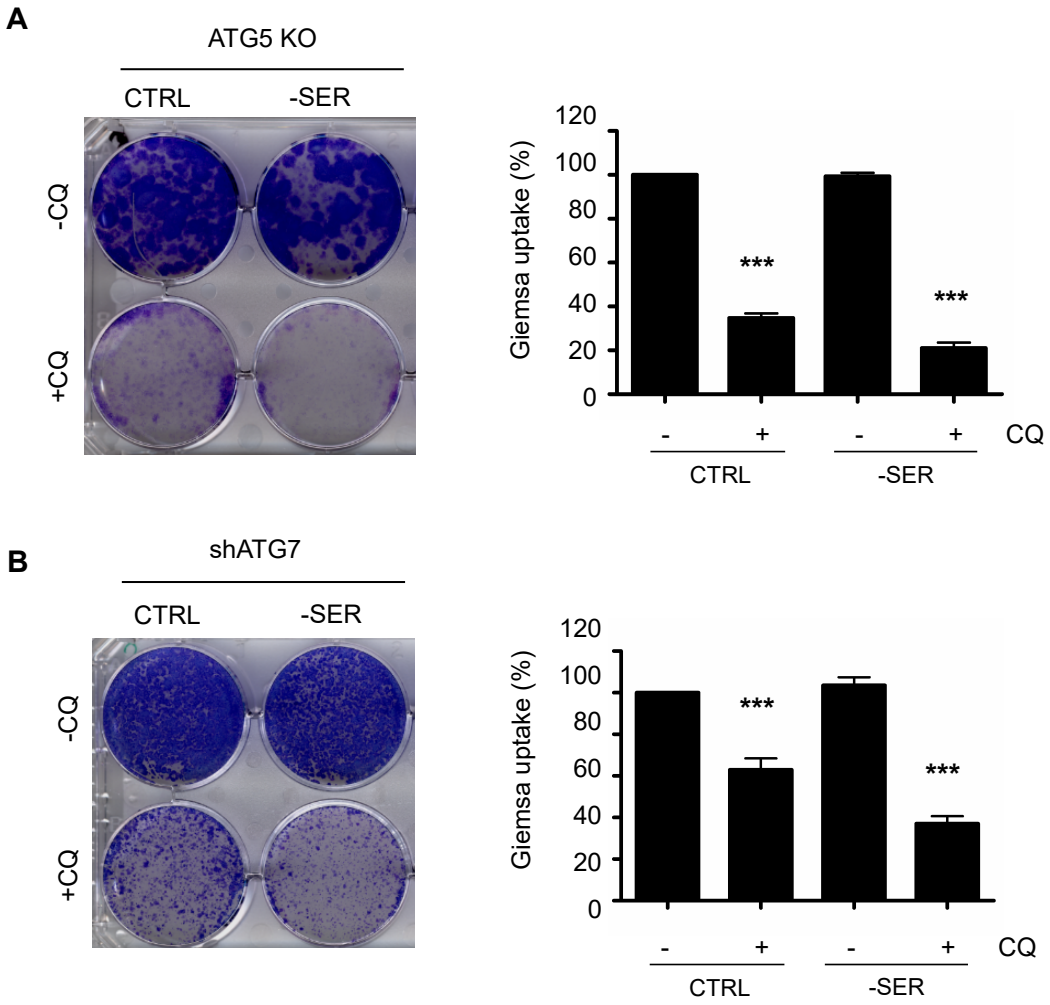

Fig3.10：CQ still sensitises to growth factor deprivation in cells with genetically impaired autophagy

(A) ATG5 KO MEFs or **(B)** shATG7 4T1 cells were treated with full nutrient (CTRL) or serum-free DMEM (-SER) for 24hrs, +/- CQ (25μM) as indicated The media was replenished and 3 days later cell viability was assessed as in Fig 3.1. Giemsa uptake as % of control, one-way ANOVA with Tukey post-test, comparison to untreated control (***P<0.001), n=3 technical replicates, errors bars +/-SEM.

3.2.iv Reductions in glucose metabolic state reduce the activity of CQ.

During the course of our studies of CQ and cell stress conditions, we examined different types of nutrient starvation and responses to CQ. Our results above indicated that growth factor (serum) starvation sensitised 4T1 cells to CQ. As such, we further compared several conditions often used to elicit autophagy responses *in vitro*: glucose starvation (glucose-free DMEM with no serum (contains amino acids)), and amino acid starvation (Earle's balanced salt solution (EBSS) with no serum (contains glucose)). These 3 different nutrient starvation conditions were tested in the presence or absence of CQ.

As previously, treatment with CQ (25μM) leads to a reduction in cell survival when 4T1 cells were subjected to serum withdrawal. However, further withdrawal of glucose alongside serum starvation almost fully rescued the effect of CQ, which was entirely unexpected. In contrast, withdrawal of amino acids, alongside serum starvation, promoted CQ-effects on cell death **(Fig 3.11a)**. Time-course clonogenic assays were utilised to determine when the differences between nutrient starvation conditions became apparent. The protective effect conferred by glucose starvation was only observed after 16hrs starvation (as compared for example to 8hrs) **(Fig 3.11b)** indicating the effect is a long term response to nutrient deprivation.

To obtain better understanding of the temporal dynamics of CQ-mediated cell death, we performed live cell imaging and tracked the proliferation of the cells in the different nutrient starvations in combination with CQ. 4T1 cells were transferred into different starvation conditions (serum, serum and glucose, or serum and amino acids) in the presence or absence of CQ (25μM) and then sequentially imaged over time. In the absence of CQ, under control full nutrient conditions, cells proliferated rapidly, leading to ~doubling of confluency over the initial 24hrs **(Fig 3.12a)**. Cells under nutrient starvation conditions displayed reductions in proliferative capabilities, with alternate nutrient starvations affecting this outcome to differing extents. After the initial 24hr treatment period serum starvation only reduced the confluency by ~10%, similarly glucose starvation reduced the confluency by ~20%. However, amino starvation had the greatest effect on proliferative capabilities, with limited proliferation observed between 0 and 24 hours. After the first 24hrs in treatment conditions, cell media was replaced with new full nutrient media (indicated by the red arrow); both control and all nutrient starved cells were able to recover and continue proliferating after nutrient replenishment.

However, when combining CQ with nutrient starvations for the initial 24hr treatment only cells in full nutrient media continued proliferating, while those starved of nutrients (all conditions) showed a reduction in confluency **(Fig 3.12a)**. Upon nutrient replenishment after the first 24hrs of imaging, the cell profiles in the presence of CQ, serum starvation and/or amino acid starvation resulted in a reduction in proliferation in comparison to control cells (full nutrients). However, cells deprived of glucose displayed an increase in proliferation in comparison to serum starved and/or amino acid starved cells, suggesting glucose starved cells had a greater potential for recovery upon nutrient replenishment.

Further analysis of the 4T1 cell morphologies under different conditions supported the cell growth profiles. Live cell images taken 23hrs after nutrient starvation showed clear differences in the confluency of 4T1 cells in the different nutrient starvations on combination with CQ **(Fig 3.12b)**. A reduction in confluency was observed in CQ-treated serum starved cells and/or amino acid starved cells, while those exposed to glucose starvation showed less of a reduction in confluency, and displayed more normal, healthy cell morphologies.

To further examine if glucose vs. amino acid deprivation effects on CQ could be separated from effects of serum starvation low amounts (1% final) of dialysed foetal bovine serum were re-supplemented to the starvation media. Low amounts of FBS were proposed to replenish some baseline growth factor signalling while still synergising with CQ for cell death. On co-treatment with CQ, glucose starvation (in low FBS) was able to block death of 4T1 cells, whereas amino acid withdrawal still induced cell death (**Fig 3.13)**. This was consistent with findings described in zero serum conditions, and together supports a mechanism where glucose starvation rescues CQ-dependent cell death.

To further explore how the viability rescue effects depended on severity of glucose starvation, 4T1 cells were treated with serum-free media containing glucose in varying concentrations from 4.5g/L to 0g/L, in the presence of CQ **(Fig 3.14)**. As expected, CQ combination with serum-free media containing high glucose (4.5g/L) induced cell death. However, induction of cell death was not altered upon CQ combination with serum-free media containing mid to lower glucose concentrations (2.25g/L and 1.0g/L). Only a full rescue of cell death with serum-free media with no glucose (0g/L) was observed. These data indicted only absolute depletion of glucose rescues CQ-mediated cell death in this model.

In order to survive glucose starvation during the 24hr drug treatment period, cells must utilise other nutrient sources. Many cancer cell lines display properties of glutamine addiction, which is often linked to the over-expression of myc (Wise et al., 2008, Gao et al., 2009). Glutamine addicted cancers are highly dependent on glutamine for their growth and survival despite it being regarded as an inefficient metabolic pathway; key factors for this may be attributed to glutamine providing a nitrogen for protein synthesis and providing the essential TCA cycle energy substrate (α-ketoglutarate) (Wise and Thompson, 2010). Considering this rationale, we hypothesised that 4T1 cells were likely utilising glutamine in the media to survive starvation. As control, cells starved of serum- and glucose displayed the survival response to CQ in clonogenic assays (left panel). However, further withdrawal of glutamine from glucose-free media in combination with CQ led to a loss of cell viability (right panel). Even glucose starved cells in the absence of CQ had reduced cell viability when glutamine was depleted **(Fig 3.15)**. Thus, upon glucose starvation, dependency on glutamine is generally enhanced. When we replenished the glucose-free glutamine-free media with glutamine, this rescued cell viability. These data suggested that 4T1 cells are indeed glutamine addicted, and in the absence of glucose utilise this amino acid as a key nutrient source in order to survive. Indeed, a recent study described 4T1 cells as possessing metabolic plasticity: the ability to readily adapt and switch between glycolysis and oxidative phosphorylation in response to extracellular cues (Simoes et al., 2015). Furthermore, in concert with our findings, it was identified that 4T1 cells are heavily reliant of glutamine for their growth. These data corroborate our findings supporting a role of glutamine in 4T1 cell survival in response to glucose withdrawal.

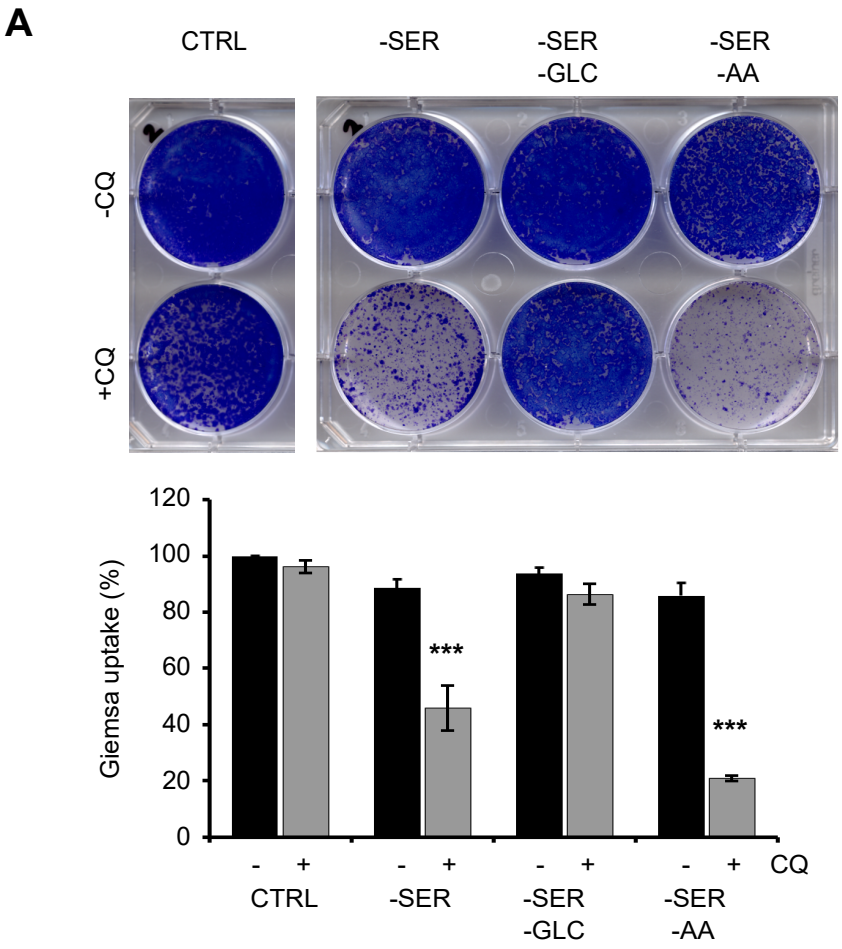
A
CTRL
-SER
-SER
-GLC
-SER
-AA
-CQ
+CQ
Giemsa uptake (%)
120
100
80
60
40
20
0
***
***
- + - + - + - + CQ
CTRL
-SER
-SER
-GLC
-SER
-AA

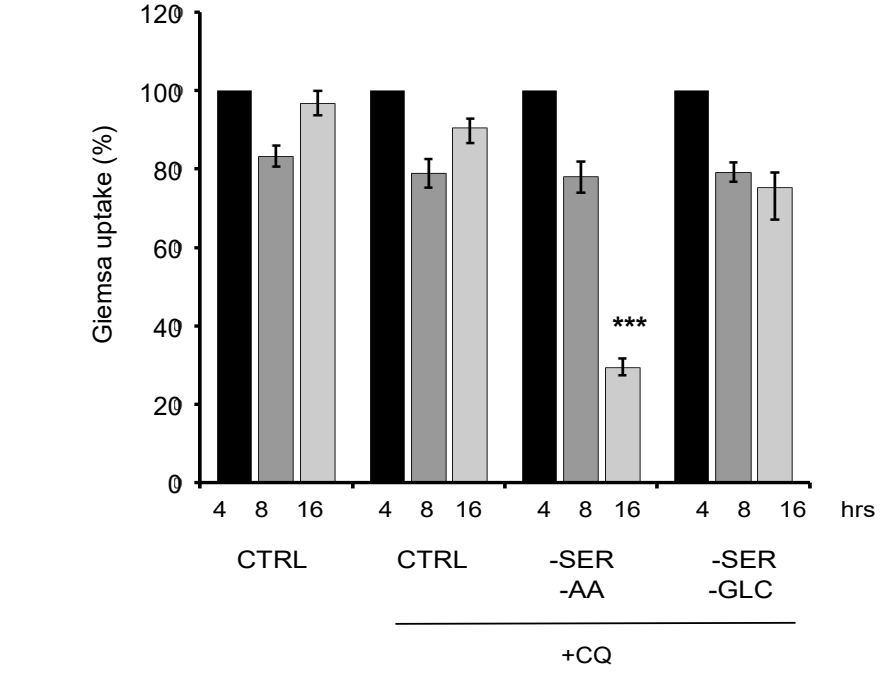
B
Giemsa uptake (%)
120
100
80
60
40
20
0
***
4 8 16 4 8 16 4 8 16 4 8 16 hrs
CTRL
CTRL
-SER
-AA
-SER
-GLC
+CQ

Fig 3.11 (previous page): Glucose starvation rescues CQ sensitised cell death, in a time dependent manner

(A) 4T1 cells were treated with full nutrient (CTRL), serum-free DMEM (-SER), glucose-free and serum-free DMEM (-SER-GLC), or amino acid-free and serum-free media (-SER-AA) +/- CQ (25μM) as indicated for 24hrs. Media was replenished and 3 days later cell viability was assessed as in Fig 3.1. Giemsa uptake shown as % of control, one-way ANOVA with Tukey post-test, comparison to untreated control (***P<0.001), n=3 technical replicates, errors bars +/-SEM.

(B) 4T1 cells were nutrient starved as indicated +/- CQ (25μM) for 4, 8, or 16hrs. Media was replenished and 3 days later cell viability was assessed as in Fig 3.1. Giemsa uptake shown as % of control, one-way ANOVA with Tukey post-test, comparison to respective time-point control (***P<0.001), n=3 technical replicates, errors bars +/-SEM.

Fig 3.12 (next page): CQ sensitisation to cell death is dependent on specific nutrient availability.

(A) 4T1 cells were treated with full nutrient (CTRL), serum-free DMEM (-SER), glucose-free and serum-free DMEM (-SER-GLC), or amino acid-free and serum-free media (-SER-AA) +/- CQ (25μM) as indicated for 24hrs. Media was replenished (as indicated by the arrows) and left for a further 24hrs to analyse recovery. Confluency of the cells was measured from time-lapse microscopy over 48hrs and analysed as described in Methods.

(B) Still images were taken from time-lapse microscopy videos after 23hrs treatment to represent the differences in cell death and morphology between nutrient starvation conditions.

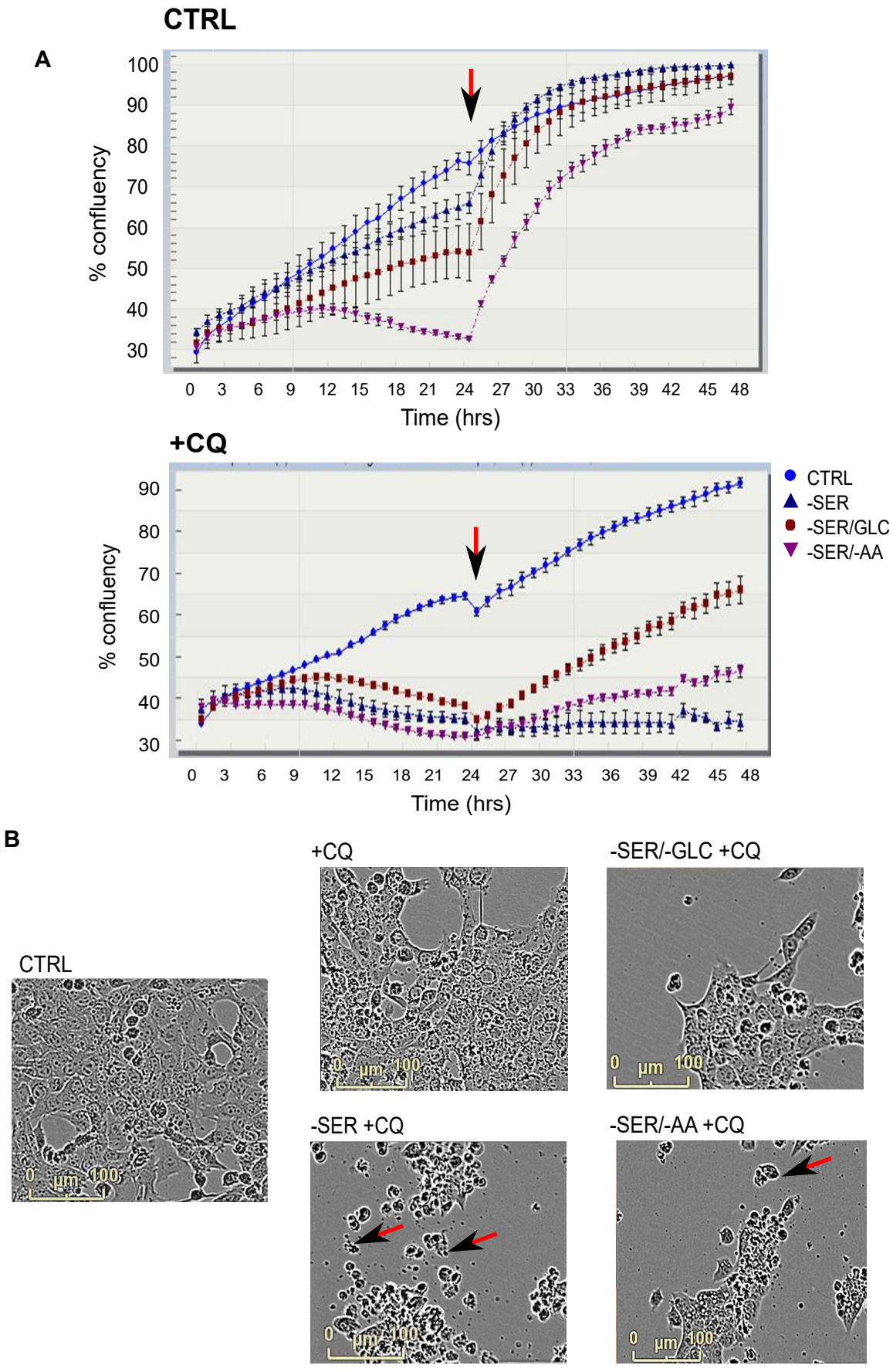
A
CTRL
% confluency
Time (hrs)
+CQ
% confluency
Time (hrs)
CTRL
-SER
-SER/GLC
-SER/-AA
B
CTRL
+CQ
-SER/-GLC +CQ
-SER +CQ
-SER/-AA +CQ
0 µm 100

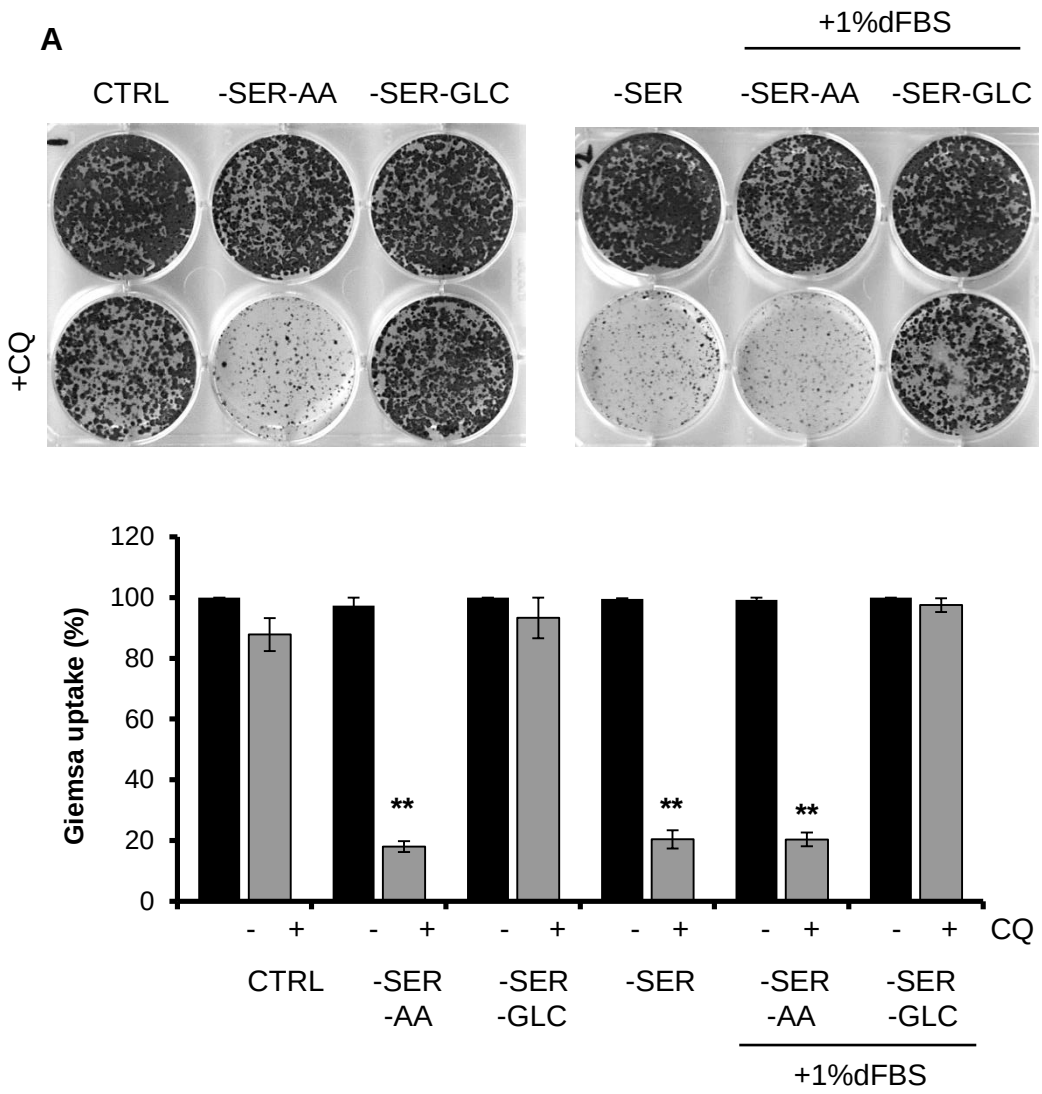

Fig 3.13: Glucose starvation rescues cell viability independently of serum starvation.

(A) 4T1 cells were treated with full nutrient (CTRL), amino acid-free and serum-free media (-SER-AA), glucose-free and serum-free DMEM (-SER-GLC), or serum-free DMEM (-SER), +/- CQ (25μM) as indicated for 24hrs. Alternatively, cells were treated with -SER-AA media or -SER-GLC media supplemented with dialysed FBS (1%) for 24hrs to examine the effects on single nutrient starvation. Media was replenished and 3 days later cell viability was assessed as in Fig 3.1. Giemsa uptake shown as % of control, n=3 technical replicates, one-way ANOVA with Tukey post-test, comparison to untreated control (**P<0.01), errors bars +/-SEM.

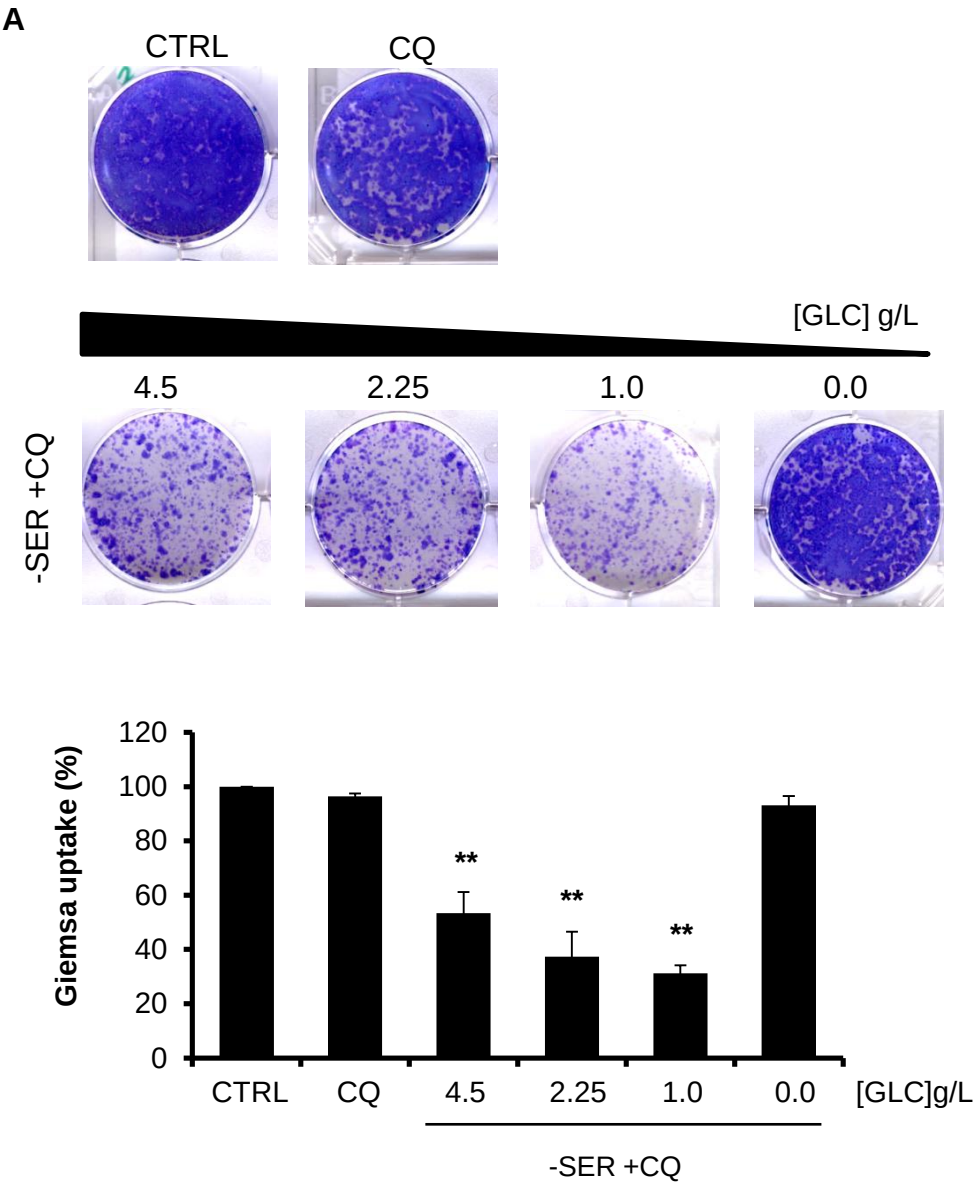

Fig 3.14: Glucose starvation mediated rescue of cell viability is not glucose concentration dependent

(A) 4T1 cells were treated with full nutrient DMEM (CTRL), or serum-free DMEM (-SER) containing differing glucose concentrations as indicated, +CQ (25μM) for 24hrs. Media was replenished and 3 days later cell viability was assessed as in Fig 3.1. Giemsa uptake shown as % of control, n=3 technical replicates, one-way ANOVA with Tukey post-test, comparison to untreated control (**p<0.01), errors bars +/-SEM.

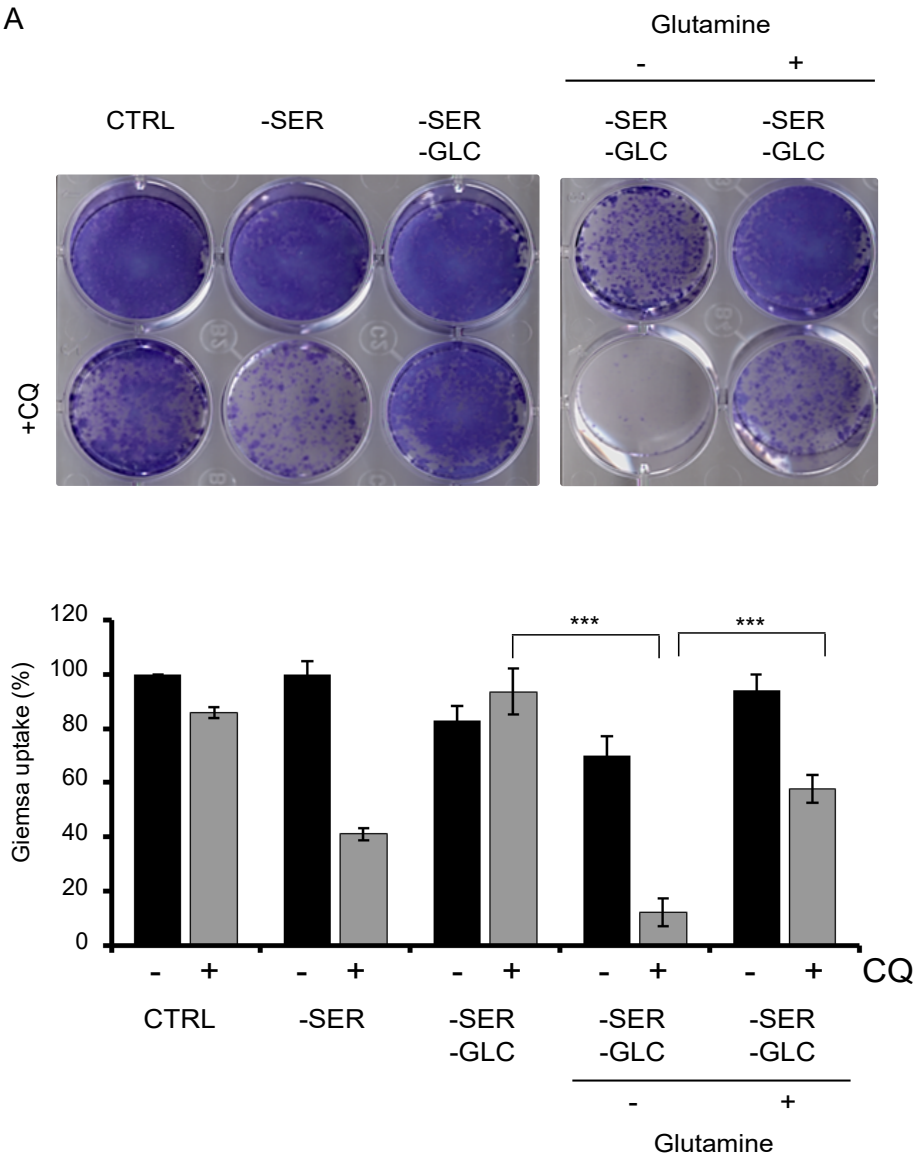

Fig 3.15: Glutamine is the key nutrient source required for survival in glucose-starved 4T1 cells

(A) 4T1 cells were treated with full nutrient (CTRL), serum -free DMEM (-SER), glucose-free and serum -free DMEM (-SER-GLC), +/- CQ (25μM) for 24hrs. Alternatively, cells were treated with glucose -free and serum -free DMEM (-SER-GLC) -/+ Glutamine (4mM) +/-CQ (25μM). Media was replenished and 3 days later cell viability was assessed as in Fig 3.1. Giemsa uptake as % of control, n=4 technical replicates, one-way ANOVA with Tukey post-test, comparisons as indicated (***p<0.001), errors bars +/-SEM.

3.2.v Is glucose withdrawal providing a protective effect through glycolysis inhibition?

Considering our observations, it was becoming apparent that glucose starvation protects 4T1 cells from death induced by CQ coupled to serum starvation. To further explore the key interrelationship between glucose metabolism and cell survival, the ability of the glycolysis inhibitor, 2-deoxyglucose (2-DG), to rescue serum starvation-induced cell death was examined. 2-DG is a glucose analogue that inhibits glycolysis via interference with the rate-limiting enzyme, hexokinase (Parniak and Kalant, 1985). 2-DG is phosphorylated by hexokinase to generate 2-DG-P which cannot be further metabolized, thus leading to accumulation of 2-DG-P and depletion in ATP. Interestingly, addition of 2-DG (2.5mM or 5mM) promoted a cell survival response to CQ-treated serum starved cells. The level of protection from 2-DG was comparable to that of glucose withdrawal **(Fig 3.16)**. Thus, interference with the glycolysis pathway leads to a protective effect against serum starvation and CQ–mediated cell death.

To further investigate the relationship between glucose starvation and glycolysis inhibition, the potential of downstream inhibitors of glycolysis to confer the same protective advantage as 2-DG were explored. Gossypol and dichloroacetate (DCA) were utilised as downstream glycolysis inhibitors. Gossypol is a lactate dehydrogenase inhibitor, thereby inhibiting the enzyme which converts lactate to pyruvate before entry into the TCA cycle (Yu et al., 2001). DCA inhibits pyruvate dehydrogenase kinase (PDK). During glycolysis PDK phosphorylates and inactivates the enzyme pyruvate dehydrogenase (PDH) (Clark et al., 1987). This interference with the enzyme PDH, which is typically responsible for the conversion of pyruvate to acetyl-CoA, pushes metabolic pathways towards the cytoplasmic glycolysis that cancer cells prefer as oppose to glucose oxidation in the mitochondria. Therefore, inhibition of PDK by DCA prevents inactivation of PDH and in turn switches cancer cells from utilising glycolysis to glucose oxidation. Interestingly, both of these glycolysis inhibitors have been studied with a view to developing potential anti-cancer therapies, making them attractive compounds to use in our investigations. For example, a derivative of gossypol was shown to induce oxidative stress and inhibit progression of pancreatic cancer in xenograft models (Le et al., 2010). Gossypol has previously been investigated in clinical trials as a potential treatment for refractory metastatic breast cancer (Van Poznak et al.,

2001). Similarly, DCA has also shown anti-cancer effects when applied to multiple cancer cell lines, including glioblastoma and breast (Bonnet et al., 2007). Other studies have also demonstrated DCA to affect cell proliferation (Delaney et al., 2015). Since these compounds have had these strong effects in cancer cell death, we utilised these glycolysis inhibitors to compare upstream vs. downstream glycolysis inhibition in our model.

CQ alone induced a mild reduction in cell viability and consistent with our previous findings, glucose starvation rescued cell death associated with CQ and serum starvation combination. While 2-DG conferred a rescue of cell viability, gossypol and DCA failed to provide any protection upon serum starvation and CQ combination **(Fig 3.17a)**. However, under serum starvation, gossypol also induced a significant reduction in cell viability in the absence of CQ compared to control cells, whereas DCA did not. To confirm that these effects were due to the drugs in combination with serum starvation, we also examined the effects of DCA and gossypol in full nutrient media +/- CQ. The vehicle control, DMSO, was not detrimental to cell health and behaved like the untreated control set. 2-DG and DCA did not induce cell death in full nutrient media, and no enhancement was seen in cell death when combined with CQ (in comparison to CQ alone). However, gossypol induced cell death as a single agent, shown as a significant reduction in cell survival upon addition of the drug alone **(Fig 3.17b)**.

These studies indicated that inhibition of glycolysis at the very upstream stages, such as complete glucose withdrawal or hexokinase inhibition is protective against CQ-mediated cell death. However, interference with glycolysis enzymes important in pyruvate metabolism did not provide a protective advantage. As outcomes from these different strategies of glycolysis inhibition varied, overall our data suggests that only certain inhibitory compounds are able to mimic glucose withdrawal to provide resistance to CQ.

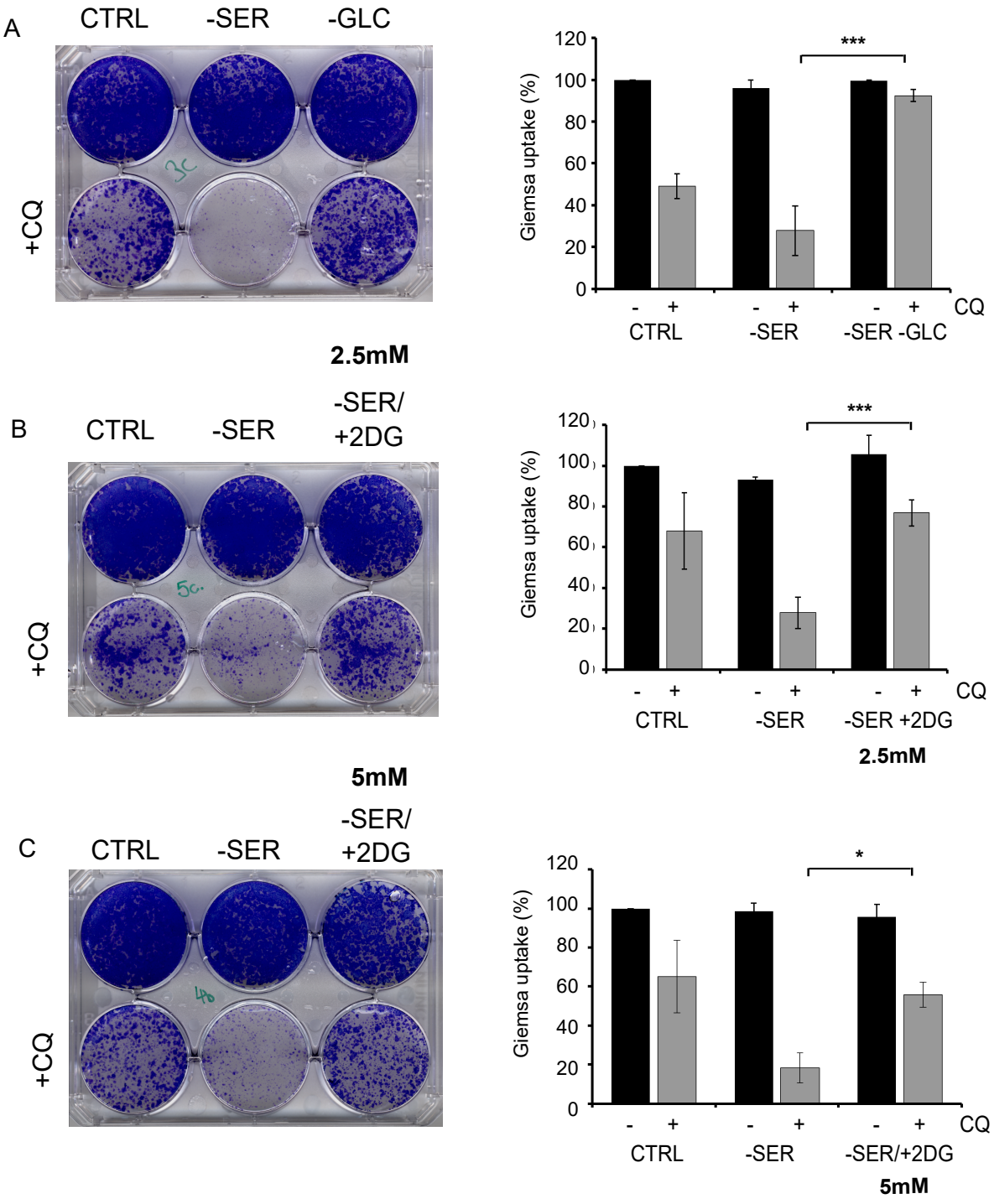

Fig 3.16: The hexokinase inhibitor, 2-deoxyglucose, rescues CQ sensitised cell death

4T1 cells were treated with **(A)** full nutrient (CTRL), serum -free DMEM (-SER), glucose-free and serum -free DMEM (-SER-GLC), +/ - CQ (25μM) for 24hrs. **(B)** Nutrient starvations as indicated or 2-deoxyglucose (2DG) 2.5mM +/ - CQ (25μM). **(C)** Nutrient starvations as indicated or 2DG 5mM +/ - CQ (25μM) . Media was replenished and 3 days later cell viability was assessed as in Fig 3.1. Giemsa uptake as % of control, n=3 technical replicates, one-way ANOVA with Tukey post-test, comparison as indicated (*p<0.05, ***p<0.001), errors bars +/- SEM

A

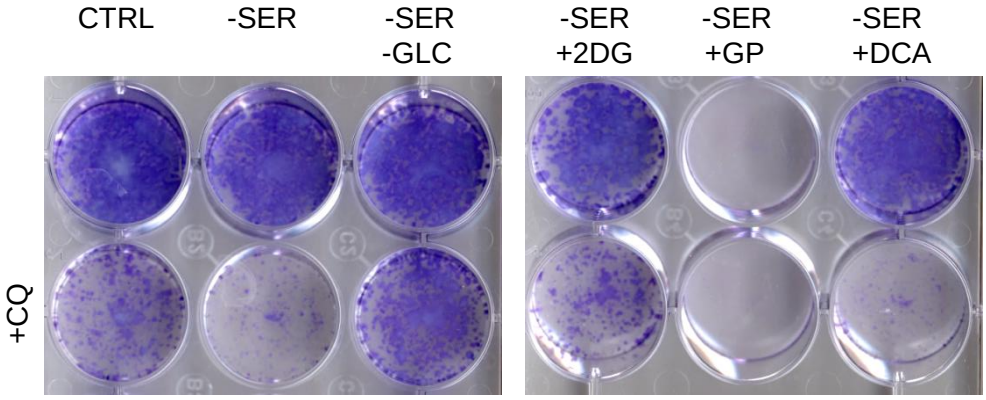
CTRL
-SER
-SER -GLC
-SER +2DG
-SER +GP
-SER +DCA
+CQ

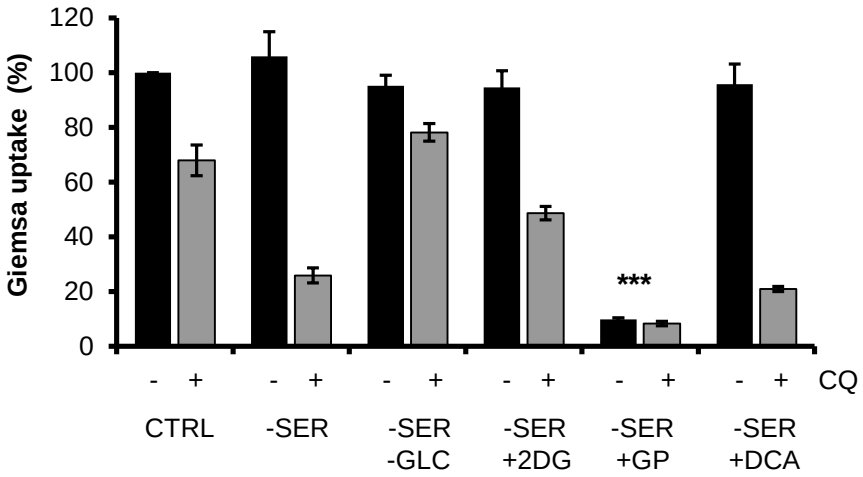
Giemsa uptake (%)
120
100
80
60
40
20
0
***
- + - + - + - + - + - + CQ
CTRL
-SER
-SER -GLC
-SER +2DG
-SER +GP
-SER +DCA

B

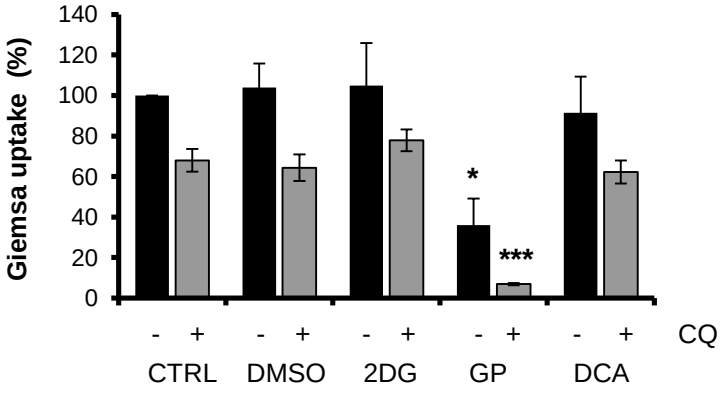
Giemsa uptake (%)
140
120
100
80
60
40
20
0
*
***
- + - + - + - + - + CQ
CTRL
DMSO
2DG
GP
DCA

Fig 3.17: Downstream glycolysis inhibitors did not rescue CQ sensitised cell death

(A) 4T1 cells were treated with **(A)** full nutrient (CTRL), serum-free DMEM (-SER), glucose-free and serum-free DMEM (-SER-GLC), +/- CQ (25μM) for 24hrs. Alternatively, serum starved (-SER) cells were treated with 2DG (2.5mM), GP (20μM), or DCA (5mM). **(B)** Cells were treated with the vehicle control, DMSO, or 2DG (2.5mM), GP (20μM), or DCA (5mM) in full nutrient media +/- CQ (25μM) for 24hrs. Media was replenished and 3 days later cell viability was assessed as in Fig 3.1. Giemsa uptake shown as % of control, n=3 technical replicates, one-way ANOVA with Tukey post-test, comparison to untreated controls (*$p<0.05$, ***$p<0.001$) errors bars +/-SEM.

3.2.vi AMPK signalling does not contribute to the protective mechanism induced by glucose starvation

Glucose starvation is known to activate the AMPK signalling pathway (Laderoute et al., 2006, Priebe et al., 2011). It has also previously been demonstrated that AMPK can support cell survival in glucose-limiting conditions (Chaube et al., 2015). Therefore, we hypothesised that activation of AMPK following glucose starvation could elicit a cell survival response in 4T1 cells. To further explore the involvement of AMPK in our cell system, the activation of the AMPK pathway (using phospho-acetyl-CoA Carboxylase (ACC) as a marker) after different starvation conditions was first biochemically confirmed. ACC is a key enzyme involved in the biosynthesis and oxidation of fatty acids; ACC is activated following phosphorylation at Ser79 by AMPK, and therefore this phosphorylation level is often used as a marker of AMPK signalling activation (Ha et al., 1994). Glucose starvation induced a greater activation of the AMPK pathway compared to serum or serum and amino acid starvations as quantified by pACC/Actin. For comparison the AMPK activator, AICAR was used; AMPK signalling was activated by AICAR, as shown by a greater than 3-fold increase in p-ACC/Actin ratios **(Fig 3.18a)**. These results confirmed that AMPK activation was induced by glucose starvation or pharmacological activators to a similar degree, whereas alternative nutrient starvations of serum or amino acid starvation did not have the potential to induce AMPK activation.

As 2-DG mimicked the cytoprotective effects of glucose starvation in relation in CQ treatment, the potential for 2-DG to also activate the AMPK pathway was explored. As a secondary method of detecting AMPK activation, AMPK (T172) phosphorylation levels were measured; Thr172 has been identified as one of the key regulatory phosphorylation sites within the AMPK activation loop (Woods et al., 2003). Here, glucose starvation induced a marked increase in pAMPK levels in comparison to control or serum-starved cells. Similarly, 2DG treatment also induced greater phosphorylation of AMPK at the T172 site in comparison to control cells, although not to as great an extent as glucose starvation **(Fig 3.18b).** As observed in our initial studies, glucose starvation induced a greater induction of pACC expression compared to control or serum starved cells and treatment with 2DG (at both 2.5mM and 5mM) mimicked this response.

Our results above provided some clarification of AMPK activation following glucose starvation and 2-DG treatment, in addition to evidence for the effectiveness of the

AMPK activating compounds. We thus aimed to further test the possibility that AMPK activation was driving the resistance to CQ and increased survival response under glycolytic inhibition conditions. We tested the AMPK activator AICAR on CQ-dependent clonogenic survival. If protection to cell death is conferred by AMPK signalling, we would predict AMPK activators to rescue cell death induced by CQ and serum starvation combination.

As seen previously, serum starvation in the presence of CQ induced a large reduction in cell survival, and concurrent glucose starvation rescued cell viability. Under combined serum starvation and CQ treatment, co-incubation with AICAR (AMPK activation) (1mM) did not improve cell viability compared to cells in the absence of AICAR **(Fig 3.19b).** Addition of AICAR also did not provide a further CQ-protective effect onto that from glucose starvation. These data suggest that activation of the AMPK pathway by glucose starvation is not contributing to the cell survival mechanism. To further explore if AMPK was involved in survival to CQ, we also attempted to determine if inhibition of AMPK altered the glucose starvation-mediated pro-survival effect using the AMPK inhibitor, compound C. Unfortunately, incubation with compound C for 24hrs, even at low doses (10μM), was toxic to 4T1 cells (data not shown). From all available data, we conclude that increased survival in glucose starved cells is independent of AMPK signalling.

Since the increased survival that we observed was indicated to be independent of AMPK activation, we hypothesised the survival responses in glucose-deprived 4T1 cells may be related to overall decreased levels of metabolism. To test this idea, methyl pyruvate (MP), a cell-permeant intermediate of glucose metabolism, was used. MP is converted by pyruvate dehydrogenase to generate Acetyl-CoA for the TCA cycle, and thus would be expected to replenish cellular ATP stores via oxidative phosphorylation even during glucose starvation (Lembert et al., 2001). Using this approach, we reasoned that we may get insight into whether glucose starvation-mediated cell survival was dependent on a reduction in cellular energy levels; if indeed this was the case, we would expect addition of MP to reverse the glucose-starvation mediated rescue of cell viability. MP was added to the glucose starved rescue condition; surprisingly, addition of MP (10mM) did not affect the ability of glucose starvation to promote cell survival **(Fig 3.20)**. As an alternative method of replenishing cellular energy galactose was utilised; this alternate carbon source is proposed to remodel oxidative energy metabolism, pushing energy

production towards mitochondrial driven pathways (Kase et al., 2013, Aguer et al., 2011). However, supplementation of galactose again did not alter the CQ-protective response induced by glucose starvation.

Our studies so far suggest that glucose starvation-mediated cell survival is independent of changes in energy as activation of the AMPK energy sensing pathway in serum starved cells did not alter cell survival. Furthermore, replenishment of cellular energy via alternative sources failed to reverse glucose-starvation dependent cell survival.

Another key survival signal is activation of the AKT-PI3K pathway (Mundi et al., 2016). The possibility for glucose starvation-mediated activation of this pathway for cell survival was investigated by employing API-2, a selective inhibitor of AKT (Yang et al., 2004b). API-2 (also known as triciribine) inhibited cell survival mediated by glucose starvation **(Fig 3.21)**. However, API-2 also reduced cell viability in all nutrient conditions whether in the presence or absence of CQ, suggesting that inhibition of AKT-derived survival signals over 24hrs simply cannot be tolerated and is not the pathway specific to glucose starvation.

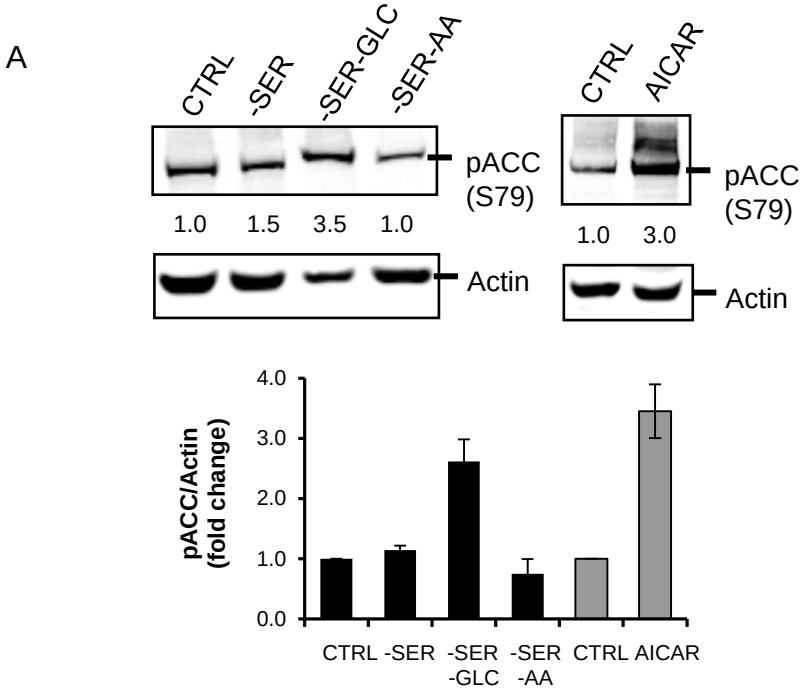
A
CTRL
-SER
-SER-GLC
-SER-AA
pACC
(S79)
1.0
1.5
3.5
1.0
Actin
CTRL
AICAR
pACC
(S79)
1.0
3.0
Actin
pACC/Actin
(fold change)
4.0
3.0
2.0
1.0
0.0
CTRL -SER -SER -GLC -SER -AA CTRL AICAR

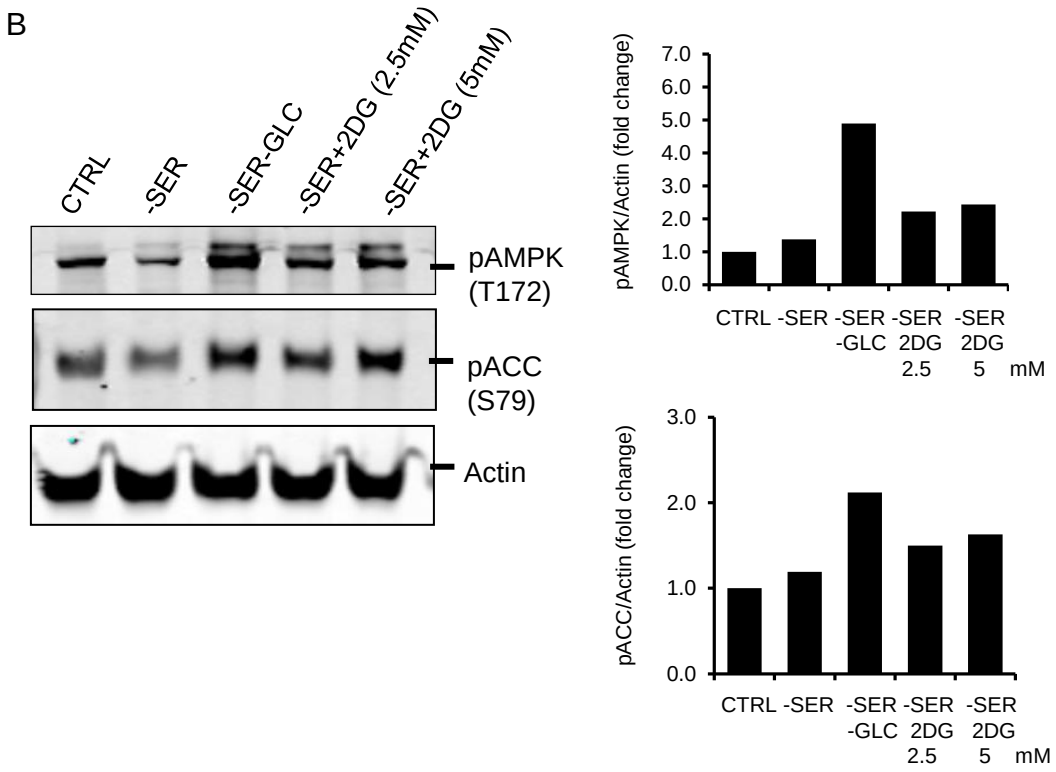
B
CTRL
-SER
-SER-GLC
-SER+2DG (2.5mM)
-SER+2DG (5mM)
pAMPK
(T172)
pACC
(S79)
Actin
pAMPK/Actin (fold change)
7.0
6.0
5.0
4.0
3.0
2.0
1.0
0.0
CTRL -SER -SER -GLC -SER 2DG 2.5 -SER 2DG 5 mM
pACC/Actin (fold change)
3.0
2.0
1.0
0.0
CTRL -SER -SER -GLC -SER 2DG 2.5 -SER 2DG 5 mM

Fig 3.18 (previous page): Glucose starvation or 2-DG treatment induces AMPK activation

(A) 4T1 cells were treated with full nutrient DMEM (CTRL), serum-free DMEM (-SER), serum-free and glucose-free DMEM (-SER-GLC), or serum-free and amino acid-free media (-SER-AA) for 24hrs. Alternatively, cells were treated with the AMPK activator, AICAR (1mM), for 24hrs. Cells were lysed and measured for pACC (S79) expression by western blot analysis. Actin was using as a loading control. Immunoblotting was quantified as described in Methods and expressed as ratios indicated (arbitrary units). Fold change in protein expression is shown in bottom panels, n=3 independent experiments, errors bars +/-SEM.

(B) 4T1 cells were treated with full nutrient DMEM (CTRL), serum-free DMEM (-SER), serum-free and glucose-free DMEM (-SER-GLC), or serum-free media with 2-DG at the indicated concentrations for 4hrs. Cells were lysed and measured for pACC (S79) and pAMPK (T172) protein expression by western blot analysis. Actin was using as a loading control. Immunoblotting was quantified as described in Methods and expressed as ratios indicated (arbitrary units). Fold change in protein phosphorylation is shown in bottom panels, n=2 independent experiments.

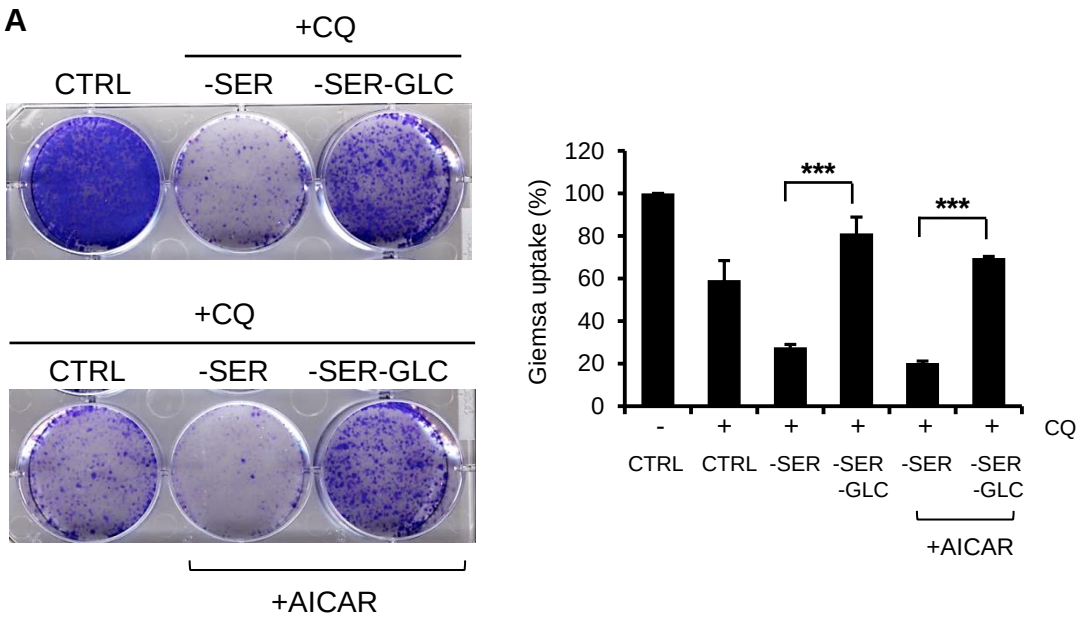

Fig 3.19: Glucose starvation mediated cyto-protection is not dependent on AMPK signalling upregulation.

(A) 4T1 cells were treated with full nutrient DMEM (CTRL), serum-free DMEM (-SER), or serum-free and glucose-free DMEM (-SER-GLC), + CQ (25μM) for 24hrs. Alternatively, cells treated with serum-free DMEM (-SER), or serum- and glucose-free DMEM (-SER-GLC) + CQ (25μM) were examined in the presence of AICAR (1mM). Media was replenished and 3 days later cell viability was assessed as in Fig 3.1. Giemsa uptake shown as % of control, n=3 technical replicates, one-way ANOVA with Tukey post-test, comparison as indicated (***p<0.001), errors bars +/-SEM.

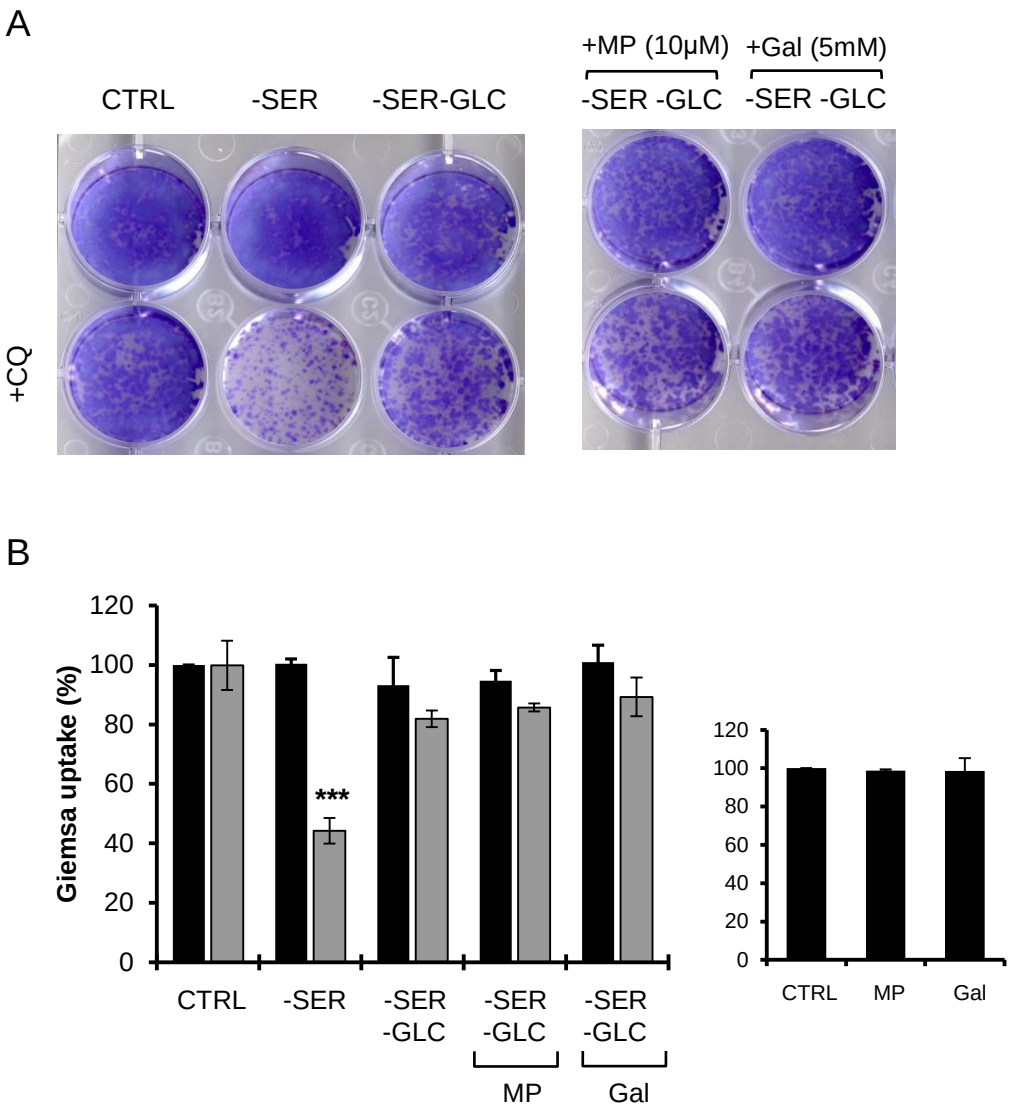

Fig 3.20: Restoring energy does not inhibit glucose-starvation mediated protection against cell death

(A) 4T1 cells were treated with full nutrient DMEM (CTRL), serum-free DMEM (-SER), or serum-free and glucose-free DMEM (-SER-GLC), + CQ (25μM) for 24hrs. Cells incubated with serum- and glucose-free DMEM (-SER-GLC) +/- CQ (25μM) were examined with the further addition of methyl pyruvate (MP, 10mM) or Galactose (Gal, 5mM). Media was replenished and 3 days later cell viability was assessed (bottom panel) as in Fig 3.1. **(B)** Giemsa uptake shown as % of control, n=3 technical replicates, one-way ANOVA with Tukey post-test, comparison to untreated control (***p<0.001), errors bars +/-SEM.

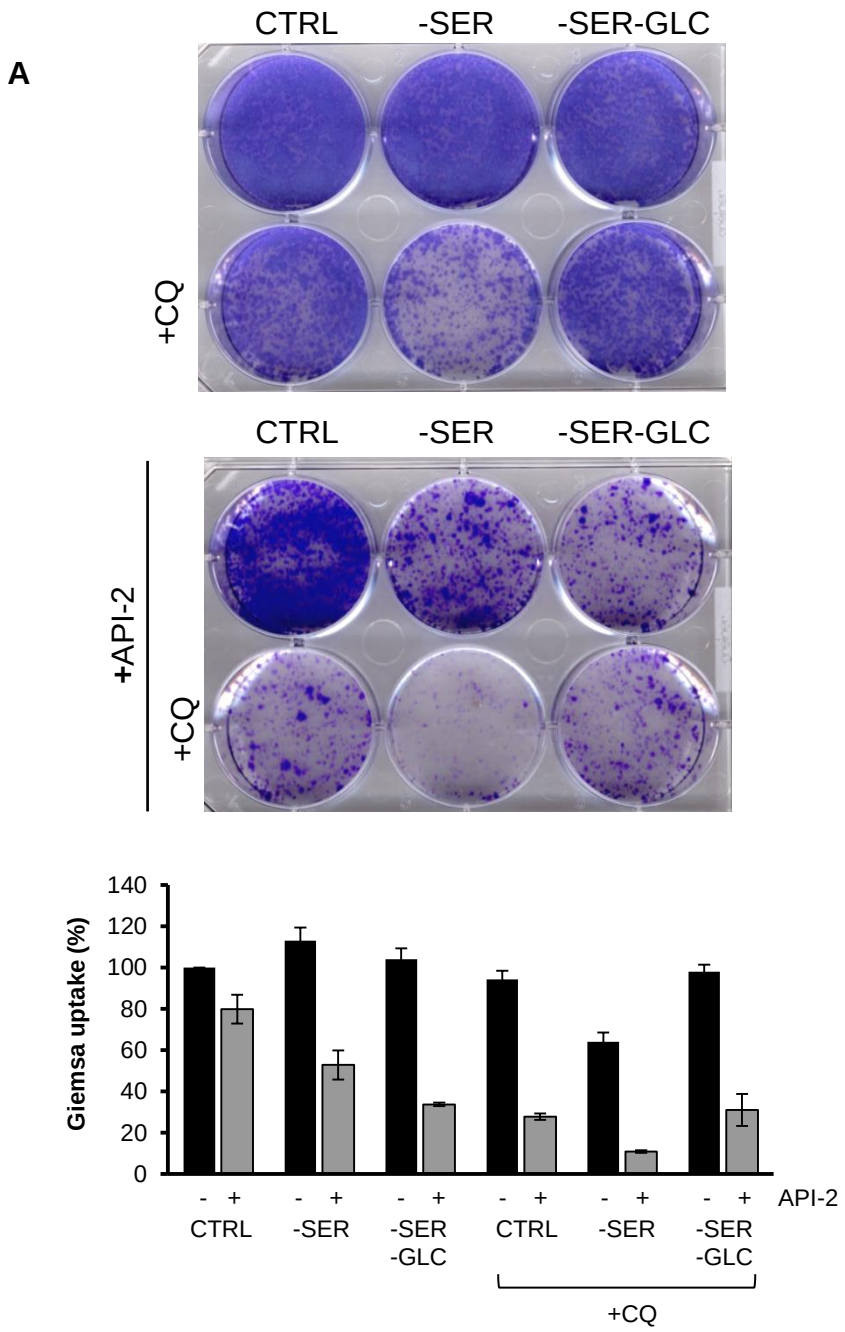

Fig 3.21: Inhibition of AKT reduces cell viability in all nutrient starved conditions. **(A)** 4T1 cells were treated with full nutrient DMEM (CTRL), serum-free DMEM (-SER), or serum-free and glucose-free DMEM (-SER-GLC), +/- CQ (25μM) for 24hrs +/- API-2 (5μM). Media was replenished and 3 days later cell viability was assessed (bottom panel) as in Fig 3.1. Giemsa uptake shown as % of control, n=3 technical replicates, errors bars +/-SEM.

3.3 Discussion

The overall aim of the project was to study the role of autophagy in breast cancer cell survival, using *in vitro* approaches in the first instance. During our initial work using CQ, a drug classified as an autophagy-lysosomal inhibitor (Bellodi et al., 2009, Amaravadi et al., 2007), we observed that CQ sensitised 4T1 cells to serum starvation-induced cell death. Unexpectedly, further glucose withdrawal or addition of an early glycolysis inhibitor reversed this reduction in cell survival. The mechanism behind this interaction became an interesting focus in my project due to the overall importance of cross-talk between cell metabolism in autophagy, cancer biology and drug resistance.

3.3.i CQ potentiates a range of cellular stressors to induce death.

In the first instance, we aimed to assess the potential of autophagy inhibition to sensitise the 4T1 metastatic breast cancer cell line to a range of cellular stressors. We utilised the autophagy-lysosomal inhibitor CQ in doing these studies. CQ had previously been demonstrated to sensitise a range of cancer cell lines to varied cancer therapeutics such as TKIs, anti-angiogenic, and platinum-derivative drugs (Bellodi et al., 2009, Selvakumaran, 2013, Liang et al., 2016) and the sensitisation effects of CQ have been attributed to inhibition of autophagy (Bellodi et al., 2009, Liang et al., 2014). Our data demonstrated that CQ sensitised 4T1 cells to a range of cellular stressors: serum starvation, PI3K-mTOR inhibition, and γ-irradiation. This potentiation effect of CQ was in agreement with previously published work. CQ has been shown to enhance cell death in response to serum starvation in a range of cancer cell lines *in vitro* – glioma, melanoma, and fibrosarcoma (Harhaji-Trajkovic et al., 2012). This was further confirmed in an *in vivo* calorie restricted mouse melanoma model, where CQ inhibited melanoma growth in mice with reduced calorie intakes. Interestingly, in concert with our own findings, CQ activity in these cell lines was also not mimicked by genetic ablation of autophagy (via shRNA towards LC3b) suggesting autophagy-independent effects were essential to this compounds anti-cancer activity.

Another cellular stressor potentiated by CQ was inhibition of the PI3K-mTOR signalling proteins via NVP-BEZ235. This combination was proven to induce cell death in neuroblastoma cell lines (Seitz et al., 2013), and these results were

replicated in our 4T1 cell model. Further evidence using alternative PI3K inhibitors has also shown the therapeutic combination of CQ with inhibition of the PI3K signalling axis to be a promising strategy (Firat et al., 2012, Echeverry et al., 2015, Mirzoeva et al., 2011). The AKT inhibitor, AZD5363, induced enhanced cell death when in combination with pharmacological inhibitors of autophagy in prostate cancer cell lines (Lamoureux, 2013). Interestingly, in this model, potentiation of AZD was also seen using genetic ablation of autophagy, in contrast to our studies. In addition to targeting PI3K using small molecule inhibitors, genetic silencing of AKT has also been shown to induce accelerated cell death when in combination with CQ (Degtyarev, 2008). Therefore, our data showing CQ mediated sensitisation to PI3K inhibition via BEZ235 is in general concert with published data, and supports this potential therapeutic combination strategy.

Our data also agree with published findings showing CQ to be an effective radio-sensitiser. Interestingly, CQ has exhibited radio-sensitising properties in both preclinical *in vitro* studies and in clinical trials. In separate studies, CQ was shown to enhance γ-irradiation associated cell death in radio-resistant primary stem-like glioma cells (Firat et al., 2012) and in colorectal cancer cell lines (Schonewolf et al., 2014). Furthermore, results from a phase II clinical trial showed that concomitant CQ treatment with whole brain irradiation increased the progression-free survival and suppression of brain metastases in comparison to patients receiving only radiation therapy (Rojas-Puentes et al., 2013). We were able to show CQ is a radio-sensitiser in the 4T1 metastatic breast cancer cell line. Interestingly, our positive data here contrasts with work by Bristol *et al*., 2013. In their studies of the 4T1 cell model, CQ treatment did not potentiate cell death triggered by irradiation in clonogenic assays, nor did it show any benefits on reducing tumour size compared to irradiation alone *in vivo* (Bristol et al., 2013). However, both Bristol *et al*. and our group pre-treated cells with CQ prior to irradiation and so the treatment protocols were overall similar. Regardless, we were able to clearly detect positive cell killing effects of CQ in combination with radiation. Our data on sensitisation by CQ agree with the wide array of studies from different cancer models reinforcing that CQ may be useful as an anti-cancer sensitising agent.

3.3.ii Nutrient-dependent differences in autophagy flux activation

Nutrient starvation is well characterised as an essential modulator of autophagy induction; thus, cells deprived of nutrients in our cell model could be dependent on autophagy for continued cell survival. However, the signalling mechanisms by which alternate nutrient starvations initiate autophagy can differ (glucose starvation vs. amino acid starvation) (Kim et al., 2011). Furthermore there is some controversy as to the potential of different nutrient conditions to activate autophagy (Ramirez-Peinado et al., 2013, Moruno-Manchon et al., 2013). We aimed to assess the capability of alternate nutrient starvations to induce autophagy in our 4T1 cell model using biochemical analysis of classical autophagy markers. In doing this work, we have highlighted key differences in autophagic flux activation under specific nutrient starvation conditions. Our data indicates that contrary to the accepted dogma, glucose starvation mediates a block of autophagic flux rather than activation. It is well recognised that depletion of glucose, and in turn ATP, can activate autophagy through the energy sensing kinase, AMPK (Kim et al., 2011). This important energy sensor can activate autophagy either indirectly through mTORC1 inhibition (Gwinn et al., 2008, Inoki et al., 2003), or directly through phosphorylation of ULK1 at S317 and S777 (Kim et al., 2011). However, the importance of the glucose starvation-driven AMPK signalling axis in the induction of autophagy conflicts with opposing data indicating that glucose is required for the assembly of the v-ATPase (Dechant et al., 2010, Sautin et al., 2005), an essential proton pump involved in acidification of the lysosomes and activation of autophagy. Based on our data indicating glucose starvation does not activate autophagic flux in the 4T1 cell line, despite activating AMPK signalling, and further evidence showing lysosomal acidification is not induced to as great an extent in glucose starved cells in comparison to alternative nutrient starvations (as described in chapter 4), we are in agreement with the latter studies. In relation to our cell model, we postulate that in the absence of glucose, the v-ATPase pump assembly is compromised, and this could be related to the lack of autophagy flux we observe.

Indeed, other studies using alternative cell lines have also observed a block of autophagy upon glucose starvation. Munoz-Pinedo *et al.,* 2013 showed that while withdrawal of glucose led to mTOR inactivation and AMPK activation, it did not induce autophagic flux (Ramirez-Peinado et al., 2013). Interestingly, it has also been shown that the presence of glucose, rather than depletion, can induce autophagy;

this was dependent on ATP, as a drop in ATP levels was correlated with a reduction in autophagosomes (Moruno-Manchon et al., 2013). Again, AMPK activation and mTOR inactivation was seen upon glucose starvation in these studies, confirming that changes in these key regulatory pathways are not an indicator of autophagy activation upon glucose starvation. Indeed, in yeast glucose starvation has also been shown to inactivate autophagy (Lang et al., 2014).

To further assess nutrient-dependent differences in autophagy activation, we examined mitochondrial morphology in response to alternate nutrient starvations. It has been established that upon depletion of essential nutrients, mitochondria exhibit a tubulated morphology to avoid autophagic degradation, thus allowing this metabolic organelle to maintain a supply of ATP to starving cells (Gomes et al., 2011, Rambold et al., 2011). Indeed, we showed clear differences in the mitochondrial morphology between amino acid and glucose starvation conditions. In response to amino acid withdrawal, mitochondria became elongated and formed tubulated structures, which may represent the organelle survival response to avoid mitophagy as proposed. In contrast, mitochondrial fission or fragmentation was predominant upon glucose withdrawal. As we and others have shown tubulated mitochondria are only present after amino acid starvation and not glucose starvation (Rambold et al., 2011), this again suggests that glucose withdrawal does not activate autophagy flux. Taken together with our biochemical analysis of autophagy, we provide evidence that alternate nutrient starvations differentially regulate the induction of autophagy.

3.3.iii CQ has autophagy-independent activity in promoting cell death.

We confirmed that CQ had sensitising properties to a range of cellular stressors in our 4T1 cell model. Furthermore, serum starvation had the potential to induce autophagy activation as measured by LC3-I to LC3-II conversion. Therefore, we aimed to determine whether the CQ-mediated potentiation of cell death in response to serum starvation was dependent on autophagy inhibition. Using biochemical methods, we showed CQ indeed had the potential to inhibit autophagic flux over long term treatment in 4T1 cells. However, our work utilising knock down of key autophagy proteins, and autophagy-deficient knockout MEFs showed CQ to be potentiating cell death through an autophagy-independent mechanism. We are not

the first to identify this unexpected effect; Maycotte *et al.,* 2012, showed CQ sensitisation of 4T1 cells to the PI3K inhibitor, LY294002, and MTOR inhibitor, Rapamycin, was not mimicked by ATG12 or Beclin1 knockdown. In addition, sensitisation still occurred even in the absence of these key autophagy proteins (Maycotte et al., 2012). Similarly, we also showed CQ to sensitise to growth factor starvation in both autophagy-deficient 4T1 cells and MEFs. Further work has been shown reinforcing the autophagy-independent anti-cancer effects of CQ. Eng *et al*., 2016, echoed our data in that knockdown of ATG7 in a KRAS-driven tumour cell lines, Panc 10.05 and HCT116, did not sensitise to irradiation or TKIs, erlotinib and sunitinib (Eng et al., 2016). In these models, CQ was able to sensitise the cells to these agents to a similar extent in both wild-type and ATG7-deificient cell lines, indicating the effects of CQ were independent of autophagy.

Although CQ may not be primarily acting by blocking autophagy in our cell model, we should highlight the other contrasting data supporting the role of autophagy in cancer. For example, genetic knockdown of ATG5/7 was shown to increase apoptosis alone or in combination with mTOR inhibitors in neuroendocrine tumour BON1 cells. The authors stated this mimicked their results with CQ (Avniel-Polak et al., 2015). In addition, the ability of CQ to enhance the efficacy of TKI Imatinib mesylate in CML blast crisis cell lines was replicated by ATG5 or ATG7 knockdown (Bellodi et al., 2009). Further work by Eileen White has shown ATG7 and HCQ treatment to similarly induce cell death in *N-Ras* or *Braf* driven melanoma cell lines (Xie et al., 2013). This dependency of *Ras* driven tumours (this time *K-Ras*) on autophagy was confirmed in mouse models of non-small cell lung cancer; here genetic deletion of ATG7 resulted in accumulation mitochondria, induction of p53 and inhibition of proliferation. These results suggested that Ras-driven tumours required autophagy to maintain functional mitochondria (Guo et al., 2013). Taking these data and our own work into consideration it is evident that the sensitisation benefits of CQ may be mediated through both autophagy-dependent and independent mechanisms and this may be related to the cell model and combination therapy used.

Alternative autophagy-independent mechanisms of CQ have been identified in multiple cell studies, many of which are linked to the concentration applied. One such example is the evidence of CQ interaction with nucleotides, specifically the purine and pyrimidine bases. Work conducted in the 1960s assessing the interaction

of CQ with DNA via spectrophotometric studies identified a binding interaction between the protonated ring system with CQ and anionic phosphate groups within DNA, with more specific interactions occurring between the CQ aromatic ring and nucleotide bases (Cohen and Yielding, 1965). Further work has shown that CQ (at doses between 100-500μM) caused oxidative damage of purine and pyrimidine bases, and increased DNA strand breaks in rat liver cells in a dose-dependent manner (Farombi, 2006). However, as the concentrations needed to elicit these DNA interactions are high we would speculate that it is unlikely these effects would be observed in humans. Furthermore, it is not clear how CQ-DNA binding alters cancer cell behaviour.

A further autophagy-independent effect of CQ identified is the potential of CQ to normalise the tumour vasculature *in vivo* (Maes et al., 2014). Maes *et al*., 2014, showed that upon CQ administration, melanoma cells lines had signs of autophagy inhibition, i.e. increased LC3-II and p62, and in addition, CQ inhibited tumour growth in both A375m and B19 F10 derived tumours *in vivo*. When investigating the tumours more closely, the authors noted CQ-treated mice had a decreased tumour vessel density and less chaotic or less twisted vasculature. While inhibition of autophagy via genetic knockdown of ATG5 did reduce cancer cell proliferation and colony formation under metabolic stress *in vitro* (and reduced the metastatic potential of melanoma cells *in vivo)*, it was observed that ATG5 deficiency increased vascular deformations. In contrast, CQ treatment led to normalisation of the vasculature. Further work was able to attribute these effects to CQ-mediated activation of Notch 1 signalling in endothelial cells. In effect, a model was proposed where CQ normalised tumour vasculature, which then increased the delivery of chemotherapeutics deeper into the tumour (in this case cisplatin), thus improving efficacy of treatment. Taking these studies into consideration with our data, there is clearly potential for CQ to exert its anti-cancer activity through autophagy independent events, whether that is through modulating tumour vasculature, interacting with DNA or other mechanism yet to be identified.

3.3.iv Alterations in glucose availability confers protection against the cytotoxic effects of CQ

From our initial studies, we identified that CQ had the potential to sensitise to nutrient stress in the form of serum starvation. However, cancer cells can be subjected to multiple energetic and/or metabolic stress conditions with the tumour mass (Reid and Kong, 2013). Therefore, we aimed to examine the potential of CQ to sensitise to alternate nutrient starvation conditions, and whether this had an impact on the ability of CQ to potentiate cell death. Indeed, in performing such studies we identified an unexpected interaction whereby reduced glucose availability conferred protection against CQ-induced cell death. In assessing the mechanism behind this glucose-dependent increase in cell survival, we hypothesised that decreases in glycolytic metabolism may play a role in this cytoprotective response. Cancer cells are widely regarded as exhibiting altered metabolism compared to normal tissue cells (Warburg, 1956, Warburg et al., 1927); it has long been recognised that cancer cells in general utilise glycolysis to produce ATP, even in aerobic conditions (Elstrom et al., 2004, Nolop et al., 1987). Termed the Warburg effect, this dependence on glycolysis classically features directing metabolism away from mitochondrial pathways (TCA cycle), as opposed to the situation in normal cells which produce energy through glucose catabolism and oxidative phosphorylation in the mitochondria (Zheng, 2012). While glycolysis is a fairly inefficient process for generating energy, it meets the needs of rapidly proliferating cancer cells (Lunt and Vander Heiden, 2011), and is suggested to allow cells to survive where oxygen levels fluctuate (i.e. within hypoxic tumours) (Guillaumond et al., 2013, Robey et al., 2005). However, the Warburg effect suggests cancer cells are more reliant on glucose for energy production and growth (Warburg, 1956). Based on the Warburg effect alone, we would hypothesise a reduction in cell survival on glucose withdrawal; in contrast, we see the opposite effect in our clonogenic assays whereby glucose depletion promotes cell survival in response to serum starvation and CQ combination. In addition, the glycolysis inhibitor, 2-DG, also rescued serum starvation and CQ-mediated cell death. Considering these findings, our data are in contrast to the Warburg theory as instead of depending on glucose for survival, we observe that glucose withdrawal leads to significant cell survival in response to CQ.

To examine the link between glycolysis inhibition and cell survival in response to CQ further, we studied the effects of two widely used inhibitors of glycolysis,

dichloroaceate (DCA) (Clark et al., 1987) and Gossypol (Wang et al., 2012). In contrast to glucose withdrawal or 2DG treatment, these downstream glycolysis inhibitors surprisingly did not protect against CQ-mediated cell death. Furthermore, gossypol demonstrated potent cytotoxic effects as a single agent in 4T1 cells. Our data from clonogenic assays using DCA and gossypol therefore agree with published findings demonstrating these compounds to be potent anti-cancer drugs. Gossypol has been shown to induce cancer cell death and inhibit proliferation in a range of cancer cell lines, including prostate (Volate et al., 2010), breast and fibrosarcoma (Ligueros et al., 1997). DCA has also shown potent anti-cancer effects in prostate cancer, sensitising both normal and radio-resistant cells to *in vitro* radiation treatment. These findings correlated with significant alterations in mitochondria membrane potential in DCA treated cells and increased rates of apoptosis (Cao et al., 2008). Alternatively, DCA has also been shown to induce apoptosis in a range of endometrial cancer cell lines while intriguingly, showing no induction of apoptosis in non-cancerous cells such as HEK-293T (Wong et al., 2008). These data indicate that downstream glycolysis inhibition has the potential to be an effective anti-cancer therapy. However, some caveats should be noted. Wong *et al*., 2008 observed that highly invasive cancer cell lines were resistant to DCA (Wong et al., 2008). Furthermore, a recent report by Delaney *et al*., 2015, suggested that the effects of DCA were via anti-proliferative mechanisms rather than alteration of cell survival responses (Delaney et al., 2015). In any case, our observations suggest that only early inhibition of glycolysis (with 2DG) (but not later stage inhibition) can induce protection against the effects of CQ.

An interesting question to us was how cells could have higher rates of survival with lower glucose metabolism. What energy sources were the cells using during the 24 hour treatment? Our data suggested that in the absence of glucose, 4T1 cells use primarily glutamine for cell survival, as withdrawal of this key amino acid led to a reduction in cell viability. Although many cancers have shown reliance on glucose to meet their energy needs, some cancer phenotypes can be heavily reliant on glutamine metabolism. Glutaminolysis begins by conversion of glutamine to glutamate in reactions mediated by glutaminases (GLS). Some of these GLS enzymes have been shown to have oncogenic properties. Not only have transformed cells and cancer cell lines been shown to have elevated GLS activity (Wang et al., 2010, Gao et al., 2009, Lobo et al., 2000), inhibition of GLS can also inhibit oncogenic growth. Importantly, glutamine provides a key alternative nutrient

and energy source when glucose is not freely available. Using a MYC-inducible human Burkitt lymphoma model P493 cell line, one study showed increased TCA cycle intermediates derived from [U-$^{13}C^{15}N$]-labelled glutamine under glucose depleted conditions (Le et al., 2012). After its conversion to glutamate, labelled glutamine was further catabolized to form α-ketoglutarate, an intermediate of the TCA cycle. This metabolic pathway is shown to be essential for cell survival when glucose metabolism is impaired (Yang et al., 2009). A key oncogenic driver of glutaminolysis is c-myc (Gao et al., 2009, Wise et al., 2008), and indeed 4T1 cells exhibit elevated myc expression in comparison to their less metastatic counterparts (Tao et al., 2008). With this known, it would be intriguing to investigate if the less metastatic 67NR and 168FARN cell lines (originally isolated in parallel with the 4T1 line) also show a dependence on glutamine in the absence of glucose.

3.3.v Glucose starvation: activation of AMPK is independent of glucose-depletion mediated cell survival.

As different nutrient starvations are known to activate alternative signalling pathways, our initial hypothesis was that glucose starvation may induce a cell survival response via activation of AMPK. AMPK monitors and maintains energy homeostasis at the cellular level (Hardie, 2014). Furthermore, recent evidence has pointed towards AMPK playing a role in cancer cell survival during bioenergetic stress (Chaube et al., 2015, Song et al., 2014, Jeon et al., 2012). AMPK activation was shown to prolong cell survival during energy stress in A549 adenocarcinoma human alveolar basal epithelial cells (Jeon et al., 2012). Furthermore, inhibition of the AMPK pathway, via shRNA-mediated knockdown of LKB1, induced cell death in response to glucose starvation. Alternatively, restoration of AMPK functions via LKB1 expression protected A549 cells from glucose starvation-induced cell death. The authors concluded AMPK activation helped maintain NADPH levels by inhibiting ACC1 and/or ACC2, and that this function was critical for cancer cell survival. AMPK activation was also shown to be a key survival mechanism in other cancer cell lines (Chhipa et al., 2010) in earlier studies. Here, blockade of AMPK activation, via expression of dominant negative AMPK or treatment with an AMPK inhibitor (compound C) increased apoptotic cell death in the androgen-independent prostate cancer cell line C4-2. In more recent work, Chaube et al., 2015, showed AMPK to protect H1299 non-small cell lung cancer cells from cell death under glucose limiting conditions. This cell survival mechanism was facilitated by AMPK induction of

mitochondrial metabolism of non-glucose substrates such as glutamine and increased OXPHOS activity (Chaube et al., 2015). Interestingly we identified that glucose starvation induced AMPK activation and in separate studies that glucose starved cells are reliant on glutamine for survival.

In concert with the literature, glucose deprivation induced activation of AMPK in 4T1 breast carcinoma cells. In addition, treatment with 2DG also induced activation of AMPK. As both of these methods of altering glycolysis conferred protection against CQ-mediated cell death, we examined whether AMPK activation was driving the resistance to cell death. However, incubation of 4T1 cells with the AMPK activator AICAR during serum starvation and CQ co-treatment did not alter the cell survival responses. Based on these data, we concluded that activation of AMPK was not the signal underlying glucose starvation-mediated resistance to CQ-induced cell death. Although we determined the survival mechanism induced by glucose withdrawal to be AMPK-independent, the work described by Chaube *et al*., 2015, may suggest AMPK is the switch from glycolysis to mitochondrial glutamine metabolism in our cell model.

Following from our findings on AMPK, we conducted further studies to ascertain whether our observations relating to glucose starvation protection of CQ-induced cell death were due to generally decreased metabolism. We utilised MP, a cell-permeant intermediate of glucose metabolism and precursor of Acetyl-CoA, to replenish ATP stores within the cells via the TCA cycle (Lembert et al., 2001). Alternatively, we promoted cellular energy levels using galactose, a carbon source proposed to enhance oxidative metabolism and drive mitochondrial energy production (Aguer et al., 2011). However, we observed no differences in cell survival upon MP supplementation. Similarly, no differences were observed after addition of galactose. Based on this work, we concluded that glucose-dependent resistance to CQ-mediated cell death was not driven by changes in energy sensing pathways (AMPK) or alternatively reduced cellular energy levels.

3.3.vi Glucose starvation and the AKT survival signal.

As we understood that glucose starvation-mediated cell survival was not dependent on the energy sensing via AMPK, we assessed whether alternative pro-survival pathways could be maintaining cell survival under glucose-depleted conditions in

our cell model. Glucose starvation has also been shown to activate AKT signalling. Gao *et al*. (Gao et al., 2013) demonstrated prolonged glucose starvation (16hrs) induced a selective phosphorylation of AKT at Thr308, a key activating site within the AKT protein kinase domain (Vincent et al., 2011). Activation of AKT led to further downstream cell survival in response to metabolic stress in HeLa cells. Furthermore, the AKT inhibitor, MK2206, reduced the percentage of cells able to survive long-term glucose starvation, indicating cell survival was dependent on AKT signalling. In accordance with these findings, MacFarlane *et al*. (MacFarlane et al., 2012) found that glucose deprivation could abrogate TRAIL-induced cell death. Z138 cells, a chronic lymphocytic leukaemia cell line, were conditioned for 2 weeks to inhibit glycolysis. This conditioned cell line was found to be less sensitive to TRAIL-induced cell death, as well as cell death induced by radiation and ABT-737, a Bcl-2 inhibitor. Intriguingly, AKT was found to be hyper-activated in these conditioned cells, suggesting AKT signalling could be a driving factor promoting cell survival in response to prolonged glucose starvation. Our investigations found that inhibition of AKT (using compound API-2) also reduced cell survival in glucose free conditions. However, API-2 also reduced cell viability in all other nutrient starved conditions, suggesting AKT to perhaps be a general survival signal, consistent with its widely accepted cellular role.

3.4 Conclusions

In this chapter, we confirmed that CQ was robust and effective at sensitising 4T1 breast carcinoma cells to a range of cellular stressors to induce cell death. In comparing the effects of CQ-mediated sensitisation to those of genetic ablation of autophagy (ATG7 and ATG5), we found the mechanism of CQ potentiation to be independent of autophagy inhibition. Further work assessing the ability of CQ to sensitise 4T1 cells to differential nutrient starvation conditions uncovered an unexpected resistance mechanism linked to glucose metabolism. Serum starvation in combination with CQ led to strong cell death. However, further glucose depletion led to substantially higher cell survival. This response was replicated using the glycolysis inhibitor, 2DG, but not alternative downstream glycolysis inhibitors that inhibited pyruvate metabolism. We were also able to demonstrate that two key cell survival pathways, AMPK and AKT, were not the key effectors of this cell survival response.

Chapter 4

CQ-mediated effects on lysosomal morphology and interaction with metabolic pathways

4.1 Introduction

The use of CQ as an autophagy inhibitor has primarily been due to its potent lysosomotropic properties. CQ, like other lysosomal inhibitors, block the end stages of autophagy trafficking and prevents the degradative flux of all autophagic cargo. As highlighted in the preceding chapter, we and others are finding that the anti-cancer effects of CQ are primarily through autophagy-independent mechanisms (Maycotte et al., 2012, Eng et al., 2016).

Indeed, CQ activity is attributed to its rapid diffusion along an acidic gradient into sites with a low pH, such as the lysosome (or in malaria parasites, the food vacuole), where it becomes protonated and in turn accumulates (Homewood et al., 1972, Seglen and Gordon, 1980). In creating a more basic environment, CQ interferes with the activity of degradative proteases, such as cathepsins, that are dependent on an acidic environment for optimal activity (Turk et al., 1994, Turk et al., 1995). This chapter investigates and discusses the lysosomal events following CQ treatment to assess whether these contribute to the anti-cancer therapeutic potential of CQ.

One essential event to ensure efficient functionality of the lysosomes is the acidification of the lysosomal lumen, which is highly dependent on v-ATPase proton pumps present in the lysosomal membrane. These hetero-multimeric enzymes composed of 2 core components (catalytic V1 subunit, membrane-bound V0 subunit) maintain the acidic environment of the lysosome via ATP-driven transport of protons into the lysosomal lumen (Mindell, 2012). The v-ATPase inhibitor, Bafilomycin A1, is widely used to disrupt autophagic flux (Mauvezin and Neufeld, 2015). Indeed, it was previously proposed that lysosomal acidification was a prerequisite for autophagosome-lysosome fusion. However, recent work using *Drosophila* presented a refined model (Mauvezin et al., 2015); in this work, inhibition of core V-ATPase subunits led to the accumulation of dysfunctional lysosomes and a block in autophagic flux (as expected), but these non-functional lysosomes still retained the ability to fuse with autophagosomes and endosomes. Thus, this work was able to separate lysosomal acidification events from fusion events within autophagy trafficking.

It has been more recently appreciated that lysosomal acidification mechanisms are also tightly linked to mTORC1 and AMPK regulation at the lysosome (Zhang et al.,

2014a, Zoncu et al., 2011, Al-Bataineh et al., 2015) thus highlighting how nutrient-dependent signalling is intimately linked with lysosomal biology. Indeed, the v-ATPase has been shown to bind to Ragulator, a resident lysosomal protein complex to activate mTORC1 (Efeyan et al., 2013). Additional work has shown v-ATPase engagement with Ragulator to be amino acid sensitive, and is necessary for amino acids to activate mTORC1 at the lysosome (Zoncu et al., 2011). Furthermore, a recent paper identified v-ATPase as the common activator for both AMPK and mTORC1 (Zhang et al., 2014a). Here the authors outline a model whereby v-ATPase and Ragulator are required for mTORC1 activation under nutrient replete conditions. However, during energy stress these same regulatory proteins were needed for AMPK activation, via a mechanism dependent on LKB1-bound AXIN (Zhang et al., 2014a). These data support the argument that v-ATPase can indeed mediate nutrient-dependent effects upon metabolic signalling pathways, although exactly how alternate nutrient deficient conditions may promote its activity is not clear. For example, glucose has been shown to be required for assembly of the v-ATPase pump (Kane, 1995, Sautin et al., 2005), therefore whether this pump would remain functional under glucose-deplete conditions is questionable. Considering this, we proposed that different nutrient starvation conditions may induce lysosomal acidification to differing extents, thus potentially influencing CQ activity at the lysosome. We aim to address this by measuring lysosomal acidity under alternative nutrient starvation conditions in the presence and absence of CQ.

In addition to studying the CQ-dependent lysosomal changes, in this chapter we also tested the efficacy of several other CQ-related quinoline compounds and their effects on lysosomal morphology. Based on the pre-clinical success of CQ in cancer models and clinical trials, there has been an interest in repurposing other known anti-malarial compounds for use as adjuvant therapies for cancer. Indeed, two such compounds, primaquine (PQ) and amodiaquine (AQ) have shown anti-cancer activity in oral squamous cell carcinoma and melanoma, respectively (Kim et al., 2013b, Qiao et al., 2013). AQ has shown efficacy in sensitising A375 melanoma cells to starvation (amino acids) or chemotherapeutic (Cisplatin and Doxorubicin) associated cell death, in addition to inducing an autophagy-lysosomal blockade (Qiao et al., 2013). Similarly, in multi-drug resistant oral squamous cancer cells, KBC20C, PQ showed potentiation of the anti-mitotic drug, Vinblastine. However, this was suggested to be due to inhibitory actions on p-glycoprotein, rather than autophagy (Kim et al., 2013b). In addition, an alternative quinoline, quinacrine (QC),

has displayed anti-cancer activity, decreasing both anchorage dependent and independent growth and leading to the induction of apoptosis in breast cancer cells (without affecting normal epithelial breast cells) (Preet et al., 2012). These results were further validated in the context of human gastric cancer (Wu et al., 2012). Since these alternative quinolines have anti-cancer properties like CQ (and in some cases demonstrate increased potency over CQ (Qiao et al., 2013)), the rationale for further developing these compounds is clear. Indeed, clinical trials assessing mefloquine and quinacrine have already been initiated for use in a range of cancers, including glioblastoma (NCT01430351), non-small cell lung cancer (NCT01839955) and prostate cancers (NCT00417274).

In this chapter, a comparative analysis of CQ against alternative quinoline compounds in relation to cell death and lysosomal biology was carried out. Furthermore, the effects of CQ on lysosomal morphology and regulation of lysosomal acidity under differential nutrient conditions was characterised.

The main objectives were to:

(1) Examine lysosomal morphology after CQ treatment, and assess any potential differences following nutrient starvation.

(2) Assess whether CQ-mediated lysosomal effects are conserved across other cancer cell types, and whether effects are still observed in autophagy-deficient contexts.

(3) Investigate whether HK inhibition mimics glucose starvation with respect to effects on lysosomal biology.

(4) Compare the lysosomal acidification response in relation to alternate nutrient starvations, both in the presence and absence of CQ.

(5) Compare both cell viability and lysosomal changes induced by CQ vs. alternative quinoline compounds (primaquine and amodiaquine).

4.2. Results

4.2i CQ induces lysosomal enlargement, which is abrogated by reduced glucose availability.

Chloroquine (CQ) is a lysosomotropic agent that prevents acidification of the lysosome/endosome. CQ accumulates in the lysosome where it inhibits enzymes such as cathepsins, which require an acidic pH. CQ also prevents fusion of lysosomes with autophagosomes, thus preventing protein degradation. We hypothesised that cell death induced by CQ and serum starvation co-treatment was related to the lysosomal targeting of CQ, rather than inhibition of autophagy. Lysosomal size and morphology was measured in 4T1 cells under the alternate nutrient starvations by staining for lysosome-associated membrane protein-1 (LAMP-1) **(Fig 4.1)**. Both serum starvation and glucose starvation alone did not alter the lysosomal morphology. However, on addition of CQ, a dramatic increase in lysosomal size was observed. The lysosomal compartments appeared swollen in morphology, with a significant 2.5 fold increase in diameter. CQ-treated serum starved cells also showed significantly increased lysosomal diameter. However, in glucose starved and CQ-treated cells, lysosomal size was significantly reduced back to control levels. Upon quantification of lysosomal sizes, it became apparent that the responses were remarkably robust and uniform; on a cell-by-cell comparison, all cells elicited similar changes with few outliers. The differences we observed in lysosomal morphology upon serum vs. serum and glucose starvation closely correlated with our results from clonogenic cell survival assays. Lysosomal enlargement occurred in nutrient conditions which also elicited cell death, whereas in glucose-free conditions that increased cell survival we see no effect on lysosomal morphology.

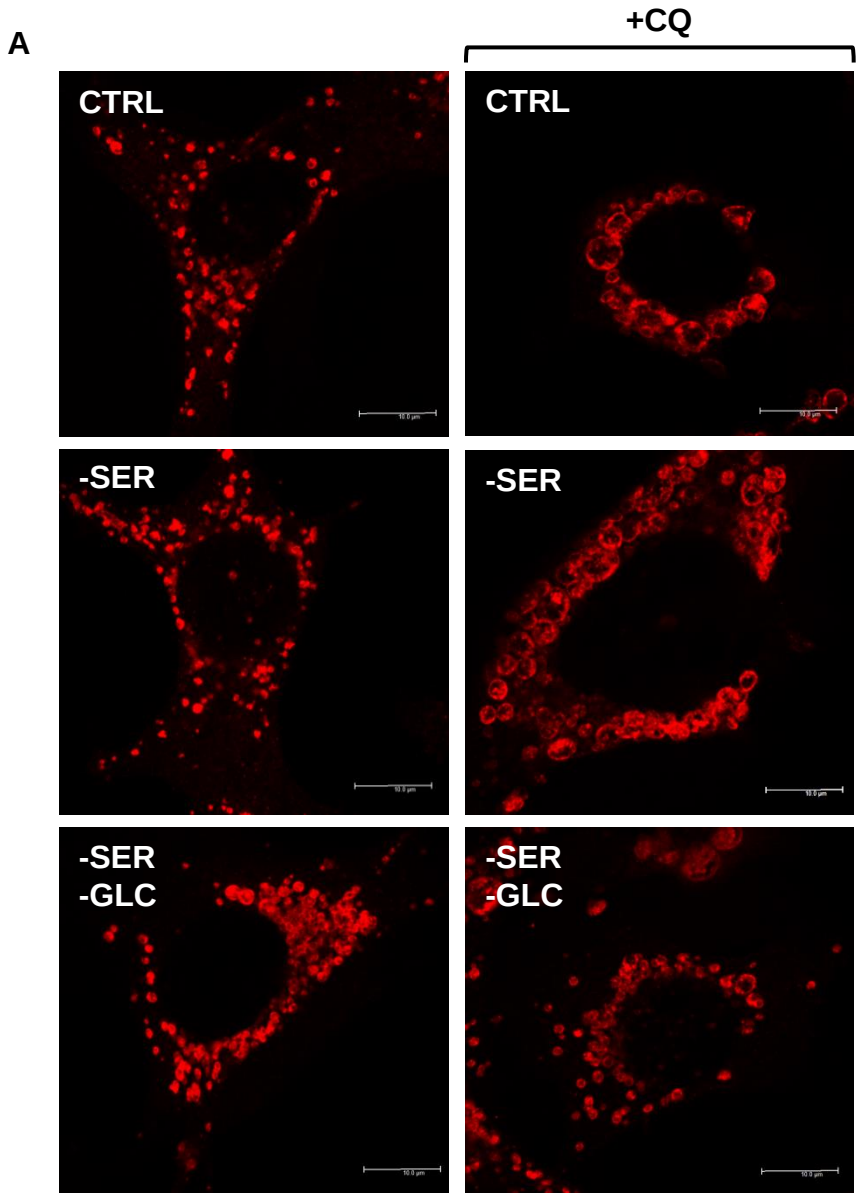
A
+CQ
CTRL
CTRL
-SER
-SER
-SER
-GLC
-SER
-GLC

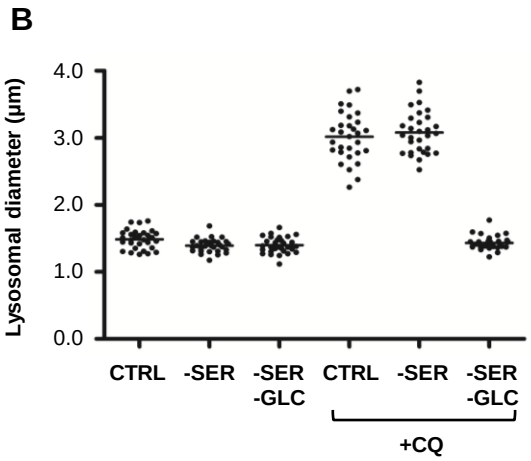
B
Lysosomal diameter (µm)
4.0
3.0
2.0
1.0
0.0
CTRL
-SER
-SER -GLC
CTRL
-SER
-SER -GLC
+CQ

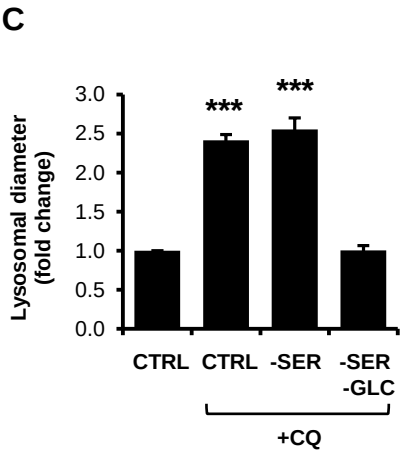
C
Lysosomal diameter (fold change)
3.0
2.5
2.0
1.5
1.0
0.5
0.0
***
***
CTRL
CTRL
-SER
-SER -GLC
+CQ

Fig 4.1 (previous page): CQ induces exaggerated lysosomal enlargement in 4T1 cells which is abrogated by reduced glucose availability.

(A) 4T1 cells were treated with full nutrient media (CTRL), starved of serum (-SER), or starved of serum and glucose (-SER-GLC) +/-CQ (25μM) as indicated for 8hrs. Cells were fixed, and stained for lysosomal associated membrane protein-1 (LAMP-1). Images were captured by confocal microscopy, and average lysosomal diameter measured for 30 cells per condition as described in Methods. Scale bar 10μm. (B) Each data point represents average lysosomal diameter per cell, and graph is representative of 3 independent experiments. (C) Average lysosomal diameter expressed as a fold change, n=3 independent experiments (One way ANOVA with Tukey post-test, comparison to control ***$p < 0.001$), error bars +/- SEM.

4.2ii Glucose starvation mediated protection of lysosomal dysfunction is a conserved event.

We examined if relationships between lysosomal morphology induced by CQ and glucose metabolism were conserved in other cell types. One such cell type used were the UVW glioma cells; glioblastoma multiforme is one such cancer phenotype that CQ is proposed to have the potential to treat (Kim et al., 2010, M.R. Rosenfeld, 2014), therefore this cell type was clinically relevant in our investigations. Measurement of the lysosomes of UVW glioma cells showed this cancer cell line to contain smaller lysosomes than the 4T1 control cell line, at approximately 0.8μm (UVW) compared to 1.5μm (4T1). However, despite differences in lysosomal size under control conditions, UVW cells exhibited the same responses to CQ treatment as 4T1 cells **(Fig 4.2)**. A significant 3.5-fold and 4-fold increase in lysosomal diameter (from control cells) was observed in CQ-treated cells and serum starved CQ-treated cells respectively. Conversely CQ-induced lysosomal enlargement was not seen in glucose-starved cells. This data showed that CQ-induced lysosomal enlargement and more importantly the resistance conferred by glucose starvation in protection of lysosomal integrity was indeed a conserved response is alternative cancer cell lines.

To further extend our observations, wild-type (1SVN) **(Fig 4.3)** and ULK1/2 double knock-out (4SVN) **(Fig 4.4)** MEFs were studied. Similar to UVW cells, the basal lysosomal size of both MEF cell lines was smaller than 4T1 cells, at approximately 1μm. As with the other cell types analysed, CQ alone induced significant lysosomal enlargement compared to control cells in both wild-type and ULK knock-out MEFs. Under serum starvation conditions coupled with CQ both MEF lines showed significant increases in lysosomal diameter, but no significant increases were induced in glucose starved cells. This data showed that the glucose-starvation mediated resistance to CQ-induced lysosomal alterations was conserved in MEF cells. Our work in MEFs, both wild-type and ULK double knock-out, is further evidence of CQ working via an autophagy independent mechanism, as changes in lysosomal morphology were conserved in both the autophagy competent and autophagy-deficient MEF lines.

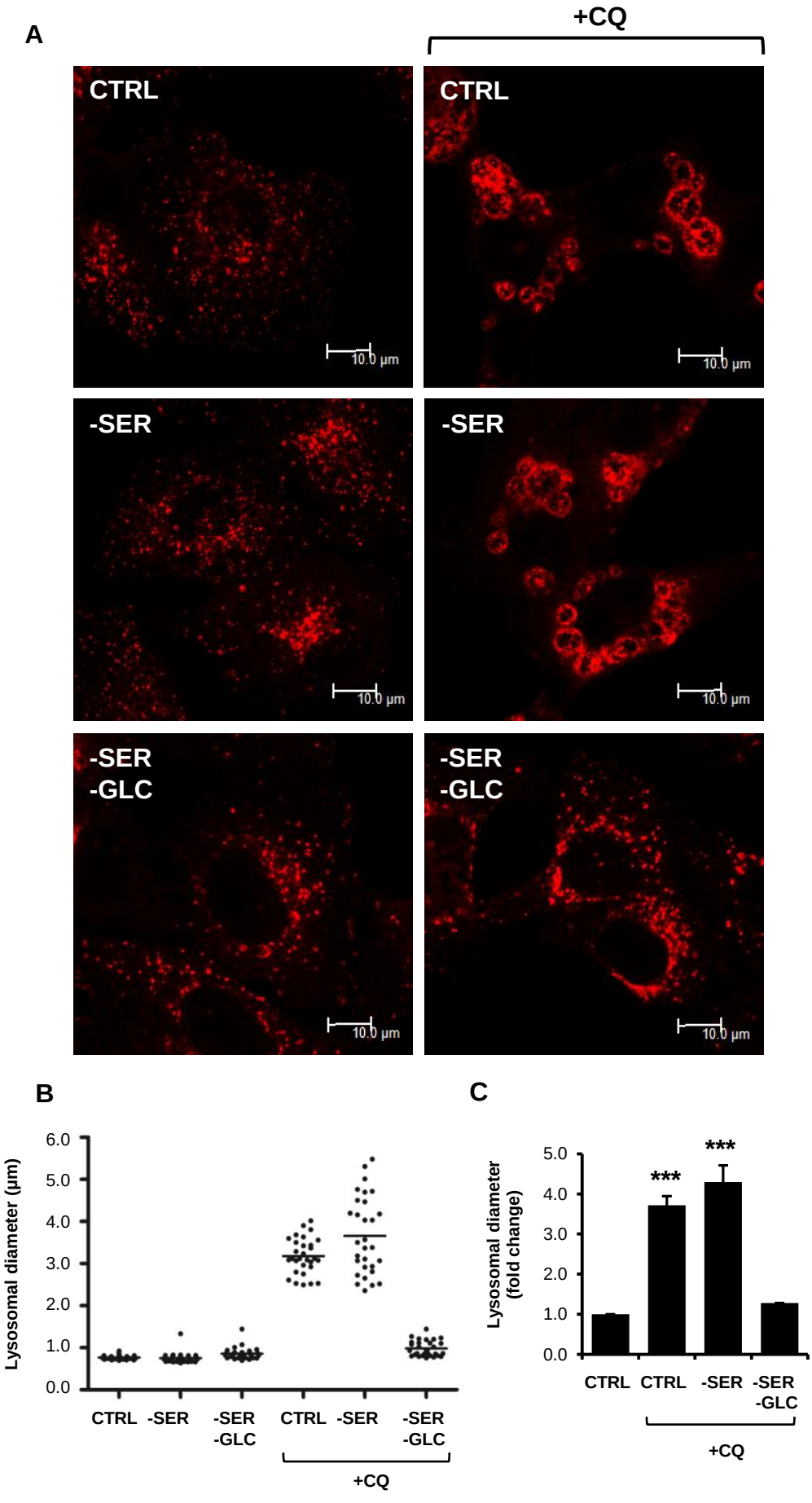
A
+CQ
CTRL
CTRL
-SER
-SER
-SER
-GLC
-SER
-GLC
10.0 µm
B
Lysosomal diameter (µm)
6.0
5.0
4.0
3.0
2.0
1.0
0.0
CTRL
-SER
-SER -GLC
CTRL
-SER
-SER -GLC
+CQ
C
Lysosomal diameter (fold change)
5.0
4.0
3.0
2.0
1.0
0.0
***
***
CTRL
CTRL
-SER
-SER -GLC
+CQ

Fig 4.2 (previous page): CQ and nutrient withdrawal lysosomal phenotypes are conserved in UVW glioma cells

(A) UVW cells were treated with full nutrient media (CTRL), or starved of serum (-SER) or serum and glucose (-SER-GLC) +/-CQ (25μM) as indicated for 8hrs. Cells were fixed, stained for LAMP-1, and quantified as in Fig 4.1. Scale bar 10μm. (B) Each data point represents average lysosomal diameter per cell (30 per condition), representative graph of 3 independent experiments. (C) Average lysosomal diameter expressed as a fold change, n=3 independent experiments (One way ANOVA with Tukey post-test, comparison to control ***p < 0.001), error bars +/- SEM.

Fig 4.3 (next page): CQ and nutrient withdrawal lysosomal phenotypes are conserved in autophagy competent wild-type MEF

(A) Wild-type (1SVN) MEFs were treated with full nutrient media (CTRL), or nutrient starved (-SER or –SER-GLC) +/-CQ (25μM) as indicated for 8hrs. Cells were fixed, stained for LAMP-1, and quantified as in Fig 4.1. Scale bar 10μm. (B) Each data point represents average lysosomal diameter per cell (30 per condition), representative graph of 3 independent experiments. (C) Average lysosomal diameter expressed as a fold change, n=3 independent experiments (One way ANOVA with Tukey post-test, comparison to control ***p < 0.001), error bars +/- SEM.

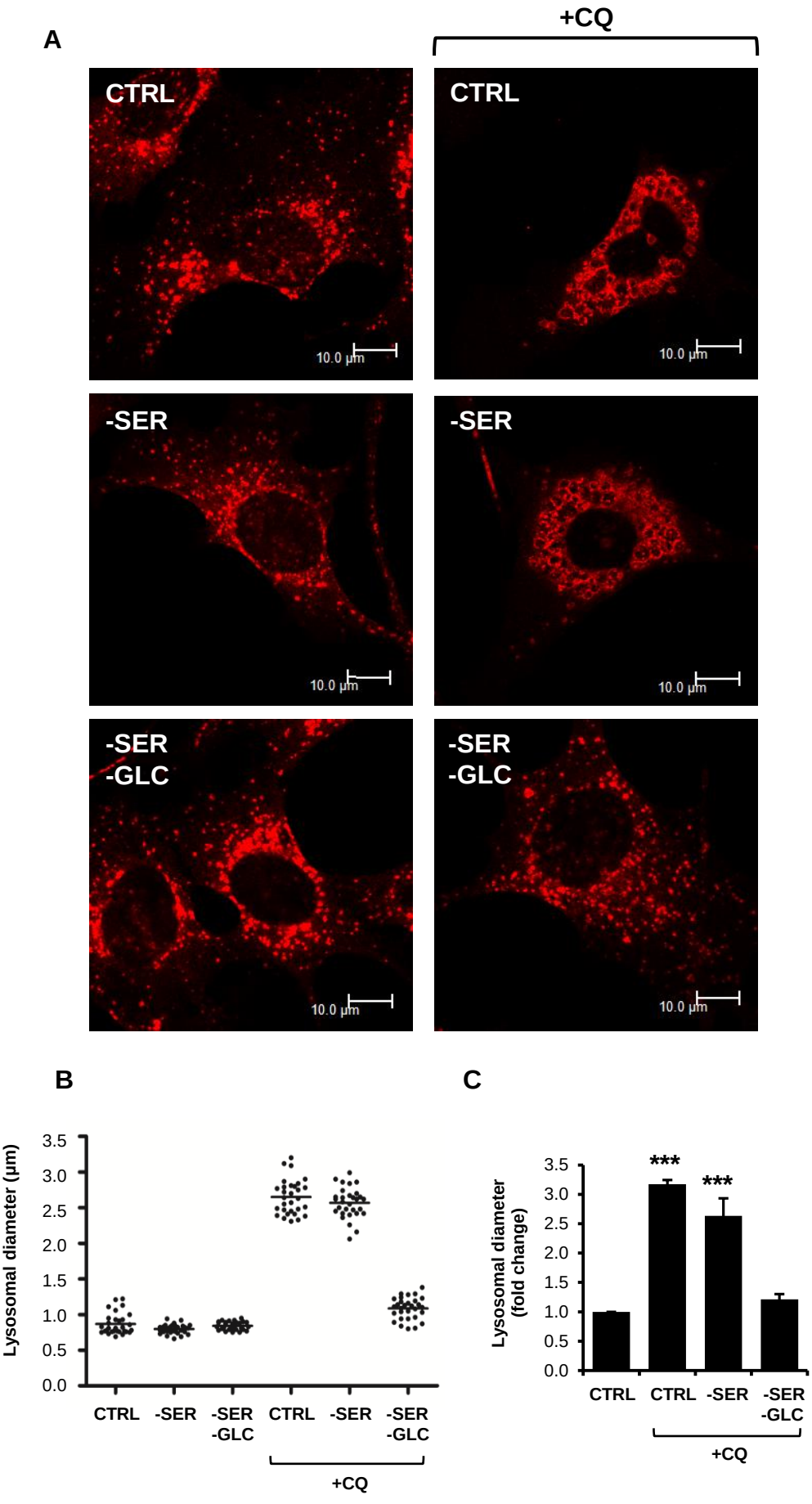
A
+CQ
CTRL
CTRL
-SER
-SER
-SER
-GLC
-SER
-GLC
10.0 µm
B
Lysosomal diameter (µm)
3.5
3.0
2.5
2.0
1.5
1.0
0.5
0.0
CTRL
-SER
-SER -GLC
CTRL
-SER
-SER -GLC
+CQ
C
Lysosomal diameter (fold change)
***
***
CTRL
CTRL
-SER
-SER -GLC
+CQ

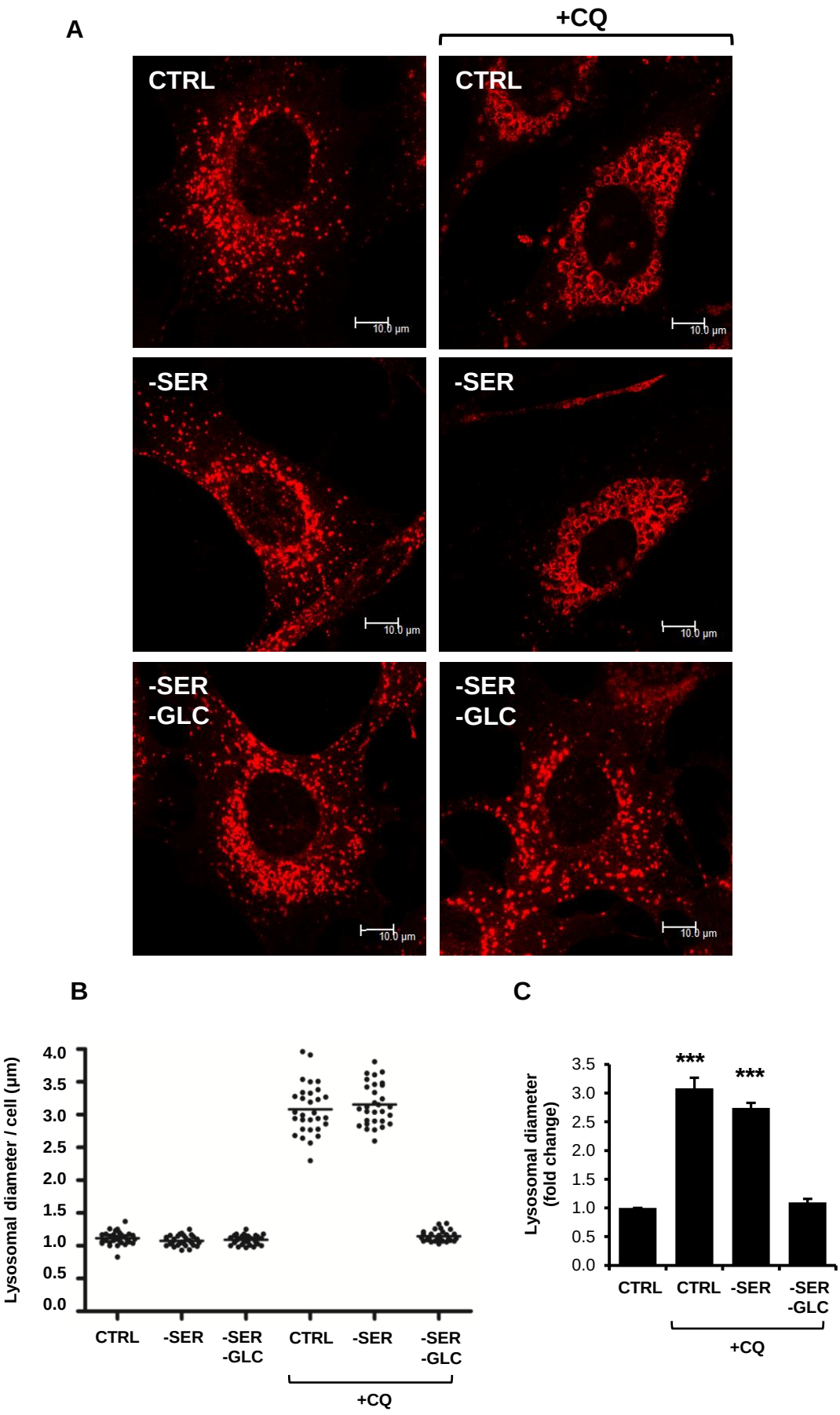
A
+CQ
CTRL
CTRL
-SER
-SER
-SER
-GLC
-SER
-GLC
10.0 µm
B
Lysosomal diameter / cell (µm)
4.0
3.5
3.0
2.5
2.0
1.5
1.0
0.5
0.0
CTRL
-SER
-SER
-GLC
CTRL
-SER
-SER
-GLC
+CQ
C
Lysosomal diameter
(fold change)
3.5
3.0
2.5
2.0
1.5
1.0
0.5
0.0
***
***
CTRL
CTRL
-SER
-SER
-GLC
+CQ

<u>Fig 4.4 (previous page):</u> CQ and nutrient withdrawal lysosomal phenotypes are conserved in autophagy deficient ULK1/2 DKO MEF

(A) ULK1/2 DKO (4SVN) MEFs were treated with full nutrient media (CTRL), or nutrient starved (-SER or –SER-GLC) +/-CQ (25μM) as indicated for 8hrs. Cells were analysed as in Fig 4.1. Scale bar 10μm. (B) Average lysosomal diameter per cell (30 cells). (C) Average lysosomal diameter expressed as fold change, n=3 independent experiments (One way ANOVA with Tukey post-test, comparison to control ***$p < 0.001$), error bars +/- SEM.

4.2iii Targeting of Hexokinase with 2DG reduced lysosomal enlargement.

In the previous chapter the glycolysis inhibitor, 2-DG, rescued serum starvation and CQ-induced cell death. Therefore, the potential for 2-DG to also reduce CQ-driven lysosomal swelling **(Fig 4.5)** was examined. Interestingly, treatment of 4T1 cells with 2-DG, both at 2.5mM and 5mM, resulted in a significant reduction in lysosomal diameter in comparison to CQ-treated cells. These data indicate that suppression of the glycolysis pathway, through 2-DG or removal of glucose, can confer protection to the lysosomes against the activity of CQ.

As 2DG is an inhibitor of hexokinase (HK) enzymes, replication of this effect using CRISPR-Cas9 technology to ablate HK2 expression in 4T1 cells was expected. To date, 4 isoforms of HK (I - IV) have been identified in mammalian cells, but the HK2 isoform has specifically been linked to cancer malignancies and has been shown to be up-regulated in many cancers (Mathupala et al., 2001, Wolf et al., 2011). Multiple CRISPR-Cas9 targeting constructs using the LentiCRISPRv2 one-vector system were re-derived (Sanjana et al., 2014) (further detailed in Methods) (**Fig 4.6A).** 4T1 cells were transduced with lentivirus containing these vectors and multiple puromycin-resistant clones were isolated. Near-complete ablation of HK2 protein expression was achieved in around 50% of clones and the best 4 clonal lines are shown in **Fig 4.6B.**

Having confirmed HK2 targeting, the effects of HK2 knockout upon CQ-induced lysosomal enlargement were examined. Surprisingly, upon comparison of HK2 targeted CRISPR-Cas9 cells against WT cells, there were no differences in their responses to CQ treatment; CQ was still able to induce lysosomal enlargement in HK2 ablated cells (**Fig 4.7**). Furthermore, glucose starvation was still able to inhibit enlargement of the acidic vesicles in both WT and CRISPR-Cas9 HK2 cells. Based on this, we reasoned that other isoforms of HK may be compensating for the loss of HK2. This is supported by the observation that further glucose starvation (thus full inhibition of glycolysis) can block enlargement of the lysosome in HK2 deficient cells. However, we would need to confirm this further by studying metabolic pathways in our HK2 targeted lines.

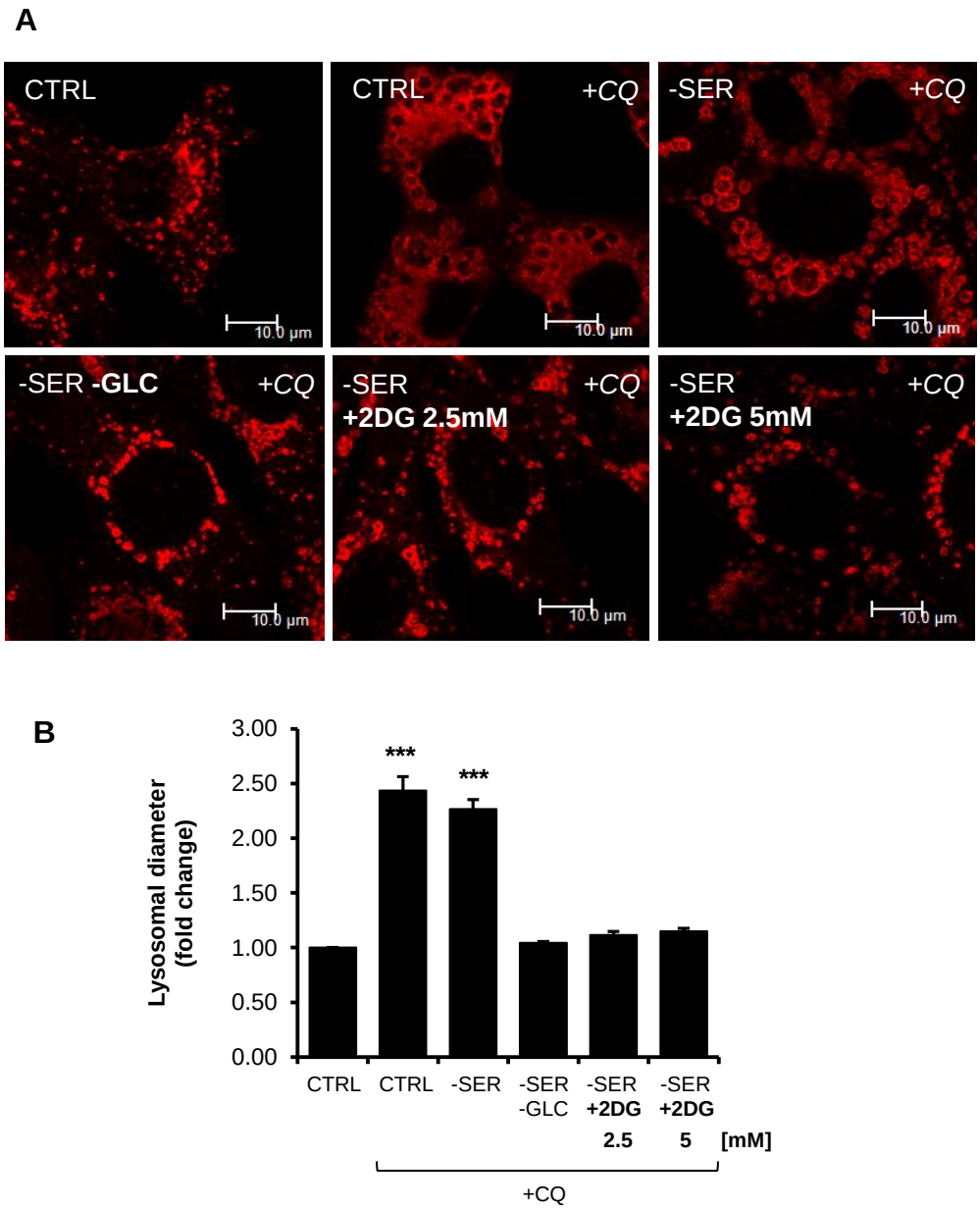

Fig 4.5: Hexokinase inhibitor, 2DG, rescues CQ-induced lysosomal enlargement in 4T1 cells. (A) 4T1 cells were treated with full nutrient media (CTRL), or nutrient starved (-SER or –SER-GLC) or alternatively treated with 2DG (2.5mM or 5mM) +/-CQ (25µM) as indicated for 8hrs. Cells were fixed, stained for LAMP-1, and quantified as in Fig 4.1. Scale bar 10µm. (B) Average lysosomal diameter expressed as a fold change, n=3 independent experiments (One way ANOVA with Tukey post-test, comparison to control ***$p < 0.001$), error bars +/- SEM.

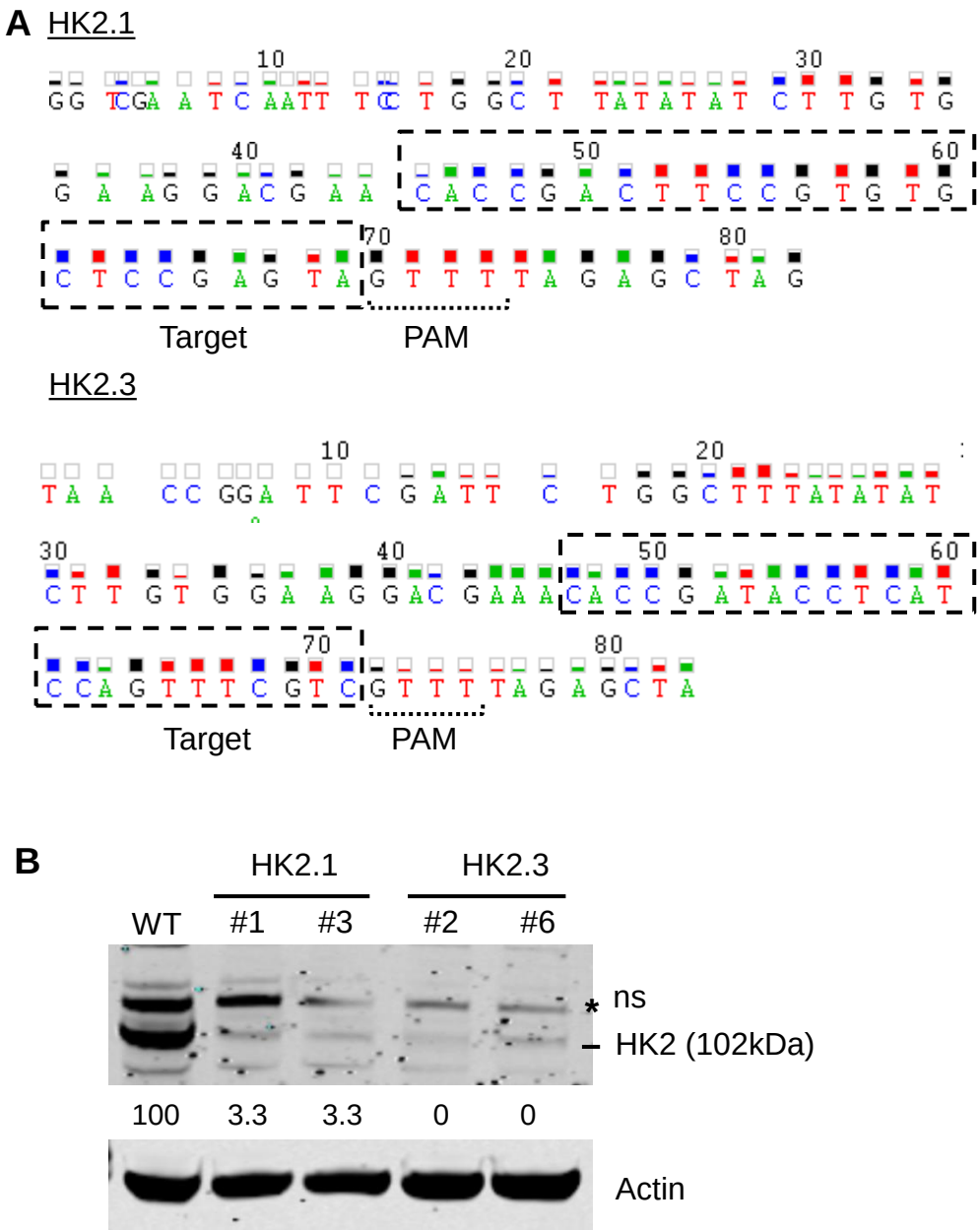

Fig 4.6: CRISPR-Cas9 mediated knock down of HK2 protein in 4T1 cells. (A) Two LentiCRISPRv2-Cas9 plasmids targeting mouse HK2 were re-derived and confirmed by sequencing (described further in Methods). Boxed area depicts target guide sequences oligos. (B) 4T1 wild type (WT) or HK2 CRISPR targeted clones (HK2.1 or HK2.3, # clone number) were assessed for HK2 levels via western blot. Actin was used as loading control. Immunoblotting was quantified as described in Methods and expressed as HK2 normalised to Actin (% of wild-type).

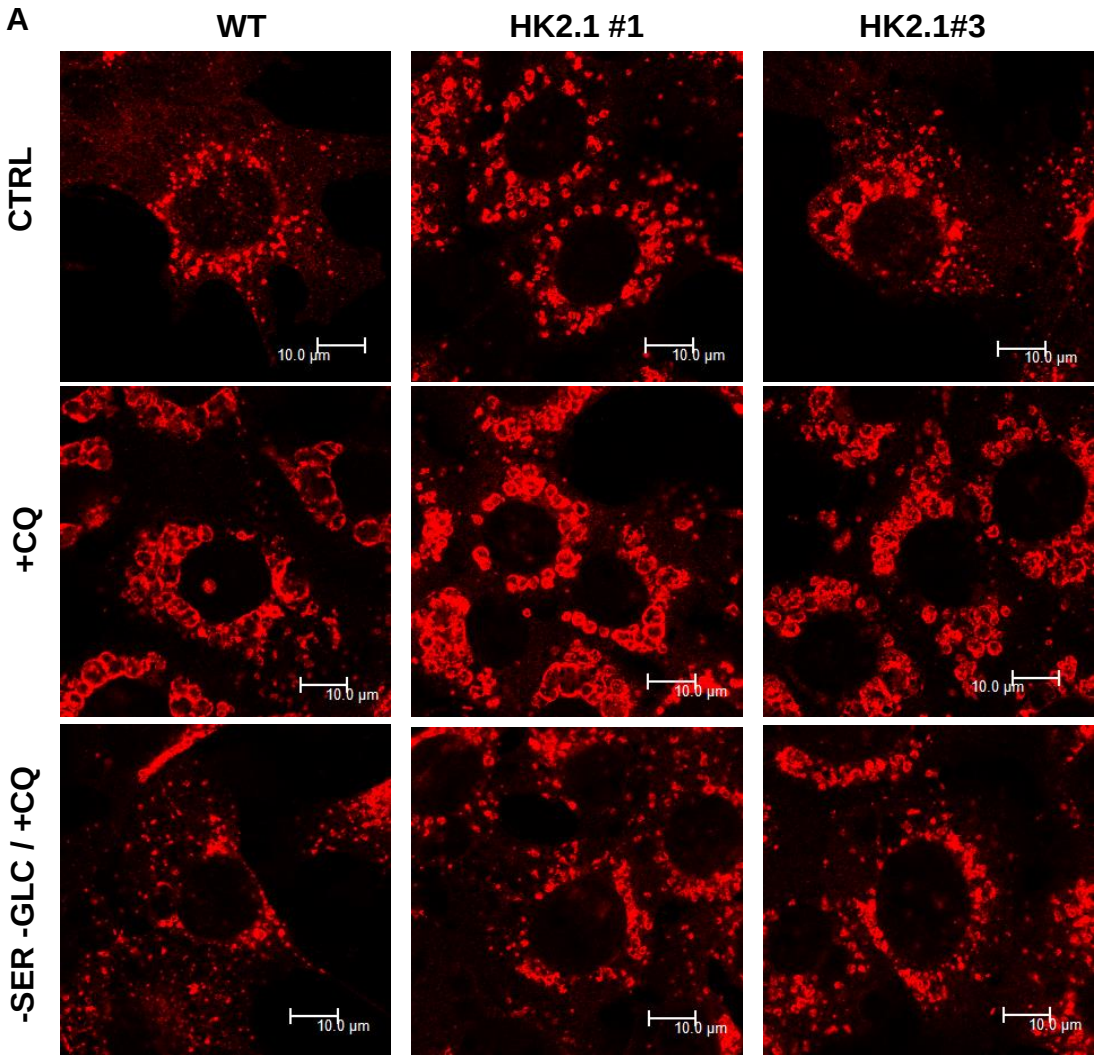
A
WT
HK2.1 #1
HK2.1#3
CTRL
+CQ
-SER -GLC / +CQ
10.0 µm

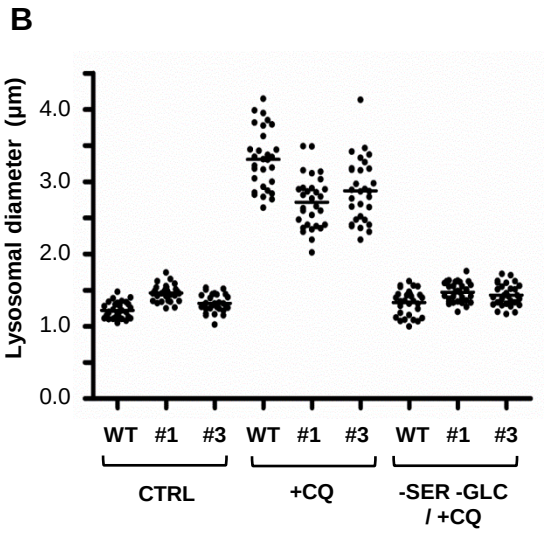
B
Lysosomal diameter (µm)
0.0
1.0
2.0
3.0
4.0
WT #1 #3 WT #1 #3 WT #1 #3
CTRL
+CQ
-SER -GLC / +CQ

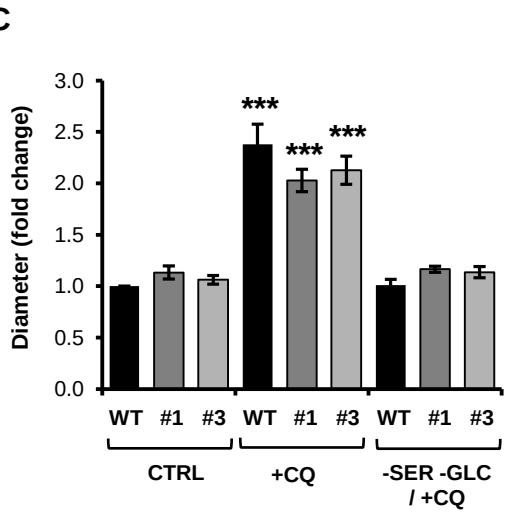
C
Diameter (fold change)
0.0
0.5
1.0
1.5
2.0
2.5
3.0
***
***
***
WT #1 #3 WT #1 #3 WT #1 #3
CTRL
+CQ
-SER -GLC / +CQ

<u>Fig 4.7:</u> HK2 silencing does not rescue CQ-induced lysosomal enlargement in 4T1 cells

(A) 4T1 wild type (WT) or HK2 CRISPR (HK2.1 #1 and #2) cells were treated with full nutrient media (CTRL) +/-CQ (25μM), or starved of serum and glucose (-SER-GLC) +CQ (25μM) as indicated for 8hrs. Cells were fixed, and stained for LAMP-1, and quantified as in Fig 4.1. Scale bar 10μm. (B) Each data point represents average lysosomal diameter per cell, representative graph of 3 independent experiments. (C) Average lysosomal diameter expressed as a fold change, n=3 independent experiments (One way ANOVA with Tukey post-test, comparison to respective wild-type or clonal control ***$p < 0.001$), error bars +/- SEM.

4.2iv Glucose starvation does not block CQ mediated de-acidification of the lysosome.

Based on our findings using 2DG and glucose withdrawal, we hypothesised that CQ fails to target the lysosome upon interference with glucose metabolism.

Pellegrini *et al*., 2014, (Pellegrini, 2014) recently showed HCT116 colon carcinoma and Me30966 melanoma cells were resistant to CQ cytotoxic activity when cultured under acidic stress. The authors attributed this loss of efficacy to a dramatic reduction in CQ uptake in an extracellular acidic environment. It is possible that the weak base of CQ is protonated in an acidic environment, resulting in a reduced capacity to freely diffuse across the lysosomal or even cell membranes. Using pH-sensitive GFP derivatives, it has been shown that yeast cells fermenting glucose have a mildly alkaline intracellular pH of 7.2, whereas cells subjected to glucose starvation have an acidic pH of 6.0 (Martinez-Munoz and Kane, 2008, Orij et al., 2009). This could support the rationale that glucose starvation leads to an intracellular acidic stress, and thus inhibits the diffusion potential of CQ to cross the lysosomal membranes. Alternatively, it has also been shown that the presence of glucose is intimately linked to formation of the v-ATPase proton pump (Kane, 1995, Sautin et al., 2005), a key mediator of lysosomal acidification which provides an acidic gradient for CQ to diffuse into the lysosomal compartment. Therefore, in the absence of glucose formation of this essential complex is compromised and the acidic gradient required for CQ to freely diffuse across membranes could be altered. Based on these theories, we could hypothesise that inhibition of glucose metabolism lowers the potential of CQ to freely diffuse across the lysosomal membranes and thus exert its basic activity at the target site of the lysosome.

Lysotracker Red DND-99 (LTR), a fluorescent dye highly selective for acidic vesicles, was utilised to ascertain if glucose starvation reduced lysosomal acidity and thus blocked CQ activity at the lysosome (**Fig 4.8A**). In the first instance, during our LTR studies key differences in the induction of acidic vesicles between different nutrient conditions were observed. Serum-starvation induced a 2.5-fold increase in LTR intensity from basal conditions, whilst serum- and glucose-starvation only induced a small increase in LTR intensity (**Fig 4.8**). Alternatively, serum- and amino acid-starvation induced a 2.5-fold increase in acidification, consistent with serum starvation alone. An increase in LTR intensity would suggest an increase in autophagosome and autolysosome formation, pointing to activation of autophagic

flux. However, as this was not the case in glucose starved cells, one could reason that autophagic flux is not activated by glucose depletion. Thus these findings correlate with the LC3 and p62 data described in chapter 3 (**Fig 3.3 & 3.4**), in which we show evidence that glucose starvation mediates a block of autophagy rather than an induction.

Whilst there were differences observed in the propensity of serum starved or glucose starved cells to induce acidification of the lysosome, the presence of CQ in all nutrient conditions led to complete deacidification of the lysosomes. These CQ induced changes were further apparent when LTR staining intensity was quantified (**Fig 4.8B**). CQ was able to significantly reduce the acidic LTR signal in all nutrient-deplete conditions in comparison to their nutrient starved control in the absence of CQ ($p<0.05$). This indicated that while glucose starvation was preventing lysosomal enlargement, it did not block CQ activity within the lysosome, and indeed CQ was still able to target to the lysosomes.

Fig 4.8 (next page): CQ de-acidifies the lysosomal compartment in 4T1 cells in all nutrient starvation conditions

(A) 4T1 cells were treated with full nutrient media (CTRL), or starved of serum (-SER), serum and glucose (-SER-GLC), or serum and amino acids (-SER-AA) +/-CQ (25μM) as indicated for 4hrs. LTR DND-99 (50nM) was added for the final 30mins of treatment. Cells were fixed and images captured by confocal microscopy. Scale bar 20μm. (B) LTR intensity was measured as described in Methods, and expressed as a fold change (30 cells per condition). n=3 independent experiments (One-way ANOVA with Tukey post-test, comparison to respective nutrient condition matched control *$p < 0.05$ compared to respective nutrient starvation without CQ), error bars +/- SEM.

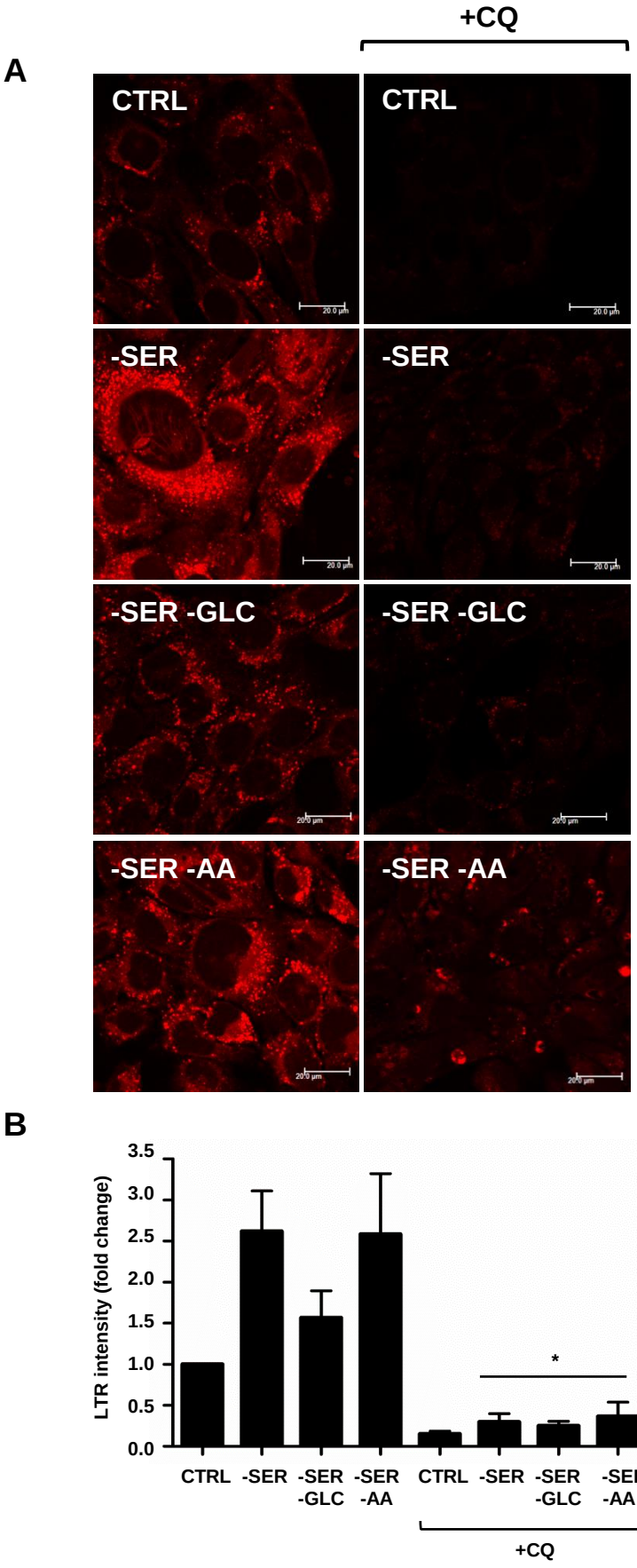
A
+CQ
CTRL
CTRL
-SER
-SER
-SER -GLC
-SER -GLC
-SER -AA
-SER -AA
B
LTR intensity (fold change)
3.5
3.0
2.5
2.0
1.5
1.0
0.5
0.0
*
CTRL
-SER
-SER -GLC
-SER -AA
CTRL
-SER
-SER -GLC
-SER -AA
+CQ

4.2v Equimolar quinoline compounds exert differential effects on lysosomal morphology and cell viability.

CQ belongs to a large family of 4-aminoquinoline compounds and members of this family are now being more widely explored as cancer therapeutics. For example, Amodiaquine (AQ), a member of this structural family, and Primaquine (PQ), belonging to the related 8-aminoquinolines, have been studied as potential anti-cancer therapies (Qiao et al., 2013, Kim et al., 2013b). We hypothesised these compounds would also display an interaction with differential nutrient starvation conditions, and this may be related to actions on the lysosome as with CQ. As such, the effects of PQ and AQ in 4T1 cells were examined using fluorescent imaging and clonogenic assays. Again, as control, CQ induced enlargement of lysosomes and these changes were abrogated on the withdrawal of glucose (**Fig 4.9**). Surprisingly, PQ and AQ both only induced small increases in lysosomal diameter, which were minimal in comparison to CQ. Interestingly, these small increases were again abrogated by glucose deprivation.

To ascertain whether these 4- and 8-aminoquinoline compounds de-acidified the lysosome (and when onset of lysosomal enlargement occurred) LTR analysis was carried out in conjunction with LAMP1 staining over a time course of up to 4hrs. All aminoquinoline compounds – CQ, PQ, AQ – de-acidified the lysosome within 30mins (and remained suppressed up to 4 hrs) (**Fig 4.10A**, $p<0.01$). In this regard, CQ and AQ at equimolar concentrations were more potent than PQ, which still had strong de-acidification properties.

In contrast, enlargement of the lysosomes by CQ was not detected until at least 1hr treatment ($p<0.01$), further increasing in a time-dependent manner up to 4hrs (**Fig 4.10B**, $p<0.001$). Also of interest, PQ and AQ again only produced minimal swelling of the lysosome which was not observed until after 4hrs exposure to the drugs. Altogether, these data indicated that lysosomal deacidification occurred before lysosomal enlargement. In addition, while PQ and AQ were still able to deacidify the lysosomes, they did not induce changes in lysosomal morphology to the same extent as CQ at equimolar concentrations.

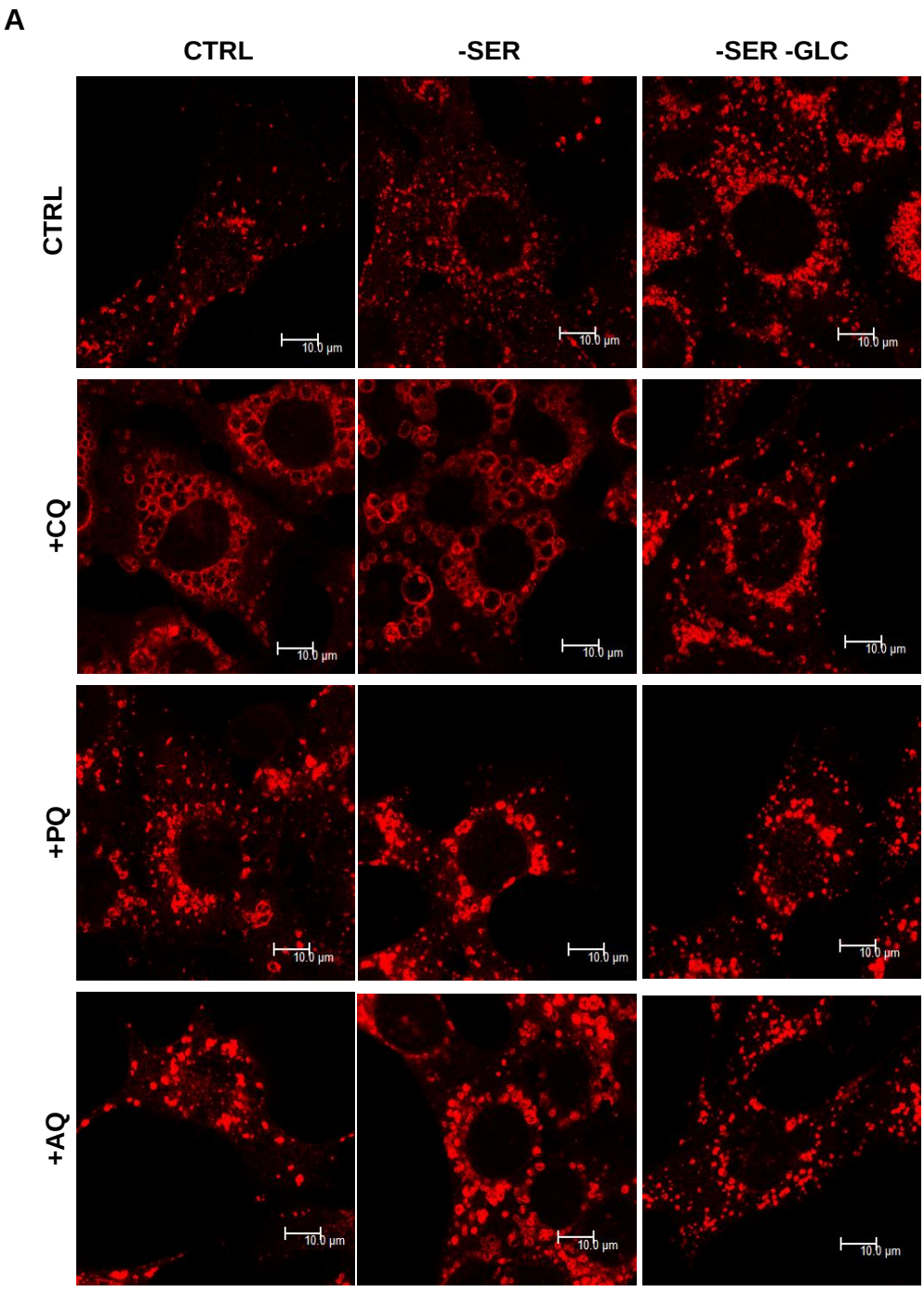

Figure legend on next page

B

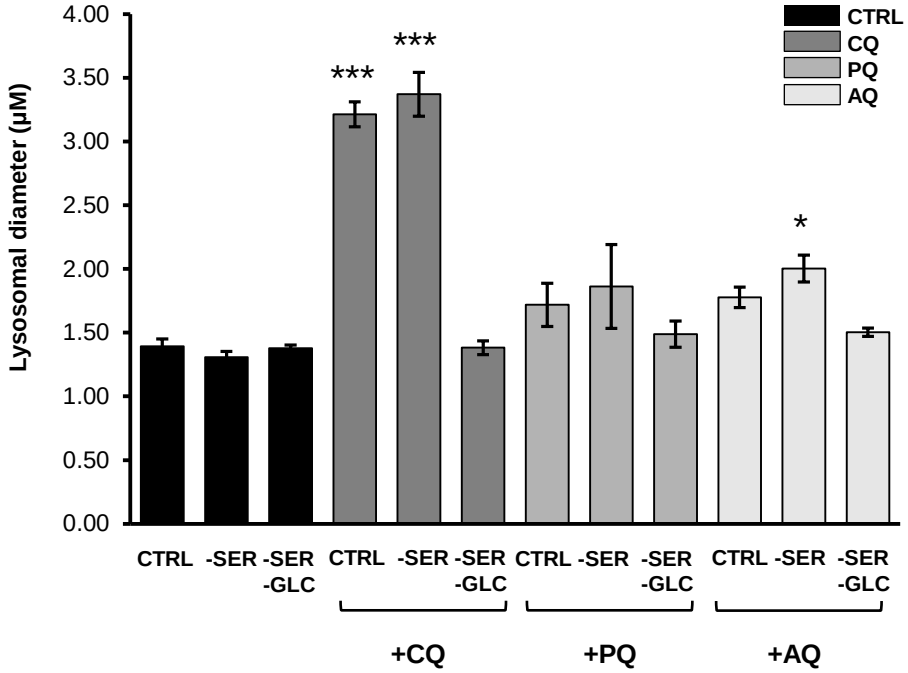

C

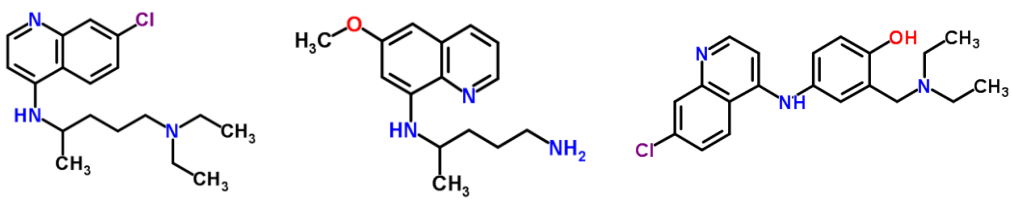

Chloroquine (CQ) **Primaquine (CQ)** **Amodiaquine (CQ)**

<u>Fig 4.9:</u> Lysosomal enlargement is not as severe with equimolar concentrations of structurally-related quinoline compounds. (A) 4T1 cells were treated with full nutrient media (CTRL), or starved of serum (-SER), or serum and glucose (-SER-GLC) +/- CQ, PQ or AQ (25µM) as indicated for 8hrs. Cells were fixed, stained for LAMP-1. Scale bar 10µm. (B) Quantified as described in Fig 4.1 (30 cells per condition), n=3 independent experiments (One-way ANOVA with Tukey post-test, comparison to untreated control ***$p < 0.001$, *$p < 0.05$), errors bars +/-SEM. (C) Structures of Chloroquine and the alternative quinoline compounds are shown.

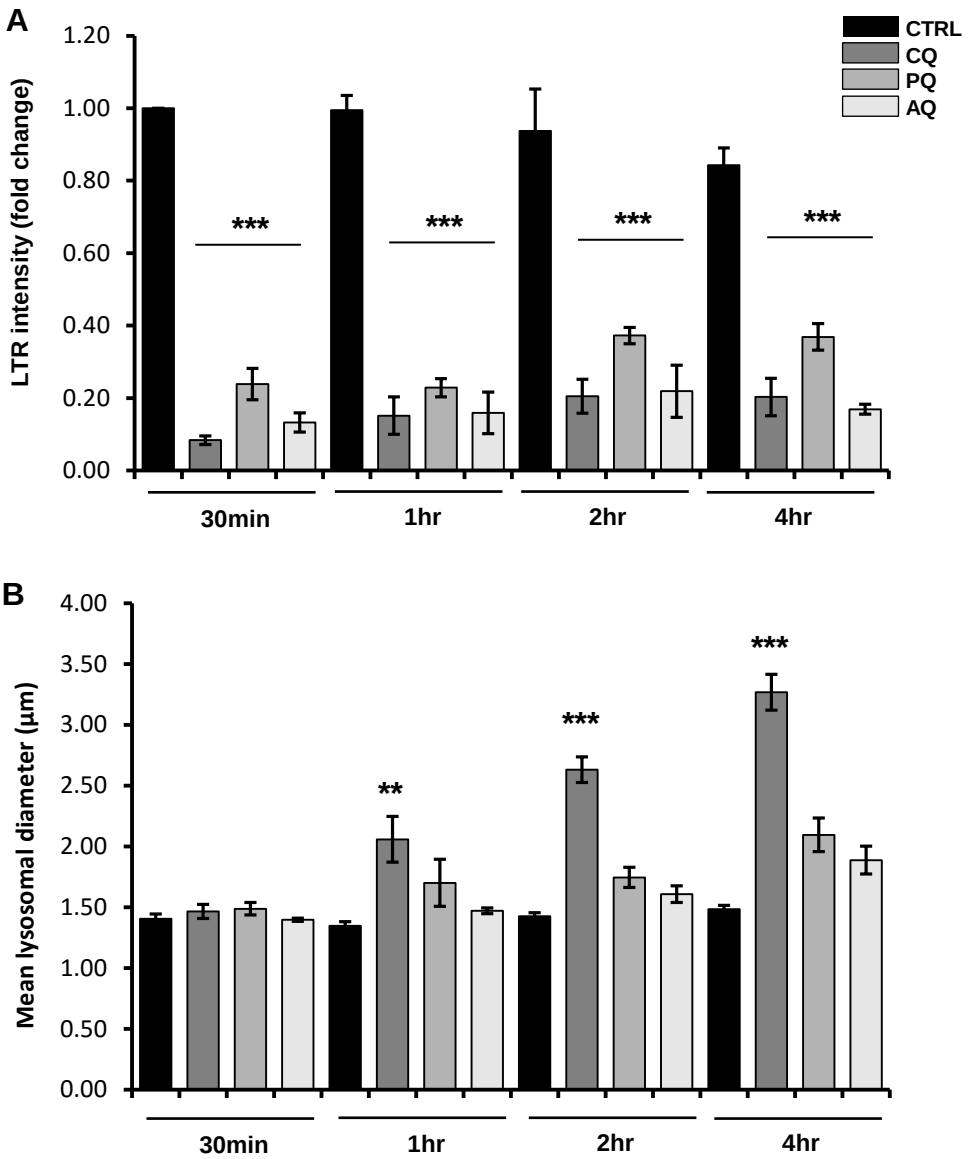

Fig 4.10: CQ and its structurally-related family members rapidly deacidify the lysosomes, before enlargement of the vesicles occurs. 4T1 cells were treated with full nutrient media (CTRL), in comparison to CQ, PQ, or AQ (all 25µM) for the times indicated. **(A)** LTR DND-99 (50nM) was added for the final 30mins of treatment. Cells were fixed, and images captured by confocal microscopy. LTR intensity was measured (30 cells per condition), and expressed as a fold change as in Fig 4.8. **(B)** Cells were fixed, and stained for LAMP-1. Images were captured by confocal microscopy, and average lysosomal diameter measured for 30 cells per condition as described in Fig 4.1. n=3 independent experiments (One-way ANOVA with Tukey post-test, comparison to respective time-point control ***$p < 0.001$, **$p < 0.01$), error bars +/- SEM.

A working model for CQ proposes that this drug de-acidifies the lysosome causing extreme swelling of these compartments, and coupled with growth factor or amino acid withdrawal, triggers cell death. This chain of events is inhibited by glucose deprivation. We confirmed above that PQ and AQ only produce a subset of effects from CQ (e.g. de-acidification). Thus, comparison of CQ, PQ, and AQ in clonogenic survival assays in different nutrient conditions examined if PQ and AQ displayed cell killing properties that were starvation dependent. In concert with our previous results, nutrient starvation conditions on their own were minimally cytotoxic, but combination of CQ and serum starvation led to a reduction in cell viability ($p<0.001$) (**Fig 4.11**). As previously established, further withdrawal of glucose blocked CQ-dependent cell killing. In line with the negligible effect on lysosomal enlargement, PQ did not induce a loss of viability, even when combined with serum starvation. In further contrast, AQ alone induced significant reductions in cell viability, and this was potentiated by serum starvation alone. Interestingly, glucose starvation did not have any effect in blocking the action of AQ. Considering AQ did not induce large increases in lysosomal diameter over 8hrs, these data do not correlate with our proposed model, and could suggest potential for the alternative quinoline compounds to induce cell death via different mechanisms or pathways despite being structurally similar.

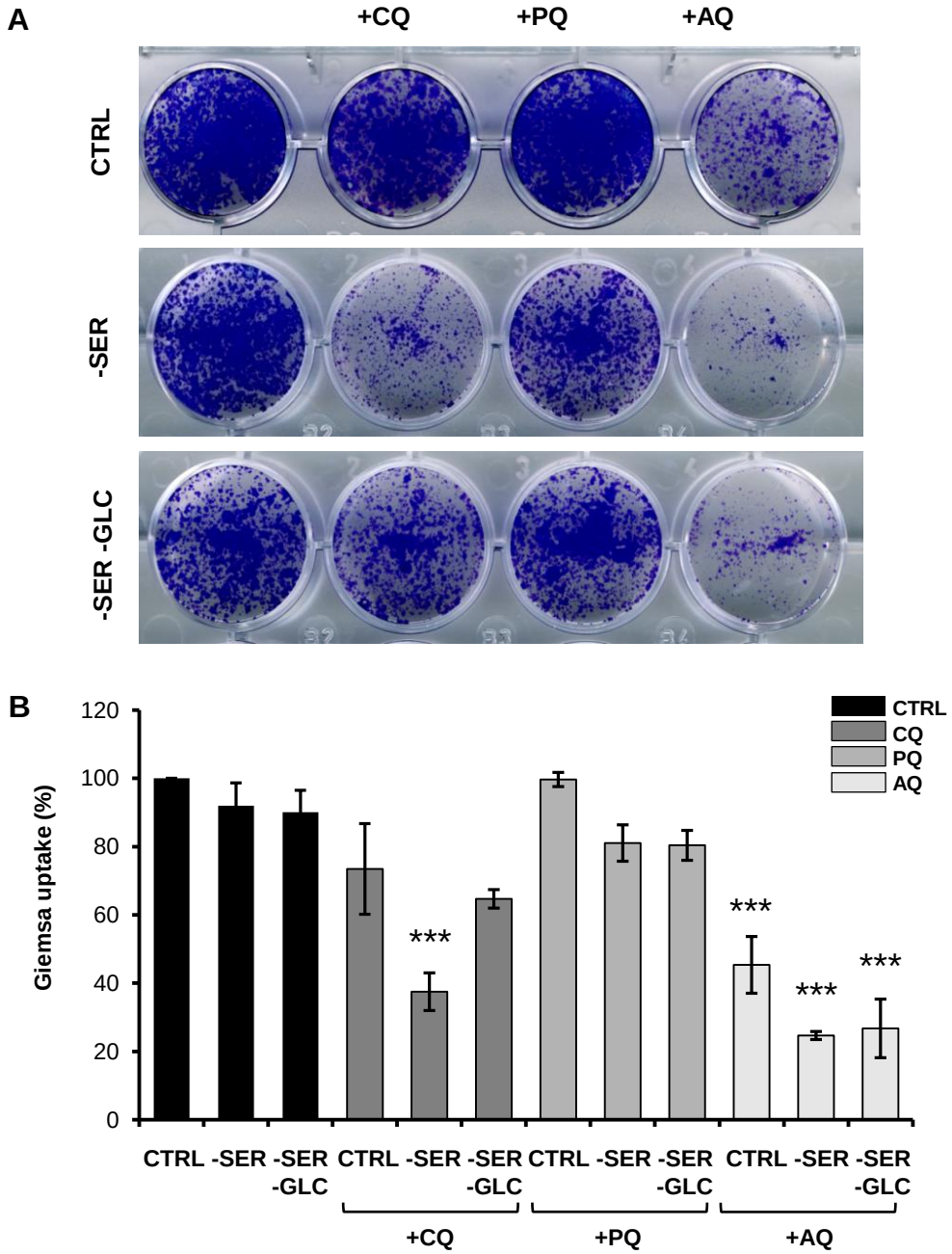

Fig 4.11: Quinoline compounds, Amodiaquine and Primaquine, exhibit differential effects on cell viability. (A) 4T1 cells were treated with full nutrient media (CTRL) or starved of serum (-SER), or serum and glucose (-SER-GLC) +/- CQ, PQ, or AQ (all 25μM) as indicated for 24hrs. The media was changed to normal full nutrient drug-free growth media and after 3 days cells were stained with Giemsa blue, and cell viability quantified as described in Fig 3.1 and Methods. (B) Giemsa uptake shown as % of control, n=3 independent experiments (One-way ANOVA with Tukey post-test, comparison to untreated control ***P < 0.001), errors bars +/-SEM.

4.3 Discussion

4.3i Glucose starvation mediated protection of CQ-induced lysosomal enlargement.

Our studies in this chapter focused on the changes in lysosomal morphology upon CQ treatment. We observed significant and dramatic increases in lysosomal diameter in 4T1 cells exposed to CQ alone or in combination with serum starvation; however, CQ did not cause lysosomal swelling on combined withdrawal of glucose and serum. This was conserved in other cancer cells such as UVW glioma, as well as autophagy competent and autophagy-deficient MEFs. Indeed, lysosomal enlargement induced by CQ was noted as early as the 1980s in rat kidney lysosomes and mouse peritoneal macrophages (Ohkuma, 1981, Ngaha, 1982). More recently, CQ-induced enlargement of acidic vesicles has been observed in ARPE-19 cells (Yoon et al., 2010, Chen et al., 2011a) where it is implicated in CQ-induced retinotoxicity. In our hands, lysosomal swelling correlated well with induction of cell death in clonogenic assays; we thus became interested in the underlying mechanism of glucose-deprivation mediated cell survival and lysosome protection. We hypothesised that under glucose withdrawal, CQ no longer targeted to the lysosome. However, CQ still showed ability to de-acidify the lysosome under glucose starvation conditions, so accessibility of CQ to the lysosome does not seem to be the issue.

4.3ii Genetic targeting of HK2 has no influence on CQ-induced lysosomal effects, while non-targeted HK inhibition does.

HK is the first enzyme involved in glycolysis; glucose is phosphorylated by HK at position C-6 to make G-6-P, with the phosphate donated from ATP. By catalysing the phosphorylation of glucose to G-6-P, HK enzymes promote and sustain a concentration gradient that facilitates glucose entry into cells and the initiation of all major pathways of glucose utilization (Roberts and Miyamoto, 2015). There are 4 known isoforms of HK (I - IV); but it is HK2 that has been shown to be up-regulated in phenotypically aggressive cancers (Coelho et al., 2015, Zhang et al., 2016) and much of the evidence published to date supports a pro-oncogenic role for HK2.

As well as its role in promoting the glycolytic pathway in cancer cells (Warburg effect), the anchoring of HK2 to the mitochondria via voltage-dependent anion channels (VDACs) is suggested to inhibit apoptotic signalling thereby promoting survival of cancer cells (Majewski et al., 2004). The accepted mechanism behind this role of HK2 is that the binding of HK2 to VDAC prevents the interaction of VDAC with activated pro-apoptotic factors, Bad and Bax, at the mitochondria (Pastorino et al., 2002).

In light of these oncogenic mechanisms, HK enzyme activity has been linked to aggressiveness of breast cancer tumours (Coelho et al., 2015). Coelho *et al*., 2015, measured breast cancer samples from patients, and correlated markers of aggressiveness and invasiveness, such as HER-2, p53, and Ki67, with HK activity. In general, the more aggressive tumour phenotypes had higher HK activity. For example, larger tumours, class IV tumours and triple negative tumours demonstrated the highest HK activity. HK2 has also been implicated in breast cancer using mouse models of ErbB2-driven cancer (Patra et al., 2013). In HK2-/- MEFs, loss of HK2 inhibited anchorage dependent growth in soft agar (transformation measure), thus HK2 was needed for oncogenic transformation in this model. In addition, HK2 deletion reduced tumour incidence and delayed the onset of tumour formation *in vivo*, and knockdown of HK2 in MDA-MB-453 breast cancer cells, which display ErbB2 amplification, impaired their ability to form orthotopic tumors in nude mice. Interestingly, HK inhibitors are now being proposed as anti-tumour drugs. One such inhibitor, 3-bromopyruvate, led to an induction of autophagy, and as such combination with CQ synergistically decreased MDA-MB-435 breast cancer cell viability (Zhang et al., 2014b). Our results do not reflect this as in our model, hexokinase inhibition with 2DG protected cells from CQ-driven lysosomal enlargement and cell death. However, our work in chapter 3 using alternative downstream inhibitors of glycolysis, DCA and gossypol, did not lead to protection of CQ-mediated cell death, this could suggest that the glucose starvation-dependent mechanism of cell survival is driven by upstream mediators of glycolysis. Therefore, we would propose to examine the effects of alternative hexokinase inhibitors in our cell model to confirm the beneficial effects we observe with 2DG. Furthermore, we could target other upstream glycolytic enzymes such as glucose-6-phosphate isomerase (GPI). Nevertheless, these studies show a clear oncogenic role for HK2 in breast cancer, and this role has been further confirmed in other cancer cell types, including pancreatic (Ogawa et al., 2015), prostate (Sadeghi et al.,

2015, Zhou et al., 2015, Ben Sahra et al., 2010) and hepatocellular carcinoma (HCC) (Dai et al., 2015).

Our data here suggest that dependency on HK2 is not straightforward, at least in 4T1 cells. While both inhibition of hexokinase with 2DG or glucose deprivation both rescued CQ-mediated lysosomal enlargement (and cell survival), specific targeting of HK2 expression using CRISPR-Cas9 gene editing could not block CQ in enlarging the lysosomal compartments. Other isoforms of HK or residual trace amounts of HK2 may be compensatory mechanisms in our HK2 CRISPR experiments here. Further studies are thus needed to be able to successfully mimic glucose starvation (or 2DG) effects by genetic methods.

4.3iii CQ exhibits activity at the lysosome, independently of pH acidification mechanisms.

We hypothesised that under glucose withdrawal, CQ may no longer target lysosomes due to loss of the acidic gradient. However, using Lysotracker red approaches, we observed that CQ still exerted its de-acidification activity at the lysosome under both glucose replete and deplete conditions. Interestingly, we also observed that in the absence of CQ, glucose withdrawal did not significantly increase the basal acidity of the lysosomes, an event that would be expected on induction of autophagy. In contrast, both serum deprivation and amino acid (+serum) deprivation induced significant acidification of the lysosome. These data are in concert with our previous findings that glucose starvation does not induce autophagic flux, but rather inhibits flux. In the current context, the data suggest that the lack of lysosomal enlargement upon CQ treatment in glucose starved cells may be due to low flux through the autophagy pathway, thus low traffic of new autophagosomes or other membranes for fusion with the lysosome.

Indeed, we are not the only group to observe nutrient dependent differences in lysosomal acidification and the mechanisms that drive this process. As outlined in chapter 3, glucose is required for assembly of the v-ATPase pump, which drives acidification of the lysosome. In *yeast cells,* the assembly of the v-ATPase pump has been shown to be driven by glucose; depriving these cells of glucose leads to rapid disassembly of the complex into its two subunits V_1 and V_0 (Kane, 1995, Dechant et

al., 2010), and leading to a rapid translocation of these subunits from the vacuolar membrane to the cytoplasm (Dechant et al., 2010). Furthermore, reassembly can be triggered by addition of glucose (Dechant et al., 2010, Kane, 1995). This has also been confirmed in mammalian cells, where glucose levels induce assembly of this ATP-driven proton pump and acidification of intracellular compartments as measured by DAMP (*N*-(3-((2,4-dinitrophenyl)amino)propyl)-*N*-(3-aminopropyl) methylamine) (Sautin et al., 2005). As we and others show glucose starvation inhibits v-ATPase assembly and does not induce significant acidification of lysosomes, we would further confirm this result in our cell system by performing double starvations, examining if glucose deprivation could abrogate the acidification induced by amino acid or serum withdrawal. To further analyse the influence of glucose on the v-ATPase complex and whether this impacts CQ-induced lysosomal enlargement, it would be interesting to examine whether inhibition of this complex via pharmacological or genetic means could abrogate the increased lysosomal sizes observed upon serum-starvation and CQ co-treatment.

4.3iv Related quinoline compounds exert differential effects at the lysosome and in cell death assays.

Recently, other quinoline drugs have been considered as an alternative to CQ for use in cancer therapy. For instance, a recent phase I clinical trial has been started assessing multiple combination therapies in glioblastoma multiforme (GBM), one of which is combination of temozolomide with mefloquine (Clinical trials identifier; NCT01430351). In addition, clinical trials investigating the benefits of quinacrine in multiple cancer types, including non-small cell lung cancer (NCT01839955) and prostate (NCT00417274) are also underway or have been completed.

Of note, so far no results from clinical trials with alternative anti-malarial drugs have been published. However, pre-clinical studies provide some rationale for use of alternative quinoline drugs as potential autophagy-lysosomal inhibitors for use in cancer therapy. Work done in U20S cells expressing tandem fluorescent-tagged LC3 has shown both AQ and PQ to inhibit autophagy with an EC_{50} of 15μM and 50μM respectively, in comparison to CQ at 15μM (Goodall et al., 2014). The 4-aminoquinoline, AQ, is known to be more potent for targeting malaria than its parent compound, CQ, so there is some precedent that this could also be the case for

cancer (Hawley et al., 1996). For instance, AQ has been shown to be cytotoxic alone, possessing a higher potency than CQ as measured by calculating the GI_{50} (drug concentration to induce a 50% reduction in cell number): 17.80μM vs. 24.36μM respectively (Zhang et al., 2008). The cytotoxicity of the compounds was shown to be cell type dependent, with MCF-7 cells being more sensitive to both AQ and CQ than MDA-MB-468 cells (Zhang et al., 2008). Indeed, AQ has further been shown to sensitise melanoma cells to starvation- and chemotherapeutic cell death (Qiao et al., 2013). In human A375 melanoma cells, AQ induced accumulation of LC3-II and p62 proteins, and LC3 puncta with impaired acidification, all indicative of a block in the autophagy-lysosomal pathway. AQ also led to increased cell killing when combined with two chemotherapeutic drugs, doxorubicin and cisplatin, compared to the drugs individually, or in combination with amino acid starvation. Indeed, experiments directly comparing AQ with CQ clearly indicated AQ to be more potent at inhibiting melanoma cell proliferation. In our work here, we also see AQ comparatively to be more potent than CQ and PQ in 4T1 cells.

In another direct comparison of quinine-based drugs, Yoon et al., 2013, used the most common anti-malarials: Atovaquine, CQ, PQ, Mefloquine (MQ), Artesunate, and doxycycline in tests for anti-cancer activities, such as the potential to reduce cell viability and induce apoptosis (Kim et al., 2013b). In the oral squamous cancer cell line KB and anti-mitotic drug resistant KBV20C, only PQ and MQ showed sensitisation effects to Vinblastine treatment, with MQ the more potent of the two drugs. A suggested mechanism of sensitisation was attributed to p-glycoprotein inhibition by PQ and MQ. P-glycoprotein is an ATP-dependent resident membrane efflux pump, which has been implicated in promoting multiple drug-resistant phenotypes (Ambudkar et al., 2003); thereby inhibition of this protein by PQ and MQ is proposed to in turn abrogate vinblastine efflux. However, CQ was also shown to have the same effects on p-glycoprotein, yet did not sensitise to Vinblastine treatment. Thus, the precise mechanistic differences between CQ, PQ and MQ remain controversial. The efficacy of these anti-cancer anti-malarial drugs are most likely highly dependent on cell type, drug combinations, and concentrations.

In 4T1 cells, we saw marked differences in cell viability after CQ, PQ, and AQ treatment. While PQ showed minimal effects in clonogenic assays, CQ and AQ induced cell death upon combination with serum starvation. However, only CQ efficacy appeared to be reduced by withdrawal of glucose. Interestingly, AQ was

also more potent at equimolar concentrations as a single agent in comparison to CQ. As well as differences in cell viability, we observed clear differences in the drug-induced changes in lysosomal morphology. In our work, CQ induced robust and exaggerated lysosomal enlargement, which was reversed by glucose withdrawal. However, no other quinoline compounds tested similarly increased lysosomal size, even AQ which was more potent in clonogenic death assays. These data are seemingly at odds with our working model in which lysosomal enlargement (and damage) was driving cell death. One such explanation for this could be that multiple mechanisms of cell death may be induced by the quinoline compounds, despite the general structural similarities of the compounds. Although understanding of cell quinolone-related cell death is limited, AQ has been shown to induce apoptosis in rat germ cells (Niu et al., 2016). The mechanisms of cell death from the different quinoline compounds are explored in more detail in the following chapter.

The majority of studies on CQ in cancer therapy focus on its sensitising effects to chemo- or radiotherapy, as CQ had been shown to have limited efficacy as a single agent. In our model, CQ has limited activity on cell viability alone. In addition, a major problem identified in clinical trials is the efficacy of CQ at tolerable doses in efficiently inhibiting autophagy or targeting cancer cell viability in patients. However, McAfee *et al*. (McAfee et al., 2012), have developed modified CQ derivatives with increased potency in blocking autophagy as well as decreasing tumour growth as a single agent. The lead compound in this study (Lys-01) has 2 aminoquinoline rings, a triamine linker, and C-7 chlorine added to the original structure of CQ. As a compound leading to autophagy blockade, the authors showed Lys01 was 10-fold more potent than CQ or HCQ. In addition, Lys01 induced near complete cell death in melanoma (1205Lu) and CQ-resistant (HCC827) cell lines. Lys05, a more soluble analogue of Lys01, enabled *in vivo* studies, and this potently reduced tumour volume and weight, and induced a greater number of autophagic vesicles in tumour cells than HCQ. Furthermore, lower doses of Lys05 could produce anti-tumour activity without dose-limiting toxicity. These data all suggest new CQ derivatives that might prove more promising at eventually treating cancer than the original quinolone compounds. However, as we have shown different quinoline derivative drugs to have different effects on lysosomal morphology (and multiple mechanisms may exist), it remains unclear if Lys01 and Lys05 trigger cell death via lysosomal enlargement. Furthermore, it is unclear if blockade of glucose metabolism would similarly lead to resistance to Lys01/05.

4.4 Conclusions

In summary, our data in this chapter indicate that CQ induces rapid de-acidification and enlargement of the lysosomal compartments in a number of cancer and normal cell types. We have identified CQ activity to be highly dependent on nutrient availability, as glucose withdrawal or glycolytic inhibition prevents CQ-mediated lysosomal swelling. Similarly, we identified that glucose withdrawal does not stimulate acidification of the lysosome in contrast to serum starvation, which in concert with our data from chapter 3 suggests that glucose starvation inhibits autophagy flux. However, we determined glucose starvation-mediated reduction in lysosomal acidification did not contribute to the mechanism of cell survival, as CQ was still able to target the lysosomes under glucose-deplete conditions. Our work with alternative quinoline compounds identified CQ to be unique in its ability to induce lysosomal swelling and cell death. Furthermore, other quinolines such as AQ did not show decreased efficacy upon glucose starvation. This suggests that, in agreement with studies assessing varied potency of quinolines, other repurposed CQ derivatives might be overall more beneficial in patients.

Chapter 5

Characterisation of cell death pathways induced by Chloroquine in 4T1 breast carcinoma cells

5.1 Introduction

As described by Hanahan and Weinberg, one of the key hallmarks of cancer is the evasion of cell death (Hanahan and Weinberg, 2011). We have shown in the preceding chapters that reduced glucose availability allows 4T1 breast cancer cells to resist CQ-dependent cell death. However, it is unclear from our studies as to the form of cell death being triggered by CQ. As such in this chapter, we characterised the mode of cell death induced by CQ.

Perhaps the best characterised cell death pathway with relation to cancer is apoptosis, a form of programmed cell death with morphological features including DNA fragmentation and blebbing of the plasma membrane. The induction of apoptosis is driven by activation of caspase family enzymes which can occur downstream of both the intrinsic or extrinsic apoptosis pathways. The extrinsic pathway is dependent on binding of ligands to their respective death receptors, for example in the cases of TNF-R1, FasR, and TRAIL-R1. A key event downstream of receptors to these ligands is the proteolytic cleavage of the upstream-acting caspase-8 to its active form, which in turn cleaves downstream caspase-3 and/or caspase-7 to promote apoptosis (Fulda and Debatin, 2006). Alternatively, the intrinsic apoptosis pathway is tightly centred on mitochondrial events, and can be promoted by cancer therapeutics such as chemo- and radio-therapy or growth factor withdrawal. Here, damaged mitochondria release cytochrome C to activate the apoptosome complex; the essential role of the apoptosome complex is to induce activation of upstream-acting caspase-9, which in turn cleaves pro-caspase 3/7 to activate apoptosis (Zou et al., 2003). As both intrinsic and extrinsic pathways converge on caspase 3/7 to promote the final stage of the apoptosis cascade, this proteolytic enzyme is regarded as the essential driving effector of apoptotic cell death (Woo et al., 1998, Blanc et al., 2000, Devarajan et al., 2002).

Indeed, caspase-3 has previously been used a readout for apoptosis with respect to CQ-induced cell death; here, CQ induced marked activation of caspase-3 which suggested CQ triggered apoptosis in glioma cells (Kim et al., 2010). CQ also induced apoptosis in melanoma cell lines (Lakhter et al., 2013), and also could enhance apoptosis induced by extrinsic apoptotic signals such as TRAIL (Park et al., 2016) and cancer therapeutics such as γ-irradiation (Firat et al., 2012). However, whether CQ activates apoptosis in all cancer cell phenotypes is not clear and could depend on the cell model and combination treatments used. As such, we aimed to

ascertain whether CQ-mediated cell death in our 4T1 cell model was dependent on apoptotic or non-apoptotic cell death mechanisms.

One alternative mechanism of cell death we investigated with respect to CQ was necroptosis. This form of regulated necrosis can be induced by much of the same stimuli as apoptosis such as: engagement of TNF receptors (Holler et al., 2000, He et al., 2009); toll-like receptors (TLRs) (He et al., 2011, Kaiser et al., 2013), and potential anti-cancer therapeutics (Locatelli et al., 2014, Saddoughi et al., 2013, Nehs et al., 2011). The key downstream effector eliciting necroptosis is a group of proteins termed the necrosome. Comprised of receptor-interacting protein kinase-1 (RIP1), RIP3, and the mixed lineage kinase domain-like protein (MLKL), the necrosome mediates the essential necroptotic events leading to cell death, for instance plasma membrane permeabilisation and generation of ROS (Su et al., 2016). This alternative mechanism of cell death is beginning to emerge as being a potential target for cancer therapeutics, particularly in cases where cancer cells are able to evade apoptosis. Indeed, a variety of cancer cell lines have been shown to be susceptible to necroptosis-inducing drug combinations (e.g. TNF plus apoptosis inhibitors) (Jouan-Lanhouet et al., 2012, Bonapace et al., 2010, Chromik et al., 2014), supporting the rationale of driving cancer cells to undergo necroptosis when conventional apoptosis is compromised.

Under certain contexts, CQ has demonstrated the ability to induce necroptosis. Combination of mTOR inhibitor, CCI-779, and CQ has been shown to induce RIPK-dependent necroptosis, and this was abrogated by the RIPK1 inhibitor, necrostatin-1 (Bray et al., 2012). In addition, CQ combination with ceramide has also been shown to trigger necroptosis (Zhu et al., 2014). Thus, similar to apoptosis, the potential for CQ to trigger necroptosis may be dependent on the combination treatment used. Here, we examined whether combination of CQ and serum starvation (growth factor withdrawal) induces necroptosis as a form of alternative cell death.

As a third and final mechanism of cell death, we are aiming to investigate the potential of CQ to induce lysosomal membrane permeabilisation (LMP) and the contribution of this pathway to the reduction in 4T1 cell viability. LMP is typically characterised through leakage of the lysosomal contents, in particular degradative proteases, into the cytosol to trigger controlled cell death (Boya and Kroemer, 2008). Such lysosomal proteases implicated include the cathepsins, more specifically Cathepsins B, D, and L (Boya and Kroemer, 2008, Oberle et al., 2010), as unlike

alternative lysosomal enzymes these degradative proteases have been shown to retain activity even under neutral pH conditions. The leakage of the cathepsin proteases has been shown to induce secondary apoptotic signalling, such as activation of the apoptotic machinery not limited to but including mitochondria and the caspases (Boya et al., 2003, Droga-Mazovec et al., 2008). Numerous activators of LMP have been defined, including viral proteins, reactive oxygen species, and the cathepsin proteases themselves (Boya and Kroemer, 2008). However, we have focused on the potential for lysosomal detergents to induce LMP. It has long been characterised that lysosomotropic drugs can damage the lysosomal membranes and thus it was suggested they could be potent inducers of LMP. Indeed both sphingosine (Kagedal et al., 2001, Ullio et al., 2012) and siramesine (Cesen et al., 2013, Dielschneider et al., 2016) have been shown to require the lysosomal cathepsins to mediate cell death and to be potent inducers of LMP. More recent research has identified the lysosomal detergent, Leucyl-Leucyl-O-methyl ester (LLOME) to induce significant lysosomal membrane damage and induce cell death (Aits et al., 2015b).

Despite advancements in the understanding of the LMP process, it remains difficult to detect and pinpoint as the mode of cell death in *in vitro* studies. However, a number of successful methods are frequently used for the detection of LMP. Boya *et al*, 2003, showed two well-known quinolone antibiotics, ciprofloxacin and norfloxacin, had the potential to induce LMP through immunofluorescent staining studies highlighting the translocation of cathepsins B and D from the lysosomes to the cytosol (Boya et al., 2003). Alternatively, in a method developed by Jaattela *et al*, 2007, LMP can be detected through increases in the cytosolic cathepsin activity using a digitonin based extraction method for whole cell and cytosolic fractions. Here the anti-mitotic drug Vincristine was shown to induce marked LMP in HeLa and MCF-7 cancer cell lines (Groth-Pedersen et al., 2007). Interestingly, Vincristine also led to an increase in the lysosomal size which corresponded with an increase in cytosolic cathepsin activity. In chapter 4, we showed CQ induces rapid changes in lysosomal morphology, significantly increasing the diameter of the lysosomal lumen, therefore we hypothesised this could be an indicator of LMP occurring in response to CQ treatment in our cell model. Indeed, CQ has been shown to induce LMP in other cancer cell systems, including breast cancer (Liang et al., 2015), neuroblastoma (Seitz et al., 2013), and lung carcinoma (Enzenmuller et al., 2013). Furthermore, work by Hasan *et al*., 2008, has shown lysosomal enlargement to be

an event that precedes LMP (Hasan, 2008). Using compounds shown to induce LMP and methods identified to detect LMP in other cell models, we aim to examine the potential of LMP to be contributing to the mechanism of cell death induced by CQ.

In this chapter, the mode of cell death induced by CQ was investigated in 4T1 cells. The objectives were to:

(1) Examine whether CQ induces apoptosis and if the cell death we observe is dependent on this pathway using apoptosis inhibitors.

(2) Investigate the contribution of alternative modes of cell death, such as necroptosis, to the responses observed in our clonogenic cell model using pharmacological inhibitors.

(3) Assess whether LMP plays a role in CQ-mediated cell death via parallel comparative studies with known LMP inducing compounds.

5.2 Results

5.2.i CQ-mediated cell death is not dependent on the classical apoptotic, necroptotic, or ROS-mediated cell death pathways.

The mode of cell death induced by CQ treatment is still widely debated, ranging from inhibition of the pro-survival autophagy pathway to inducing apoptosis. More recently, CQ has been linked to lysosomal membrane permeabilisation (LMP), where integrity of the membrane is compromised and degradative enzymes, mainly cathepsins, leak into the cytosol initiating cell death (Boya and Kroemer, 2008). CQ-induced death by time-lapsed microscopy (chapter 3), and 4T1 cells seemed to exhibit cell rounding following by lysis after 18hrs in serum starved conditions coupled with CQ treatment. Here, we aimed to further investigate the mode of cell death induced by CQ in our cell model, and began by examining the classical modes of cell death; apoptosis and necroptosis.

Two well characterised molecular indicators of classical apoptosis are poly ADP ribose polymerase (PARP) cleavage and caspase 3 activation. Cleaved caspase 3, also known as pro-caspase 3, is activated by both the intrinsic and extrinsic apoptosis pathways, and is recognised as a key executioner in both apoptotic cascades (McIlwain et al., 2013). PARP is a nuclear enzyme involved in DNA repair, and is one of the key targets of caspase 3 (Boulares et al., 1999). Cleavage of PARP inhibits its enzymatic activity, therefore interfering with DNA repair and maintenance of cell viability.

First the apoptosis inducer, Staurosporine (STS), was utilised to examine the typical biochemical apoptotic response in 4T1 cells (**Fig 5.1A**). PARP and caspase-3 cleavages with this treatment were induced after just 4hrs. Additionally, long term (24hr) STS treatment also led to strong PARP and caspase 3 cleavage signals. This identified that 4T1 cells exhibit the typical biochemical response associated with apoptosis when this cell death pathway is engaged. To explore the cell death mechanism induced in our cell model further we measured the extent that CQ and serum starvation co-treatment induced apoptosis via western blot analysis for PARP and caspase 3 cleavage events **(Fig 5.1B)**. Here co-treatment with CQ and serum starvation led to cleavage of both PARP and caspase 3. Further analysis into whether the activation of caspase 3 we observed with CQ-serum starvation co-

treatment could be abrogated with an inhibitor of apoptosis used the caspase-3 specific inhibitor, z-DEVD-FMK. This compound blocked PARP and caspase 3 cleavages associated with CQ-serum starvation.

Having observed that: 1) apoptosis pathways were activated following CQ treatment (in combination with serum starvation); and 2) that caspase inhibitors were able to suppress this, we aimed to use this approach to rescue cell death. As such, the potential for z-DEVD-FMK to also inhibit serum starvation-induced cell death in the clonogenic assay **(Fig 5.2)** was explored. In the control samples, serum starvation +CQ co-treatment led to a 75% decrease in viability. Surprisingly, addition of z-DEVD-FMK was not able to provide any suppression of cell killing in all conditions analysed, including the key condition of this thesis, namely, serum starvation + CQ combination. This suggests that while serum starvation and CQ co-treatment does induce some activation of the apoptotic machinery (PARP and caspase 3 cleavage), the final cell death process is not solely reliant on classical caspase-dependant apoptosis.

An alternative form of programmed cell death we considered was necroptosis. This form of cell death is typically amplified by the RIP1 and RIP3 signalling molecules (Silke et al., 2015). To explore this idea, CQ and serum starvation co-treatment in the presence and absence of a RIP1 inhibitor, Necrostatin-1 **(Fig 5.3)** was compared. Inhibition of RIP1 did not alter the ability of CQ and serum starvation co-treatment to reduce cell viability in the clonogenic assay. Taken together, our data suggest that 2 major pathways of programmed cell death, apoptosis and necroptosis, are not involved in CQ-mediated cell death.

There is long-standing evidence to suggest oxidative free radicals and ROS are directly responsible for oxidative damage in cells, leading to programmed cell death (Jacobson, 1996). Thus, there was a rationale for investigation into the potential for ROS scavenging to suppress cell death **(Fig 5.4)**. For this test, N-Acetyl-L-Cysteine (NAC), was used to reduced ROS present in the cells (Sun, 2010). Treatment with NAC alone did not alter cell viability in control samples. Moreover, NAC did not alter cell viability where serum starvation or CQ was given as individual treatments. Importantly, NAC did not block serum starvation and CQ combination-induced cell death. These data indicate that ROS do not play a role in CQ-mediated cell death in our cell model. Overall, our data suggest that CQ induces a unique form of cell

death that is unrelated to ROS production, and also independent of classical apoptotic or necroptotic pathways.

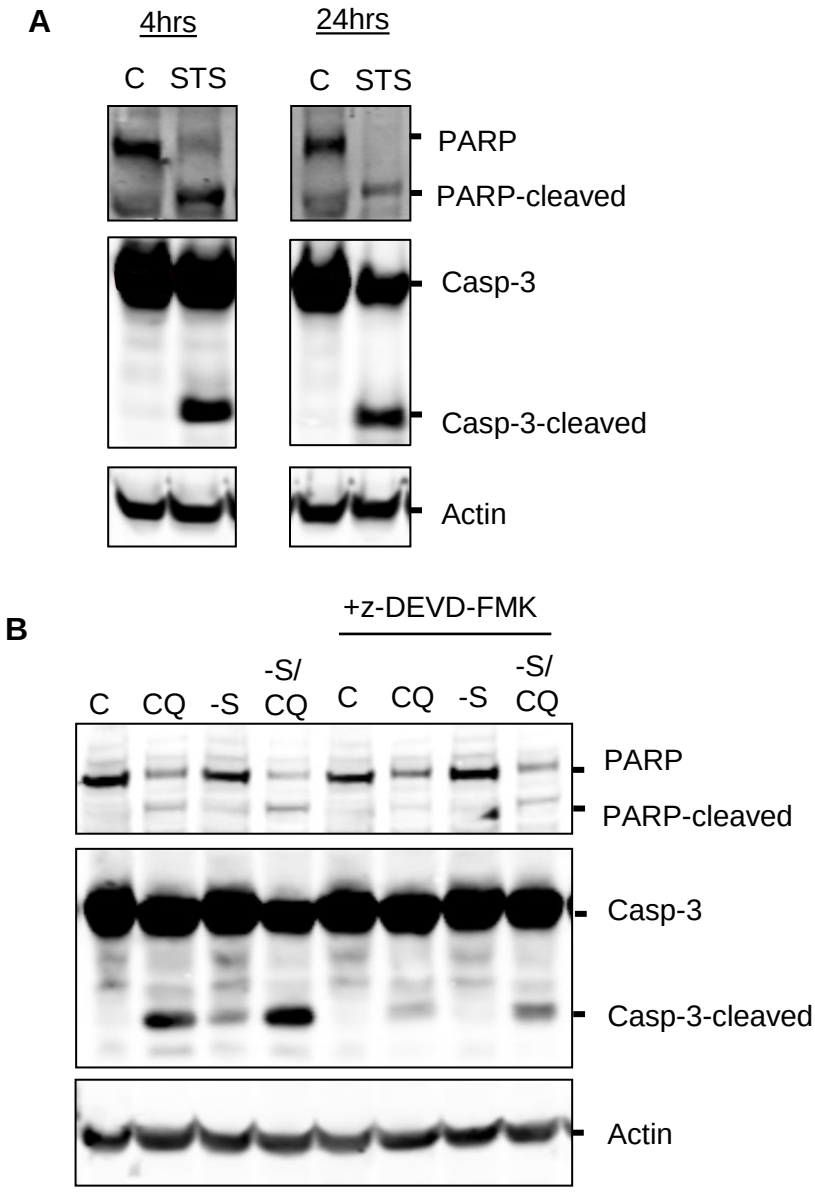

Fig 5.1: CQ-serum starvation co-treatment induces proteolytic activation of pro-apoptotic proteins. **(A)** 4T1 cells were treated for 4 or 24hrs with full nutrient media (C) or with 1μM Staurosporine (STS) as indicated. **(B)** 4T1 cells were treated with full nutrient media (C), CQ (25μM), serum starvation (-S), or a combination of serum starvation and CQ (-S/CQ). Cells were treated in the absence or presence of the caspase-3 inhibitor, Z-DEVD-FMK (10μM), as indicated for 24hrs. Following treatment cells were lysed, and PARP and Caspase 3 cleavage analysed via western blot. Actin was used as a loading control. Gel is representative of 3 independent experiments.

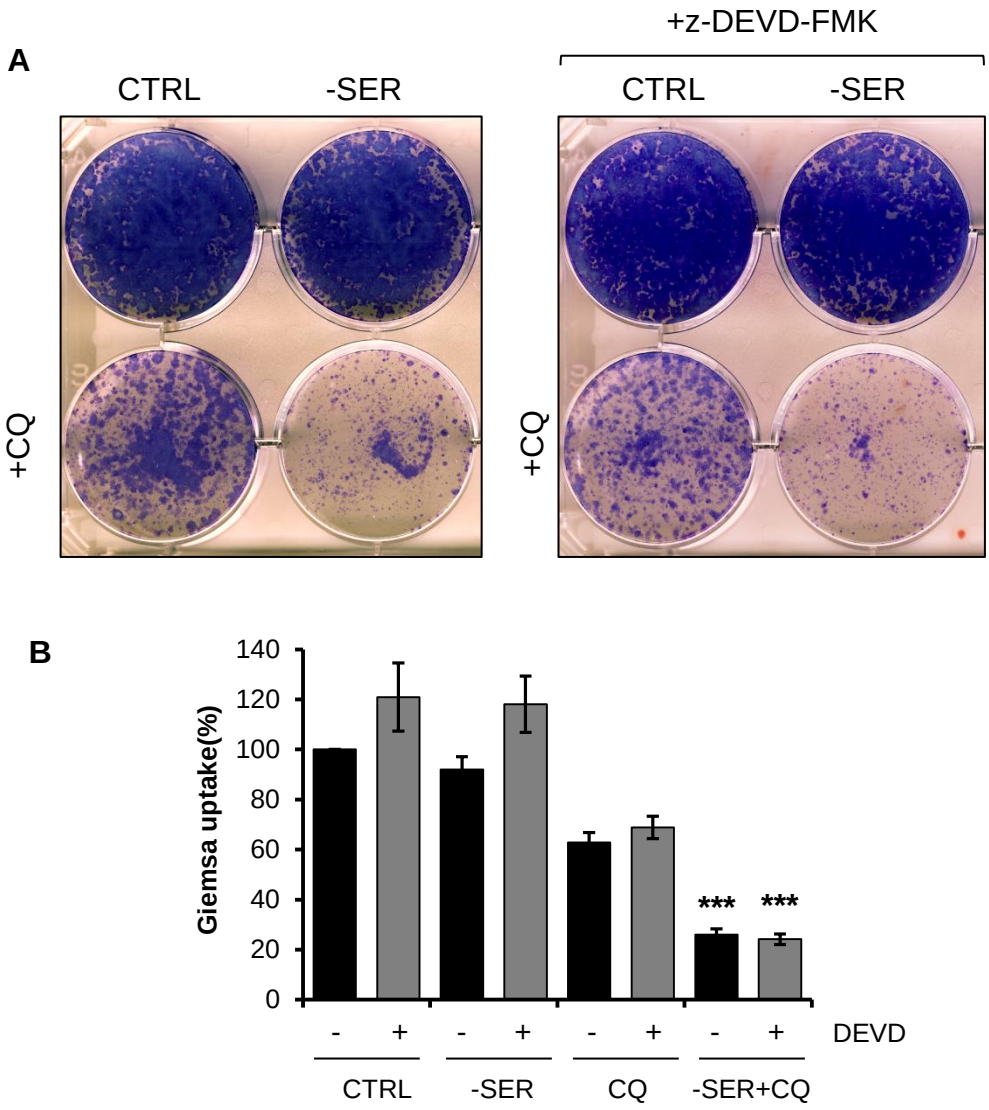

Fig 5.2: Inhibition of Caspase-3 does not block CQ-mediated cell death. (A) 4T1 cells were treated with full nutrient media (CTRL) or starved of serum (-SER) +/- CQ (25μM). Cells were treated in the absence or presence of the caspase-3 inhibitor, Z-DEVD-FMK (10μM), as indicated for 24hrs. The media was changed to normal full nutrient drug-free growth media and after 3 days cells were stained with Giemsa blue, and cell viability quantified as described in Methods. (B) Giemsa uptake shown as % of control, n=3 technical replicates (One-way ANOVA with Tukey post test, comparisons to untreated controls, ***P < 0.001), errors bars +/-SEM.

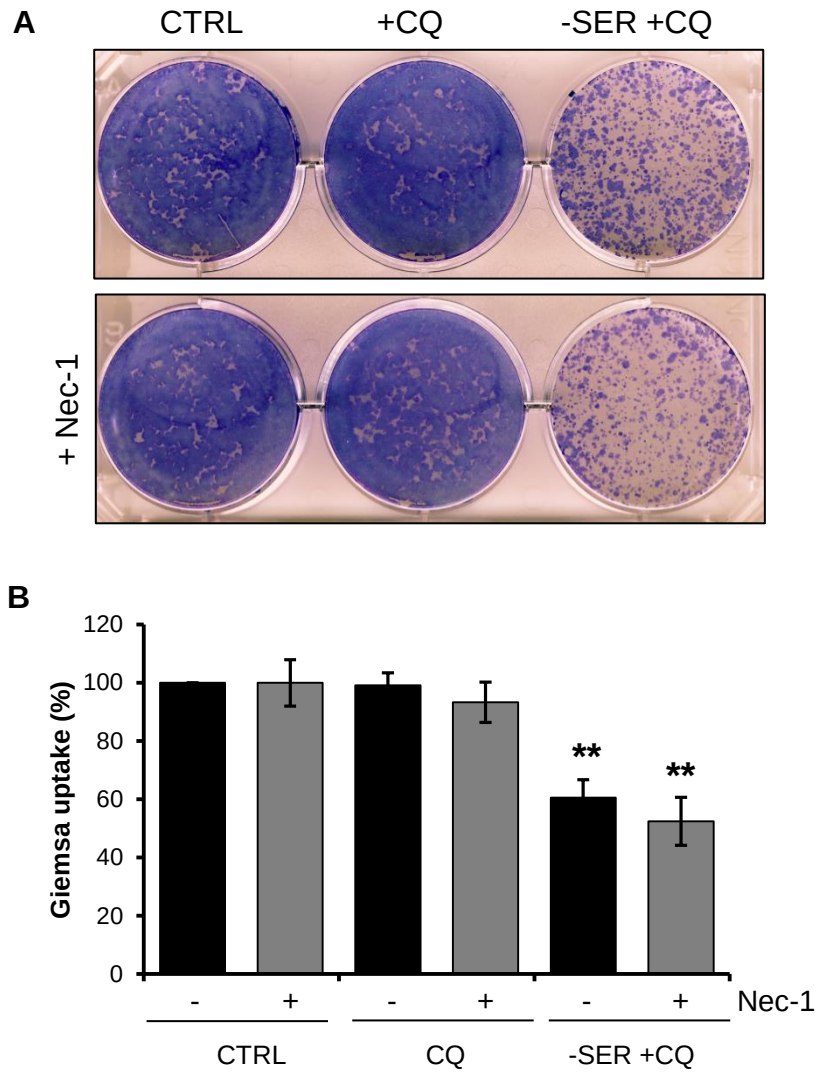

Fig 5.3: CQ-mediated cell death is not prevented by inhibition of Necroptosis. (A) 4T1 cells were treated with full nutrient media (CTRL) or starved of serum (-SER) +/- CQ (25μM). Cells were treated in the absence or presence of the RIP1 kinase inhibitor, Necrostatin-1 (Nec-1, 20μM), as indicated for 24hrs. Media was replenished and cell viability assessed as in Fig 5.2. **(B)** Giemsa uptake shown as % of control, n=3 technical replicates (One-way ANOVA with Tukey post test, comparison to untreated control **P < 0.01), errors bars +/-SEM.

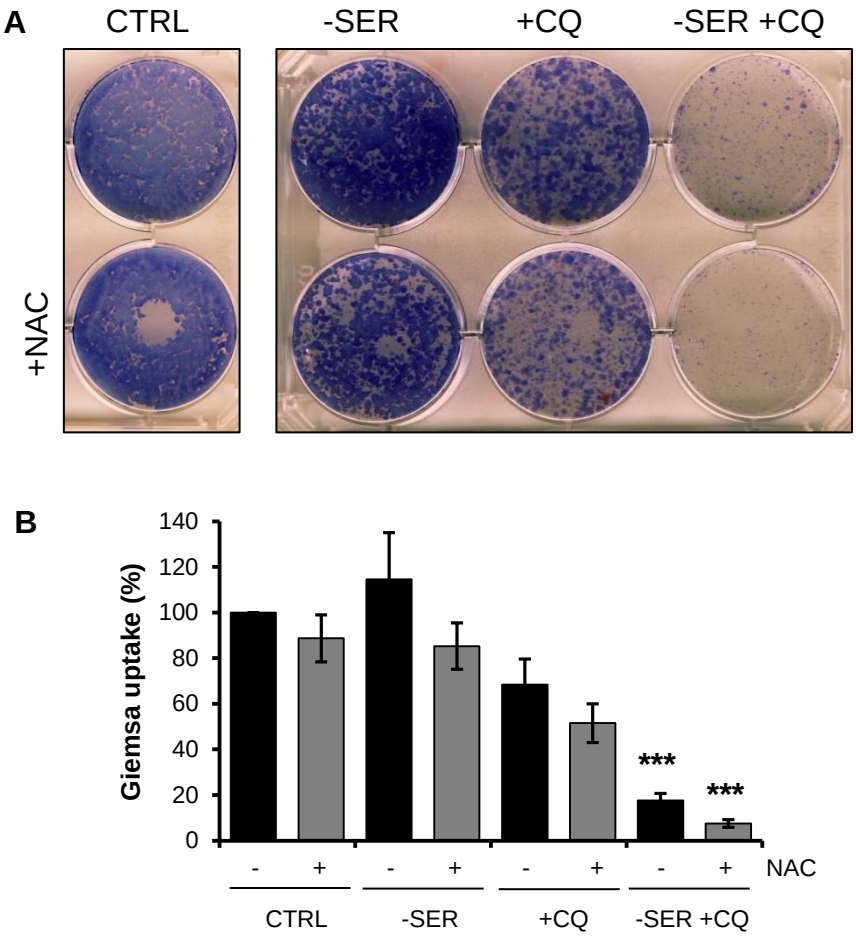

Fig 5.4: ROS scavenging does not abrogate CQ-mediated cell death. (A) 4T1 cells were treated with full nutrient media (CTRL) or starved of serum (-SER) +/- CQ (25μM). Cells were treated in the absence or presence of N-Acetyl-cysteine (NAC, 10mM) as indicated for 24hrs. Media was replenished and cell viability assessed as in Fig 5.2 **(B)** Giemsa uptake shown as % of control, n=3 technical replicates (One-way ANOVA with Tukey post test, comparison to untreated control, ***P < 0.001), errors bars +/-SEM.

5.2.ii LMP-inducing compounds do not exert the same activity as CQ in cell death and lysosomal enlargement.

The lack of effect from apoptosis and necroptosis inhibitors, coupled with the changes in lysosomal morphology observed in the previous chapter, led to the hypothesis that CQ-induced cell death may be linked to lysosomal membrane permeabilisation (LMP). This mode of cell death is characterised by leakage of cathepsins and other degradative proteases from the lysosome, which in turn can lead to either activation of caspases to trigger secondary apoptosis or lead to pH-dependent cathepsin mediated breakdown of cellular organelles.

To examine whether CQ was related to LMP, comparative cell death assays against 2 compounds previously characterised for LMP: Leu-Leu methyl ester (LLOME) (Aits et al., 2015b, Maejima et al., 2013) and ciprofloxacin (CPX) (Boya et al., 2003, Liang et al., 2015, Hasan, 2008) were performed. As control in this test, again nutrient starvations or CQ treatment alone had no effect on 4T1 cell viability. However, co-treatment with CQ and serum-starvation led to ~60% cell killing and this was rescued by glucose starvation **(Fig 5.5)**. In marked contrast, LLOME showed no efficacy in inducing cell death, either alone or when combined with serum starvation. Furthermore, serum and glucose withdrawal, which blocked the effects of CQ, promoted cell killing by LLOME. In further contrast, CPX showed no activity alone and showed no functional interaction with either nutrient starvation conditions. These results were unexpected, but highlight how CQ was targeting the cell differently than other known LMP inducers.

To further elucidate mechanistic differences between these drugs the effects of the LMP inducing compounds on lysosomal enlargement in the 4T1 cell model **(Fig 5.6)** were examined. As control, both CQ treatments alone or in combination with serum starvation induced dramatic enlargement of LAMP1+ lysosomes, which could be abrogated by glucose withdrawal. Unexpectedly, neither LLOME nor CPX showed any ability to induce enlargement of the lysosomes, either alone or in concert with nutrient starvation.

These data thus far, showing negligible effects of previously characterised LMP inducers on lysosomal enlargement, were perplexing. Especially since these compounds both showed some bioactivity and cytotoxicity in 4T1 cells (albeit with different profile from CQ). In any case, to further ascertain how these LMP drugs

target the lysosome, their actions were compared against CQ, monitoring in parallel the lysosomal morphology and acidification (LTR staining) over a time course of 30mins to 4hrs **(Fig 5.7)**. As seen previously, CQ rapidly de-acidified the lysosomal compartment within 30mins, an event that just preceded the onset of lysosomal enlargement which occurred after 1hr. Strikingly, LLOME also rapidly de-acidified lysosomes within 30mins, and generally these remained de-acidified over the 4hrs. Interestingly, while LLOME targeted and de-acidified the lysosome, it failed to induce any lysosomal enlargement. In comparison, CPX neither de-acidified nor enlarged the lysosomal compartments. In sum, this analysis could confirm LLOME was active at the lysosome but exhibits differential effects to CQ.

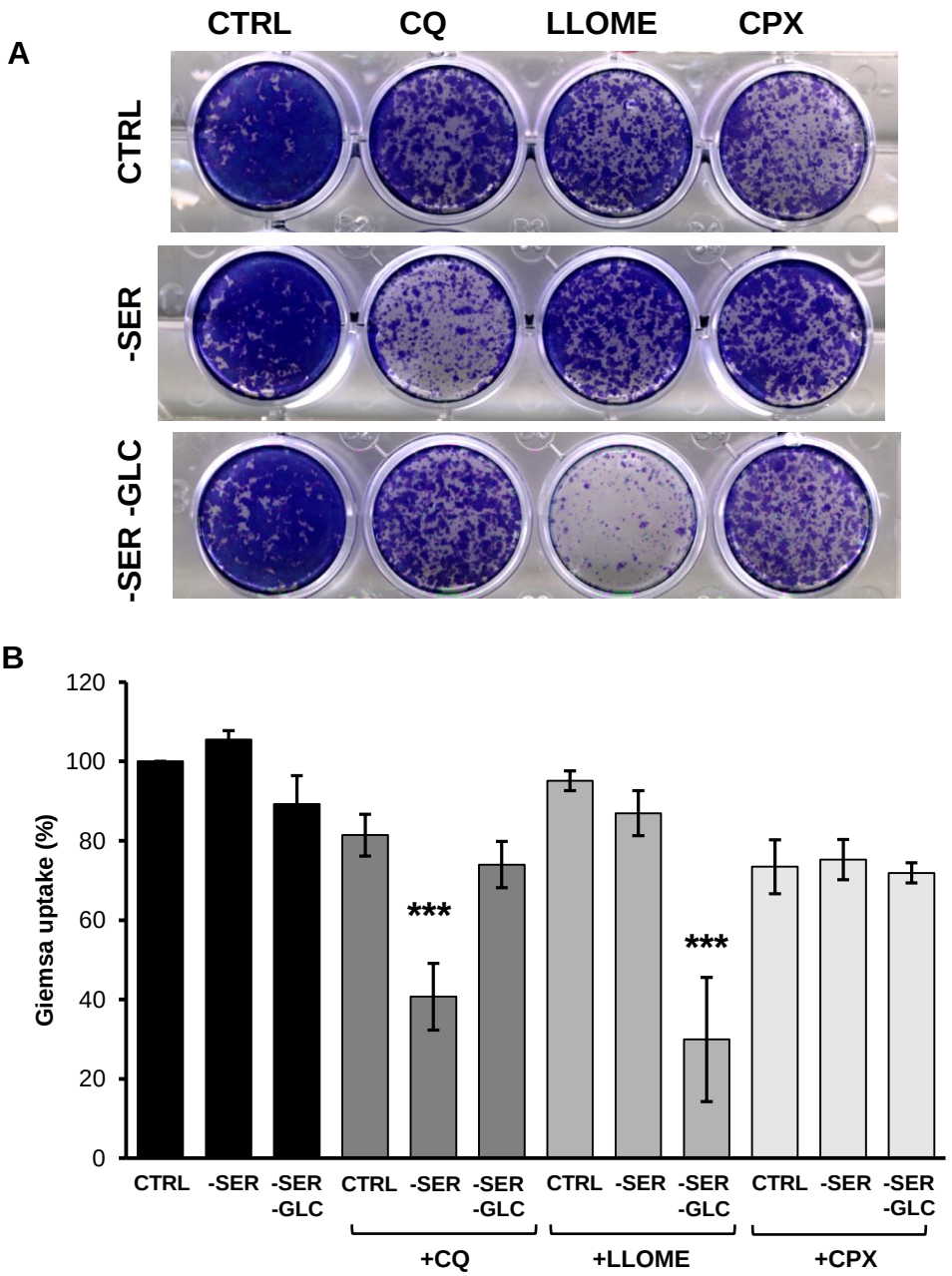

Fig 5.5: LMP inducing compounds, LLOME and CPX, exhibit differential effects on cell viability. (A) 4T1 cells were treated with full nutrient media (CTRL) or starved of serum (-SER), or serum and glucose (-SER-GLC) +/- CQ (25μM), LLOME (5mM), or CPX (150μg/mL) as indicated for 24hrs. Media was replenished and cell viability assessed as in Fig 5.2. **(B)** Giemsa uptake shown as % of control, n=3 biological replicates (One-way ANOVA with Tukey post test, comparison to untreated control, ***P < 0.001), errors bars +/-SEM.

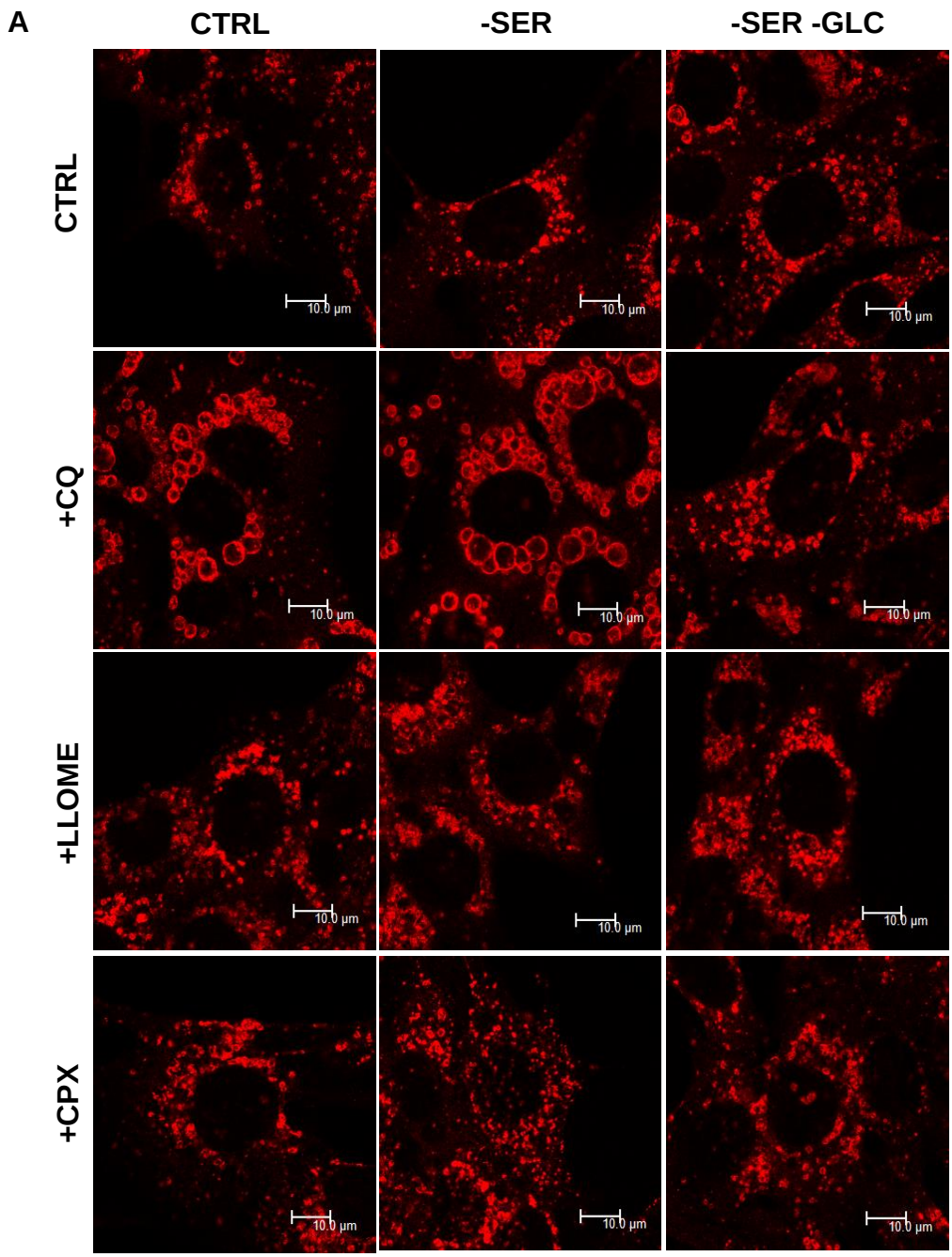

Quantification and Figure legend on next page

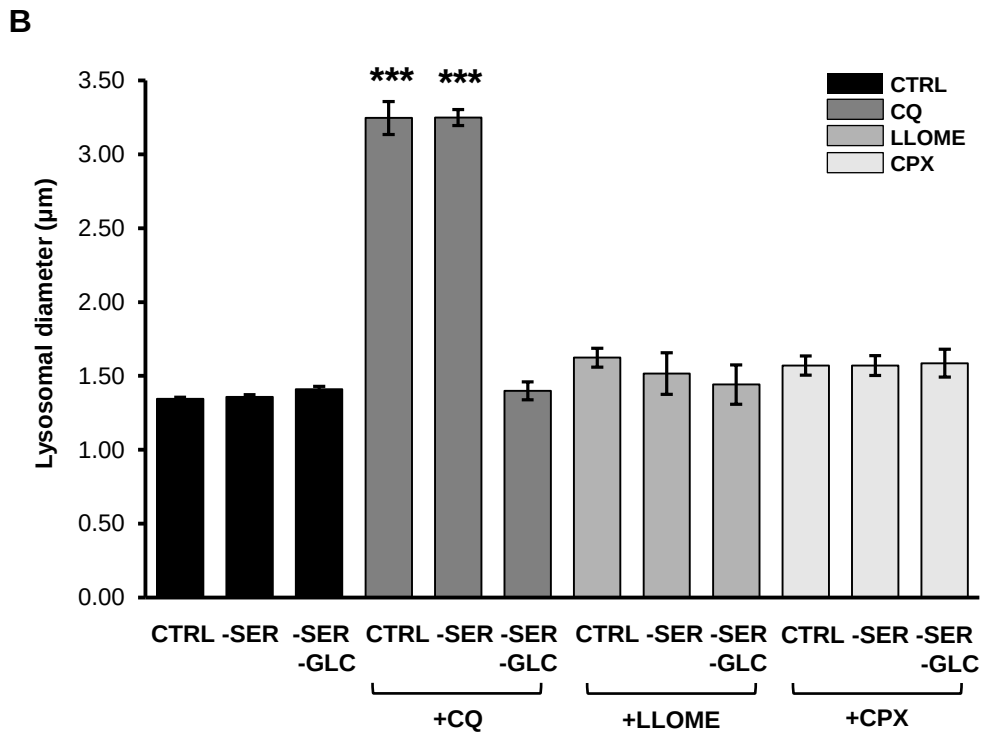

Fig 5.6: LMP inducers, LLOME and CPX, do not induce lysosomal enlargement as oppose to CQ. **(A)** 4T1 cells were treated with full nutrient media (CTRL), or starved of serum (-SER), or serum and glucose (-SER-GLC) +/-CQ (25µM), LLOME (5mM), or CPX (150µg/mL) as indicated for 8hrs. Cells were fixed, and stained for lysosomal associated membrane protein-1 (LAMP-1). Images were captured by confocal microscopy. Scale bar 10µm. **(B)** Average lysosomal diameter measured for 30 cells per condition as described in Methods. n=3 independent experiments (One-way ANOVA with Tukey post test, comparison to untreated control, ***$p < 0.001$, *$p < 0.05$), errors bars +/-SEM.

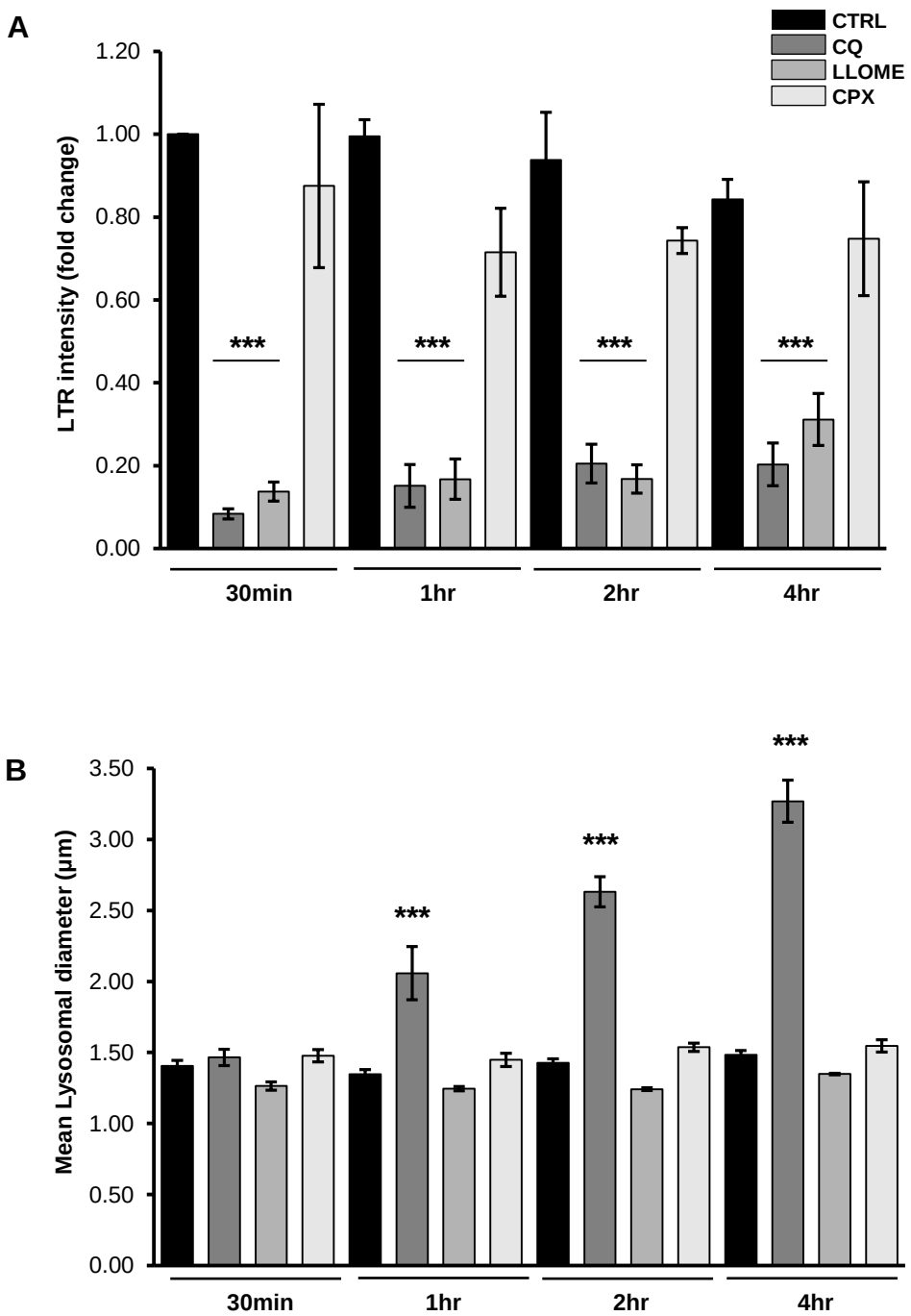
A
CTRL
CQ
LLOME
CPX
LTR intensity (fold change)
1.20
1.00
0.80
0.60
0.40
0.20
0.00
***
***
***
***
30min
1hr
2hr
4hr
B
Mean Lysosomal diameter (µm)
3.50
3.00
2.50
2.00
1.50
1.00
0.50
0.00
***
***
***
30min
1hr
2hr
4hr

Fig 5.7 (previous page): LMP inducer, LLOME, but not CPX de-acidifies the lysosomal compartments. 4T1 cells were treated with full nutrient media (CTRL), in comparison to CQ (25μM), LLOME (5mM), or CPX (150μg/mL) for the times indicated. **(A)** LTR DND-99 (50nM) was added for the final 30mins of treatment. Cells were fixed, and images captured by confocal microscopy. LTR intensity was measured as described in Methods, and expressed as a fold change. **(B)** Cells were fixed, and stained for lysosomal associated membrane protein-1 (LAMP-1). Images were captured by confocal microscopy, and average lysosomal diameter measured for 30 cells per condition as described in Methods. n=3 independent experiments (One-way ANOVA with Tukey post test, comparison to respective time-point control, ***$p < 0.001$, **$p < 0.01$), error bars +/- SEM.

5.2.iii CQ does not lead to cathepsin accumulation in the cytosol.

Previous assays established that LLOME, a well characterised LMP inducing compound, exhibited different effects than CQ on lysosomal morphology, despite targeting lysosomal acidification. Since CQ-induced death was best associated with lysosomal swelling (consistent with cathepsin leakage), we aimed to more directly detect events associated with lysosomal damage using a digitonin extraction protocol that has been a classical assay for LMP (Groth-Pedersen et al., 2007, Aits et al., 2015a). This assay measures cathepsin activity that escapes into the cytosol after drug and/or nutrient starvation treatment. The definitive feature of LMP is the leakage of cathepsins into the cytosol. Therefore on induction of LMP, an increase in cathepsin activity in the cytosolic fractions should be observed.

In our initial studies, 4T1 cells were treated with CQ alone or in combination with serum starvation or serum- and glucose-starvation in comparison to untreated controls over 8, 16, and 24hrs. Cytosolic fractions were extracted using a relatively low digitonin concentration as compared to total activity (cytosol + lysosomal contents) from parallel treated cells extracted with a high concentration of digitonin. Activity in extracts was then detected using a cathepsin B specific fluorogenic substrate. Unexpectedly at all time points tested no cathepsin activity was detected leaking into the cytosol following CQ treatment in comparison to untreated control cells (**Fig 5.8**). Furthermore, there was a clear trend that CQ-treatment (as early as 8hrs) reduced total cathepsin B activity in the whole cell fractions, a result that was independent of nutrient starvation (**Fig 5.8**). These results indicate that CQ-treatment led to inactivation of general cathepsin activity, which may be why there was no detection of leakage into the cytosol.

The above results were unexpected so further studies were needed to ascertain the optimal cytosolic extraction methodology, since digitonin concentration conditions required for efficient extraction of the cytosol vs. whole cell can differ depending on the cell type (Jaattela, 2015). In other findings, the cytosol was extracted using a range of 25-50µg/mL and the whole cell fraction at 200-300µg/mL of digitonin. Thus, we detected escaped cytosolic cathepsin activity in CQ-treated cells using a range of digitonin extraction concentrations (**Fig 5.9**) at 16hrs. In the untreated samples, some cathepsin activity extracted by up to 50µg/mL digitonin was detected, which we interpret to represent cytosolic signals under basal conditions. Extraction with 200µg/mL or greater led to strong increases in activity, which

represent whole cell amounts including lysosomal contents. Consistent with earlier experiments, again there were total reductions in cathepsin activity (in both cytosolic and whole cell extraction conditions) upon CQ treatment, irrespective of nutrient availability. These data suggest that CQ therefore does not induce leakage of active cathepsin into the cytoplasm but rather has the opposing effect, a general quenching of degradative cathepsin activity.

To further explore this further digitonin assays comparing CQ against the quinoline compounds, AQ and PQ, or alternatively the known LMP inducers, LLOME and CPX (**Fig 5.10**) were performed. Again there was a reduction in cathepsin activity in both whole cell and cytosolic fractions on CQ treatment. Conversely, PQ did not alter the cathepsin activity in either the whole cell or cytosolic fractions, whereas AQ strongly abrogated cathepsin activity in both cellular fractions. These results further highlight differences between the activities of equimolar quinoline compounds, summarised in **Table 5.1** in the discussion. On comparison with known LMP inducing compounds, LLOME did not alter the cathepsin activity in either fraction; here an increase in the cytosolic fraction would have been an indicator of the induction of LMP. Interestingly, CPX decreased the whole cell fraction and increased the cytosolic, a pattern hinting towards induction of LMP, yet this compound showed no activity in clonogenic survival assays, lysosomal deacidification and lysosomal enlargement. The results of our digitonin assay showed that CQ-mediated reductions in cathepsin activity did not correlate with the LMP inducing compounds, in addition to no correlation being observed between CQ and LMP inducers activity in clonogenic assays, as described above. Therefore, from these data the mode of cell death induced by CQ cannot be identified, and alternative studies and methods are required to elucidate this.

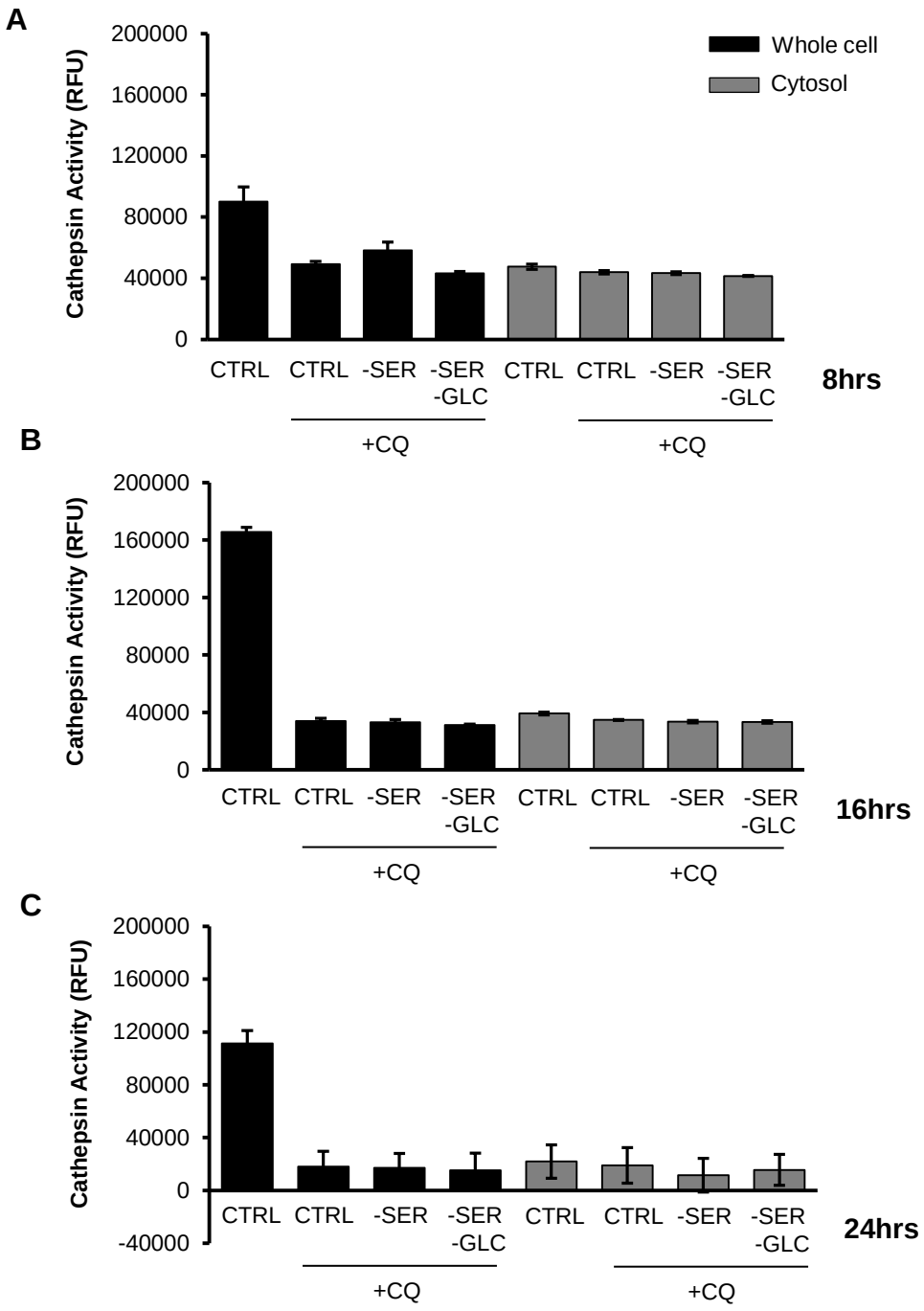

Fig 5.8: CQ blocks cathepsin activity in a Digitonin extraction assay. 4T1 cells were treated with full nutrient media (CTRL) +/- CQ, or starved of serum (-SER), or serum and glucose (-SER-GLC) +CQ (25μM) for **(A)** 8hrs **(B)** 16hr and **(C)** 24hrs. Cytosolic vs. whole cell fractions were extracted with 25μg/mL (Cytosol) or 200μg/mL (whole cell) digitonin and cathepsin activity (RFU) measured as described in Methods. n=3 technical replicates, errors bars +/- SEM.

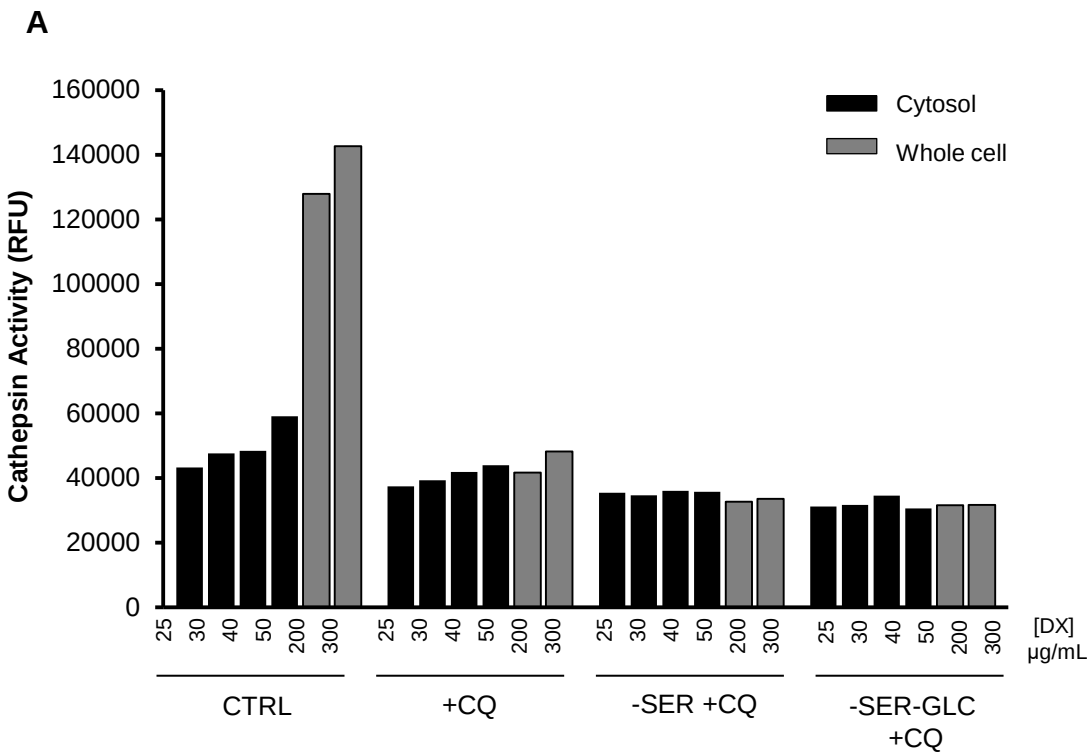

Fig 5.9: Inhibition of cathepsin activity by CQ was not dependent on Digitonin extraction concentrations. **(A)** 4T1 cells were treated with full nutrient media (CTRL) +/- CQ, or starved of serum (-SER), or serum and glucose (-SER-GLC) +CQ (25µM) for 16hrs. Cytosolic vs. whole cell fractions were extracted with digitonin concentrations as indicated and cathepsin activity (RFU) measured as described in Methods. n=2 biological replicates.

A

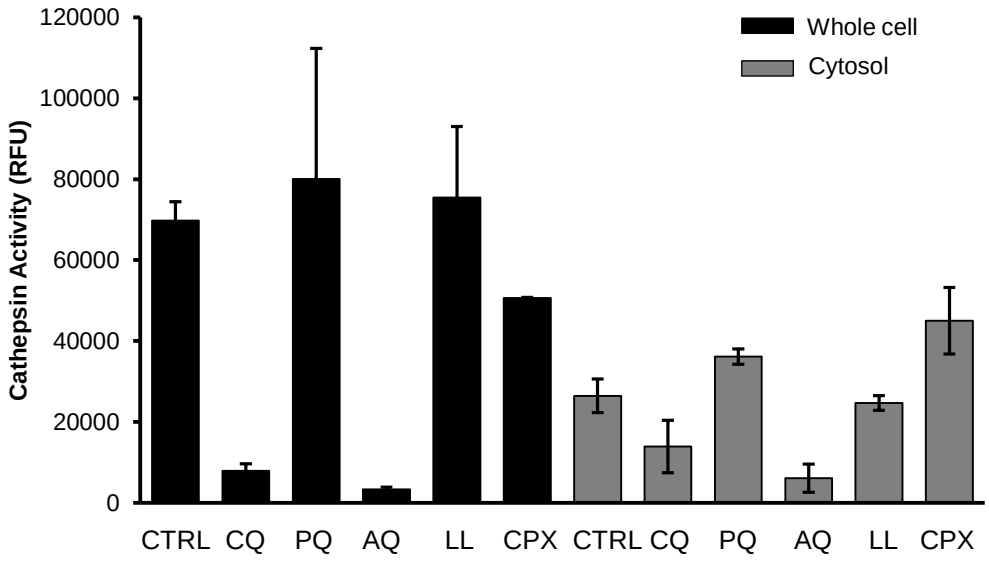

Fig 5.10: Quinoline compounds do not replicate the results of LMP inducers, LLOME and CPX, in a digitonin extraction assay. (A) 4T1 cells were treated with full nutrient media (CTRL) in comparison to CQ (25μM), PQ (25μM), AQ (25μM), LLOME (5mM), or CPX (150μg/mL) for 16hrs. Cytosolic vs. whole cell fractions were extracted with 50μg/mL (Cytosol) or 300μg/mL (whole cell) digitonin and cathepsin activity (RFU) measured as described in Methods. n=3 technical replicates, errors bars +/- SEM.

5.3 Discussion

5.3.i Chloroquine-mediated induction of classical cell death pathways does not impact overall viability.

In this chapter, the mode of cell death induced by CQ in our cell model was examined. The broad range of published work discussed below would suggest the mechanism of cell death induced by CQ is varied between cell types, ranging from apoptosis, necrosis, and LMP. However, our experiments using inhibitors of the classical cell death pathways in clonogenic assays indicated these did not play a role in CQ-mediated loss of 4T1 cell viability. Based on these findings we utilised more focused approaches to examine the potential for CQ to induce LMP in our cell model and for this to be the contributing mechanism of cell death.

As inferred to, the mechanisms of cell death induced by CQ are varied; one prominent model for CQ-induced death highlights a role for p53 and apoptosis. In a range of glioblastoma cell lines, CQ was shown to directly stabilise the p53 protein and up-regulate pro-apoptotic target proteins such as Bax (Kim et al., 2010). Furthermore, knockdown of p53 in U87MG and G120 glioma cell lines significantly reduced CQ-induced caspase-3 activation, suggesting that CQ stimulated apoptosis in glioma cells through the p53 pathway.

In this regard, we also observed caspase-3 activation upon serum deprivation and CQ treatment of 4T1 cells. However, we identified this executioner step to be largely dispensable for cell death since inhibition of this proteolytic cleavage with a commonly used inhibitor did not rescue cell viability. In agreement with our data, other studies using a range of human glioblastoma multiforme cell lines, including U87 glioma, showed CQ-mediated cell death to be caspase-independent (Geng et al., 2010). In this work, the general caspase inhibitor, boc-aspartate fluoromethylketone strongly inhibited caspase-3 but could not block cell death induced by CQ. As such, the contribution for caspase 3 downstream of CQ-induced death remains unclear.

In addition, studies on glioma demonstrated that p53-independent pathways also contributed to cell viability in response to CQ. Kim *et al*., 2010, noted that cell death was observed upon CQ treatment in p53 mutated, null, or wild-type cells, although WT p53 glioma cells were more sensitive. 4T1 breast carcinoma cells have been

shown to be p53 null (Yerlikaya et al., 2012), yet we observed sensitivity to CQ and induction of cell death, particularly on combination with serum starvation or other cellular stressors such as irradiation. This is in agreement with the previous studies findings that CQ can induce cell death in p53 null cell lines.

While the p53 status of cancer cells can influence sensitivity to CQ, this lysosomotropic drug has also been shown to activate apoptosis through direct action on the pro-apoptotic protein, PUMA. Lakhter *et al*., 2013 found that CQ killed a range of melanoma cell lines and this correlated with levels of caspase 3/7 activation (Lakhter et al., 2013). The mechanism here was attributed to CQ-mediated stabilisation and accumulation of PUMA protein (but not at the transcript level). Furthermore, siRNA depletion of PUMA markedly reduced the percentage of apoptotic cells on CQ treatment. Although, the data shown in these studies highlights how CQ can have direct interactions with essential pro-apoptotic proteins, p53 and PUMA, to induce cell death, there are caveats to these findings with CQ able to induce cell death in the absence of p53. This is particularly important with respect to our studies as we observe CQ-induced cell death in 4T1 cells, a p53-null cell line (Yerlikaya et al., 2012).

Looking more broadly across the literature, one can note that some studies show that CQ can induce apoptosis as a single agent (Geng et al., 2010, Kim et al., 2010), while the majority of studies use CQ as part of a combination therapy to enhance the efficacy of other apoptosis inducing drugs (Shi et al., 2015, Avniel-Polak et al., 2015, Park et al., 2016). This range of evidence on responses to CQ highlights likely pleiotropic effects; furthermore, while the apoptotic machinery is engaged by CQ, it may not be the sole driver of cell death. Indeed, other programmed cell death pathways can act as alternatives to apoptosis, and are suggested to be targets for cancer therapy in situations where cancer cells avoid apoptotic cell death (Su et al., 2016). As described previously, necroptosis is a form of regulated necrosis, dependent on the RIP1-RIP3-MLKL axis, typically downstream of the TNFR an inflammatory cell death pathway (Silke et al., 2015). However, there is some evidence linking CQ and necroptosis. For example, CQ has been shown to enhance necroptosis induced by ceramide in head and neck squamous cell carcinoma, but it did not activate necroptosis itself (Zhu et al., 2014). Despite this, we were able to discount necroptosis as a contributing mechanism of cell killing in our cell model, as

the RIP1 inhibitor, Necrostatin-1 did not alter cell viability in serum deprived, CQ-treated cells.

So far, we have found that two of the classical programmed cell death pathways, apoptosis and necroptosis, were not the driving mechanisms behind the cell killing in our experimental system. In addition to these processes, ROS have been implicated in cell death pathways, specifically linking with apoptosis (Fleury et al., 2002). CQ has been shown to induce ROS formation in human astroglial cells for chemokine expression suggesting that a similar pathway could be killing 4T1 cells in our hands (Park et al., 2004). Moreover, CQ has been shown to synergistically promote ROS production alongside HDAC inhibitors in CML cell lines, and this was linked to a role in induction of cell death via apoptosis (Carew et al., 2007). Importantly, in this cell system, the ROS scavenger NAC reduced the percentage of apoptotic cells. In contrast to these points, our data suggest that ROS free radical species are not involved in CQ-mediated killing; NAC was not able to rescue any cell viability in serum-starved and CQ treated cells. At present, it remains unclear if cell specific differences are the main basis behind these conflicting findings.

In conclusion, our studies investigating mechanisms of cell death have shown that CQ-mediated killing in our 4T1 cell model was independent of apoptosis, necroptosis and ROS production. Based on these data and our observations of lysosomal enlargement upon CQ treatment, we next hypothesised that cell death may be caused by the lysosomal membrane permeabilisation pathway.

5.3.ii CQ-mediated induction of alternative cell death pathway, lysosomal membrane permeabilisation.

The lysosome has long been known to be involved in degradation of endocytic cargo and macromolecules, including those sequestered by autophagosomes. The degradation of waste material transported to lysosomes is mainly carried out by hydrolytic proteases and lipases. The best studied of the proteases are the cathepsins, divided into cysteine, aspartate, and serine proteases. As well as protein turnover within the lysosome, these enzymes are now understood to be related to cell death pathways such as apoptosis and LMP (Droga-Mazovec et al., 2008, Oberle et al., 2010, Aits and Jaattela, 2013).

During LMP, lysosome homeostasis is impaired and the contents of these acidic organelles are released into the cytosol leading to abnormal degradation of cell constituents and activation of cell death pathways. The most common endpoints from LMP are osmotic lysis of the lysosome, where the lysosome bursts due to an excess of water in the process releasing these hydrolytic enzymes, or alternatively direct permeabilisation of the membrane, creating pores for cathepsins to leak into the cytosol (Repnik et al., 2014). The release of hydrolytic cathepsin proteases during this process can be a fatal event for the cell, triggering cell death pathways as adhered to previously through events such as the activation of apoptotic effector proteins, the caspases (Droga-Mazovec et al., 2008, Conus et al., 2008). Alternatively, LMP has been shown to trigger cell death through a series of mitochondrial events such as mitochondrial membrane permeabilisation (MMP) and to directly affect the conformation of pro-apoptotic proteins Bax and Bak (Boya et al., 2003).

One challenge has been that LMP has been characterised to display both necrotic and apoptotic-like features, making it difficult to definitively discern as a mechanism of cell death. In chapter 4, we presented evidence of CQ-induced lysosomal enlargement across multiple cell types. Indeed, this type of change has been shown to precede LMP in breast cancer cell lines (Hasan, 2008) supporting our hypothesis that LMP was involved in CQ-mediated cell death. Furthermore, CQ has been shown to induce LMP in other cancer cell systems, including breast cancer (Liang et al., 2015), neuroblastoma (Seitz et al., 2013), and lung carcinoma (Enzenmuller et al., 2013).

Although CQ-induced lysosomal swelling and damage are entirely with the notion of LMP, our further work comparing the effects of CQ and two known LMP inducers on clonogenic cell survival and lysosomal enlargement highlighted marked differences. Our main effect has been CQ induced lysosomal enlargement and cell death in combination with serum starvation. In contrast, the compound LLOME did not lead to similar lysosomal swelling, even though the lysosome acidification was clearly being targeted in treated cells.

This clear difference between CQ and LLOME action was surprising to us. LLOME has been shown to induce lysosomal damage in MEF and murine macrophage cells at concentrations 5-fold lower than that which we used (Maejima et al., 2013). In this report, up to 1mM LLOME induced release of cathepsin D into the cytosol, indicating

damaged lysosomal membranes; and furthermore, the number of Galectin3-positive puncta (marker for damaged lysosomes), increased dose-dependently with LLOME treatment. Other papers using LLOME as a standard stimulant of LMP have used doses lower than 5mM, and found this lysosomotropic drug to be strongly active (Aits et al., 2015b).

As another reported compound from the literature, CPX has also been shown to induce LMP at concentrations lower than that which we used. For example, Cathepsin D was shown to have leaked and distributed throughout the cytosol of MCF-7 cells following 10μM CPX treatment (Liang et al., 2015). However, while CPX induced LMP in this study, it did not induce swelling of the lysosome. In contrast, LMP induced by CQ was accompanied by lysosomal enlargement. In an alternative study, CPX (30μM) was also shown to induce LMP in HeLa cells, as the translocation of Cathepsins B and D from lysosomes to the cytosol (Boya et al., 2003). In contrast our experiments using 0.45mM CPX did not mimic the findings of previous publications. CPX did not show any activity in our hands at: reducing lysosomal acidity, inducing lysosomal swelling, or inducing cell death. As such, these data sets indicated that CQ was more potent at inducing lysosomal swelling and cell killing with a set of effects distinct from other compounds previously characterised to trigger LMP.

Because we saw unexpected different profiles of lysosomal activity, we performed further classical biochemical assays to more directly detect LMP in our cell model. We utilised a widely described digitonin extraction assay (Groth-Pedersen et al., 2007, Jaattela, 2015) in which low concentrations of this detergent would permeablise just the plasma membrane to extract a cytosolic fraction. Cathepsins should not normally be detected in the cytosol, but are expected to be present in the cytosol following LMP. High concentrations of digitonin are also used to permeablise all intracellular membranes to obtain whole cell reference readings. This digitonin extraction approached could detect cathepsin leakage into the cytosol, for example as initially described in ME-180as human cervix carcinoma cells stimulated with TNFα (Foghsgaard et al., 2001). Furthermore, this assay has been used to detect leakage of cathepsin activity in response to chemotherapeutic drugs, such as Vincristine, in MCF-7 breast carcinoma cells (Groth-Pedersen et al., 2007); and in response to siramesine in U-87MG glioblastoma cells (Cesen et al., 2013).

In our studies, we unexpectedly could not observe increases in cytosolic cathepsin activity upon CQ treatment, either alone or in combination with nutrient starvation. In fact, the overwhelming effect with CQ was an apparent quenching in overall whole cell cathepsin activity. In addition, CQ targeted cathepsin activity under full nutrient and all nutrient starvation conditions, even after serum-glucose withdrawal which blocks CQ induced lysosomal swelling and cell killing. Our data thus suggest that CQ inhibits cathepsin activity rather than promoting leakage of these enzymes into the cytosol, raising questions on the assumption that cathepsin activity was driving a LMP-related cell death pathway.

To further understand LMP, some insights were gained by comparison of CQ effects vs. those from LMP inducers, LLOME and CPX. LLOME has been previously shown to induce LMP by measuring cathepsin distribution in the cytosol through fluorescence microscopy (Maejima et al., 2013) However, in our hands, we could not detect any increased cathepsin activity in cytosolic fractions following LLOME treatment. However, we could detect increased levels of cathepsin activity in the cytosol following CPX treatment. As such, this compound was able to induce some degree of LMP signal in the digitonin assay, despite showing no activity in lysosomal deacidification, lysosomal enlargement, or cell death assays.

As we showed in chapter 4, CQ also displayed differential properties in cell killing, lysosomal enlargement and lysosomal deacidification (summarised in **Table 5.1**) to the alternative quinoline compounds AQ and PQ. Thus we also compared the potential of CQ, AQ and PQ to inhibit cathepsin activity. Interestingly, AQ mirrored the effects of CQ in abrogating both whole cell and cytosolic cathepsin activity, whereas PQ had no effect. These data could reflect our observations that both CQ and AQ induce strong lysosomal deacidification and cell death, whilst PQ only mildly de-acidified the lysosome and showed no efficacy in clonogenic assays. Although oppose to our hypothesis of CQ-induction of LMP, this pattern of results could imply that 4T1 cell death arises from deacidification of the lysosome and inhibition of cathepsin activity. However, the caveat to this is the observations that in contrast to CQ, AQ did not induce lysosomal swelling.

Table 5.1: Summary and comparison of results for alternative quinoline and LMP inducing compounds. The conclusions from cell death and lysosome activity assays when using quinoline compounds and LMP inducers in comparison to CQ are summarised below.

Compound	Cell death	Lysosome enlargement	Glucose rescue	Lysosome de-acidification	Cathepsin activity
CQ (25μM)	✓	✓	✓	✓	↓
AQ (25μM)	✓	×	×	✓	↓
PQ (25μM)	×	×	×	✓ (mild)	No change
LLOME (5mM)	×	×	×	✓	No change
CPX (0.4mM)	×	×	×	×	↑

Based on these inconclusive outcomes further work is required here to dissect the role of LMP in CQ-mediated cell death and any potential differences in cell death mechanisms between the alternate quinoline compounds.

Alternative assays available for the detection of LMP include measuring cathepsin enzymes in the cytosol through western blotting or immunofluorescent imaging (Maejima et al., 2013), or use of a Galectin3 probe which labels damaged lysosomes. The galectin3 assay is suggested to offer more sensitive detection of LMP, and was shown to be a general marker of leaky and damaged lysosomes, irrespective of the agent used to initiate membrane disruption (Aits et al., 2015b). During this assay, galactin3 translocated from a diffuse cytosolic staining pattern in control cells to punctate structures which co-localised with lysosomal markers, such as LAMP1 and 2, under conditions which promoted LMP. We propose further experiments using the Galectin3 assay would detect if CQ does indeed induce LMP in our cell model.

5.4 Conclusions

In conclusion of our data described here, we have shown the mechanism of cell death induced by CQ to be independent of classical apoptosis, necroptosis, and ROS-driven pathways. Based on our observations of CQ-mediated lysosomal enlargement, an event suggested to precede lysosomal membrane permeabilisation (Hasan, 2008), we hypothesised LMP to be the mechanism of cell death induced in our experimental model. CQ has been shown to induce LMP in a range of alternative cancer cell lines (Liang et al., 2015, Seitz et al., 2013, Enzenmuller et al., 2013), providing rationale for this argument. Despite these published findings, we observed stark differences between CQ and two known LMP inducing drugs, LLOME and CPX, in both clonogenic and lysosomal staining assays. Furthermore, marked differences between these compounds were also detected during digitonin extraction cathepsin activity assays, a method often used to detect LMP induction. At odds with studies using alternative methods of LMP detection (Galectin3 assays), in our hands both LLOME and CPX did not induce detectable LMP in digitonin extraction experiments. Based on the data presented here we cannot conclude CQ-mediated cell death is directly driven by LMP and further work is required to fully elucidate the mode of cell death driving the loss of viability in our 4T1 cell model.

Chapter 6

General Discussion

6.1 Main findings and implications

6.1.i Aims and Importance

CQ has been shown to be a potential beneficial therapeutic strategy for targeting autophagy in a cancer setting, leading to sensitisation to a range of cellular stressors and ultimately reducing cancer cell viability (Amaravadi et al., 2007, Bellodi et al., 2009, Cufi et al., 2013, Wang et al., 2014). Because of this, there are now more than 50 clinical trials worldwide examining the potential of CQ or its derivative HCQ in cancer (from clinicaltrials.gov). Despite the clearly defined rationale for using CQ, questions still surround its specific mechanism of action. Considering this, the objectives of this thesis were to examine the potential of autophagy inhibition via CQ to sensitise an aggressive metastatic breast cancer cell line to a range of cellular stressors, including radiation, chemotherapeutic compounds, and metabolic deficiencies. Furthermore, we aimed to ascertain the mechanism by which CQ sensitised to cellular stress.

6.1.ii CQ action is autophagy-independent

Autophagy has been shown to be cancer promoting (Hu et al., 2012, Kim et al., 2015, Strohecker et al., 2013, Guo et al., 2013) in a range of settings supporting clear rationale for targeting autophagy in well-established tumours. Indeed, CQ is widely described as an autophagy-lysosomal inhibitor, inhibiting late stage autophagy flux rather than formation of autophagosomes (Pasquier, 2016).

The work outlined here examined the potential of CQ to sensitise to cellular stressors in a 4T1 metastatic breast carcinoma cell model. In concert with previous studies, we found that CQ could strongly sensitise to radiation, PI3K inhibition, and growth factor depletion, to drive cell death. This clearly reflected the rationale for use of CQ in pre-clinical, and importantly, clinical studies as an adjuvant cancer therapy. We hypothesised the beneficial effects of CQ to be driven by inhibition of autophagy according to the wider dogma. However, despite CQ showing clear evidence of autophagy inhibition, genetic ablation of autophagy did not mimic the effects of CQ in clonogenic assays. Our data showing CQ to be acting independently of autophagy were in concert with other more recent studies (Maycotte et al., 2012, Eng et al., 2016). As such, the mechanism of CQ as a cancer therapeutic is not as straightforward as originally proposed. Considering this,

the results of clinical trials should be reviewed with these insights as any beneficial properties of CQ may not be arising as a result of autophagy inhibition. Indeed, the emergence of more specific ULK1 and VPS34 inhibitors (Egan et al., 2015, Petherick et al., 2015, Ronan, 2014 #617, Dowdle et al., 2014)} will provide further insight into the potential of targeting autophagy pharmacologically in pre-clinical and possible future clinical trials. As such, this work supports rationale for autophagy-independent based anti-cancer treatments. However, there is clearly rationale for more specific autophagy inhibitors to help kill cancer cells. In principle, these strategies could be further combined.

6.1.iii CQ efficacy is intricately linked to glucose availability

In analysing the sensitisation properties of CQ, we examined its potential to sensitise to different nutrient and energetic conditions as typically found with a tumour mass (Reid and Kong, 2013). In doing these studies, interesting and unexpected interrelationships between CQ action and glucose metabolism were uncovered.

In general, cancer cells have long been noted to have an altered metabolic profile in comparison to normal, healthy cells (Warburg et al., 1927, Warburg, 1956), preferentially relying on glycolysis as the main ATP production pathway. However, my findings here are seemingly at odds with this predominant addiction to glucose -- while CQ and serum starvation induced cell death, further withdrawal of glucose conferred protection against this response. In further support of these findings, the upstream glycolysis inhibitor 2-DG, also rescued cell death induced by serum starvation and CQ. However, more late-stage inhibitors of glycolysis (DCA and gossypol), did not confer the same protective advantage.

Taken together, our studies suggested that early-stage inhibition of glycolysis interfered with the ability of CQ to target the cell. We have thus uncovered a previously undocumented glucose-dependent resistance mechanism to CQ. Our finding also raises questions as to whether targeting the glycolytic pathway could really be a beneficial treatment strategy for all cancer contexts (for example, not recommended in combination with CQ).

Indeed, advances in cancer metabolism have highlighted that tumour cells can be heavily reliant on alternative nutrient sources, such as glutamine, often termed

'glutamine-addiction', especially in glucose-low conditions (Le et al., 2012, Yang et al., 2009). Here, it was further confirmed that glutamine is an essential nutrient source maintaining cell viability under glucose-starved conditions. Interestingly, reliance on glutamine is correlated with increased expression of the oncogenic protein c-myc (Wise et al., 2008, Gao et al., 2009). 4T1 cells have been shown to have elevated c-myc levels over their less metastatic sibling cell lines (Tao et al., 2008). Therefore it stands to reason that 4T1 cells would be more reliant on glutamine for cell survival. Based on our data and others showing glutamine addiction in certain cancer settings, there is further rationale to target glutamine metabolism alongside CQ treatment.

6.1.iv CQ-induced damage to the lysosome drives cancer cell death

After determining that CQ action was intricately linked to nutrients, experiments were designed to identify the specific mechanism of resistance under glucose-starvation. Possible roles of activating classical cell survival pathways including AMPK and AKT were ruled out. While there were observed increases in AMPK signalling after glycolysis inhibition, pharmacological activation of AMPK could not mimic the rescue on cell death. This was at odds with published work identifying AMPK to prolong cell survival under energetic stress and maintain cell viability under glucose-depleted conditions (Jeon et al., 2012, Chaube et al., 2015, Song et al., 2014). We concluded that AMPK was not a major part of the resistance to CQ.

Our work also determined AKT signalling to be a general survival signal but activation of this was not the basis of the specific glucose starvation-driven resistance. Our conclusion here was unexpected and in contrast to Gao *et al.,* 2013, who demonstrated AKT was phosphorylated and activated in cells subjected to long-term glucose starvation as a key survival signal (Gao et al., 2013). Comparison of our data summarised above with published work showing AMPK and AKT to be key survival signals under energetic stress highlights the wide variety of different mechanisms that can be hijacked by cells to endure and circumvent cytotoxic insults.

Importantly, in exploring the mechanism of cell survival induced by glucose starvation, it was identified that CQ-mediated cell death was closely associated with lysosomal enlargement and damage. These studies demonstrated that CQ had a significant and conserved impact on lysosomal morphology and this was abrogated

by inhibition of glycolysis. Observations of CQ-induced lysosomal damage in both autophagy-competent and -deficient MEF supported our conclusions that CQ effects were not mediated through autophagy, but rather through lysosomal targeting. The specific glycolytic event that mediates cell survival has not as yet been fully determined. Targeted CRISPR knockout of HK2, the isoform of hexokinase shown to be up-regulated across multiple cancers (Coelho et al., 2015, Zhang et al., 2016), could not protect against CQ-induced lysosomal enlargement. It is possible that there were compensatory effects from other HK isoforms, and inhibition of all isoforms (as with 2DG) is required for full HK inhibition.

We had hypothesised that under glucose starvation, CQ could no longer target the lysosomes and this could be the potential mechanism for cell survival and lysosome protection. Interestingly, the presence of glucose has been shown to be intimately linked to assembly of the v-ATPase pump, an essential component involved in lysosome acidification (Kane, 1995, Dechant et al., 2010, Sautin et al., 2005). Therefore, our initial rationale was that glucose deprivation could disrupt the acidic gradient and block CQ to access the lysosomal lumen. However, our studies using lysotracker dye showed that CQ still exhibited its de-acidification activity at the lysosome in all nutrient conditions, irrespective of glucose availability. This demonstrated that CQ targeting to the lysosome lumen was not affected by glucose starvation and thus was not the mechanism of survival promoted by glucose withdrawal.

Taken together, our results from cell viability and lysosomal assays support a model whereby CQ enters the lysosome leading to rapid de-acidification and enlargement (damage). Further cellular stress, such as serum starvation, cooperates with the cytotoxic damage from lysosomal proteolytic enzymes leaking into the cytoplasm, together triggering a cell death pathway. Under glucose-depleted conditions, while CQ still rapidly de-acidifies the lysosome, swelling and leakage does not occur to contribute to cell death **(Fig 6.1).** This model highlights the unexpected nutrient-dependent resistance mechanism to CQ. In addition, this scheme begins to shed light on the mechanism of action linked to CQ anti-cancer activity.

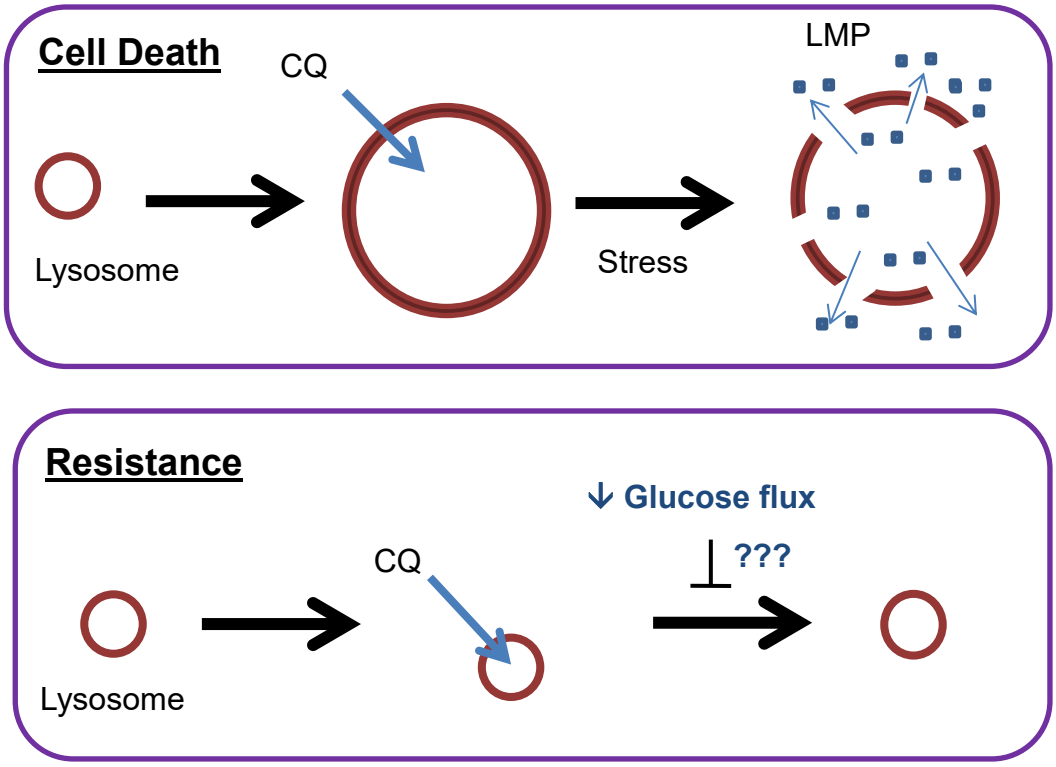

Fig 6.1 A proposed model of CQ-mediated cell death and the potential for glucose starvation to promote resistance CQ leads to rapid deacidification and enlargement of the lysosome, and event which correlates with reduction in cell viability. However, in glucose-depleted conditions, the lysosomal swelling induced by CQ is abrogated, despite evidence of CQ activity at the lysosome. This protection of lysosome morphology correlates with a cytoprotective response in clonogenic assays. Thus our model suggests the glucose withdrawal inhibits CQ-mediated cell death, potentially through interfering with the process of LMP or lysosomes.

6.1.v Glucose starvation blocks autophagy

Separate from our data analysing CQ, we also identified intriguingly that glucose vs. amino acid starvation differentially regulated the autophagy pathway. While amino acid starvation appeared to activate proper autophagic degradative flux, glucose starvation induced biochemical signals that conversely indicated a block in autophagic flux. In examining acidification of the lysosome, we demonstrated that while serum or serum and amino acid starvation led to marked lysosomal acidification, glucose withdrawal did not activate the lysosome. These data fit with published work showing glucose is necessary for formation of the v-ATPase pump and proper activation of autophagy (Sautin et al., 2005, Dechant et al., 2010). Taken together, our data lead us to conclude that glucose starvation blocks autophagy flux in contrast with dogma (for example: evidence for glucose starvation inducing autophagy through AMPK signalling (Kim et al., 2011)). However, other studies have also highlighted that glucose starvation in fact blocks autophagy flux (Ramirez-Peinado et al., 2013, Moruno-Manchon et al., 2013). Our work in combination with others challenges the current prevalent model in which amino acid and glucose starvation represent alternate types of nutrient deprivation that both promote autophagy.

6.1.vi Quinoline compounds may be better re-purposed anti-cancer agents

CQ belongs to a wider family of quinoline anti-malarial compounds. Therefore, the anti-cancer potential for these alternative quinoline drugs and whether they were also susceptible to nutrient dependent resistance was examined. Both AQ and PQ have been suggested to be effective anti-cancer agents in vitro. AQ has been shown to block autophagy, impair acidification, and enhance cisplatin and amino acid cell killing in human A375 melanoma cells (Qiao et al., 2013). In oral squamous cell carcinoma KB, PQ demonstrated sensitisation capabilities to vinblastine (Kim et al., 2013b). Interestingly, these compounds (despite similar parent chemical structure) displayed quite different profiles across the mechanistic assays used in this thesis (as summarised in **Table 5.1**). Equimolar concentrations of CQ, AQ, and PQ induced differential effects on the lysosome and cell death. These clear differences point towards potent structure-activity relationships. Importantly, it was established that AQ was a more potent anticancer drug irrespective of nutrient supply and therefore may represent a better option for repurposing drugs in the quinoline

classification. In this respect, AQ has a large aromatic ring (not present in CQ and PQ) attached to the central amine group, which may be driving different interactions in the cell.

6.1.vii CQ-induced cell death is a distinct form of LMP

While CQ is being used in patients to help kill cancer cells, this compound so far has been linked to pleiotropic mechanisms of cell death (Lakhter et al., 2013, Zhu et al., 2014, Liang et al., 2015). Therefore, we aimed to better define the pathway of action for CQ, for example, in relation to autophagy, lysosomes and glucose utilisation. Above, lysosomal damage and leakage was proposed as the key event for cell death (**Figure 6.1)**. Exploration of classical cell death pathways through a series of experiments utilising pharmacological inhibitors of apoptosis, ROS-linked death and necroptosis aimed to confirm this. The outcome of cell death assays concluded that CQ-mediated death did not rely on canonical apoptotic pathways. Thus, although speculative, if CQ was promoting alternative forms of cell death distinct from apoptosis, this could be further clinical potential for treating tumour cells with mutations to bypass apoptosis, for example, categories lacking p53 or other pro-apoptotic machinery.

If CQ was not driving apoptosis, it could be hypothesised that cell death induced by CQ in our system was closely linked to, or directly, LMP (Hasan, 2008). Indeed, CQ has been linked to LMP in multiple cancer cells, including breast, neuroblastoma and lung (Liang et al., 2015, Seitz et al., 2013, Enzenmuller et al., 2013). However, in our studies, CQ induced a distinct set of responses that did not match those of other characterised LMP-inducing compounds (see **Table 5.1**). CQ induced severe lysosomal enlargement while both LLOME and CPX did not. In lysotracker assays, CQ and LLOME both rapidly de-acidified the lysosome, whereas CPX showed no activity in this assay. Furthermore, while CQ mediated lysosomal enlargement and de-acidification correlated with clonogenic cell death, LLOME treatment only induced cell death in combination with glucose starvation, despite no effects on lysosomal swelling. This is in contrast with our findings whereby glucose starvation confers a cytoprotective effect to CQ. As such, the LMP cell death triggered by LLOME was not dependent on any nutrient specificity.

Due to the distinct patterns obtained using CQ and LMP inducers, we aimed to directly measure any changes or leakage of cathepsin activity after CQ treatment.

Using a digitonin extraction assay, it is expected that cathepsin activity leaking into the cytosol upon LMP would be detected (Groth-Pedersen et al., 2007, Jaattela, 2015). However, with CQ treatment we observed an overall overwhelming quenching of cathepsin activity throughout the whole cell. In concert with the effects of CQ on lysosomal de-acidification, this reduction in cathepsin activity occurred independently of nutrient starvation. Further insight was gained by comparing CQ to LMP inducers in the digitonin assay. Again distinct patterns of results were observed across all compounds tested. These data indicated that CQ was not inducing LMP, at least not by classical markers of the pathway or by a mechanism similar to other established LMP inducing compounds.

Our data from lysotracker and digitonin assays indicate that acidification of the lysosome is intricately linked to overall cathepsin activity. Drugs which induced lysosomal de-acidification did not cause any detectable leaked cathepsin activity indicative of LMP (CQ, AQ, LLOME), whereas those drugs which did not de-acidify the lysosome (CPX) gave some increases in cytosolic cathepsin activity, akin to LMP. Whether these data show that: 1) CQ does not induce LMP; or 2) that LMP cannot be detected because of dominant effects from CQ on lysosomal pH; needs further dissection. Alternative approaches are available for more sensitive detection of LMP.

6.2 Future work

As inconsistencies were observed when comparing CQ with the other known LMP inducers, further questions revolve around clarifying LMP as the mode of CQ-dependent cell death in the 4T1 model. A recently described Galectin 3 approach (Aits et al., 2015b) may offer an alternative and more sensitive approach for detection of LMP. Here, stably expressed Galactin 3 translocates to leaky and damaged lysosomes e.g. during LMP. Alternatively, translocation of cathepsin enzymes from the lysosome to the cytosol can also be visualised by imaging (Boya et al., 2003, Maejima et al., 2013). Future studies would propose to next probe the interplay between CQ and LMP using these alternative methods.

A question still also remains over the exact mechanism driving resistance to CQ under glucose-depleted conditions. We hypothesise the basis of this mechanism lies within metabolic switching of the cancer cells, and propose further work using additional glycolytic inhibitors to tease out the key stages of metabolic switch-over.

So far, early inhibition of glycolysis via glucose starvation or hexokinase inhibition promoted lysosomal functionality and cell survival. However, it should be considered that these metabolic steps also lie upstream of the pentose phosphate pathway (PPP) (Patra and Hay, 2014). Therefore, increased cell survival could be caused by a depression of the PPP, glycolysis, or both. This could be elucidated using inhibitors of PPP under the alternate nutrient conditions, for example, inhibition of the PPP rate limiting enzyme glucose-6-phosphate dehydrogenase. Two compounds *dehydroepiandrosterone* and 6-aminonicotinamide were recently evaluated as potent inhibitors of this enzyme (Preuss et al., 2013). Here, if cell survival was controlled by the PPP, blocking the PPP pathway using one of these drugs might offer same levels of protection to CQ as 2-deoxyglucose.

In this regard, it would be intriguing to determine the metabolic pathway supporting survival in glucose-deplete condition. We would hypothesise this to be mitochondria-dependent as we have already shown glutamine reliance for cell survival. Glutaminolysis has been shown to drive ATP production through direct access to the mitochondrial TCA cycle (Le et al., 2012). Furthermore, mitochondrial uncoupling has been shown to re-direct energy pathways towards glycolysis (Si et al., 2009). Therefore, it stands to reason that inhibition of glycolysis in cancer cells with metabolic plasticity would lead to increased mitochondrial metabolism.

A potential study to confirm this would be to utilise TCA uncoupling compounds under glucose-deplete conditions, and then to examine the effect of these on lysosomal functionality and cell death. Examples of standard uncoupling compounds could be carbonilcyanide *m*-cholorophenylhydrazone (CCCP) (Hirose et al., 1974), carbonilcyanide *p*-triflouromethoxyphenylhydrazone (FCCP) (Benz and Mclaughlin, 1983, Lou et al., 2007), or more direct TCA cycle enzyme inhibitors for instance α-ketoglutarate dehydrogenase inhibitor, succinyl phosphonate (Bunik et al., 2005). Alternatively, use of a radio-labelled glutamine (as in (Le et al., 2012)) could be used to track increases in TCA cycle intermediates derived from glutamine under both glucose replete and deplete conditions.

Based on the outcomes of *in vitro* studies outlined and discussed, further *in vivo* work exploring the translation of *in vitro* results to an *in vivo* setting is warranted. To examine the potential of upstream glycolytic inhibition to protect against CQ-induced cancer cell death in an *in vivo* 4T1 mammary fat pad model (Tao et al., 2008) two

potential lines of experimental methodology are proposed. Withdrawal of glucose conferred protection against CQ-mediated cell death *in vitro*, therefore to mimic these conditions *in vivo* a calorie restricted or low sugar diet may be utilised (to limits as allowed within ethical guidelines of animal work). Alternatively, a more direct method would be to use the glycolytic inhibitor 2-DG as used in *in vitro* studies; here if *in vitro* outcomes were to be translated *in vivo*, expected outcomes of these mouse models would show CQ to decrease tumour size while combination with 2-DG would show no changes in tumour sizes.

Chapter 7

References

7.1 References

Aas, T., Borresen, A. L., Geisler, S., Smithsorensen, B., Johnsen, H., Varhaug, J. E., Akslen, L. A. & Lonning, P. E. 1996. Specific P53 mutations are associated with de novo resistance to doxorubicin in breast cancer patients. *Nature Medicine,* 2**,** 811-814.

Aguer, C., Gambarotta, D., Mailloux, R. J., Moffat, C., Dent, R., Mcpherson, R. & Harper, M. E. 2011. Galactose enhances oxidative metabolism and reveals mitochondrial dysfunction in human primary muscle cells. *Plos One,* 6**,** e28536.

Ahuja, A., Gupta, N., Srinivasan, R., Kalra, N., Chawla, Y., Rajwanshi, A. 2007. Differentiation of hepatocellular carcinoma from metastatic carcinoma of the liver - clinical and cytological features. *Journal of Cytology* 24**,** 125-129.

Aits, S. & Jaattela, M. 2013. Lysosomal cell death at a glance. *Journal of Cell Science,* 126**,** 1905-1912.

Aits, S., Jaattela, M. & Nylandsted, J. 2015a. Methods for the quantification of lysosomal membrane permeabilization: A hallmark of lysosomal cell death. *Lysosomes and Lysosomal Diseases,* 126**,** 261-285.

Aits, S., Kricker, J., Liu, B., Ellegaard, A. M., Hamalisto, S., Tvingsholm, S., Corcelle-Termeau, E., Hogh, S., Farkas, T., Jonassen, A. H., Gromova, I., Mortensen, M. & Jaattela, M. 2015b. Sensitive detection of lysosomal membrane permeabilization by lysosomal galectin puncta assay. *Autophagy,* 11**,** 1408-1424.

Al-Bataineh, M., Li, H., Marciszyn, A., Bhalla, V., Hallows, K. & Pastor-Soler, N. 2015. AMPK Regulates the Vacuolar H+-ATPase via 14-3-3 Proteins. *Faseb Journal,* 29.

Alessi, D. R., James, S. R., Downes, C. P., Holmes, A. B., Gaffney, P. R. J., Reese, C. B. & Cohen, P. 1997. Characterization of a 3-phosphoinositide-dependent protein kinase which phosphorylates and activates protein kinase B alpha. *Current Biology,* 7**,** 261-269.

Amaravadi, R. K., Yu, D. N., Lum, J. J., Bui, T., Christophorou, M. A., Evan, G. I., Thomas-Tikhonenko, A. & Thompson, C. B. 2007. Autophagy inhibition enhances

therapy-induced apoptosis in a Myc-induced model of lymphoma. *Journal of Clinical Investigation,* 117**,** 326-336.

Ambudkar, S. V., Kimchi-Sarfaty, C., Sauna, Z. E. & Gottesman, M. M. 2003. P-glycoprotein: from genomics to mechanism. *Oncogene,* 22**,** 7468-7485.

Amiard, S., Doudeau, M., Pinte, S., Poulet, A., Lenain, C., Faivre-Moskalenko, C., Angelov, D., Hug, N., Vindigni, A., Bouvet, P., Paoletti, J., Gilson, E. & Giraud-Panis, M. J. 2007. A topological mechanism for TRF2-enhanced strand invasion. *Nature Structural & Molecular Biology,* 14**,** 147-154.

Andjelkovic, M., Alessi, D. R., Meier, R., Fernandez, A., Lamb, N. J. C., Frech, M., Cron, P., Cohen, P., Lucocq, J. M. & Hemmings, B. A. 1997. Role of translocation in the activation and function of protein kinase B. *Journal of Biological Chemistry,* 272**,** 31515-31524.

Aslakson, C. J. & Miller, F. R. 1992. Selective Events in the Metastatic Process Defined by Analysis of the Sequential Dissemination of Subpopulations of a Mouse Mammary-Tumor. *Cancer Research,* 52**,** 1399-1405.

Avniel-Polak, S., Leibowitz, G., Riahi, Y., Glaser, B., Gross, D. J. & Grozinsky-Glasberg, S. 2015. Abrogation of Autophagy by Chloroquine Alone or in Combination with mTOR Inhibitors Induces Apoptosis in Neuroendocrine Tumor Cells. *Neuroendocrinology*.

Axe, E. L., Walker, S. A., Manifava, M., Chandra, P., Roderick, H. L., Habermann, A., Griffiths, G. & Ktistakis, N. T. 2008. Autophagosome formation from membrane compartments enriched in phosphatidylinositol 3-phosphate and dynamically connected to the endoplasmic reticulum. *Journal of Cell Biology,* 182**,** 685-701.

Aylett, C. H., Sauer, E., Imseng, S., Boehringer, D., Hall, M. N., Ban, N. & Maier, T. 2016. Architecture of human mTOR complex 1. *Science,* 351**,** 48-52.

Bach, M., Larance, M., James, D. E. & Ramm, G. 2011. The serine/threonine kinase ULK1 is a target of multiple phosphorylation events. *Biochemical Journal,* 440**,** 283-91.

Bar-Peled, L., Chantranupong, L., Cherniack, A. D., Chen, W. W., Ottina, K. A., Grabiner, B. C., Spear, E. D., Carter, S. L., Meyerson, M. & Sabatini, D. M. 2013. A

Tumor Suppressor Complex with GAP Activity for the Rag GTPases That Signal Amino Acid Sufficiency to mTORC1. *Science,* 340**,** 1100-1106.

Bar-Peled, L., Schweitzer, L. D., Zoncu, R. & Sabatini, D. M. 2012. Ragulator Is a GEF for the Rag GTPases that Signal Amino Acid Levels tomTORC1. *Cell,* 150**,** 1196-1208.

Bartlett, B. J., Isakson, P., Lewerenz, J., Sanchez, H., Kotzebue, R. W., Cumming, R. C., Harris, G. L., Nezis, I. P., Schubert, D. R., Simonsen, A. & Finley, K. D. 2011. p62, Ref(2)P and ubiquitinated proteins are conserved markers of neuronal aging, aggregate formation and progressive autophagic defects. *Autophagy,* 7**,** 572-83.

Batlle, E., Sancho, E., Franci, C., Dominguez, D., Monfar, M., Baulida, J. & De Herreros, A. G. 2000. The transcription factor Snail is a repressor of E-cadherin gene expression in epithelial tumour cells. *Nature Cell Biology,* 2**,** 84-89.

Bellodi, C., Lidonnici, M. R., Hamilton, A., Helgason, G. V., Soliera, A. R., Ronchetti, M., Galavotti, S., Young, K. W., Selmi, T., Yacobi, R., Van Etten, R. A., Donato, N., Hunter, A., Dinsdale, D., Tirro, E., Vigneri, P., Nicotera, P., Dyer, M. J., Holyoake, T., Salomoni, P. & Calabretta, B. 2009. Targeting autophagy potentiates tyrosine kinase inhibitor-induced cell death in Philadelphia chromosome-positive cells, including primary CML stem cells. *Journal of Clinical Investigation,* 119**,** 1109-1123.

Belmokhtar, C. A., Hillion, J. & Segal-Bendirdjian, E. 2001. Staurosporine induces apoptosis through both caspase-dependent and caspase-independent mechanisms. *Oncogene,* 20**,** 3354-3362.

Ben Sahra, I., Laurent, K., Giuliano, S., Larbret, F., Ponzio, G., Gounon, P., Le Marchand-Brustel, Y., Giorgetti-Peraldi, S., Cormont, M., Bertolotto, C., Deckert, M., Auberger, P., Tanti, J. F. & Bost, F. 2010. Targeting cancer cell metabolism: the combination of metformin and 2-deoxyglucose induces p53-dependent apoptosis in prostate cancer cells. *Cancer Res,* 70**,** 2465-75.

Benz, R. & Mclaughlin, S. 1983. The Molecular Mechanism of Action of the Proton Ionophore Fccp (Carbonylcyanide Para-Trifluoromethoxyphenylhydrazone). *Biophysical Journal,* 41**,** 381-398.

Bertoni, J. M. 1981. Competitive-Inhibition of Rat-Brain Hexokinase by 2-Deoxyglucose, Glucosamine, and Metrizamide. *Journal of Neurochemistry,* 37**,** 1523-1528.

Bingle, L., Brown, N.J., Lewis, C.E. 2002. The role of tumour-associated macrophages in tumour progression: implications for new anticancer therapies. . *Journal of Pathology,* 192**,** 254-265.

Blanc, C., Deveraux, Q. L., Krajewski, S., Janicke, R. U., Porter, A. G., Reed, J. C., Jaggi, R. & Marti, A. 2000. Caspase-3 is essential for procaspase-9 processing and cisplatin-induced apoptosis of MCF-7 breast cancer cells. *Cancer Res,* 60**,** 4386-90.

Boffa, D. J., Luan, F., Thomas, D., Yang, H., Sharma, V. K., Lagman, M. & Suthanthiran, M. 2004. Rapamycin inhibits the growth and metastatic progression of non-small cell lung cancer. *Clin Cancer Res,* 10**,** 293-300.

Bonapace, L., Bornhauser, B. C., Schmitz, M., Cario, G., Ziegler, U., Niggli, F. K., Schafer, B. W., Schrappe, M., Stanulla, M. & Bourquin, J. P. 2010. Induction of autophagy-dependent necroptosis is required for childhood acute lymphoblastic leukemia cells to overcome glucocorticoid resistance. *Journal of Clinical Investigation,* 120**,** 1310-23.

Bonnet, S., Archer, S. L., Allalunis-Turner, J., Haromy, A., Beaulieu, C., Thompson, R., Lee, C. T., Lopaschuk, G. D., Puttagunta, L., Harry, G., Hashimoto, K., Porter, C. J., Andrade, M. A., Thebaud, B. & Michelakis, E. D. 2007. A mitochondria-K+ channel axis is suppressed in cancer and its normalization promotes apoptosis and inhibits cancer growth. *Cancer Cell,* 11**,** 37-51.

Boulares, A. H., Yakovlev, A. G., Ivanova, V., Stoica, B. A., Wang, G., Iyer, S. & Smulson, M. 1999. Role of poly(ADP-ribose) polymerase (PARP) cleavage in apoptosis. Caspase 3-resistant PARP mutant increases rates of apoptosis in transfected cells. *J Biol Chem,* 274**,** 22932-40.

Boya, P., Andreau, K., Poncet, D., Zamzami, N., Perfettini, J. L., Metivier, D., Ojcius, D. M., Jaattela, M. & Kroemer, G. 2003. Lysosomal membrane permeabilization induces cell death in a mitochondrion-dependent fashion. *Journal of Experimental Medicine,* 197**,** 1323-1334.

Boya, P. & Kroemer, G. 2008. Lysosomal membrane permeabilization in cell death. *Oncogene,* 27**,** 6434-6451.

Boyd, M., Mairs, R. J., Mairs, S. C., Wilson, L., Livingstone, A., Cunningham, S. H., Brown, M. M., Quigg, M. & Keith, W. N. 2001. Expression in UVW glioma cells of the noradrenaline transporter gene, driven by the telomerase RNA promoter, induces active uptake of [I-131]MIBG and clonogenic cell kill. *Oncogene,* 20**,** 7804-7808.

Brandizzi, F. & Barlowe, C. 2013. Organization of the ER-Golgi interface for membrane traffic control. *Nature Reviews Molecular Cell Biology,* 14**,** 382-392.

Bray, K., Mathew, R., Lau, A., Kamphorst, J. J., Fan, J., Chen, J., Chen, H. Y., Ghavami, A., Stein, M., Dipaola, R. S., Zhang, D., Rabinowitz, J. D. & White, E. 2012. Autophagy suppresses RIP kinase-dependent necrosis enabling survival to mTOR inhibition. *Plos One,* 7**,** e41831.

Bristol, M. L., Di, X., Beckman, M. J., Wilson, E. N., Henderson, S. C., Maiti, A., Fan, Z. & Gewirtz, D. A. 2012. Dual functions of autophagy in the response of breast tumor cells to radiation: cytoprotective autophagy with radiation alone and cytotoxic autophagy in radiosensitization by vitamin D 3. *Autophagy,* 8**,** 739-53.

Bristol, M. L., Emery, S. M., Maycotte, P., Thorburn, A., Chakradeo, S. & Gewirtz, D. A. 2013. Autophagy inhibition for chemosensitization and radiosensitization in cancer: do the preclinical data support this therapeutic strategy? *J Pharmacol Exp Ther,* 344**,** 544-52.

Broccoli, D., Smogorzewska, A., Chong, L. & Delange, T. 1997. Human telomeres contain two distinct Myb-related proteins, TRF1 and TRF2. *Nat Genet,* 17**,** 231-235.

Browning, D. J. 2014. Hydroxychloroquine and chloroquine retinopathy. New York: Springer.

Buchler, P., Reber, H. A., Buchler, M., Shrinkante, S., Buchler, M. W., Friess, H., Semenza, G. L. & Hines, O. J. 2003. Hypoxia-inducible factor 1 regulates vascular endothelial growth factor expression in human pancreatic cancer. *Pancreas,* 26**,** 56-64.

Budanov, A. V. & Karin, M. 2008. p53 target genes Sestrin1 and Sestrin2 connect genotoxic stress and mTOR signaling. *Cell,* 134**,** 451-460.

Bunik, V. I., Denton, T. T., Xu, H., Thompson, C. M., Cooper, A. J. L. & Gibson, G. E. 2005. Phosphonate analogues of alpha-ketoglutarate inhibit the activity of the alpha-ketoglutarate dehydrogenase complex isolated from brain and in cultured cells. *Biochemistry,* 44**,** 10552-10561.

Cai, S. L., Tee, A. R., Short, J. D., Bergeron, J. M., Kim, J., Shen, J. J., Guo, R. F., Johnson, C. L., Kiguchi, K. & Walker, C. L. 2006. Activity of TSC2 is inhibited by AKT-mediated phosphorylation and membrane partitioning. *Journal of Cell Biology,* 173**,** 279-289.

Cancer Research Uk. 2013. *Breast cancer statistics* [Online]. Available: http://www.cancerresearchuk.org/health-professional/cancer-statistics/statistics-by-cancer-type/breast-cancer#heading-Zero [Accessed 5th Sept 2016].

Cao, W., Yacoub, S., Shiverick, K. T., Namiki, K., Sakai, Y., Porvasnik, S., Urbanek, C. & Rosser, C. J. 2008. Dichloroacetate (DCA) sensitizes both wild-type and over expressing Bcl-2 prostate cancer cells in vitro to radiation. *Prostate,* 68**,** 1223-31.

Carew, J. S., Medina, E. C., Esquivel, J. A., Mahalingam, D., Swords, R., Kelly, K., Zhang, H., Huang, P., Mita, A. C., Mita, M. M., Giles, F. J. & Nawrocki, S. T. 2010. Autophagy inhibition enhances vorinostat-induced apoptosis via ubiquitinated protein accumulation. *Journal of Cellular and Molecular Medicine,* 14**,** 2448-2459.

Carew, J. S., Nawrocki, S. T., Kahue, C. N., Zhang, H., Yang, C., Chung, L., Houghton, J. A., Huang, P., Giles, F. J. & Cleveland, J. L. 2007. Targeting autophagy augments the anticancer activity of the histone deacetylase inhibitor SAHA to overcome Bcr-Abl-mediated drug resistance. *Blood,* 110**,** 313-22.

Carmeliet, P. 2005. VEGF as a key mediator of angiogenesis in cancer. *Oncology,* 69 Suppl 3**,** 4-10.

Carpenter, C. L., Duckworth, B. C., Auger, K. R., Cohen, B., Schaffhausen, B. S. & Cantley, L. C. 1990. Purification and Characterization of Phosphoinositide 3-Kinase from Rat-Liver. *Journal of Biological Chemistry,* 265**,** 19704-19711.

Carriere, A., Cargnello, M., Julien, L. A., Gao, H., Bonneil, E., Thibault, P. & Roux, P. P. 2008. Oncogenic MAPK signaling stimulates mTORC1 activity by promoting RSK-mediated Raptor phosphorylation. *Current Biology,* 18**,** 1269-1277.

Cesen, M. H., Repnik, U., Turk, V. & Turk, B. 2013. Siramesine triggers cell death through destabilisation of mitochondria, but not lysosomes. *Cell Death & Disease,* 4.

Chaachouay, H., Ohneseit, P., Toulany, M., Kehlbach, R., Multhoff, G. & Rodemann, H. P. 2011. Autophagy contributes to resistance of tumor cells to ionizing radiation. *Radiotherapy and Oncology,* 99**,** 287-292.

Chan, E. Y. W., Longatti, A., Mcknight, N. C. & Tooze, S. A. 2009. Kinase-Inactivated ULK Proteins Inhibit Autophagy via Their Conserved C- Terminal Domains Using an Atg13-Independent Mechanism. *Molecular and Cellular Biology,* 29**,** 157-171.

Chang, E. H., Gonda, M. A., Ellis, R. W., Scolnick, E. M. & Lowy, D. R. 1982. Human Genome Contains 4 Genes Homologous to Transforming Genes of Harvey and Kirsten Murine Sarcoma-Viruses. *Proceedings of the National Academy of Sciences of the United States of America-Biological Sciences,* 79**,** 4848-4852.

Chantranupong, L., Scaria, S. M., Saxton, R. A., Gygi, M. P., Shen, K., Wyant, G. A., Wang, T., Harper, J. W., Gygi, S. P. & Sabatini, D. M. 2016. The CASTOR Proteins Are Arginine Sensors for the mTORC1 Pathway. *Cell,* 165**,** 153-164.

Chantranupong, L., Wolfson, R. L., Orozco, J. M., Saxton, R. A., Scaria, S. M., Bar-Peled, L., Spooner, E., Isasa, M., Gygi, S. P. & Sabatini, D. M. 2014. The Sestrins Interact with GATOR2 to Negatively Regulate the Amino-Acid-Sensing Pathway Upstream of mTORC1. *Cell Reports,* 9**,** 1-8.

Chaube, B., Malvi, P., Singh, S. V., Mohammad, N., Viollet, B. & Bhat, M. K. 2015. AMPK maintains energy homeostasis and survival in cancer cells via regulating p38/PGC-1α-mediated mitochondrial biogenesis. *Cell Death Discovery,* 1**,** 15063.

Chen, P. M., Gombart, Z. J. & Chen, J. W. 2011a. Chloroquine treatment of ARPE-19 cells leads to lysosome dilation and intracellular lipid accumulation: possible implications of lysosomal dysfunction in macular degeneration. *Cell Biosci,* 1**,** 10.

Chen, Q., Liang, Z., Sun, T., Sun, X. 2011. Grape Skin Polyphenols (GSPs) Inhibit the Migration of Mouse Mammary Carcinoma 4T1 Cells *in Vitro Clinical Oncology Cancer Research,* 8**,** 33-37.

Chen, Y., Hou, Q. Y., Yan, W. X., Luo, J., Chen, D., Liu, Z. G., He, S. Q. & Ding, X. Q. 2011b. PIK3CA Is Critical for the Proliferation, Invasiveness, and Drug Resistance of Human Tongue Carcinoma Cells. *Oncology Research,* 19**,** 563-571.

Cheng, Q. & Chen, J. D. 2010. Mechanism of p53 stabilization by ATM after DNA damage. *Cell Cycle,* 9**,** 472-478.CHHIPA, R. R., WU, Y., MOHLER, J. L. & IP, C. 2010. Survival advantage of AMPK activation to androgen-independent prostate cancer cells during energy stress. *Cellular Signalling,* 22**,** 1554-1561.

Chipuk, J. E., Kuwana, T., Bouchier-Hayes, L., Droin, N. M., Newmeyer, D., Schuler, M. & Green, D. R. 2004. Direct activation of Bax by p53 mediates mitochondrial membrane permeabilization and apoptosis. *Science,* 303**,** 1010-1014.

Chipuk, J. E., Maurer, U., Green, D. R. & Schuler, M. 2003. Pharmacologic activation of p53 elicits Bax-dependent apoptosis in the absence of transcription. *Cancer Cell,* 4**,** 371-381.

Chromik, J., Safferthal, C., Serve, H. & Fulda, S. 2014. Smac mimetic primes apoptosis-resistant acute myeloid leukaemia cells for cytarabine-induced cell death by triggering necroptosis. *Cancer Letters,* 344**,** 101-9.

Ciani, B., Layfield, R., Cavey, J. R., Sheppard, P. W. & Searle, M. S. 2003. Structure of the ubiquitin-associated domain of p62 (SQSTM1) and implications for mutations that cause Paget's disease of bone. *J Biol Chem,* 278**,** 37409-12.

Clark, A. S., Mitch, W. E., Goodman, M. N., Fagan, J. M., Anwargoheer, M. & Curnow, R. T. 1987. Dichloroacetate Inhibits Glycolysis and Augments Insulin-Stimulated Glycogen-Synthesis in Rat Muscle. *Journal of Clinical Investigation,* 79**,** 588-594.

Codogno, P., Mehrpour, M. & Proikas-Cezanne, T. 2012. Canonical and non-canonical autophagy: variations on a common theme of self-eating? *Nature Reviews Molecular Cell Biology,* 13**,** 7-12.

Coelho, R. G., Calaca, I. C., Celestrini, D. M., Correia-Carneiro, A. H., Costa, M. M., Zancan, P. & Sola-Penna, M. 2015. Hexokinase and phosphofructokinase activity and intracellular distribution correlate with aggressiveness and invasiveness of human breast carcinoma. *Oncotarget,* 6**,** 29375-87.

Cohen, S. N. & Yielding, K. L. 1965. Spectrophotometric Studies of the Interaction of Chloroquine with Deoxyribonucleic Acid. *J Biol Chem,* 240**,** 3123-31.

Conus, S., Perozzo, R., Reinheckel, T., Peters, C., Scapozza, L., Yousefi, S. & Simon, H. U. 2008. Caspase-8 is activated by cathepsin D initiating neutrophil apoptosis during the resolution of inflammation. *Journal of Experimental Medicine,* 205**,** 685-698.

Cufi, S., Vazquez-Martin, A., Oliveras-Ferraros, C., Corominas-Faja, B., Cuyas, E., Lopez-Bonet, E., Martin-Castillo, B., Joven, J. & Menendez, J. A. 2013. The anti-malarial chloroquine overcomes primary resistance and restores sensitivity to trastuzumab in HER2-positive breast cancer. *Sci Rep,* 3**,** 2469.

Dai, W., Wang, F., Lu, J., Xia, Y., He, L., Chen, K., Li, J., Li, S., Liu, T., Zheng, Y., Wang, J., Lu, W., Zhou, Y., Yin, Q., Abudumijiti, H., Chen, R., Zhang, R., Zhou, L., Zhou, Z., Zhu, R., Yang, J., Wang, C., Zhang, H., Xu, L. & Guo, C. 2015. By reducing hexokinase 2, resveratrol induces apoptosis in HCC cells addicted to aerobic glycolysis and inhibits tumor growth in mice. *Oncotarget,* 6**,** 13703-17.

Dechant, R., Binda, M., Lee, S. S., Pelet, S., Winderickx, J. & Peter, M. 2010. Cytosolic pH is a second messenger for glucose and regulates the PKA pathway through V-ATPase. *Embo Journal,* 29**,** 2515-2526.

Degenhardt, K., Mathew, R., Beaudoin, B., Bray, K., Anderson, D., Chen, G., Mukherjee, C,. Shi, Y., Gelinas, C., Fan, Y., Et Al 2006. Autophagy promotes tumor cell survival and restricts necrosis, inflammation, and tumorigenesis. *Cancer Cell,* 10**,** 51-64

Degterev, A., Hitomi, J., Germscheid, M., Ch'en, I. L., Korkina, O., Teng, X., Abbott, D., Cuny, G. D., Yuan, C., Wagner, G., Hedrick, S. M., Gerber, S. A., Lugovskoy, A. & Yuan, J. 2008. Identification of RIP1 kinase as a specific cellular target of necrostatins. *Nature Chemical Biology,* 4**,** 313-321.

Degterev, A., Huang, Z. H., Boyce, M., Li, Y. Q., Jagtap, P., Mizushima, N., Cuny, G. D., Mitchison, T. J., Moskowitz, M. A. & Yuan, J. Y. 2005. Chemical inhibitor of nonapoptotic cell death with therapeutic potential for ischemic brain injury. *Nature Chemical Biology,* 1**,** 112-119.

Degtyarev, M., De Maziere, A., Orr, C., Lin, J., Lee, Bb., Tien, Jy., Prior, Ww., Van Dijk, S., Wu, H., Gray, Dc., Davis, Dp., Stern, Hm., Murray, Lj., Hoeflich, Kp., Klumperman, J., Friedman, Ls., Lin, K. 2008. Akt inhibition promotes autophagy and sensitizes PTEN-null tumors to lysosomotrophic agents *J Cell Biol,* 183**,** 101-116.

Delaney, L. M., Ho, N., Morrison, J., Farias, N. R., Mosser, D. D. & Coomber, B. L. 2015. Dichloroacetate affects proliferation but not survival of human colorectal cancer cells. *Apoptosis,* 20**,** 63-74.

Demetriades, C., Doumpas, N. & Teleman, A. A. 2014. Regulation of TORC1 in Response to Amino Acid Starvation via Lysosomal Recruitment of TSC2. *Cell,* 156**,** 786-799.

Devarajan, E., Sahin, A. A., Chen, J. S., Krishnamurthy, R. R., Aggarwal, N., Brun, A. M., Sapino, A., Zhang, F., Sharma, D., Yang, X. H., Tora, A. D. & Mehta, K. 2002. Down-regulation of caspase 3 in breast cancer: a possible mechanism for chemoresistance. *Oncogene,* 21**,** 8843-51.

Dibble, C. C., Elis, W., Menon, S., Qin, W., Klekota, J., Asara, J. M., Finan, P. M., Kwiatkowski, D. J., Murphy, L. O. & Manning, B. D. 2012. TBC1D7 Is a Third Subunit of the TSC1-TSC2 Complex Upstream of mTORC1. *Mol Cell,* 47**,** 535-546.

Dielschneider, R. F., Eisenstat, H., Mi, S., Curtis, J. M., Xiao, W., Johnston, J. B. & Gibson, S. B. 2016. Lysosomotropic agents selectively target chronic lymphocytic leukemia cells due to altered sphingolipid metabolism. *Leukemia,* 30**,** 1290-1300.

Dooley, H. C., Razi, M., Polson, H. E. J., Girardin, S. E., Wilson, M. I. & Tooze, S. A. 2014. WIPI2 Links LC3 Conjugation with PI3P, Autophagosome Formation, and Pathogen Clearance by Recruiting Atg12-5-16L1. *Mol Cell,* 55**,** 238-252.

Dowdle, W. E., Nyfeler, B., Nagel, J., Elling, R. A., Liu, S. M., Triantafellow, E., Menon, S., Wang, Z. C., Honda, A., Pardee, G., Cantwell, J., Luu, C., Cornella-Taracido, I., Harrington, E., Fekkes, P., Lei, H., Fang, Q., Digan, M. E., Burdick, D., Powers, A. F., Helliwell, S. B., D'aquin, S., Bastien, J., Wang, H., Wiederschain, D., Kuerth, J., Bergman, P., Schwalb, D., Thomas, J., Ugwonali, S., Harbinski, F., Tallarico, J., Wilson, C. J., Myer, V. E., Porter, J. A., Bussiere, D. E., Finan, P. M., Labow, M. A., Mao, X. H., Hamann, L. G., Manning, B. D., Valdez, R. A., Nicholson, T., Schirle, M., Knapp, M. S., Keaney, E. P. & Murphy, L. O. 2014. Selective VPS34

inhibitor blocks autophagy and uncovers a role for NCOA4 in ferritin degradation and iron homeostasis in vivo. *Nature Cell Biology,* 16**,** 1069-+.

Droga-Mazovec, G., Bojic, L., Petelin, A., Ivanova, S., Romih, R., Repnik, U., Salvesen, G. S., Stoka, V., Turk, V. & Turk, B. 2008. Cysteine cathepsins trigger caspase-dependent cell death through cleavage of Bid and antiapoptotic Bcl-2 homologues. *Journal of Biological Chemistry,* 283**,** 19140-19150.

Duffy, A., Le, J., Sausville, E. & Emadi, A. 2015. Autophagy modulation: a target for cancer treatment development. *Cancer Chemotherapy and Pharmacology,* 75**,** 439-447.

Dunn, W. A. 1990. Studies on the Mechanisms of Autophagy - Formation of the Autophagic Vacuole. *Journal of Cell Biology,* 110**,** 1923-1933.

Echeverry, N., Ziltener, G., Barbone, D., Weder, W., Stahel, R. A., Broaddus, V. C. & Felley-Bosco, E. 2015. Inhibition of autophagy sensitizes malignant pleural mesothelioma cells to dual PI3K/mTOR inhibitors. *Cell Death & Disease,* 6**,** e1757.

Eckhardt, B. L., Parker, B. S., Van Laar, R. K., Restall, C. M., Natoli, A. L., Tavaria, M. D., Stanley, K. L., Sloan, E. K., Moseley, J. M. & Anderson, R. L. 2005. Genomic analysis of a spontaneous model of breast cancer metastasis to bone reveals a role for the extracellular matrix. *Molecular Cancer Research,* 3**,** 1-13.

Efeyan, A., Zoncu, R., Chang, S., Gumper, I., Snitkin, H., Wolfson, R. L., Kirak, O., Sabatini, D. D. & Sabatini, D. M. 2013. Regulation of mTORC1 by the Rag GTPases is necessary for neonatal autophagy and survival. *Nature,* 493**,** 679-+.

Egan, D. F., Chun, M. G. H., Vamos, M., Zou, H. X., Rong, J., Miller, C. J., Lou, H. J., Raveendra-Panickar, D., Yang, C. C., Sheffler, D. J., Teriete, P., Asara, J. M., Turk, B. E., Cosford, N. D. P. & Shaw, R. J. 2015. Small Molecule Inhibition of the Autophagy Kinase ULK1 and Identification of ULK1 Substrates. *Mol Cell,* 59**,** 285-297.

Egan, D. F., Shackelford, D. B., Mihaylova, M. M., Gelino, S., Kohnz, R. A., Mair, W., Vasquez, D. S., Joshi, A., Gwinn, D. M., Taylor, R., Asara, J. M., Fitzpatrick, J., Dillin, A., Viollet, B., Kundu, M., Hansen, M. & Shaw, R. J. 2011. Phosphorylation of ULK1 (hATG1) by AMP-activated protein kinase connects energy sensing to mitophagy. *Science,* 331**,** 456-61.

Elstrom, R. L., Bauer, D. E., Buzzai, M., Karnauskas, R., Harris, M. H., Plas, D. R., Zhuang, H., Cinalli, R. M., Alavi, A., Rudin, C. M. & Thompson, C. B. 2004. Akt stimulates aerobic glycolysis in cancer cells. *Cancer Res,* 64**,** 3892-9.

Eng, C. H., Wang, Z., Tkach, D., Toral-Barza, L., Ugwonali, S., Liu, S., Fitzgerald, S. L., George, E., Frias, E., Cochran, N., De Jesus, R., Mcallister, G., Hoffman, G. R., Bray, K., Lemon, L., Lucas, J., Fantin, V. R., Abraham, R. T., Murphy, L. O. & Nyfeler, B. 2016. Macroautophagy is dispensable for growth of KRAS mutant tumors and chloroquine efficacy. *Proc Natl Acad Sci U S A,* 113**,** 182-7.

Enzenmuller, S., Gonzalez, P., Debatin, K. M. & Fulda, S. 2013. Chloroquine overcomes resistance of lung carcinoma cells to the dual PI3K/mTOR inhibitor PI103 by lysosome-mediated apoptosis. *Anticancer Drugs,* 24**,** 14-9.

Erdal, H., Berndtsson, M., Castro, J., Brunk, U., Shoshan, M. C. & Linder, S. 2005. Induction of lysosomal membrane permeabilization by compounds that activate p53-independent apoptosis. *Proceedings of the National Academy of Sciences of the United States of America,* 102**,** 192-197.

Falkenberg, K. J. & Johnstone, R. W. 2014. Histone deacetylases and their inhibitors in cancer, neurological diseases and immune disorders. *Nature Reviews Drug Discovery,* 13**,** 673-691.

Fan, W., Nassiri, A. & Zhong, Q. 2011. Autophagosome targeting and membrane curvature sensing by Barkor/Atg14(L). *Proceedings of the National Academy of Sciences of the United States of America,* 108**,** 7769-7774.

Farombi, E. O. 2006. Genotoxicity of chloroquine in rat liver cells: protective role of free radical scavengers. *Cell Biol Toxicol,* 22**,** 159-67.

Firat, E., Weyerbrock, A., Gaedicke, S., Grosu, A. L. & Niedermann, G. 2012. Chloroquine or Chloroquine-PI3K/Akt Pathway Inhibitor Combinations Strongly Promote gamma-Irradiation-Induced Cell Death in Primary Stem-Like Glioma Cells. *Plos One,* 7.

Fleury, C., Mignotte, B. & Vayssiere, J. L. 2002. Mitochondrial reactive oxygen species in cell death signaling. *Biochimie,* 84**,** 131-41.

Foghsgaard, L., Wissing, D., Mauch, D., Lademann, U., Bastholm, L., Boes, M., Elling, F., Leist, M. & Jaattela, M. 2001. Cathepsin B acts as a dominant execution protease in tumor cell apoptosis induced by tumor necrosis factor. *Journal of Cell Biology,* 153**,** 999-1009.

Forbes, S. A., Bindal, N., Bamford, S., Cole, C., Kok, C. Y., Beare, D., Jia, M. M., Shepherd, R., Leung, K., Menzies, A., Teague, J. W., Campbell, P. J., Stratton, M. R. & Futreal, P. A. 2011. COSMIC: mining complete cancer genomes in the Catalogue of Somatic Mutations in Cancer. *Nucleic Acids Research,* 39**,** D945-D950.

Forsythe, J. A., Jiang, B. H., Iyer, N. V., Agani, F., Leung, S. W., Koos, R. D. & Semenza, G. L. 1996. Activation of vascular endothelial growth factor gene transcription by hypoxia-inducible factor 1. *Molecular and Cellular Biology,* 16**,** 4604-13.

Fouche, N., Cesare, A. J., Willcox, S., Ozgur, S., Compton, S. A. & Griffith, J. D. 2006. The basic domain of TRF2 directs binding to DNA junctions irrespective of the presence of TTAGGG repeats. *Journal of Biological Chemistry,* 281**,** 37486-37495.

Fujita, N., Itoh, T., Omori, H., Fukuda, M., Noda, T. & Yoshimori, T. 2008. The Atg16L complex specifies the site of LC3 lipidation for membrane biogenesis in autophagy. *Molecular Biology of the Cell,* 19**,** 2092-2100.

Fulda, S. & Debatin, K. M. 2006. Extrinsic versus intrinsic apoptosis pathways in anticancer chemotherapy. *Oncogene,* 25**,** 4798-811.

Fung, C., Lock, R., Gao, S., Salas, E., Debnath, J. 2008. Induction of autophagy during extracellular matrix detachment promotes cell survival. *Molecular Biology of the Cell,* 19**,** 797-806.

Furman, R. R., Sharman, J. P., Coutre, S. E., Cheson, B. D., Pagel, J. M., Hillmen, P., Barrientos, J. C., Zelenetz, A. D., Kipps, T. J., Flinn, I., Ghia, P., Eradat, H., Ervin, T., Lamanna, N., Coiffier, B., Pettitt, A. R., Ma, S., Stilgenbauer, S., Cramer, P., Aiello, M., Johnson, D. M., Miller, L. L., Li, D., Jahn, T. M., Dansey, R. D., Hallek, M. & O'brien, S. M. 2014. Idelalisib and Rituximab in Relapsed Chronic Lymphocytic Leukemia. *New England Journal of Medicine,* 370**,** 997-1007.

Ganley, I. G., Lam, D. H., Wang, J. R., Ding, X. J., Chen, S. & Jiang, X. J. 2009. ULK1 center dot ATG13 center dot FIP200 Complex Mediates mTOR Signaling and Is Essential for Autophagy. *Journal of Biological Chemistry,* 284**,** 12297-12305.

Gao, M., Liang, J. Y., Lu, Y. L., Guo, H. F., German, P., Bai, S. S., Jonasch, E., Yang, X. S., Mills, G. B. & Ding, Z. Y. 2013. Site specific activation of AKT protects cells from death induced by glucose deprivation. *Cancer Research,* 73.

Gao, P., Tchernyshyov, I., Chang, T. C., Lee, Y. S., Kita, K., Ochi, T., Zeller, K. I., De Marzo, A. M., Van Eyk, J. E., Mendell, J. T. & Dang, C. V. 2009. c-Myc suppression of miR-23a/b enhances mitochondrial glutaminase expression and glutamine metabolism. *Nature,* 458**,** 762-5.

Gasparini, G. 2000. Prognostic value of vascular endothelial growth factor in breast cancer. *Oncologist,* 5 Suppl 1**,** 37-44.

Ge, L., Melville, D., Zhang, M. & Schekman, R. 2013. The ER-Golgi intermediate compartment is a key membrane source for the LC3 lipidation step of autophagosome biogenesis. *Elife,* 2.

Ge, L., Zhang, M. & Schekman, R. 2014. Phosphatidylinositol 3-kinase and COPII generate LC3 lipidation vesicles from the ER-Golgi intermediate compartment. *Elife,* 3.

Geng, Y., Kohli, L., Klocke, B. J. & Roth, K. A. 2010. Chloroquine-induced autophagic vacuole accumulation and cell death in glioma cells is p53 independent. *Neuro Oncol,* 12**,** 473-81.

Gerber, H. P., Dixit, V. & Ferrara, N. 1998. Vascular endothelial growth factor induces expression of the antiapoptotic proteins Bcl-2 and A1 in vascular endothelial cells. *J Biol Chem,* 273**,** 13313-6.

Gomes, L. C., Di Benedetto, G. & Scorrano, L. 2011. During autophagy mitochondria elongate, are spared from degradation and sustain cell viability. *Nature Cell Biology,* 13**,** 589-U207.

Gong, J. G., Costanzo, A., Yang, H. Q., Melino, G., Kaelin, W. G., Levrero, M. & Wang, J. Y. J. 1999. The tyrosine kinase c-Abl regulates p73 in apoptotic response to cisplatin-induced DNA damage. *Nature,* 399**,** 806-809.

Goodall, M. L., Wang, T., Martin, K. R., Kortus, M. G., Kauffman, A. L., Trent, J. M., Gately, S. & Mackeigan, J. P. 2014. Development of potent autophagy inhibitors that sensitize oncogenic BRAF V600E mutant melanoma tumor cells to vemurafenib. *Autophagy,* 10**,** 1120-1136.

Grabiner, B. C., Nardi, V., Birsoy, K., Possemato, R., Shen, K., Sinha, S., Jordan, A., Beck, A. H. & Sabatini, D. M. 2014. A Diverse Array of Cancer-Associated MTOR Mutations Are Hyperactivating and Can Predict Rapamycin Sensitivity. *Cancer Discovery,* 4**,** 554-563.

Groth-Pedersen, L., Ostenfeld, M. S., Hoyer-Hansen, M., Nylandsted, J. & Jaattela, M. 2007. Vincristine induces dramatic lysosomal changes and sensitizes cancer cells to lysosome-destabilizing siramesine. *Cancer Research,* 67**,** 2217-2225.

Guillaumond, F., Leca, J., Olivares, O., Lavaut, M. N., Vidal, N., Berthezene, P., Dusetti, N. J., Loncle, C., Calvo, E., Turrini, O., Iovanna, J. L., Tomasini, R. & Vasseur, S. 2013. Strengthened glycolysis under hypoxia supports tumor symbiosis and hexosamine biosynthesis in pancreatic adenocarcinoma. *Proc Natl Acad Sci U S A,* 110**,** 3919-24.

Guo, J. Y., Chen, H. Y., Mathew, R., Fan, J., Strohecker, A. M., Karsli-Uzunbas, G., Kamphorst, J. J., Chen, G. H., Lemons, J. M. S., Karantza, V., Coller, H. A., Dipaola, R. S., Gelinas, C., Rabinowitz, J. D. & White, E. 2011. Activated Ras requires autophagy to maintain oxidative metabolism and tumorigenesis. *Genes Dev,* 25**,** 460-470.

Guo, J. Y., Karsli-Uzunbas, G., Mathew, R., Aisner, S. C., Kamphorst, J. J., Strohecker, A. M., Chen, G. H., Price, S., Lu, W. Y., Teng, X., Snyder, E., Santanam, U., Dipaola, R. S., Jacks, T., Rabinowitz, J. D. & White, E. 2013. Autophagy suppresses progression of K-ras-induced lung tumors to oncocytomas and maintains lipid homeostasis. *Genes Dev,* 27**,** 1447-1461.

Gupta, G. P. & Massague, J. 2006. Cancer metastasis: Building a framework. *Cell,* 127**,** 679-695.

Gwinn, D. M., Shackelford, D. B., Egan, D. F., Mihaylova, M. M., Mery, A., Vasquez, D. S., Turk, B. E. & Shaw, R. J. 2008. AMPK phosphorylation of raptor mediates a metabolic checkpoint. *Mol Cell,* 30**,** 214-26.

Ha, J., Daniel, S., Broyles, S. S. & Kim, K. H. 1994. Critical Phosphorylation Sites for Acetyl-Coa Carboxylase Activity. *Journal of Biological Chemistry,* 269**,** 22162-22168.

Hahn, W. C., Counter, C. M., Lundberg, A. S., Beijersbergen, R. L., Brooks, M. W. & Weinberg, R. A. 1999. Creation of human tumour cells with defined genetic elements. *Nature,* 400**,** 464-8.

Hailey, D. W., Rambold, A. S., Satpute-Krishnan, P., Mitra, K., Sougrat, R., Kim, P. K. & Lippincott-Schwartz, J. 2010. Mitochondria Supply Membranes for Autophagosome Biogenesis during Starvation. *Cell,* 141**,** 656-667.

Han, W. D., Pan, H. M., Chen, Y., Sun, J., Wang, Y. S., Li, J., Ge, W. T., Feng, L. F., Lin, X. Y., Wang, X. J., Wang, X. & Jin, H. C. 2011. EGFR Tyrosine Kinase Inhibitors Activate Autophagy as a Cytoprotective Response in Human Lung Cancer Cells. *Plos One,* 6.

Hanahan, D. & Weinberg, R. A. 2000. The hallmarks of cancer. *Cell,* 100**,** 57-70.

Hanahan, D. & Weinberg, R. A. 2011. Hallmarks of Cancer: The Next Generation. *Cell,* 144**,** 646-674.

Hara, T., Takamura, A., Kishi, C., Iemura, S. I., Natsume, T., Guan, J. L. & Mizushima, N. 2008. FIP200, a ULK-interacting protein, is required for autophagosome formation in mammalian cells. *Journal of Cell Biology,* 181**,** 497-510.

Hardie, D. G. 2014. AMP-activated protein kinase: maintaining energy homeostasis at the cellular and whole-body levels. *Annu Rev Nutr,* 34**,** 31-55.

Harhaji-Trajkovic, L., Arsikin, K., Kravic-Stevovic, T., Petricevic, S., Tovilovic, G., Pantovic, A., Zogovic, N., Ristic, B., Janjetovic, K., Bumbasirevic, V. & Trajkovic, V. 2012. Chloroquine-Mediated Lysosomal Dysfunction Enhances the Anticancer Effect of Nutrient Deprivation. *Pharmaceutical Research,* 29**,** 2249-2263.

Hasan, N., Greenwood, T., Glunde, K. 2008. Lysosome swelling precedes lysosomal membrane permeabilization in breast cancer cells. *Cancer Res,* 68**,** LB-51.

Hawley, S. R., Bray, P. G., Park, B. K. & Ward, S. A. 1996. Amodiaquine accumulation in Plasmodium falciparum as a possible explanation for its superior antimalarial activity over chloroquine. *Molecular and Biochemical Parasitology,* 80**,** 15-25.

Hayashi-Nishino, M., Fujita, N., Noda, T., Yamaguchi, A., Yoshimori, T. & Yamamoto, A. 2009. A subdomain of the endoplasmic reticulum forms a cradle for autophagosome formation. *Nature Cell Biology,* 11**,** 1433-U102.

He, S. D., Liang, Y. Q., Shao, F. & Wang, X. D. 2011. Toll-like receptors activate programmed necrosis in macrophages through a receptor-interacting kinase-3-mediated pathway. *Proceedings of the National Academy of Sciences of the United States of America,* 108**,** 20054-20059.

He, S. D., Wang, L., Miao, L., Wang, T., Du, F. H., Zhao, L. P. & Wang, X. D. 2009. Receptor Interacting Protein Kinase-3 Determines Cellular Necrotic Response to TNF-alpha. *Cell,* 137**,** 1100-1111.

Heerboth, S., Housman, G., Leary, M., Longacre, M., Byler, S., Lapinska, K., Willbanks, A. & Sarkar, S. 2015. EMT and tumor metastasis. *Clin Transl Med,* 4**,** 6.

Hernandez, C. P., Morrow, K., Lopez-Barcons, L. A., Zabaleta, J., Sierra, R., Velasco, C., Cole, J. & Rodriguez, P. C. 2010. Pegylated arginase I: a potential therapeutic approach in T-ALL. *Blood,* 115**,** 5214-5221.

Hirose, S., Yaginuma, N. & Inada, Y. 1974. Disruption of Charge Separation Followed by That of Proton Gradient in Mitochondrial-Membrane by Cccp. *Journal of Biochemistry,* 76**,** 213-216.

Holler, N., Zaru, R., Micheau, O., Thome, M., Attinger, A., Valitutti, S., Bodmer, J. L., Schneider, P., Seed, B. & Tschopp, J. 2000. Fas triggers an alternative, caspase-8-independent cell death pathway using the kinase RIP as effector molecule. *Nat Immunol,* 1**,** 489-495.

Homewood, C. A., Warhurst, D. C., Peters, W. & Baggaley, V. C. 1972. Lysosomes, pH and the anti-malarial action of chloroquine. *Nature,* 235**,** 50-2.

Horiuchi, A., Imai, T., Shimizu, M., Oka, K., Wang, C., Nikaido, T. & Konishi, I. 2002. Hypoxia-induced changes in the expression of VEGF, HIF-1 alpha and cell cycle-related molecules in ovarian cancer cells. *Anticancer Res,* 22**,** 2697-702.

Hosokawa, N., Hara, T., Kaizuka, T., Kishi, C., Takamura, A., Miura, Y., Iemura, S., Natsume, T., Takehana, K., Yamada, N., Guan, J. L., Oshiro, N. & Mizushima, N. 2009a. Nutrient-dependent mTORC1 association with the ULK1-Atg13-FIP200 complex required for autophagy. *Mol Biol Cell,* 20**,** 1981-91.

Hosokawa, N., Sasaki, T., Iemura, S., Natsume, T., Hara, T. & Mizushima, N. 2009b. Atg101, a novel mammalian autophagy protein interacting with Atg13. *Autophagy,* 5**,** 973-9.

Houghtaling, B. R., Cuttonaro, L., Chang, W. & Smith, S. 2004. A dynamic molecular link between the telomere length regulator TRF1 and the chromosome end protector TRF2. *Current Biology,* 14**,** 1621-1631.

Hu, Y. L., Delay, M., Jahangiri, A., Molinaro, A. M., Rose, S. D., Carbonell, W. S. & Aghi, M. K. 2012. Hypoxia-induced autophagy promotes tumor cell survival and adaptation to antiangiogenic treatment in glioblastoma. *Cancer Res,* 72**,** 1773-83.

Huai, J. S., Vogtle, F. N., Jockel, L., Li, Y. B., Kiefer, T., Ricci, J. E. & Borner, C. 2013. TNF alpha-induced lysosomal membrane permeability is downstream of MOMP and triggered by caspase-mediated NDUFS1 cleavage and ROS formation. *Journal of Cell Science,* 126**,** 4015-4025.

Ichimura, Y., Kumanomidou, T., Sou, Y. S., Mizushima, T., Ezaki, J., Ueno, T., Kominami, E., Yamane, T., Tanaka, K. & Komatsu, M. 2008. Structural basis for sorting mechanism of p62 in selective autophagy. *J Biol Chem,* 283**,** 22847-57.

Ikenouchi, J., Matsuda, M., Furuse, M. & Tsukita, S. 2003. Regulation of tight junctions during the epithelium-mesenchyme transition: direct repression of the gene expression of claudins/occludin by Snail. *Journal of Cell Science,* 116**,** 1959-1967.

Inoki, K., Li, Y., Zhu, T. Q., Wu, J. & Guan, K. L. 2002. TSC2 is phosphorylated and inhibited by Akt and suppresses mTOR signalling. *Nature Cell Biology,* 4**,** 648-657.

Inoki, K., Zhu, T. & Guan, K. L. 2003. TSC2 mediates cellular energy response to control cell growth and survival. *Cell,* 115**,** 577-90.

Irwin, M., Marin, M. C., Phillips, A. C., Seelan, R. S., Smith, D. I., Liu, W. G., Flores, E. R., Tsai, K. Y., Jacks, T., Vousden, K. H. & Kaelin, W. G. 2000. Role for the p53 homologue p73 in E2F-1-induced apoptosis. *Nature,* 407**,** 645-648.

Isakoff, S. J., Engelman, J. A., Irie, H. Y., Luo, J., Brachmann, S. M., Pearline, R. V., Cantley, L. C. & Brugge, J. S. 2005. Breast cancer-associated PIK3CA mutations are oncogenic in mammary epithelial cells. *Cancer Research,* 65**,** 10992-11000.

Ishigami, S. I., Arii, S., Furutani, M., Niwano, M., Harada, T., Mizumoto, M., Mori, A., Onodera, H. & Imamura, M. 1998. Predictive value of vascular endothelial growth factor (VEGF) in metastasis and prognosis of human colorectal cancer. *Br J Cancer,* 78**,** 1379-84.

Itakura, E., Kishi, C., Inoue, K. & Mizushima, N. 2008. Beclin 1 Forms Two Distinct Phosphatidylinositol 3-Kinase Complexes with Mammalian Atg14 and UVRAG. *Molecular Biology of the Cell,* 19**,** 5360-5372.

Itakura, E. & Mizushima, N. 2010. Characterization of autophagosome formation site by a hierarchical analysis of mammalian Atg proteins. *Autophagy,* 6**,** 764-776.

Itakura, E. & Mizushima, N. 2011. p62 Targeting to the autophagosome formation site requires self-oligomerization but not LC3 binding. *Journal of Cell Biology,* 192**,** 17-27.

Jaattela, M., Nylandsted, J. 2015. Quantification of Lysosomal Membrane Permeabilization by Cytosolic Cathepsin and β-N-Acetyl-Glucosaminidase Activity Measurements. *Cold Spring Harbor Protocols*.

Jacobson, M. D. 1996. Reactive oxygen species and programmed cell death. *Trends in Biochemical Sciences,* 21**,** 83-86.

Jeon, S. M., Chandel, N. S. & Hay, N. 2012. AMPK regulates NADPH homeostasis to promote tumour cell survival during energy stress. *Nature,* 485**,** 661-+.

Ji, Y., Di, W., Yang, Q., Lu, Z., Cai, W. & Wu, J. 2015. Inhibition of Autophagy Increases Proliferation Inhibition and Apoptosis Induced by the PI3K/mTOR Inhibitor NVP-BEZ235 in Breast Cancer Cells. *Clin Lab,* 61**,** 1043-51.

Jiang, P. D., Zhao, Y. L., Deng, X. Q., Mao, Y. Q., Shi, W., Tang, Q. Q., Li, Z. G., Zheng, Y. Z., Yang, S. Y. & Wei, Y. Q. 2010. Antitumor and antimetastatic activities

of chloroquine diphosphate in a murine model of breast cancer. *Biomedicine & Pharmacotherapy,* 64**,** 609-14.

Jo, G. H., Bogler, O., Chwae, Y. J., Yoo, H., Lee, S. H., Park, J. B., Kim, Y. J., Kim, J. H. & Gwak, H. S. 2015. Radiation-induced autophagy contributes to cell death and induces apoptosis partly in malignant glioma cells. *Cancer Res Treat,* 47**,** 221-41.

Joo, J. H., Dorsey, F. C., Joshi, A., Hennessy-Walters, K. M., Rose, K. L., Mccastlain, K., Zhang, J., Iyengar, R., Jung, C. H., Suen, D. F., Steeves, M. A., Yang, C. Y., Prater, S. M., Kim, D. H., Thompson, C. B., Youle, R. J., Ney, P. A., Cleveland, J. L. & Kundu, M. 2011. Hsp90-Cdc37 chaperone complex regulates Ulk1- and Atg13-mediated mitophagy. *Mol Cell,* 43**,** 572-85.

Jouan-Lanhouet, S., Arshad, M. I., Piquet-Pellorce, C., Martin-Chouly, C., Le Moigne-Muller, G., Van Herreweghe, F., Takahashi, N., Sergent, O., Lagadic-Gossmann, D., Vandenabeele, P., Samson, M. & Dimanche-Boitrel, M. T. 2012. TRAIL induces necroptosis involving RIPK1/RIPK3-dependent PARP-1 activation. *Cell Death and Differentiation,* 19**,** 2003-14.

Jung, C. H., Jun, C. B., Ro, S. H., Kim, Y. M., Otto, N. M., Cao, J., Kundu, M. & Kim, D. H. 2009. ULK-Atg13-FIP200 Complexes Mediate mTOR Signaling to the Autophagy Machinery. *Molecular Biology of the Cell,* 20**,** 1992-2003.

Kagedal, K., Zhao, M., Svensson, I. & Brunk, U. T. 2001. Sphingosine-induced apoptosis is dependent on lysosomal proteases. *Biochemical Journal,* 359**,** 335-343.

Kaiser, W. J., Sridharan, H., Huang, C. Z., Mandal, P., Upton, J. W., Gough, P. J., Sehon, C. A., Marquis, R. W., Bertin, J. & Mocarski, E. S. 2013. Toll-like Receptor 3-mediated Necrosis via TRIF, RIP3, and MLKL. *Journal of Biological Chemistry,* 288**,** 31268-31279.

Kandoth, C., Mclellan, M. D., Vandin, F., Ye, K., Niu, B. F., Lu, C., Xie, M. C., Zhang, Q. Y., Mcmichael, J. F., Wyczalkowski, M. A., Leiserson, M. D. M., Miller, C. A., Welch, J. S., Walter, M. J., Wendl, M. C., Ley, T. J., Wilson, R. K., Raphael, B. J. & Ding, L. 2013. Mutational landscape and significance across 12 major cancer types. *Nature,* 502**,** 333+.

Kane, P. M. 1995. Disassembly and Reassembly of the Yeast Vacuolar H+-Atpase in-Vivo. *Journal of Biological Chemistry,* 270**,** 17025-17032.

Kang, M. R., Kim, M. S., Oh, J. E., Kim, Y. R., Song, S. Y., Kim, S. S., Ahn, C. H., Yoo, N. J. & Lee, S. H. 2009. Frameshift mutations of autophagy-related genes ATG2B, ATG5, ATG9B and ATG12 in gastric and colorectal cancers with microsatellite instability. *J Pathol,* 217**,** 702-6.

Kang, S. A., Pacold, M. E., Cervantes, C. L., Lim, D., Lou, H. J., Ottina, K., Gray, N. S., Turk, B. E., Yaffe, M. B. & Sabatini, D. M. 2013. mTORC1 Phosphorylation Sites Encode Their Sensitivity to Starvation and Rapamycin. *Science,* 341**,** 364-+.

Kang, Y., Siegel, P. M., Shu, W., Drobnjak, M., Kakonen, S. M., Cordon-Cardo, C., Guise, T. A. & Massague, J. 2003. A multigenic program mediating breast cancer metastasis to bone. *Cancer Cell,* 3**,** 537-49.

Karanasios, E., Walker, S. A., Okkenhaug, H., Manifava, M., Hummel, E., Zimmermann, H., Ahmed, Q., Domart, M. C., Collinson, L. & Ktistakis, N. T. 2016. Autophagy initiation by ULK complex assembly on ER tubulovesicular regions marked by ATG9 vesicles. *Nat Commun,* 7**,** 12420.

Karayiannakis, A. J., Syrigos, K. N., Polychronidis, A., Zbar, A., Kouraklis, G., Simopoulos, C. & Karatzas, G. 2002. Circulating VEGF levels in the serum of gastric cancer patients: correlation with pathological variables, patient survival, and tumor surgery. *Ann Surg,* 236**,** 37-42.

Kase, E. T., Nikolic, N., Bakke, S. S., Bogen, K. K., Aas, V., Thoresen, G. H. & Rustan, A. C. 2013. Remodeling of oxidative energy metabolism by galactose improves glucose handling and metabolic switching in human skeletal muscle cells. *Plos One,* 8**,** e59972.

Kim, E., Goraksha-Hicks, P., Li, L., Neufeld, T. P. & Guan, K. L. 2008. Regulation of TORC1 by Rag GTPases in nutrient response. *Nature Cell Biology,* 10**,** 935-945.

Kim, E. L., Wustenberg, R., Rubsam, A., Schmitz-Salue, C., Warnecke, G., Bucker, E. M., Pettkus, N., Speidel, D., Rohde, V., Schulz-Schaeffer, W., Deppert, W. & Giese, A. 2010. Chloroquine activates the p53 pathway and induces apoptosis in human glioma cells. *Neuro Oncol,* 12**,** 389-400.

Kim, J., Kim, Y. C., Fang, C., Russell, R. C., Kim, J. H., Fan, W., Liu, R., Zhong, Q. & Guan, K. L. 2013a. Differential regulation of distinct Vps34 complexes by AMPK in nutrient stress and autophagy. *Cell,* 152**,** 290-303.

Kim, J., Kundu, M., Viollet, B. & Guan, K. L. 2011. AMPK and mTOR regulate autophagy through direct phosphorylation of Ulk1. *Nature Cell Biology,* 13**,** 132-U71.

Kim, J. H., Choi, A. R., Kim, Y. K. & Yoon, S. 2013b. Co-treatment with the anti-malarial drugs mefloquine and primaquine highly sensitizes drug-resistant cancer cells by increasing P-gp inhibition. *Biochemical and Biophysical Research Communications,* 441**,** 655-660.

Kim, N. W., Piatyszek, M. A., Prowse, K. R., Harley, C. B., West, M. D., Ho, P. L., Coviello, G. M., Wright, W. E., Weinrich, S. L. & Shay, J. W. 1994. Specific association of human telomerase activity with immortal cells and cancer. *Science,* 266**,** 2011-5.

Kim, S. E., Park, H. J., Jeong, H. K., Kim, M. J., Kim, M., Bae, O. N. & Baek, S. H. 2015. Autophagy sustains the survival of human pancreatic cancer PANC-1 cells under extreme nutrient deprivation conditions. *Biochem Biophys Res Commun,* 463**,** 205-10.

Kuma, A., Hatano, M., Matsui, M., Yamamoto, A., Nakaya, H., Yoshimori, T., Ohsumi, Y., Tokuhisa, T. & Mizushima, N. 2004. The role of autophagy during the early neonatal starvation period. *Nature,* 432**,** 1032-1036.

Laderoute, K. R., Amin, K., Calaoagan, J. M., Knapp, M., Le, T., Orduna, J., Foretz, M. & Viollet, B. 2006. 5 '-AMP-activated protein kinase (AMPK) is induced by low-oxygen and glucose deprivation conditions found in solid-tumor microenvironments. *Molecular and Cellular Biology,* 26**,** 5336-5347.

Lakhter, A. J., Sahu, R. P., Sun, Y., Kaufmann, W. K., Androphy, E. J., Travers, J. B. & Naidu, S. R. 2013. Chloroquine promotes apoptosis in melanoma cells by inhibiting BH3 domain-mediated PUMA degradation. *J Invest Dermatol,* 133**,** 2247-54.

Lamoureux, F., Thomas, C., Crafter, C., Kumano, M., Zhang, F., Davies, B.R., Gleave, M.E., Zoubeidi, A. 2013. Blocked autophagy using lysosomotrophic agents

sensitizes resistant prostate tumor cells to the novel Akt inhibitor AZD5363. *Clinical Cancer Research,* 19**,** 833-844.

Lang, M. J., Martinez-Marquez, J. Y., Prosser, D. C., Ganser, L. R., Buelto, D., Wendland, B. & Duncan, M. C. 2014. Glucose Starvation Inhibits Autophagy via Vacuolar Hydrolysis and Induces Plasma Membrane Internalization by Down-regulating Recycling. *Journal of Biological Chemistry,* 289**,** 16736-16747.

Lazova, R., Camp, R.L., Klump,V., Siddiqui, S.F., Amaravadi, R.K., Pawelek, J.M. 2012. Punctate LC3B expression is a common feature of solid tumors and associated with proliferation, metastasis, and poor outcome. *Clinical Cancer Research,* 18**,** 370-379.

Le, A., Cooper, C. R., Gouw, A. M., Dinavahi, R., Maitra, A., Deck, L. M., Royer, R. E., Vander Jagt, D. L., Semenza, G. L. & Dang, C. V. 2010. Inhibition of lactate dehydrogenase A induces oxidative stress and inhibits tumor progression. *Proc Natl Acad Sci U S A,* 107**,** 2037-42.

Le, A., Lane, A. N., Hamaker, M., Bose, S., Gouw, A., Barbi, J., Tsukamoto, T., Rojas, C. J., Slusher, B. S., Zhang, H., Zimmerman, L. J., Liebler, D. C., Slebos, R. J., Lorkiewicz, P. K., Higashi, R. M., Fan, T. W. & Dang, C. V. 2012. Glucose-independent glutamine metabolism via TCA cycling for proliferation and survival in B cells. *Cell Metabolism,* 15**,** 110-21.

Lembert, N., Joos, H. C., Idahl, L. A., Ammon, H. P. & Wahl, M. A. 2001. Methyl pyruvate initiates membrane depolarization and insulin release by metabolic factors other than ATP. *Biochemical Journal,* 354**,** 345-50.

Li, J., Yen, C., Liaw, D., Podsypanina, K., Bose, S., Wang, S. I., Puc, J., Miliaresis, C., Rodgers, L., Mccombie, R., Bigner, S. H., Giovanella, B. C., Ittmann, M., Tycko, B., Hibshoosh, H., Wigler, M. H. & Parsons, R. 1997. PTEN, a putative protein tyrosine phosphatase gene mutated in human brain, breast, and prostate cancer. *Science,* 275**,** 1943-7.

Li, N., Zheng, Y. Y., Chen, W., Wang, C. M., Liu, X. G., He, W. G., Xu, H. M. & Cao, X. T. 2007. Adaptor protein LAPF recruits phosphorylated p53 to Lysosomes and triggers lysosomal destabilization in apoptosis. *Cancer Research,* 67**,** 11176-11185.

Li, Y. I., Libby, E. F., Lewis, M. J., Liu, J., Shacka, J. J. & Hurst, D. R. 2016. Increased autophagic response in a population of metastatic breast cancer cells. *Oncology Letters,* 12**,** 523-529.

Liang, D. H., Choi, D. S., Ensor, J. E., Kaipparettu, B. A., Bass, B. L. & Chang, J. C. 2016. The autophagy inhibitor chloroquine targets cancer stem cells in triple negative breast cancer by inducing mitochondrial damage and impairing DNA break repair. *Cancer Letters,* 376**,** 249-58.

Liang, X., Tang, J., Liang, Y., Jin, R. & Cai, X. 2014. Suppression of autophagy by chloroquine sensitizes 5-fluorouracil-mediated cell death in gallbladder carcinoma cells. *Cell Biosci,* 4**,** 10.

Liang, X., Yang, Y., Wang, L. J., Zhu, X. B., Zeng, X. W., Wu, X. J., Chen, H. B., Zhang, X. D. & Mei, L. 2015. pH-Triggered burst intracellular release from hollow microspheres to induce autophagic cancer cell death. *Journal of Materials Chemistry B,* 3**,** 9383-9396.

Liang, X. H., Jackson, S., Seaman, M., Brown, K., Kempkes, B., Hibshoosh, H. & Levine, B. 1999. Induction of autophagy and inhibition of tumorigenesis by beclin 1. *Nature,* 402**,** 672-6.

Ligueros, M., Jeoung, D., Tang, B., Hochhauser, D., Reidenberg, M. M. & Sonenberg, M. 1997. Gossypol inhibition of mitosis, cyclin D1 and Rb protein in human mammary cancer cells and cyclin-D1 transfected human fibrosarcoma cells. *Br J Cancer,* 76**,** 21-8.

Lim, J., Lachenmayer, M. L., Wu, S., Liu, W., Kundu, M., Wang, R., Komatsu, M., Oh, Y. J., Zhao, Y. & Yue, Z. 2015. Proteotoxic stress induces phosphorylation of p62/SQSTM1 by ULK1 to regulate selective autophagic clearance of protein aggregates. *PLoS Genet,* 11**,** e1004987.

Lin, T. J., Liang, W. M., Hsiao, P. W., M, S. P., Wei, W. C., Lin, H. T., Yin, S. Y. & Yang, N. S. 2015. Rapamycin Promotes Mouse 4T1 Tumor Metastasis that Can Be Reversed by a Dendritic Cell-Based Vaccine. *Plos One,* 10**,** e0138335.

Liu, T. J., Koul, D., Lafortune, T., Tiao, N., Shen, R. J., Maira, S. M., Garcia-Echevrria, C. & Yung, W. K. 2009. NVP-BEZ235, a novel dual phosphatidylinositol

3-kinase/mammalian target of rapamycin inhibitor, elicits multifaceted antitumor activities in human gliomas. *Mol Cancer Ther,* 8**,** 2204-10.

Lobo, C., Ruiz-Bellido, M. A., Aledo, J. C., Marquez, J., Nunez De Castro, I. & Alonso, F. J. 2000. Inhibition of glutaminase expression by antisense mRNA decreases growth and tumourigenicity of tumour cells. *Biochemical Journal,* 348 Pt 2**,** 257-61.

Locatelli, S. L., Cleris, L., Stirparo, G. G., Tartari, S., Saba, E., Pierdominici, M., Malorni, W., Carbone, A., Anichini, A. & Carlo-Stella, C. 2014. BIM upregulation and ROS-dependent necroptosis mediate the antitumor effects of the HDACi Givinostat and Sorafenib in Hodgkin lymphoma cell line xenografts. *Leukemia,* 28**,** 1861-1871.

Lomonaco, S. L., Finniss, S., Xiang, C. L., Decarvalho, A., Umansky, F., Kalkanis, S. N., Mikkelsen, T. & Brodie, C. 2009. The induction of autophagy by gamma-radiation contributes to the radioresistance of glioma stem cells. *International Journal of Cancer,* 125**,** 717-722.

Long, X., Lin, Y., Ortiz-Vega, S., Yonezawa, K. & Avruch, J. 2005. Rheb binds and regulates the mTOR kinase. *Current Biology,* 15**,** 702-13.

Longatti, A., Lamb, C. A., Razi, M., Yoshimura, S., Barr, F. A. & Tooze, S. A. 2012. TBC1D14 regulates autophagosome formation via Rab11-and ULK1-positive recycling endosomes. *Journal of Cell Biology,* 197**,** 659-675.

Lou, P. H., Hansen, B. S., Olsen, P. H., Tullin, S., Murphy, M. P. & Brand, M. D. 2007. Mitochondrial uncouplers with an extraordinary dynamic range. *Biochemical Journal,* 407**,** 129-140.

Lou, Y., Mcdonald, P. C., Oloumi, A., Chia, S., Ostlund, C., Ahmadi, A., Kyle, A., Auf Dem Keller, U., Leung, S., Huntsman, D., Clarke, B., Sutherland, B. W., Waterhouse, D., Bally, M., Roskelley, C., Overall, C. M., Minchinton, A., Pacchiano, F., Carta, F., Scozzafava, A., Touisni, N., Winum, J. Y., Supuran, C. T. & Dedhar, S. 2011. Targeting tumor hypoxia: suppression of breast tumor growth and metastasis by novel carbonic anhydrase IX inhibitors. *Cancer Res,* 71**,** 3364-76.

Luan, F. L., Ding, R., Sharma, V. K., Chon, W. J., Lagman, M. & Suthanthiran, M. 2003. Rapamycin is an effective inhibitor of human renal cancer metastasis. *Kidney Int,* 63**,** 917-26.

Lunt, S. Y. & Vander Heiden, M. G. 2011. Aerobic glycolysis: meeting the metabolic requirements of cell proliferation. *Annu Rev Cell Dev Biol,* 27**,** 441-64.

M Carlo., A. M., Y Lakhman., S Patil., K Woo., J Deluca., C Lee., & Jj Hsieh., D. F., Rj Motzer., Mh Vossa. 2016. A Phase Ib Study of BEZ235, aDualInhibitor of Phosphatidylinositol 3-Kinase andMammalian Target of Rapamycin, in Patients With Advanced Renal Cell Carcinoma. *The Oncologist*.

M.R. Rosenfeld, X. Y., J.G. Supko, S. Desideri, S.A. Grossman , S. Brem, T. Mikkelson, D. Wang, Y.C.Chang, J. Hu, Q. Mcafee, J.Fisher, A.Troxel, S.Piao, D.F.Heitjan, K.S.Tan, L.Pontiggia, P.J. O'dwyer, L.E. Davis, R.K. Amaravadi. 2014. A phase I/II trial of hydroxychloroquine in conjunction with radiation therapy and concurrent and adjuvant temozolomide in patients with newly diagnosed glioblastoma multiforme. *Autophagy,* 10**,** 1-10.

Ma, X. J. M. & Blenis, J. 2009. Molecular mechanisms of mTOR-mediated translational control. *Nature Reviews Molecular Cell Biology,* 10**,** 307-318.

Ma, Y. Y., Wei, S. J., Lin, Y. C., Lung, J. C., Chang, T. C., Whang-Peng, J., Liu, J. M., Yang, D. M., Yang, W. K. & Shen, C. Y. 2000. PIK3CA as an oncogene in cervical cancer. *Oncogene,* 19**,** 2739-2744.

Macfarlane, M., Robinson, G. L. & Cain, K. 2012. Glucose-a sweet way to die Metabolic switching modulates tumor cell death. *Cell Cycle,* 11**,** 3919-3925.

Macintosh, R. L., Timpson, P., Thorburn, J., Anderson, K.I., Thorburn, A., Ryan, K.M. 2012. Inhibition of autophagy impairs tumor cell invasion in an organotypic model. *Cell Cycle,* 11**,** 2022-2029.

Maclean, K. H., Dorsey, F. C., Cleveland, J. L. & Kastan, M. B. 2008. Targeting lysosomal degradation induces p53-dependent cell death and prevents cancer in mouse models of lymphomagenesis (vol 118, pg 79, 2008). *Journal of Clinical Investigation,* 118**,** 1584-1584.

Macmillan Cancer Support. 2013. *Cancer mortality trends: 1992-2020* [Online].Available:http://www.macmillan.org.uk/documents/aboutus/newsroom/mortality-trends-2013-executive-summary-final.pdf [Accessed 5th Sept 2016].

Maddams, J., Utley, M. & Moller, H. 2012. Projections of cancer prevalence in the United Kingdom, 2010-2040. *Br J Cancer,* 107**,** 1195-202.

Maehama, T. & Dixon, J. E. 1998. The tumor suppressor, PTEN/MMAC1, dephosphorylates the lipid second messenger, phosphatidylinositol 3,4,5-trisphosphate. *Journal of Biological Chemistry,* 273**,** 13375-13378.

Maejima, I., Takahashi, A., Omori, H., Kimura, T., Takabatake, Y., Saitoh, T., Yamamoto, A., Hamasaki, M., Noda, T., Isaka, Y. & Yoshimori, T. 2013. Autophagy sequesters damaged lysosomes to control lysosomal biogenesis and kidney injury. *Embo Journal,* 32**,** 2336-2347.

Maes, H., Kuchnio, A., Peric, A., Moens, S., Nys, K., De Bock, K., Quaegebeur, A., Schoors, S., Georgiadou, M., Wouters, J., Vinckier, S., Vankelecom, H., Garmyn, M., Vion, A. C., Radtke, F., Boulanger, C., Gerhardt, H., Dejana, E., Dewerchin, M., Ghesquiere, B., Annaert, W., Agostinis, P. & Carmeliet, P. 2014. Tumor Vessel Normalization by Chloroquine Independent of Autophagy. *Cancer Cell,* 26**,** 190-206.

Mahalingam, D., Mita, M., Sarantopoulos, J., Wood, L. , Amaravadi, R., Davis, L., Mita, A., Curiel, T.J., Espitia, C.M., Nawrocki, S.T., Giles, F.J., Carew, J.S. 2014. Combined autophagy and HDAC inhibition. A phase I safety, tolerability, pharmacokinetic, and pharmacodynamic analysis of hydroxychloroquine in combination with the HDAC inhibitor vorinostat in patients with advanced solid tumors. *Autophagy,* 10**,** 1403-1414.

Maira, S. M., Stauffer, F., Brueggen, J., Furet, P., Schnell, C., Fritsch, C., Brachmann, S., Chene, P., De Pover, A., Schoemaker, K., Fabbro, D., Gabriel, D., Simonen, M., Murphy, L., Finan, P., Sellers, W. & Garcia-Echeverria, C. 2008. Identification and characterization of NVP-BEZ235, a new orally available dual phosphatidylinositol 3-kinase/mammalian target of rapamycin inhibitor with potent in vivo antitumor activity. *Mol Cancer Ther,* 7**,** 1851-63.

Majewski, N., Nogueira, V., Bhaskar, P., Coy, P. E., Skeen, J. E., Gottlob, K., Chandel, N. S., Thompson, C. B., Robey, R. B. & Hay, N. 2004. Hexokinase-mitochondria interaction mediated by Akt is required to inhibit apoptosis in the presence or absence of Bax and Bak. *Mol Cell,* 16**,** 819-30.

Manning, B. D., Tee, A. R., Logsdon, N., Blenis, J. & Cantley, L. C. 2002. Identification of the tuberous sclerosis complex-2 gene product tuberin as a target of

the phosphoinositide 3-kinase/Akt pathway. *Molecular Biology of the Cell,* 13**,** 293a-293a.

Marino, G., Salvador-Montoliu, N., Fueyo, A., Knecht, E., Mizushima, N. & Lopez-Otin, C. 2007. Tissue-specific autophagy alterations and increased tumorigenesis in mice deficient in Atg4C/autophagin-3. *J Biol Chem,* 282**,** 18573-83.

Martinez-Munoz, G. A. & Kane, P. 2008. Vacuolar and plasma membrane proton pumps collaborate to achieve cytosolic pH homeostasis in yeast. *Journal of Biological Chemistry,* 283**,** 20309-20319.

Mathew, R., Karantza-Wadsworth, V., White, E. 2007. Role of autophagy in cancer. *Nature Reviews Cancer,* 7**,** 961-967.

Mathew, R., Karp, C.M., Beaudoin, B., Vuong, N., Chen, G., Chen, H.Y., Bray, K., Reddy, A,. Bhanot, G., Gelinas, C., Et Al. 2009. Autophagy suppresses tumorigenesis through elimination of p62. *Cell,* 137**,** 1062-1075.

Mathupala, S. P., Rempel, A. & Pedersen, P. L. 2001. Glucose catabolism in cancer cells: identification and characterization of a marked activation response of the type II hexokinase gene to hypoxic conditions. *J Biol Chem,* 276**,** 43407-12.

Matsumoto, G., Wada, K., Okuno, M., Kurosawa, M. & Nukina, N. 2011. Serine 403 phosphorylation of p62/SQSTM1 regulates selective autophagic clearance of ubiquitinated proteins. *Mol Cell,* 44**,** 279-89.

Matsunaga, K., Morita, E., Saitoh, T., Akira, S., Ktistakis, N. T., Izumi, T., Noda, T. & Yoshimori, T. 2010. Autophagy requires endoplasmic reticulum targeting of the PI3-kinase complex via Atg14L. *Journal of Cell Biology,* 190**,** 511-521.

Mauvezin, C., Nagy, P., Juhasz, G. & Neufeld, T. P. 2015. Autophagosome-lysosome fusion is independent of V-ATPase-mediated acidification. *Nat Commun,* 6**,** 7007.

Mauvezin, C. & Neufeld, T. P. 2015. Bafilomycin A1 disrupts autophagic flux by inhibiting both V-ATPase-dependent acidification and Ca-P60A/SERCA-dependent autophagosome-lysosome fusion. *Autophagy,* 11**,** 1437-8.

Maycotte, P., Aryal, S., Cummings, C. T., Thorburn, J., Morgan, M. J. & Thorburn, A. 2012. Chloroquine sensitizes breast cancer cells to Chemotherapy Independent Of Autophagy. *Autophagy,* 8**,** 200-212.

McAfee, Q., Zhang, Z. H., Samanta, A., Levi, S. M., Ma, X. H., Piao, S. F., Lynch, J. P., Uehara, T., Sepulveda, A. R., Davis, L. E., Winkler, J. D. & Amaravadi, R. K. 2012. Autophagy inhibitor Lys05 has single-agent antitumor activity and reproduces the phenotype of a genetic autophagy deficiency. *Proceedings of the National Academy of Sciences of the United States of America,* 109**,** 8253-8258.

McAlpine, F., Williamson, L. E., Tooze, S. A. & Chan, E. Y. W. 2013. Regulation of nutrient-sensitive autophagy by uncoordinated 51-like kinases 1 and 2. *Autophagy,* 9**,** 361-373.

McIlwain, D. R., Berger, T. & Mak, T. W. 2013. Caspase functions in cell death and disease. *Cold Spring Harb Perspect Biol,* 5**,** a008656.

Meadows, K. L. & Hurwitz, H. I. 2012. Anti-VEGF therapies in the clinic. *Cold Spring Harb Perspect Med,* 2.

Menon, S., Dibble, C. C., Talbott, G., Hoxhaj, G., Valvezan, A. J., Takahashi, H., Cantley, L. C. & Manning, B. D. 2014. Spatial Control of the TSC Complex Integrates Insulin and Nutrient Regulation of mTORC1 at the Lysosome. *Cell,* 156**,** 771-785.

Mercer, C. A., Kaliappan, A. & Dennis, P. B. 2009. A novel, human Atg13 binding protein, Atg101, interacts with ULK1 and is essential for macroautophagy. *Autophagy,* 5**,** 649-62.

Miller, F. R., Miller, B. E. & Heppner, G. H. 1983. Characterization of Metastatic Heterogeneity among Subpopulations of a Single-Mouse Mammary-Tumor - Heterogeneity in Phenotypic Stability. *Invasion & Metastasis,* 3**,** 22-31.

Mindell, J. A. 2012. Lysosomal acidification mechanisms. *Annu Rev Physiol,* 74**,** 69-86.

Minn, A. J., Gupta, G. P., Siegel, P. M., Bos, P. D., Shu, W. P., Giri, D. D., Viale, A., Olshen, A. B., Gerald, W. L. & Massague, J. 2005. Genes that mediate breast cancer metastasis to lung. *Nature,* 436**,** 518-524.

Mirzoeva, O. K., Hann, B., Hom, Y. K., Debnath, J., Aftab, D., Shokat, K. & Korn, W. M. 2011. Autophagy suppression promotes apoptotic cell death in response to inhibition of the PI3K-mTOR pathway in pancreatic adenocarcinoma. *J Mol Med (Berl),* 89**,** 877-89.

Miyashita, T. & Reed, J. C. 1995. Tumor-Suppressor P53 Is a Direct Transcriptional Activator of the Human Bax Gene. *Cell,* 80**,** 293-299.

Mizushima, N., Levine, B., Cuervo, A. M. & Klionsky, D. J. 2008. Autophagy fights disease through cellular self-digestion. *Nature,* 451**,** 1069-1075.

Mizushima, N., Noda, T., Yoshimori, T., Tanaka, Y., Ishii, T., George, M. D., Klionsky, D. J., Ohsumi, M. & Ohsumi, Y. 1998. A protein conjugation system essential for autophagy. *Nature,* 395**,** 395-398.

Morrow, K., Hernandez, C. P., Raber, P., Del Valle, L., Wilk, A. M., Majumdar, S., Wyczechowska, D., Reiss, K. & Rodriguez, P. C. 2013. Anti-leukemic mechanisms of pegylated arginase I in acute lymphoblastic T-cell leukemia. *Leukemia,* 27**,** 569-577.

Moruno-Manchon, J. F., Perez-Jimenez, E. & Knecht, E. 2013. Glucose induces autophagy under starvation conditions by a p38 MAPK-dependent pathway. *Biochemical Journal,* 449**,** 497-506.

Muller, A., Homey, B., Soto, H., Ge, N., Catron, D., Buchanan, M. E., Mcclanahan, T., Murphy, E., Yuan, W., Wagner, S. N., Barrera, J. L., Mohar, A., Verastegui, E. & Zlotnik, A. 2001. Involvement of chemokine receptors in breast cancer metastasis. *Nature,* 410**,** 50-6.

Mundi, P. S., Sachdev, J., Mccourt, C. & Kalinsky, K. 2016. Akt In Cancer: new molecular insights and advances in drug development. *Br J Clin Pharmacol*.

Murugan, A. K., Alzahrani, A. & Xing, M. Z. 2013. Mutations in Critical Domains Confer the Human mTOR Gene Strong Tumorigenicity. *Journal of Biological Chemistry,* 288**,** 6511-6521.

N. Fazio, R. B., E. Baudin, L. Antonuzzo, R. Hubner, H. Lahner, W.W. De Herder, M. Raderer, A. Teule, J. Capdevila, S. Libutti, M. Kulke, M. Shah, D. Dey, S. Turri, P. Aimone, C. Verslype, 2014. 1143P - Ph II study of BEZ235 in patients with

advanced pancreatic neuroendocrine tumors (pNET) after mTOR inhibitor therapy failure: Stage I interim results. *Annals of Oncology* 25.

Nakano, K. & Vousden, K. H. 2001. PUMA, a novel proapoptotic gene, is induced by p53. *Mol Cell,* 7**,** 683-694.

Nehs, M. A., Lin, C. I., Kozono, D. E., Whang, E. E., Cho, N. L., Zhu, K., Moalem, J., Moore, F. D. & Ruan, D. T. 2011. Necroptosis is a novel mechanism of radiation-induced cell death in anaplastic thyroid and adrenocortical cancers. *Surgery,* 150**,** 1032-1038.

Nezis, I. P., Simonsen, A., Sagona, A. P., Finley, K., Gaumer, S., Contamine, D., Rusten, T. E., Stenmark, H. & Brech, A. 2008. Ref(2)P, the Drosophila melanogaster homologue of mammalian p62, is required for the formation of protein aggregates in adult brain. *Journal of Cell Biology,* 180**,** 1065-71.

Ngaha, E., Akanji, Ma. 1982. Effect of chloroquine on the stability of rat kidney lysosomes in vivo and in vitro. *Comp Biochem Physiol* 73**,** 109-113.

Niu, Y. R., Wei, B., Chen, B., Xu, L. H., Jing, X., Peng, C. L. & Ma, T. Z. 2016. Amodiaquine-induced reproductive toxicity in adult male rats. *Molecular Reproduction and Development,* 83**,** 174-182.

Nolop, K. B., Rhodes, C. G., Brudin, L. H., Beaney, R. P., Krausz, T., Jones, T. & Hughes, J. M. 1987. Glucose utilization in vivo by human pulmonary neoplasms. *Cancer,* 60**,** 2682-9.

Nor, J. E., Christensen, J., Mooney, D. J. & Polverini, P. J. 1999. Vascular endothelial growth factor (VEGF)-mediated angiogenesis is associated with enhanced endothelial cell survival and induction of Bcl-2 expression. *Am J Pathol,* 154**,** 375-84.

O'donovan, T. R., O'sullivan, G.C., Mckenna, S.L. 2011. Induction of autophagy by drug resistant esophageal cancer cells promotes their survival and recovery following treatment with chemotherapeutics. *Autophagy,* 7**,** 509-524.

Oberle, C., Huai, J., Reinheckel, T., Tacke, M., Rassner, M., Ekert, P. G., Buellesbach, J. & Borner, C. 2010. Lysosomal membrane permeabilization and

cathepsin release is a Bax/Bak-dependent, amplifying event of apoptosis in fibroblasts and monocytes. *Cell Death and Differentiation,* 17**,** 1167-1178.

Ogawa, H., Nagano, H., Konno, M., Eguchi, H., Koseki, J., Kawamoto, K., Nishida, N., Colvin, H., Tomokuni, A., Tomimaru, Y., Hama, N., Wada, H., Marubashi, S., Kobayashi, S., Mori, M., Doki, Y. & Ishii, H. 2015. The combination of the expression of hexokinase 2 and pyruvate kinase M2 is a prognostic marker in patients with pancreatic cancer. *Mol Clin Oncol,* 3**,** 563-571.

Ohkuma, S., Poole, B. 1981. Cytoplasmic vacuolation of mouse peritoneal macrophages and the uptake into lysosomes of weakly basic substances. *J Cell Biol,* 90**,** 656-664.

Onder, T. T., Gupta, P. B., Mani, S. A., Yang, J., Lander, E. S. & Weinberg, R. A. 2008. Loss of E-cadherin promotes metastasis via multiple downstream transcriptional pathways. *Cancer Research,* 68**,** 3645-3654.

Orij, R., Postmus, J., Ter Beek, A., Brul, S. & Smits, G. J. 2009. In vivo measurement of cytosolic and mitochondrial pH using a pH-sensitive GFP derivative in Saccharomyces cerevisiae reveals a relation between intracellular pH and growth. *Microbiology-Sgm,* 155**,** 268-278.

Osorio, L. A., Farfan, N. M., Castellon, E. A. & Contreras, H. R. 2016. SNAIL transcription factor increases the motility and invasive capacity of prostate cancer cells. *Mol Med Rep,* 13**,** 778-86.

Paget, S. 1989. The distribution of secondary growths in cancer of the breast. 1889. *Cancer Metastasis Rev,* 8**,** 98-101.

Pankiv, S., Clausen, T. H., Lamark, T., Brech, A., Bruun, J. A., Outzen, H., Overvatn, A., Bjorkoy, G. & Johansen, T. 2007. p62/SQSTM1 binds directly to Atg8/LC3 to facilitate degradation of ubiquitinated protein aggregates by autophagy. *J Biol Chem,* 282**,** 24131-45.

Paoli, P., Giannoni, E. & Chiarugi, P. 2013. Anoikis molecular pathways and its role in cancer progression. *Biochimica Et Biophysica Acta-Molecular Cell Research,* 1833**,** 3481-3498.

Parada, L. F., Tabin, C. J., Shih, C. & Weinberg, R. A. 1982. Human EJ bladder carcinoma oncogene is homologue of Harvey sarcoma virus ras gene. *Nature,* 297**,** 474-8.

Park, E. J., Min, K. J., Choi, K. S., Kubatka, P., Kruzliak, P., Kim, D. E. & Kwon, T. K. 2016. Chloroquine enhances TRAIL-mediated apoptosis through up-regulation of DR5 by stabilization of mRNA and protein in cancer cells. *Sci Rep,* 6**,** 22921.

Park, J., Choi, K., Jeong, E., Kwon, D., Benveniste, E. N. & Choi, C. 2004. Reactive oxygen species mediate chloroquine-induced expression of chemokines by human astroglial cells. *Glia,* 47**,** 9-20.

Parmigiani, A., Nourbakhsh, A., Ding, B. X., Wang, W., Kim, Y. C., Akopiants, K., Guan, K. L., Karin, M. & Budanov, A. V. 2014. Sestrins Inhibit mTORC1 Kinase Activation through the GATOR Complex. *Cell Reports,* 9**,** 1281-1291.

Parniak, M. & Kalant, N. 1985. Incorporation of Glucose into Glycogen in Primary Cultures of Rat Hepatocytes. *Canadian Journal of Biochemistry and Cell Biology,* 63**,** 333-340.

Pasquier, B. 2016. Autophagy inhibitors. *Cellular and Molecular Life Sciences,* 73**,** 985-1001.

Pastorino, J. G., Shulga, N. & Hoek, J. B. 2002. Mitochondrial binding of hexokinase II inhibits Bax-induced cytochrome c release and apoptosis. *J Biol Chem,* 277**,** 7610-8.

Patra, K. C. & Hay, N. 2014. The pentose phosphate pathway and cancer. *Trends in Biochemical Sciences,* 39**,** 347-354.

Patra, K. C., Wang, Q., Bhaskar, P. T., Miller, L., Wang, Z., Wheaton, W., Chandel, N., Laakso, M., Muller, W. J., Allen, E. L., Jha, A. K., Smolen, G. A., Clasquin, M. F., Robey, R. B. & Hay, N. 2013. Hexokinase 2 is required for tumor initiation and maintenance and its systemic deletion is therapeutic in mouse models of cancer. *Cancer Cell,* 24**,** 213-28.

Pazdur, R. 2013a. *FDA Approval for Everolimus* [Online]. National Cancer Institute. Available: http://www.cancer.gov/about-cancer/treatment/drugs/fda-everolimus [Accessed 5th Sept 2016].

Pazdur, R. 2013b. *FDA Approval of Temosirolimus* [Online]. National Cancer Institute Available: http://www.cancer.gov/about-cancer/treatment/drugs/fda-temsirolimus [Accessed 5th Sept 2016].

Pecorino, L. 2008. *Molecular Biology of Cancer: Mechanisms, Targets, and Therapeutics,* New York, Oxford University Press.

Pellegrini, P., Strambi, A., Zipoli, C., Hagg-Olofsson, M., Buoncervello, M., Linder, S., De Milito, A. 2014. Acidic extracellular pH neutralises the autophagy-inhibiting activity of chloroquine. *Autophagy,* 10**,** 1-10.

Petherick, K. J., Conway, O. J. L., Mpamhanga, C., Osborne, S. A., Kamal, A., Saxty, B. & Ganley, I. G. 2015. Pharmacological Inhibition of ULK1 Kinase Blocks Mammalian Target of Rapamycin (mTOR)-dependent Autophagy. *Journal of Biological Chemistry,* 290**,** 11376-11383.

Pilli, M., Arko-Mensah, J., Ponpuak, M., Roberts, E., Master, S., Mandell, M. A., Dupont, N., Ornatowski, W., Jiang, S., Bradfute, S. B., Bruun, J. A., Hansen, T. E., Johansen, T. & Deretic, V. 2012. TBK-1 promotes autophagy-mediated antimicrobial defense by controlling autophagosome maturation. *Immunity,* 37**,** 223-34.

Preet, R., Mohapatra, P., Mohanty, S., Sahu, S. K., Choudhuri, T., Wyatt, M. D. & Kundu, C. N. 2012. Quinacrine has anticancer activity in breast cancer cells through inhibition of topoisomerase activity. *International Journal of Cancer,* 130**,** 1660-70.

Preuss, J., Richardson, A. D., Pinkerton, A., Hedrick, M., Sergienko, E., Rahlfs, S., Becker, K. & Bode, L. 2013. Identification and Characterization of Novel Human Glucose-6-Phosphate Dehydrogenase Inhibitors. *Journal of Biomolecular Screening,* 18**,** 286-297.

Priebe, A., Tan, L., Wahl, H., Kueck, A., He, G., Kwok, R., Opipari, A. & Liu, J. R. 2011. Glucose deprivation activates AMPK and induces cell death through modulation of Akt in ovarian cancer cells. *Gynecol Oncol,* 122**,** 389-95.

Puri, C., Renna, M., Bento, C. F., Moreau, K. & Rubinsztein, D. C. 2013. Diverse Autophagosome Membrane Sources Coalesce in Recycling Endosomes. *Cell,* 154**,** 1285-1299.

Qiao, S. X., Tao, S. S., De La Vega, M. R., Park, S. L., Vonderfecht, A. A., Jacobs, S. L., Zhang, D. D. & Wondrak, G. T. 2013. The antimalarial amodiaquine causes autophagic-lysosomal and proliferative blockade sensitizing human melanoma cells to starvation- and chemotherapy-induced cell death. *Autophagy,* 9**,** 2087-2102.

Rak, J., Mitsuhashi, Y., Bayko, L., Filmus, J., Shirasawa, S., Sasazuki, T. & Kerbel, R. S. 1995. Mutant ras oncogenes upregulate VEGF/VPF expression: implications for induction and inhibition of tumor angiogenesis. *Cancer Res,* 55**,** 4575-80.

Rambold, A. S., Kostelecky, B., Elia, N. & Lippincott-Schwartz, J. 2011. Tubular network formation protects mitochondria from autophagosomal degradation during nutrient starvation. *Proceedings of the National Academy of Sciences of the United States of America,* 108**,** 10190-10195.

Ramirez-Peinado, S., Leon-Annicchiarico, C. L., Galindo-Moreno, J., Iurlaro, R., Caro-Maldonado, A., Prehn, J. H. M., Ryan, K. M. & Munoz-Pinedo, C. 2013. Glucose-starved Cells Do Not Engage in Prosurvival Autophagy. *Journal of Biological Chemistry,* 288**,** 30387-30398.

Rangwala, R., . Chang, Y.C., Hu, J., Algazy, K., Evans, T., Fecher, L., Schuchter, L., Torigian, D.A., Panosian, J., Troxel, A., Tan, K., Heitjan, D.F., Demichele, A., Vaughn, D., Redlinger, M., Alavi, A., Kaiser, J., Pontiggia, L., Davis, L.E., O'dwyer, P.J., Amaravadi, R.K. 2014a. Combined MTOR and autophagy inhibition. Phase I trial of hydroxychloroquine and temsirolimus in patients with advanced solid tumors and melanoma. . *Autophagy,* 10**,** 1-12.

Rangwala, R., Leone, R., Chang, Y.C., Fecher, L., Schuchter, L.M., Kramer, A., Tan, K., Heitjan, D.F., Rodgers, G., Gallagher, M., Piao, S., Troxel, A.B., Evans, T., Demichele, A., Nathanson, K.L., O'dwyer, P.J., Kaiser, J., Pontiggia, L., Davis, L.E., Amaravadi, R.K. 2014b. Phase I trial of hydroxychloroquine with dose-intense temozolomide in patients with advanced solid tumors and melanoma. *Autophagy,* 10**,** 1-11.

Ravikumar, B., Moreau, K., Jahreiss, L., Puri, C. & Rubinsztein, D. C. 2010. Plasma membrane contributes to the formation of pre-autophagosomal structures (vol 12, pg 747, 2010). *Nature Cell Biology,* 12**,** 1021-1021.

Rebsamen, M., Pochini, L., Stasyk, T., De Araujo, M. E. G., Galluccio, M., Kandasamy, R. K., Snijder, B., Fauster, A., Rudashevskaya, E. L., Bruckner, M.,

Scorzoni, S., Filipek, P. A., Huber, K. V. M., Bigenzahn, J. W., Heinz, L. X., Kraft, C., Bennett, K. L., Indiveri, C., Huber, L. A. & Superti-Furga, G. 2015. SLC38A9 is a component of the lysosomal amino acid sensing machinery that controls mTORC1. *Nature,* advance online publication.

Reddy, B. S., Sujith, T., Kumar, M.Sathish., Babu, A.Narendra., Rao, N.Rama., Manjunathan, J. 2012. Malarial drugs got resistance. *Int J Pharm Biomed Res,* 3**,** 213-215.

Reid, M. A. & Kong, M. 2013. Dealing with hunger: Metabolic stress responses in tumors. *J Carcinog,* 12**,** 17.

Reles, A., Wen, W. H., Schmider, A., Gee, C., Runnebaum, I. B., Kilian, U., Jones, L. A., El-Naggar, A., Minguillon, C., Schonborn, I., Reich, O., Kreienberg, R., Lichtenegger, W. & Press, M. F. 2001. Correlation of p53 mutations with resistance to platinum-based chemotherapy and shortened survival in ovarian cancer. *Clinical Cancer Research,* 7**,** 2984-2997.

Repnik, U., Cesen, M. H. & Turk, B. 2014. Lysosomal membrane permeabilization in cell death: Concepts and challenges. *Mitochondrion,* 19**,** 49-57.

Ro, S. H., Semple, I. A., Park, H., Park, H. W., Kim, M., Kim, J. S. & Lee, J. H. 2014. Sestrin2 promotes Unc-51-like kinase 1 mediated phosphorylation of p62/sequestosome-1. *FEBS J,* 281**,** 3816-27.

Roberts, D. J. & Miyamoto, S. 2015. Hexokinase II integrates energy metabolism and cellular protection: Akting on mitochondria and TORCing to autophagy. *Cell Death and Differentiation,* 22**,** 248-257.

Robey, I. F., Lien, A. D., Welsh, S. J., Baggett, B. K. & Gillies, R. J. 2005. Hypoxia-inducible factor-1alpha and the glycolytic phenotype in tumors. *Neoplasia,* 7**,** 324-30.

Rojas-Puentes, L. L., Gonzalez-Pinedo, M., Crismatt, A., Ortega-Gomez, A., Gamboa-Vignolle, C., Nunez-Gomez, R., Dorantes-Gallareta, Y., Arce-Salinas, C. & Arrieta, O. 2013. Phase II randomized, double-blind, placebo-controlled study of whole-brain irradiation with concomitant chloroquine for brain metastases. *Radiat Oncol,* 8**,** 209.

Rusch, V., Klimstra, D., Venkatraman, E., Oliver, J., Martini, N., Gralla, R., Kris, M. & Dmitrovsky, E. 1995. Aberrant P53 Expression Predicts Clinical Resistance to Cisplatin-Based Chemotherapy in Locally Advanced Non-Small-Cell Lung-Cancer. *Cancer Research,* 55**,** 5038-5042.

Russell, R. C., Tian, Y., Yuan, H. X., Park, H. W., Chang, Y. Y., Kim, J., Kim, H., Neufeld, T. P., Dillin, A. & Guan, K. L. 2013. ULK1 induces autophagy by phosphorylating Beclin-1 and activating VPS34 lipid kinase. *Nature Cell Biology,* 15**,** 741-+.

Saddoughi, S. A., Gencer, S., Peterson, Y. K., Ward, K. E., Mukhopadhyay, A., Oaks, J., Bielawski, J., Szulc, Z. M., Thomas, R. J., Selvam, S. P., Senkal, C. E., Garrett-Mayer, E., De Palma, R. M., Fedarovich, D., Liu, A., Habib, A. A., Stahelin, R. V., Perrotti, D. & Ogretmen, B. 2013. Sphingosine analogue drug FTY720 targets I2PP2A/SET and mediates lung tumour suppression via activation of PP2A-RIPK1-dependent necroptosis. *Embo Molecular Medicine,* 5**,** 105-121.

Sadeghi, R. N., Karami-Tehrani, F. & Salami, S. 2015. Targeting prostate cancer cell metabolism: impact of hexokinase and CPT-1 enzymes. *Tumour Biol,* 36**,** 2893-905.

Sakoh-Nakatogawa, M., Matoba, K., Asai, E., Kirisako, H., Ishii, J., Noda, N. N., Inagaki, F., Nakatogawa, H. & Ohsumi, Y. 2013. Atg12-Atg5 conjugate enhances E2 activity of Atg3 by rearranging its catalytic site. *Nature Structural & Molecular Biology,* 20**,** 433-+.

Samuels, Y., Diaz, L. A., Schmidt-Kittler, O., Cummins, J. M., Delong, L., Cheong, I., Rago, C., Huso, D. L., Lengauer, C., Kinzler, K. W., Vogelstein, B. & Velculescu, V. E. 2005. Mutant PIK3CA promotes cell growth and invasion of human cancer cells. *Cancer Cell,* 7**,** 561-573.

Samuels, Y., Wang, Z. H., Bardelli, A., Silliman, N., Ptak, J., Szabo, S., Yan, H., Gazdar, A., Powell, D. M., Riggins, G. J., Willson, J. K. V., Markowitz, S., Kinzler, K. W., Vogelstein, B. & Velculescu, V. E. 2004. High frequency of mutations of the PIK3CA gene in human cancers. *Science,* 304**,** 554-554.

Sancak, Y., Bar-Peled, L., Zoncu, R., Markhard, A. L., Nada, S. & Sabatini, D. M. 2010. Ragulator-Rag Complex Targets mTORC1 to the Lysosomal Surface and Is Necessary for Its Activation by Amino Acids. *Cell,* 141**,** 290-303.

Sancak, Y., Peterson, T. R., Shaul, Y. D., Lindquist, R. A., Thoreen, C. C., Bar-Peled, L. & Sabatini, D. M. 2008. The Rag GTPases bind raptor and mediate amino acid signaling to mTORC1. *Science,* 320**,** 1496-1501.

Sanjana, N. E., Shalem, O. & Zhang, F. 2014. Improved vectors and genome-wide libraries for CRISPR screening. *Nature Methods,* 11**,** 783-784.

Santarpia, L., Lippman, S. M. & El-Naggar, A. K. 2012. Targeting the MAPK-RAS-RAF signaling pathway in cancer therapy. *Expert Opin Ther Targets,* 16**,** 103-19.

Santos, E., Tronick, S. R., Aaronson, S. A., Pulciani, S. & Barbacid, M. 1982. T24 human bladder carcinoma oncogene is an activated form of the normal human homologue of BALB- and Harvey-MSV transforming genes. *Nature,* 298**,** 343-7.

Sato, K., Tsuchihara, K., Fujii, S., Sugiyama, M., Goya, T., Atomi, Y., Ueno, T., Ochiai, A. & Esumi, H. 2007. Autophagy is activated in colorectal cancer cells and contributes to the tolerance to nutrient deprivation. *Cancer Res,* 67**,** 9677-84.

Sato, T., Nakashima, A., Guo, L., Coffman, K. & Tamanoi, F. 2010. Single amino-acid changes that confer constitutive activation of mTOR are discovered in human cancer. *Oncogene,* 29**,** 2746-2752.

Sautin, Y. Y., Lu, M., Gaugler, A., Zhang, L. & Gluck, S. L. 2005. Phosphatidylinositol 3-kinase-mediated effects of glucose on vacuolar H+-ATPase assembly, translocation, and acidification of intracellular compartments in renal epithelial cells. *Molecular and Cellular Biology,* 25**,** 575-589.

Sawaya, R. 2001. Considerations in the diagnosis and management of brain metastases. *Oncology-New York,* 15**,** 1144-1158.

Saxton, R. A., Chantranupong, L., Knockenhauer, K. E., Schwartz, T. U. & Sabatini, D. M. 2016a. Mechanism of arginine sensing by CASTOR1 upstream of mTORC1. *Nature,* 536**,** 229-33.

Saxton, R. A., Knockenhauer, K. E., Wolfson, R. L., Chantranupong, L., Pacold, M. E., Wang, T., Schwartz, T. U. & Sabatini, D. M. 2016b. METABOLISM Structural basis for leucine sensing by the Sestrin2-mTORC1 pathway. *Science,* 351**,** 53-58.

Schoenlein, P. V., Periyasamy-Thandavan, S., Samaddar, J. S., Jackson, W. H. & Barrett, J. T. 2009. Autophagy facilitates the progression of ERalpha-positive breast cancer cells to antiestrogen resistance. *Autophagy,* 5**,** 400-3.

Schonewolf, C. A., Mehta, M., Schiff, D., Wu, H., Haffty, B. G., Karantza, V. & Jabbour, S. K. 2014. Autophagy inhibition by chloroquine sensitizes HT-29 colorectal cancer cells to concurrent chemoradiation. *World J Gastrointest Oncol,* 6**,** 74-82.

Seglen, P. O. & Gordon, P. B. 1980. Effects of lysosomotropic monoamines, diamines, amino alcohols, and other amino compounds on protein degradation and protein synthesis in isolated rat hepatocytes. *Mol Pharmacol,* 18**,** 468-75.

Seitz, C., Hugle, M., Cristofanon, S., Tchoghandjian, A. & Fulda, S. 2013. The dual PI3K/mTOR inhibitor NVP-BEZ235 and chloroquine synergize to trigger apoptosis via mitochondrial-lysosomal cross-talk. *International Journal of Cancer,* 132**,** 2682-2693.

Selvakumaran, M., Amaravadi, R., & Vasilevskaya, I.A. 2013. Autophagy inhibition sensitises colon cancer cells to anti-angiogenic and cytotoxic therapy. *Clinical Cancer Research,* 19**,** 2995-3007.

Shang, L. B., Chen, S., Du, F. H., Li, S., Zhao, L. P. & Wang, X. D. 2011. Nutrient starvation elicits an acute autophagic response mediated by Ulk1 dephosphorylation and its subsequent dissociation from AMPK. *Proceedings of the National Academy of Sciences of the United States of America,* 108**,** 4788-4793.

Sharifi, M. N., Mowers, E. E., Drake, L. E., Collier, C., Chen, H., Zamora, M., Mui, S. & Macleod, K. F. 2016. Autophagy Promotes Focal Adhesion Disassembly and Cell Motility of Metastatic Tumor Cells through the Direct Interaction of Paxillin with LC3. *Cell Reports,* 15**,** 1660-72.

Shi, Y. M., Yang, L., Geng, Y. D., Zhang, C. & Kong, L. Y. 2015. Polyphyllin I induced-apoptosis is enhanced by inhibition of autophagy in human hepatocellular carcinoma cells. *Phytomedicine,* 22**,** 1139-49.

Shuvayeva, G., Bobak, Y., Igumentseva, N., Titone, R., Morani, F., Stasyk, O. & Isidoro, C. 2014. Single amino acid arginine deprivation triggers prosurvival autophagic response in ovarian carcinoma SKOV3. *Biomed Res Int,* 2014**,** 505041.

Si, Y., Shi, H. & Lee, K. 2009. Metabolic Flux Analysis of Mitochondrial Uncoupling in 3T3-L1 Adipocytes. *Plos One,* 4.

Sidi, S., Sanda, T., Kennedy, R. D., Hagen, A. T., Jette, C. A., Hoffmans, R., Pascual, J., Imamura, S., Kishi, S., Amatruda, J. F., Kanki, J. P., Green, D. R., D'andrea, A. A. & Look, A. T. 2008. Chk1 suppresses a caspase-2 apoptotic response to DNA damage that bypasses p53, Bcl-2, and caspase-3. *Cell,* 133**,** 864-877.

Silke, J., Rickard, J. A. & Gerlic, M. 2015. The diverse role of RIP kinases in necroptosis and inflammation. *Nat Immunol,* 16**,** 689-97.

Simoes, R. V., Serganova, I. S., Kruchevsky, N., Leftin, A., Shestov, A. A., Thaler, H. T., Sukenick, G., Locasale, J. W., Blasberg, R. G., Koutcher, J. A. & Ackerstaff, E. 2015. Metabolic plasticity of metastatic breast cancer cells: adaptation to changes in the microenvironment. *Neoplasia,* 17**,** 671-84.

Slater, A. F. G. 1993. Chloroquine - Mechanism of Drug-Action and Resistance in Plasmodium-Falciparum. *Pharmacology & Therapeutics,* 57**,** 203-235.

Solomon, V. R. & Lee, H. 2009. Chloroquine and its analogs: A new promise of an old drug for effective and safe cancer therapies. *European Journal of Pharmacology,* 625**,** 220-233.

Song, X., Huang, D., Liu, Y., Pan, X., Zhang, J. & Liang, B. 2014. AMP-activated protein kinase is required for cell survival and growth in HeLa-S3 cells in vivo. *IUBMB Life,* 66**,** 415-23.

Stambolic, V., Suzuki, A., De La Pompa, J. L., Brothers, G. M., Mirtsos, C., Sasaki, T., Ruland, J., Penninger, J. M., Siderovski, D. P. & Mak, T. W. 1998. Negative regulation of PKB/Akt-dependent cell survival by the tumor suppressor PTEN. *Cell,* 95**,** 29-39.

Steck, P. A., Pershouse, M. A., Jasser, S. A., Yung, W. K., Lin, H., Ligon, A. H., Langford, L. A., Baumgard, M. L., Hattier, T., Davis, T., Frye, C., Hu, R., Swedlund, B., Teng, D. H. & Tavtigian, S. V. 1997. Identification of a candidate tumour suppressor gene, MMAC1, at chromosome 10q23.3 that is mutated in multiple advanced cancers. *Nat Genet,* 15**,** 356-62.

Strohecker, A. M., Guo, J. Y., Karsli-Uzunbas, G., Price, S. M., Chen, G. J., Mathew, R., Mcmahon, M. & White, E. 2013. Autophagy Sustains Mitochondrial Glutamine Metabolism and Growth of Braf(V600E)-Driven Lung Tumors. *Cancer Discovery,* 3**,** 1272-1285.

Su, Z., Yang, Z., Xie, L., Dewitt, J. P. & Chen, Y. 2016. Cancer therapy in the necroptosis era. *Cell Death and Differentiation,* 23**,** 748-56.

Sullivan, D. J., Matile, H., Ridley, R. G. & Goldberg, D. E. 1998. A common mechanism for blockade of heme polymerization by antimalarial quinolines. *Journal of Biological Chemistry,* 273**,** 31103-31107.

Sun, S. Y. 2010. N-acetylcysteine, reactive oxygen species and beyond. *Cancer Biol Ther,* 9**,** 109-10.

Sun, W. L., Chen, J., Wang, Y. P. & Zheng, H. 2011. Autophagy protects breast cancer cells from epirubicin-induced apoptosis and facilitates epirubicin-resistance development. *Autophagy,* 7**,** 1035-44.

Takamura, A., Komatsu, M., Hara, T., Sakamoto, A., Kishi, C., Waguri, S., Eishi, Y., Hino, O., Tanaka, K. & Mizushima, N. 2011. Autophagy-deficient mice develop multiple liver tumors. *Genes Dev,* 25**,** 795-800.

Tao, K., Fang, M., Alroy, J. & Sahagian, G. G. 2008. Imagable 4T1 model for the study of late stage breast cancer. *Bmc Cancer,* 8.

Taparowsky, E., Shimizu, K., Goldfarb, M. & Wigler, M. 1983. Structure and activation of the human N-ras gene. *Cell,* 34**,** 581-6.

Tee, A. R., Manning, B. D., Roux, P. P., Cantley, L. C. & Blenis, J. 2003. Tuberous sclerosis complex gene products, tuberin and hamartin, control mTOR signaling by acting as a GTPase-activating protein complex toward Rheb. *Current Biology,* 13**,** 1259-1268.

Thorburn, J., Frankel, A. E. & Thorburn, A. 2009a. Regulation of HMGB1 release by autophagy. *Autophagy,* 5**,** 247-9.

Thorburn, J., Horita, H., Redzic, J., Hansen, K., Frankel, A. E. & Thorburn, A. 2009b. Autophagy regulates selective HMGB1 release in tumor cells that are destined to die. *Cell Death and Differentiation,* 16**,** 175-83.

Tian, W., Li, W., Chen, Y., Yan, Z., Huang, X., Zhuang, H., Zhong, W., Wu, W., Lin, C., Chen, H., Hou, X., Zhang, L., Sui, S., Zhao, B., Hu, Z., Li, L. & Feng, D. 2015. Phosphorylation of ULK1 by AMPK regulates translocation of ULK1 to mitochondria and mitophagy. *Febs Letters,* 589**,** 1847-54.

Tomita, Y., Marchenko, N., Erster, S., Nemajerova, A., Dehner, A., Klein, C., Pan, H. G., Kessler, H., Pancoska, P. & Moll, U. M. 2006. WT p53, but not tumor-derived mutants, bind to Bcl2 via the DNA binding domain and induce mitochondrial permeabilization. *Journal of Biological Chemistry,* 281**,** 8600-8606.

Turk, B., Bieth, J. G., Bjork, I., Dolenc, I., Turk, D., Cimerman, N., Kos, J., Colic, A., Stoka, V. & Turk, V. 1995. Regulation of the activity of lysosomal cysteine proteinases by pH-induced inactivation and/or endogenous protein inhibitors, cystatins. *Biol Chem Hoppe Seyler,* 376**,** 225-30.

Turk, B., Dolenc, I., Zerovnik, E., Turk, D., Gubensek, F. & Turk, V. 1994. Human cathepsin B is a metastable enzyme stabilized by specific ionic interactions associated with the active site. *Biochemistry,* 33**,** 14800-6.

Uemura, T., Yamamoto, M., Kametaka, A., Sou, Y., Yabashi, A., Yamada, A., Annoh, H., Kametaka, S., Komatsu, M. & Waguri, S. 2014. A Cluster of Thin Tubular Structures Mediates Transformation of the Endoplasmic Reticulum to Autophagic Isolation Membrane. *Molecular and Cellular Biology,* 34**,** 1695-1706.

Ullio, C., Casas, J., Brunk, U. T., Sala, G., Fabrias, G., Ghidoni, R., Bonelli, G., Baccino, F. M. & Autelli, R. 2012. Sphingosine mediates TNF alpha-induced lysosomal membrane permeabilization and ensuing programmed cell death in hepatoma cells. *Journal of Lipid Research,* 53**,** 1134-1143.

Unemori, E. N., Ferrara, N., Bauer, E. A. & Amento, E. P. 1992. Vascular endothelial growth factor induces interstitial collagenase expression in human endothelial cells. *J Cell Physiol,* 153**,** 557-62.

Van Poznak, C., Seidman, A. D., Reidenberg, M. M., Moasser, M. M., Sklarin, N., Van Zee, K., Borgen, P., Gollub, M., Bacotti, D., Yao, T. J., Bloch, R., Ligueros, M., Sonenberg, M., Norton, L. & Hudis, C. 2001. Oral gossypol in the treatment of patients with refractory metastatic breast cancer: a phase I/II clinical trial. *Breast Cancer Res Treat,* 66**,** 239-48.

Vander Haar, E., Lee, S. I., Bandhakavi, S., Griffin, T. J. & Kim, D. H. 2007. Insulin signalling to mTOR mediated by the Akt/PKB substrate PRAS40. *Nature Cell Biology,* 9**,** 316-23.

Vasudev, N. S. & Reynolds, A. R. 2014. Anti-angiogenic therapy for cancer: current progress, unresolved questions and future directions. *Angiogenesis,* 17**,** 471-494.

Vazquez-Martin, A., Oliveras-Ferraros, C. & Menendez, J. A. 2009. Autophagy facilitates the development of breast cancer resistance to the anti-HER2 monoclonal antibody trastuzumab. *Plos One,* 4**,** e6251.

Vincent, E. E., Elder, D. J., Thomas, E. C., Phillips, L., Morgan, C., Pawade, J., Sohail, M., May, M. T., Hetzel, M. R. & Tavare, J. M. 2011. Akt phosphorylation on Thr308 but not on Ser473 correlates with Akt protein kinase activity in human non-small cell lung cancer. *Br J Cancer,* 104**,** 1755-61.

Vistain, L. F., Yamamoto, N., Rathore, R., Cha, P. & Meade, T. J. 2015. Targeted Inhibition of Snail Activity in Breast Cancer Cells by Using a Co(III) -Ebox Conjugate. *Chembiochem,* 16**,** 2065-72.

Vogl, D. T., Stadtmauuer, E.A., Tan, K.S., Heitjan, D.F., Davis, L.E., Pontiggia, L., Rangwala, R., Piao, S., Chang, Y.C., Scott, E.C., Paul, T.M., Nichols, C.W., Porter, D.L., Kaplan, J., Mallon, G., Bradner, J.E., Amaravadi, R.K. 2014. Combined autophagy and proteasome inhibition. A phase I trial of hydroxychloroquine and bortezomib in patients with relapsed/refractory myeloma. *Autophagy,* 10**,** 1380-1390.

Volate, S. R., Kawasaki, B. T., Hurt, E. M., Milner, J. A., Kim, Y. S., White, J. & Farrar, W. L. 2010. Gossypol induces apoptosis by activating p53 in prostate cancer cells and prostate tumor-initiating cells. *Mol Cancer Ther,* 9**,** 461-70.

Wang, H. & Keiser, J. A. 1998. Vascular endothelial growth factor upregulates the expression of matrix metalloproteinases in vascular smooth muscle cells: role of flt-1. *Circulation Research,* 83**,** 832-40.

Wang, J. B., Erickson, J. W., Fuji, R., Ramachandran, S., Gao, P., Dinavahi, R., Wilson, K. F., Ambrosio, A. L., Dias, S. M., Dang, C. V. & Cerione, R. A. 2010. Targeting mitochondrial glutaminase activity inhibits oncogenic transformation. *Cancer Cell,* 18**,** 207-19.

Wang S., T. Z., Wolfson R., Shen K., Wyant G.A., Plovanich M.E., Yuan E.D., Jones T.D., Chantranupong L., Comb W., Wang T., Bar-Peled L., Zoncu R., Straub C., Kim C., Park J., Sabatini B.L., Sabatini D.M. 2015. The amino acid transporter SLC38A9 is a key component of a lysosomal membrane complex that signals arginine sufficiency to mTORC1. . *Science,* 347**,** 188-194.

Wang, Z., Shi, X., Li, Y., Fan, J., Zeng, X., Xian, Z., Sun, Y., Wang, S., Song, P., Zhao, S., Hu, H. & Ju, D. 2014. Blocking autophagy enhanced cytotoxicity induced by recombinant human arginase in triple-negative breast cancer cells. *Cell Death & Disease,* 5**,** e1563.

Wang, Z. Y., Wang, N., Chen, J. P. & Shen, J. G. 2012. Emerging Glycolysis Targeting and Drug Discovery from Chinese Medicine in Cancer Therapy. *Evidence-Based Complementary and Alternative Medicine*.

Warburg, O. 1956. On the origin of cancer cells. *Science,* 123**,** 309-14.

Warburg, O., Wind, F. & Negelein, E. 1927. The Metabolism of Tumors in the Body. *J Gen Physiol,* 8**,** 519-30.

Wattel, E., Preudhomme, C., Hecquet, B., Vanrumbeke, M., Quesnel, B., Dervite, I., Morel, P. & Fenaux, P. 1994. P53 Mutations Are Associated with Resistance to Chemotherapy and Short Survival in Hematologic Malignancies. *Blood,* 84**,** 3148-3157.

Wilkinson, S., O'prey, J., Fricker, M. & Ryan, K. M. 2009. Hypoxia-selective macroautophagy and cell survival signaled by autocrine PDGFR activity. *Genes Dev,* 23**,** 1283-8.

Wilson, E. N., Bristol, M. L., Di, X., Maltese, W. A., Koterba, K., Beckman, M. J. & Gewirtz, D. A. 2011. A switch between cytoprotective and cytotoxic autophagy in the radiosensitization of breast tumor cells by chloroquine and vitamin D. *Horm Cancer,* 2**,** 272-85.

Wise, D. R., Deberardinis, R. J., Mancuso, A., Sayed, N., Zhang, X. Y., Pfeiffer, H. K., Nissim, I., Daikhin, E., Yudkoff, M., Mcmahon, S. B. & Thompson, C. B. 2008. Myc regulates a transcriptional program that stimulates mitochondrial glutaminolysis and leads to glutamine addiction. *Proc Natl Acad Sci U S A,* 105**,** 18782-7.

Wise, D. R. & Thompson, C. B. 2010. Glutamine addiction: a new therapeutic target in cancer. *Trends in Biochemical Sciences,* 35**,** 427-33.

Wolf, A., Agnihotri, S., Micallef, J., Mukherjee, J., Sabha, N., Cairns, R., Hawkins, C. & Guha, A. 2011. Hexokinase 2 is a key mediator of aerobic glycolysis and promotes tumor growth in human glioblastoma multiforme. *Journal of Experimental Medicine,* 208**,** 313-26.

Wolfson, R. L., Chantranupong, L., Saxton, R. A., Shen, K., Scaria, S. M., Cantor, J. R. & Sabatini, D. M. 2016. Sestrin2 is a leucine sensor for the mTORC1 pathway. *Science,* 351**,** 43-8.

Wong, J. Y., Huggins, G. S., Debidda, M., Munshi, N. C. & De Vivo, I. 2008. Dichloroacetate induces apoptosis in endometrial cancer cells. *Gynecol Oncol,* 109**,** 394-402.

Wong, P. M., Feng, Y., Wang, J., Shi, R. & Jiang, X. 2015. Regulation of autophagy by coordinated action of mTORC1 and protein phosphatase 2A. *Nat Commun,* 6**,** 8048.

Woo, M., Hakem, R., Soengas, M. S., Duncan, G. S., Shahinian, A., Kagi, D., Hakem, A., Mccurrach, M., Khoo, W., Kaufman, S. A., Senaldi, G., Howard, T., Lowe, S. W. & Mak, T. W. 1998. Essential contribution of caspase 3/CPP32 to apoptosis and its associated nuclear changes. *Genes Dev,* 12**,** 806-19.

Woods, A., Vertommen, D., Neumann, D., Turk, R., Bayliss, J., Schlattner, U., Wallimann, T., Carling, D. & Rider, M. H. 2003. Identification of phosphorylation sites in AMP-activated protein kinase (AMPK) for upstream AMPK kinases and study of their roles by site-directed mutagenesis. *J Biol Chem,* 278**,** 28434-42.

Wu, X., Wang, Y., Wang, H., Wang, Q., Wang, L., Miao, J., Cui, F. & Wang, J. 2012. Quinacrine Inhibits Cell Growth and Induces Apoptosis in Human Gastric Cancer Cell Line SGC-7901. *Curr Ther Res Clin Exp,* 73**,** 52-64.

Wu, Y. L., Mehew, J. W., Heckman, C. A., Arcinas, M. & Boxer, L. M. 2001. Negative regulation of bcl-2 expression by p53 in hematopoietic cells. *Oncogene,* 20**,** 240-251.

Xie, X. Q., White, E. P. & Mehnert, J. M. 2013. Coordinate Autophagy and mTOR Pathway Inhibition Enhances Cell Death in Melanoma. *Plos One,* 8.

Xie, Z. P. & Klionsky, D. J. 2007. Autophagosome formation: Core machinery and adaptations. *Nature Cell Biology,* 9**,** 1102-1109.

Yang, C., Sudderth, J., Dang, T., Bachoo, R. M., Mcdonald, J. G. & Deberardinis, R. J. 2009. Glioblastoma cells require glutamate dehydrogenase to survive impairments of glucose metabolism or Akt signaling. *Cancer Res,* 69**,** 7986-93.

Yang, H., Hreggvidsdottir, H. S., Palmblad, K., Wang, H., Ochani, M., Li, J., Lu, B., Chavan, S., Rosas-Ballina, M., Al-Abed, Y., Akira, S., Bierhaus, A., Erlandsson-Harris, H., Andersson, U. & Tracey, K. J. 2010. A critical cysteine is required for HMGB1 binding to Toll-like receptor 4 and activation of macrophage cytokine release. *Proc Natl Acad Sci U S A,* 107**,** 11942-7.

Yang, J., Mani, S. A., Donaher, J. L., Ramaswamy, S., Itzykson, R. A., Come, C., Savagner, P., Gitelman, I., Richardson, A. & Weinberg, R. A. 2004a. Twist, a master regulator of morphogenesis, plays an essential role in tumor metastasis. *Cell,* 117**,** 927-939.

Yang, J. Y., Zong, C. S., Xia, W., Yamaguchi, H., Ding, Q., Xie, X., Lang, J. Y., Lai, C. C., Chang, C. J., Huang, W. C., Huang, H., Kuo, H. P., Lee, D. F., Li, L. Y., Lien, H. C., Cheng, X., Chang, K. J., Hsiao, C. D., Tsai, F. J., Tsai, C. H., Sahin, A. A., Muller, W. J., Mills, G. B., Yu, D., Hortobagyi, G. N. & Hung, M. C. 2008. ERK promotes tumorigenesis by inhibiting FOXO3a via MDM2-mediated degradation. *Nature Cell Biology,* 10**,** 138-48.

Yang, L., Dan, H. C., Sun, M., Liu, Q., Sun, X. M., Feldman, R. I., Hamilton, A. D., Polokoff, M., Nicosia, S. V., Herlyn, M., Sebti, S. M. & Cheng, J. Q. 2004b. Akt/protein kinase B signaling inhibitor-2, a selective small molecule inhibitor of Akt signaling with antitumor activity in cancer cells overexpressing Akt. *Cancer Res,* 64**,** 4394-9.

Yang, Z. F. & Klionsky, D. J. 2010. Eaten alive: a history of macroautophagy. *Nature Cell Biology,* 12**,** 814-822.

Ye, J. Z. S., Hockemeyer, D., Krutchinsky, A. N., Loayza, D., Hooper, S. M., Chait, B. T. & De Lange, T. 2004. POT1-interacting protein PIP1: a telomere length regulator that recruits POT1 to the TIN2/TRF1 complex. *Genes Dev,* 18**,** 1649-1654.

Yerlikaya, A., Okur, E. & Ulukaya, E. 2012. The p53-independent induction of apoptosis in breast cancer cells in response to proteasome inhibitor bortezomib. *Tumor Biology,* 33**,** 1385-1392.

Yin, T., He, S., Ye, T., Shen, G., Wan, Y. & Wang, Y. 2014. Antiangiogenic therapy using sunitinib combined with rapamycin retards tumor growth but promotes metastasis. *Transl Oncol,* 7**,** 221-9.

Yip, C. K., Murata, K., Walz, T., Sabatini, D. M. & Kang, S. A. 2010. Structure of the human mTOR complex I and its implications for rapamycin inhibition. *Mol Cell,* 38**,** 768-74.

Yonishrouach, E., Resnitzky, D., Lotem, J., Sachs, L., Kimchi, A. & Oren, M. 1991. Wild-Type P53 Induces Apoptosis of Myeloid Leukemic-Cells That Is Inhibited by Interleukin-6. *Nature,* 352**,** 345-347.

Yoon, Y. H., Cho, K. S., Hwang, J. J., Lee, S. J., Choi, J. A. & Koh, J. Y. 2010. Induction of lysosomal dilatation, arrested autophagy, and cell death by chloroquine in cultured ARPE-19 cells. *Invest Ophthalmol Vis Sci,* 51**,** 6030-7.

Yu, Y., Deck, J. A., Hunsaker, L. A., Deck, L. M., Royer, R. E., Goldberg, E. & Vander Jagt, D. L. 2001. Selective active site inhibitors of human lactate dehydrogenases A4, B4, and C4. *Biochem Pharmacol,* 62**,** 81-9.

Yue, Z., Jin, S., Yang, C., Levine, A. J. & Heintz, N. 2003. Beclin 1, an autophagy gene essential for early embryonic development, is a haploinsufficient tumor suppressor. *Proc Natl Acad Sci U S A,* 100**,** 15077-82.

Zhang, C. S., Jiang, B., Li, M., Zhu, M., Peng, Y., Zhang, Y. L., Wu, Y. Q., Li, T. Y., Liang, Y., Lu, Z., Lian, G., Liu, Q., Guo, H., Yin, Z., Ye, Z., Han, J., Wu, J. W., Yin, H., Lin, S. Y. & Lin, S. C. 2014a. The lysosomal v-ATPase-Ragulator complex is a common activator for AMPK and mTORC1, acting as a switch between catabolism and anabolism. *Cell Metabolism,* 20**,** 526-40.

Zhang, H. W., Solomon, V. R., Hu, C. K., Ulibarri, G. & Lee, H. Y. 2008. Synthesis and in vitro cytotoxicity evaluation of 4-aminoquinoline derivatives. *Biomedicine & Pharmacotherapy,* 62**,** 65-69.

Zhang, Q., Zhang, Y., Zhang, P., Chao, Z., Xia, F., Jiang, C., Zhang, X., Jiang, Z. & Liu, H. 2014b. Hexokinase II inhibitor, 3-BrPA induced autophagy by stimulating ROS formation in human breast cancer cells. *Genes Cancer,* 5**,** 100-12.

Zhang, Z. J., Huang, S., Wang, H. Y., Wu, J., Chen, D., Peng, B. G. & Zhou, Q. 2016. High expression of hexokinase domain containing 1 is associated with poor prognosis and aggressive phenotype in hepatocarcinoma. *Biochemical and Biophysical Research Communications,* 474**,** 673-679.

Zheng, J. 2012. Energy metabolism of cancer: Glycolysis versus oxidative phosphorylation (Review). *Oncology Letters,* 4**,** 1151-1157.

Zhong, Y., Wang, Q. J., Li, X. T., Yan, Y., Backer, J. M., Chait, B. T., Heintz, N. & Yue, Z. Y. 2009. Distinct regulation of autophagic activity by Atg14L and Rubicon associated with Beclin 1-phosphatidylinositol-3-kinase complex. *Nature Cell Biology,* 11**,** 468-U262.

Zhou, P., Chen, W. G. & Li, X. W. 2015. MicroRNA-143 acts as a tumor suppressor by targeting hexokinase 2 in human prostate cancer. *Am J Cancer Res,* 5**,** 2056-63.

Zhu, W., Wang, X., Zhou, Y. & Wang, H. 2014. C2-ceramide induces cell death and protective autophagy in head and neck squamous cell carcinoma cells. *Int J Mol Sci,* 15**,** 3336-55.

Zoncu, R., Bar-Peled, L., Efeyan, A., Wang, S. Y., Sancak, Y. & Sabatini, D. M. 2011. mTORC1 Senses Lysosomal Amino Acids Through an Inside-Out Mechanism That Requires the Vacuolar H+-ATPase. *Science,* 334**,** 678-683.

Zoppino, F. C. M., Militello, R. D., Slavin, I., Alvarez, C. & Colombo, M. I. 2010. Autophagosome Formation Depends on the Small GTPase Rab1 and Functional ER Exit Sites. *Traffic,* 11**,** 1246-1261.

Zou, H., Yang, R., Hao, J., Wang, J., Sun, C., Fesik, S. W., Wu, J. C., Tomaselli, K. J. & Armstrong, R. C. 2003. Regulation of the Apaf-1/caspase-9 apoptosome by caspase-3 and XIAP. *J Biol Chem,* 278**,** 8091-8.